SYNTHESIS AND ANTIDIABETIC INVESTIGATION ON THIAZOLE DERIVATIVES

Thesis

Submitted for the Award of the Degree of

DOCTOR OF PHILOSOPHY

in

Pharmaceutical Chemistry

By

Sharfuddin Mohd

Registration Number: 41700271

Supervised by
Dr. Vikas Sharma (26231)
Associate Professor
Department of Pharmaceutical Chemistry
School of Pharmaceutical Sciences
Lovely Professional University
Punjab-144411, India

Co-Supervised by
Dr. Rakesh Kumar (27441)
Assistant Professor
Department of Pharmacology
School of Pharmaceutical Sciences
Lovely Professional University
Punjab-144411, India

LOVELY PROFESSIONAL UNIVERSITY, PUNJAB
2025

DECLARATION

I, hereby declared that the presented work in the thesis entitled "**Synthesis and Antidiabetic Investigation on Thiazole Derivatives**" in fulfilment of degree of **Doctor of Philosophy (Ph.D.)** is outcome of research work carried out by me under the supervision Dr. Vikas Sharma, working as Associate Professor, in the department of pharmaceutical chemistry, school of pharmaceutical sciences, of lovely professional university, Punjab, India. In keeping with general practice of reporting scientific observations, due acknowledgements have been made whenever work described here has been based on findings of other investigator. This work has not been submitted in part or full to any other university or institute for the award of any degree.

(**Signature of scholar**)

Sharfuddin Mohd (41700271)
Department of Pharmaceutical chemistry
School of Pharmaceutical sciences,
Lovely professional university, Punjab, India.

CERTIFICATE

This is to certify that the work reported in the Ph. D. thesis entitled "**Synthesis and Antidiabetic Investigation on Thiazole Derivatives**"submitted in fulfillment of the requirement for the reward of degree of **Doctor of Philosophy (Ph.D.)** in the Department of Pharmaceutical chemistry, School of Pharmaceutical sciences, is a research work carried out by Sharfuddin Mohd (41700271), is bonafide record of his original work carried out under my supervision and that no part of thesis has been submitted for any other degree, diploma or equivalent course.

(Signature of Supervisor)
Dr. Vikas Sharma (26231)
Associate Professor
Department of Pharmaceutical Chemistry
School of Pharmaceutical Sciences
Lovely Professional University
Punjab-144411, India

(**Signature of Co-Supervisor**)
Dr. Rakesh Kumar (27441)
Assistant Professor
Department of Pharmacology
School of Pharmaceutical Sciences
Lovely Professional University
Punjab-144411, India

ABSTRACT

Diabetes Mellitus (DM) is one of the major causes of death globally after cancer and heart disease. To identify potent and selective oral hypoglycemic drugs with minimum or less side effects is a serious concern and goal of the medicinal chemists. T2DM remains a significant global health alarm, imposing the continual exploring novel therapeutic approaches. Among the therapeutic strategies, inhibition of carbohydrate-hydrolysing enzymes like pancreatic α-amylase (PAA) and intestinal α-glucosidase (IAG) has emerged as a critical target for controlling blood glucose levels after meals. The growing prevalence of T2DM underscores the need for innovative therapeutic strategies that address both insulin resistance and postprandial hyperglycemia. The investigation seeks to address the limitations of current treatment modalities and introduce pure inhibitor of the PAA and IAG enzymes that could enhance the efficacy while minimizing adverse effects. The thesis deals with the comprehensive research ideas focus on design, synthesis and antidiabetic assessment of the new naphthalene-based thiazolidinedione (**Series-I**) and quinoline-based thiazolidinedione (**Series-II**) derivatives. The study begins with an extensive literature review, which identified thiazolidinedione-based molecules as promising candidates. To explore the anti-diabetic potential of the selected compounds, their inhibitory effects were evaluated against two important carbohydrate-hydrolysing enzymes: pancreatic α-amylase (PAA) and intestinal α-glucosidase (IAG). Inhibition of PAA and IAG enzymes can effectively reduce postprandial hyperglycemia by delaying carbohydrate digestion and glucose absorption. The antioxidant potential studies were also performed and results confined that the all compound was also able to reduce the reactive oxygen species (ROS) induced diabetes. The *in silico* findings were further correlated with *in vitro* enzyme inhibition assays to validate the predictive computational models. All the synthesized compounds exhibit strong to moderate binding affinities. Additionally, molecular mechanics generalized born surface area (MM-GBSA) and molecular dynamics (MD) simulation studies also demonstrated significant ligand binding strength within PAA and IAG receptor binding pocket. *In silico* molecular properties, ADME and toxicity analyses reveals favourable physicochemical properties and feasible toxicity profiles for all synthesized compounds.

In the first series, a rational drug design approach allied with a pharmacophore-based designed strategy was applied to prepare novel compounds (**NT1**-**NT18**) with specific structural features (thiazolidinedione ring) known to treat diabetes. Target thiazolidinedione-based naphthalene derivatives were synthesized using schemes **scheme.1** includes two steps. At first, in **scheme.1** thiazolidinedione is reacted with 2-naphthaldehyde which then undergoes Knoevenagel condensation reaction in the presence of methanol and piperidine (cat) is reflux for 18 h at 70 °C to yield the intermediate. The intermediate was finally treated with different derivatives of aryl bromides, aqueous ethanolic solution and sodium hydroxide (NaOH) to yield a series of substituted analogues (**NT1-NT7**). Additionally in **scheme.1**, the same thiazolidinedione is reacted with 6-methoxy-2-naphthaldehyde in the presence of piperidine in methanol to give intermediate. These resulting intermediates were finally treated with alkyl and aryl bromides in the aqueous ethanolic solution (ethanol: water, 1:1), catalytical amount of NaOH to give final analogs (**NT8-NT18**).

The structural elucidation of each compound was proficient using advanced spectroscopic techniques, like FT-IR, MS and NMR (^{1}H & ^{13}C) spectroscopic studies. Moreover, all the synthesized compounds were screened for *In vitro* antidiabetic activity against PAA and IAG enzymes, revealed that compounds **NT7** and **NT17** was found to be the most potent exhibited high potency compared to acarbose. Notably, compound **NT17 s**hows IC_{50} value of 4.48 µM and 2.14 µM as compared with acarbose against PAA and IAG enzymes respectively. Compound **NT17** emerged as the most potent compound in the series (**NT1-NT18**), displaying an increased binding affinity of -10.7 kcal/mol with PAA receptor and -10.9 kcal/mol with receptors IGA receptor and engaging in hydrogen bond interactions with Thr163, Arg195 amino acids within the PAA active binding pocket and Arg315, Arg442 amino acids within IAG active binding pocket respectively. Subsequently, DPPH antioxidant assay demonstrates that the compound **NT7** and **NT17** are effective against ascorbic acid, indicating the effectiveness in able to reduce the reactive oxygen species (ROS) induced DM. A molecular docking and MM-GSBA studies provided insights into the interaction patterns of these compounds with PAA and IAG receptors. ADME and toxicity analysis revealed favourable physicochemical properties leads to durglikeness and manageable toxicity profiles by all compounds including compound **NT7** and **NT17**.

In the second series, quinoline-based thiazolidinedione derivatives (**QT1-QT8**) were synthesised with alkyl, haloalkyl and aromatic groups are strategically placed on amidic nitrogen of central thiazolidinedione core while a quinoline ring is introduced, attributed to the presence of the heterocyclic nitrogen, which facilitates additional hydrogen bonding and polar interactions. Which enhance the enzymes inhibition with superior control of postprandial glucose levels. Target thiazolidinedione-based quinoline derivatives were synthesized using schemes **scheme.2** includes two steps. At first, thiazolidinedione is reacted with quinoline-6-carbaldehyde, in the presence of methanol and piperidine (Knoevenagel condensation) to yield the intermediate. alkyl, haloalkyl and benzyl chloride derivatives leads to quinoline based thiazolidinediones (**QT1-QT8**).

To evaluate the antidiabetic of synthesized compounds **QT1-QT8 (**thiazolidinedione-based quinoline series), *in vitro* PAA and IAG assays were conducted. **QT8** analogue containing N-substituted bicyclic biphenyl carbonitrile on TZD, confirmed the highest biological activity with an IC_{50} value of 4.68 µM towards PAA enzyme and 2.45 µM towards IAG enzyme. Notably, compound **QT8** unveiled the highest binding affinity at -11.3 kcal/mol with PAA and -10.6 kcal/mol with IAG respectively. In contrast, standard compound acarbose (-6.7 kcal/mol) with PAA and acarbose (-8.5 kcal/mol) with IGA displayed considerably lower docking scores when compared to the synthesized compounds. The compound **QT8** formed two hydrogen bonds with Gln63 and His299 amino acid residues in PAA active binding pocket and four hydrogen bonds with Arg213, Gln279, Arg315, His351 amino residues in IAG active binding site respectively. Moreover, the pharmacokinetic analyses highlighted the satisfactory bioavailability and distribution profiles of these compounds (**QT1-QT8**), emphasizing their potential for further development.

In conclusion, this research is a promising effort to identify best inhibitors of PAA and IAG for T2DM treatment. Compounds like **NT7**, **NT17** and **QT8** shows significant potential in inhibiting PAA and IAG enzymes to treat T2DM and may offer safer alternatives to current treatments. Further *in vivo* studies using compound **NT17** and **QT8** could provide valuable insights into its potential as a novel therapeutic option, potentially improving the prognosis and treatment options for T2DM patients.

Keywords: Thiazolidinedione, Diabetes mellitus, α-amylase, α-glucosidase, DPPH assay, Molecular dynamics, ADME and toxicity

Salient features:

- Thiazolidinediones, naphthalene and quinoline moieties (scaffold) are individually showing good antidiabetic properties.
- In our present study, we have combined naphthalene based thiazolidinediones and quinoline based thiazolidinediones combinations has been shown potent antidiabetic action towards both pancreatic α-amylase (PAA) and intestinal α-glucosidase (IAG) proteins.
- The study suggests a scaffold combination concept targeting PAA and IAG.
- All synthesized compounds have studied *in vitro* antidiabetic action in different targets like PAA and IAG proteins. We have validated those in-vitro results with molecular docking studies, that revealed these molecules are having strong binding interactions towards both targets.
- Studied antioxidant activity of all synthesised compounds and results confined all compounds exhibit good antioxidant potential.
- Molecular dynamic (MD) simulations naked stability of enzyme-compound complex(s).
- The compounds demonstrated acceptable ADME and toxicity properties.

Graphical abstract

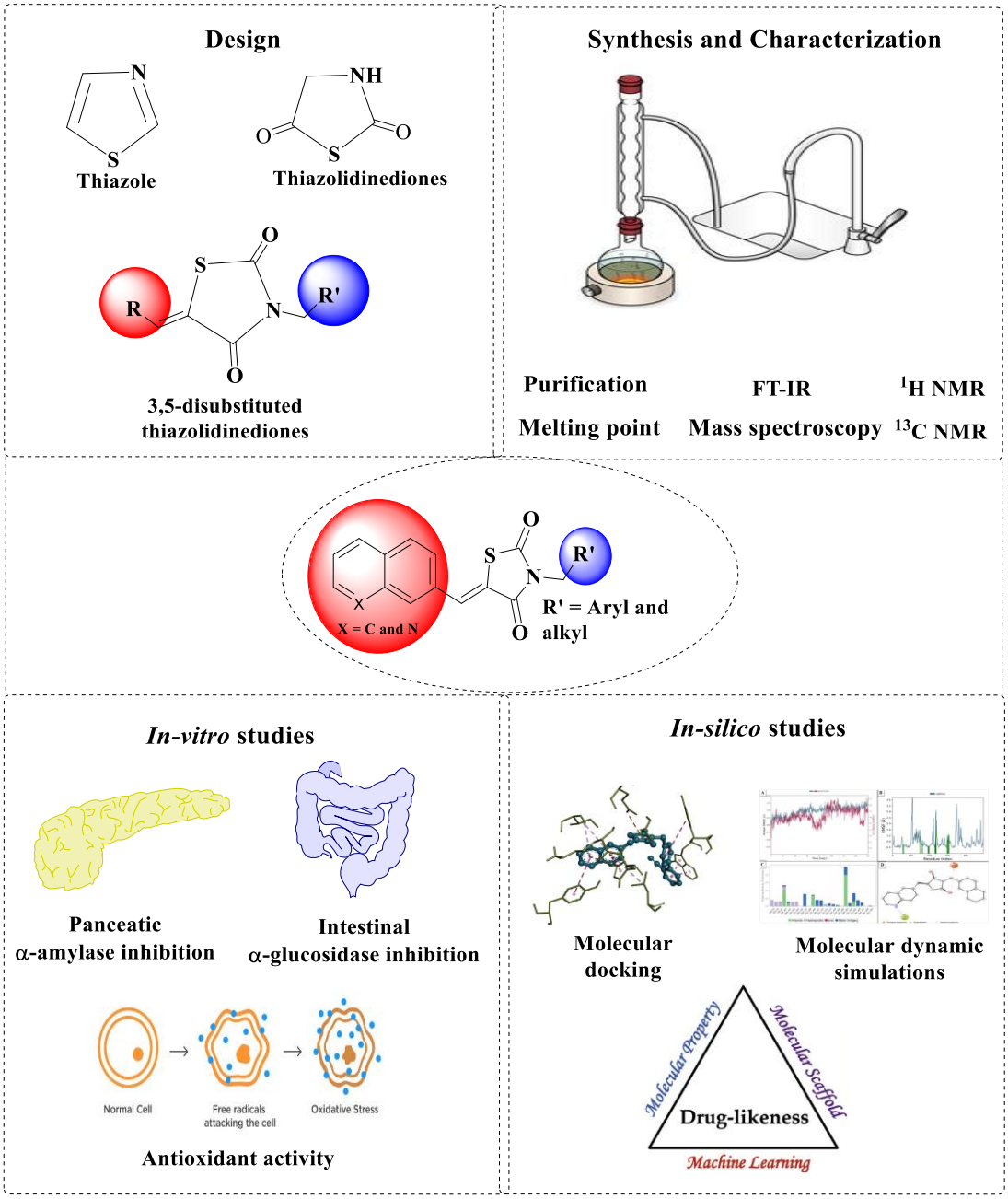

Novel thiazolidinedione derivatives as potential antidiabetic agents

ACKNOWLEDGEMENTS

Undertaking this Ph.D. has been a truly life-changing experience for me and it would not have been possible to do without the support and guidance that I received from many people. I would like to express my warm gratitude to all those helped me to make this day possible from a distant dream.

I am deeply grateful to ***Dr. Ashok Mittal, Chancellor and Mrs. Dr. Rashmi Mittal, pro-Chancellor, Lovely Professional University*** for providing me necessary infrastructure facilities as well as excellent working environment in the laboratory in order to complete my task.

I also like to express my sincere respect to ***Dr. Monica Gulati***, Professor, Ex. Dean cum Registrar, Lovely Professional University and ***Dr. Sachin Kumar Singh*** Professor and COD, Department of Pharmaceutical Chemistry, Lovely Professional University for their valuable suggestions, guidance, support and also for providing all the necessary facilities to conduct my research work.

There are no proper words to convey my deep gratitude and respect for my thesis and honoured research advisors, ***Dr. Vikas Sharma***, Professor, Department of Pharmaceutical Chemistry, Lovely Professional University and ***Dr. Rakesh Kumar*** Assistant Professor, Department of Pharmacology, Lovely Professional University. This long journey of mine has been endowed to their profound insight, valuable advice, motivation, immense knowledge, continuous support and patience during my Ph.D. study. Dr. Vikas Sharma and Dr. Rakesh had spent their precious time to guide me, and helped me to overcome the difficulty of this journey. They have inspired me to become an independent researcher and helped me realize the power of critical reasoning. Their guidance helped me in all time of research and writing of this thesis. I really feel fortunate enough to come into contact with these two eminent persons and hope that I can follow their path of dedication in my future works.

I am really grateful to ***Dr. Vancha Harish***, Associate Professor, Department of Pharmaceutics, Lovely Professional University, for giving valuable suggestions in my research work.

I specially, like to express my love and respect to ***Dr. Govindaiah Pilli***, ***Dr. B.C. Revanasiddappa***, ***Dr. Vijay Kumar and Dr. Palakurthy Yanadaiah*** who are more than a friend for me, and they have supported me in all my ups and downs throughout my journey and also provided me necessary supports in my research works and helped me cross many obstacles during my entire work period.

I would like to thank the support of ***Dr. Sheshagiri R Dixit,*** his student ***Durgesh Paresh Bidye*** and ***Dr. Nandan Kumar Duddukuri (Chief Scientific Officer at Innatura Scientific Pvt. Ltd)*** for allowing me to carry out computational and synthetic experiments in their lab.

I would like to extend my thanks to the senior faculty members ***Dr. Gurvinder Singh, Dr. Surendrs Kumar Nayak, Dr. Pankaj Wadwa, Dr. Gurdeep Singh and Dr. Iqbal Brar*** for their support and suggestions to my work as evaluation panel members.

I would always cherish the wonderful memories with my research colleagues in School of Pharmaceutical Sciences, Lovely Professional University: ***Mr. Srinivas Sutrapu, Mr. Mahender Thatikayala, Mr. Shubam Kumar, Ms. Shivani Sharma and Ms. Pooja.***

I would like to extend my thanks to the laboratory assistants, library and office staffs of School of Pharmaceutical Sciences, Lovely Professional University for their caring attitude and constant support.

I am thankful to ***Central Instrumentation Facility, Lovely Professional University*** and ***Sophisticated Analytical Instrumentation Facility*** **(SAIF)** at Panjab university for their tremendous contribution in sample analysis during my research work.

Where emotions are involved, words don't seem adequate to express. A vocabulary finds no appreciation to express my heartfelt love and thanks to my sweet sisters ***Raziya, Thasleema, Anoja*** and my brother ***Abdulla*** for their unconditional love and encouragement to enter into PhD and also for their support during the research journey.

I would like to extend my gratitude to my beloved friends ***Mr. Purna Chander Reddy, Mr. Sreekanth.E, Mr. Amar, Mr. Bhargava Raju, Mr. Srikanth.K, Mr. Anil Kumar.N and Mr. Venkatesh.V*** for their motivation and support during odd times of my journey.

I would like to extend my special thanks, love and gratitude towards my better half ***Shajahan Begum*** for her endless love and constant support, for all the late nights and early mornings, and for keeping me sane over the past few months. Thank you for being my muse, editor, proofreader and sounding board. But most of all, thank you for being my best friend. I owe you everything.

My acknowledgement would be incomplete without thanking the biggest source of my strength, my family. I am indebted to my parents ***Mr. Mahaboob Mohd***, and ***Mrs. Jainabee*** for the immutable source of information and strength to take my higher studies and completion of the same. I am proud to pay them as my parents and there are no words, only feelings to honourably pay my regards for their ceaseless perspiration, encouragement, moral support and unlimited love.

I would like to dedicate this work to my parents whose dreams for me have resulted in this achievement and without their loving, upbringing and nurturing; I would not have been where I am today and what I am today. It is true that parents are neither anchor to hold your back, nor snail to take us there, but a guiding light whose love shows us the way.

Last but not least, I acknowledge all those who knowingly and unknowingly contributed in making my work effortless and rewarding success

My journey towards Ph.D. has been a long and challenging road and I am contended that I have accomplished it successfully.

It's both an ending and beginning. Its warm memories of the past and big dreams for the future.

Thankful I ever remain

Sharfuddin Mohd

Dedicated to my

Parents and Family

LIST OF CONTENT

LIST OF FIGURES

LIST OF TABLES

SYNTHETIC SCHEMES

LIST OF ABBREVATIONS

Abbreviation/Symbol	Description
α	Alpha
β	Beta
β-cells	Beta cells of pancreas
°C	Degree Centigrade
Å	Angstrom
ADME	Absorption Distribution Metabolism Excretion
ATP	Adenosine Triphosphate
BBB	Blood Brain Barrier
BV-Score	Bioavailability-Score
CADD	Computer-aided Drug Design
CAMD	Computer-aided Molecular Design
cat	Catalyst
CH_2	Methylene
CNS	Central Nervous System
Conc	Concentrated
CYP	Cytochrome Phosphorus
d	doublet
DCM	Dichloromethane
dd	Doublet of doublet
DM	Diabetes Mellitus
DMF	N,N-Dimethylformamide
DNA	Deoxyribonucleic Acid
DPPH	Diphenyl Picrylhydrazine
ED_{25}	Effective dose 25
ESI-MS	Electrospray Ionization Mass Spectrometry
FDA	Food and Drug Administration
FT-IR	Fourier Transform Infrared Spectroscopy
GC-MS/MS	Gas Chromatography-Mass Spectrometry
GDM	Gestational Diabetes Mellitus
GI	Gastrointestinal
GIT	Gastrointestinal tract
GLP-1	Glucagon-Like Peptide-1
^1H	Hydogen-1
HBA	Hydrogen Bond Acceptor
HbA1c	glycated haemoglobin
HBD	Hydrogen Bond Donor
HCl	Hydrochloric Acid
HCN	Hydrogen cyanide
HEK293T	Human embryonic kidney 293T cells
HIA	Human Intestinal Absorption
HNF1A	Hepatocyte nuclear factors 1-alpha
HNF1B	Hepatocyte nuclear factors 1-beta
H_2O_2	Hydrogen peroxide

HPLC	High-performance liquid chromatography
hr	hour
IAG	Intestinal α-Glucosidase
IC_{50}	Inhibition concentration 50%
j	J-coupling values
KC	Knoevenagel condensation
kg	Kilograms
KOH	Potassium hydroxide
LBVS	Ligand-Based Virtual Screening
MD	Molecular Dynamic
min	Minutes
mg	milligram
MHz	Mega Hertz
mL	millimolar
µM	Micro Molar
MM-GBSA	Molecular Mechanics, General Born Surface Area
MODY	Maturity-Onset Diabetes of the Young
mp	Melting point
MR	Molar Refractivity
MS	Mass spectrometry
MW	Molecular Weight
Na^+	Sodium Ions
NaOEt	Sodium Ethoxide
NaOH	Sodium Hydroxide
NDM	Neonatal Diabetes
NIDDM	Non-Insulin Dependent Diabetes Mellitus
NMR	Nuclear Magnetic Resonance
NO_2	Nitrogen dioxide
ns	Nano seconds
%	Percentage
PAA	Pancreatic α-amylase
PDA	Photodiode Array Detector
PDB	Protein Data Bank
P-NPG	P-nitrophenol glycol
PPAR-γ	Peroxisome proliferator-activated receptor gamma
PPAR-α	Peroxisome proliferator-activated receptor alpha
QP Log $P_{o/w}$	Predicated octanal/water partition coefficient
RB	Rotatable Bonds
RBF	Round-Bottomed Flask
RG	Radius of Gyration
RMSD	Root Mean Square Deviation
RMSF	Root-mean-square fluctuation
ROS	Reactive oxygen species
s	Singlet
SAR	Structure-activity Relationship
SDM	steepest descent method

SEM	Standard error of the mean
SGLT	Sodium-glucose cotransporter
SPC	simple point charge
STD	Standard
t	Triplet
TCA	Tricarboxylic acid cycle
T1DM	Type-1 diabetes Mellitus
T2DM	Type-2 diabetes Mellitus
TLC	Thin Layer Chromatograph
TMS	Tetramethyl silane
TPSA	Total Polar Surface Area
tRNA.	Transfer ribonucleic acid
TZD	Thiazolidinedione
UV	Ultraviolet
WHO	World Health Organisation

LIST OF APPENDICES

CHAPTER-1

INTRODUCTION

CHAPTER-1
INTRODUCTION

1. Introduction

Drug discovery is a hectic and time-consuming process.it takes almost 12-15 years to develop a new drug to get from the lab to clinical use (1). From approximately 10,000-20,000 compounds in preclinical trials and animal studies, only one may reach after clinical trials for human use (2). During the primary stages of drug development, large-scale and complex chemical libraries are examined to identify new hits like, bioactive compounds, ligands, and biomarkers (3). Drug development involves the discovery and optimization of therapeutic agents that have favorable pharmacokinetic, pharmacodynamic, and toxicological characteristics (4). The number of new drug molecules coming through the drug discovery and development pipeline started dwindling in the 1980s (5) Pharmaceutical industries in the post-genomic era have a goal to discover a small molecule of drug which finds the drug target and also shows their activity at a particular site where it is needed (6). There are many examples where small molecules have been used to isolate and identify new drug targets (7). Major steps involved in the present drug discovery process are (Figure 1),

1. Disease identification,
2. Target identification,
3. Lead molecule discovery and its optimization,
4. Preclinical and clinical trials.

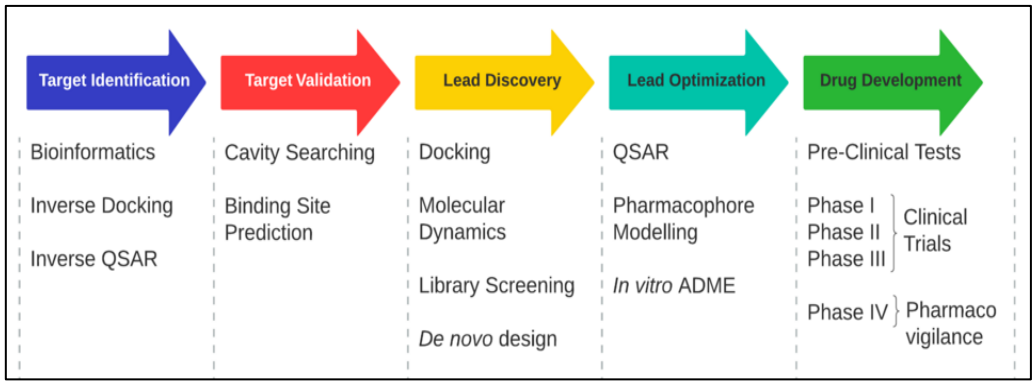

Figure 1: Steps involved in the present drug discovery process

In silico methods have obtained huge popularity and became a basic part of the academic and industrial research in drug discovery (8). In Fastly growing drug discovery process, there are new terms referred recently like bioinformatics, genomics, chemo informatics and Proteomics (9). Now-a-days many *in silico* methods and computer programme tools are representing the stability of interaction between graphical three-dimensional visualization in combination with different types of ligands and targets in order to locate the lead molecules from database (10). In order to develop smaller molecules of drug candidates against a disease, the researcher must have proper understanding over all the metabolic pathways occurring in the cell. Hence, the first and important duty in rational approach for a disease is to evaluate the disease metabolic pathways and choose the prospective target. Accordingly, recognition and progress of prospective ligands especially for a protein target shapes the initial objective in the course of drug discovery (11).

1.1. Computational approach in drug discovery

Based on the knowledge of the target, the novel drugs are invented in the process of drug design (12).The medication is commonly an organic molecule which initiates (or) prohibits the function of a protein which in turn increases the medicinal befit to the patient. In drug design, small compound and interaction of biomolecular target to it frequently relies on computer modelling techniques (13). It is referred as computer-aided drug design (CADD), computer-aided molecular design (CAMD), rational drug design or *in silico* studies. Computational methods have speed up the drug discovery and development process (14). Preferably the computational technique must be able to estimate affinity prior to a compound is synthesised (15). The basic aim is to estimate whether a known compound will bind to a target protein (or) not and if so, how much strongly. CADD utilize computational chemistry to enhance, discover (or) study drugs and equivalent biologically active compounds (16).

1.1.1. Drug likeness (or) rule of five

High-throughput screening (HTS) is an *in silico* method used to rapidly evaluate a large number of compounds for biological or biochemical activity against specific targets

(17). HTS efficiently generates vast amounts of data, enabling researchers to quickly identify hits or lead compounds (18). Lipinski's rule of five is a concept frequently used in drug discovery. This rule helps to predict if a biologically active molecule is likely to have the chemical and physical properties to be orally bioavailable (19). As per the rule of five a compound (applicable to small molecules only) is likely to exhibit drug-like properties should have hydrogen bond (Donors) less than or equal to 5, hydrogen bond (acceptors) below 10. Additionally, molecular weight (MW) less than or equal to 500 Daltons and partition coefficient (LogP) not more than 5. Drug-likeness is a crucial factor in early-stage drug discovery, as it aids in compound selection and optimization (20).

1.1.2. Molecular docking

Molecular docking, a strategic method for predicting ligand affinity towards receptor-ligand complexes in drug discovery, has been widely used in early drug development stages for understanding ligand-receptor binding interactions. This technique, first introduced in the late 1990s, is widely used in early drug development for virtual screening tools, providing valuable insights into ligand-receptor binding interactions (21). The docking process comprises three phases, with the first phase focusing on sampling, which involves generating ligand configurations and orientations relative to the target binding site. The docking score, estimated by ligand-receptor complex affinity, is used to screen the best compounds, while the binding energy is a scoring function. The most effective compounds are identified through their docking scores, at last the third phase, is a scoring function often indicating the binding energy of the complex (22). The molecular docking can provide accurate pose prediction or binding conformation of ligand in the active (binding) site of the target receptor (23). The complexity of the receptor-ligand interaction is significantly reduced. Accurate binding free energy used to rank the order of the docking poses. The docking study can aid in understanding the pharmacokinetic properties of compounds by determining the binding conformations and orientation of CYP-ligand complexes. Molecular docking also predicts the pharmacodynamic properties of the drug molecule poses of a drug molecule with its desirable or undesirable effect (24) (Figure 2).

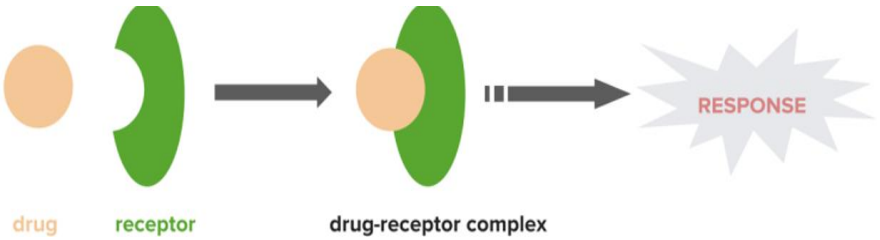

Figure 2: Drug and receptor interaction and predicting response

1.1.3. Prediction of pharmacokinetics (ADME)

Identifying absorption, distribution, metabolism, and excretion (ADME) properties and addressing potential issues early is essential for the successful progression of a drug candidate. Drug absorption in the gastrointestinal (GI) tract is a complex process influenced by the drug's physicochemical characteristics, physiological conditions and formulation design (25). For drugs targeting the central nervous system (CNS), effective permeability across the blood-brain barrier (BBB) is critical. Orally administered CNS drugs must cross the BBB to reach their targets and exert therapeutic effects. The cytochrome P450 (CYP) enzyme system plays a pivotal role in drug metabolism, significantly impacting a drug's initial bioavailability, safety, and pharmacological activity (26). Inhibition of CYP enzymes is undesirable, as it can lead to serious adverse effects through drug-drug interactions. Identifying the specific CYP isoforms involved in a drug's metabolism helps predict the primary metabolic pathway and guide safety assessments (27). Furthermore, understanding the site of metabolism on the molecular structure, where the metabolic reaction initiates, is important for optimizing metabolic stability and guiding chemical modifications during drug design (28).The drug discovery process for diabetes is a testament to scientific perseverance and innovation, continually pushing the boundaries to provide more effective, safer, and personalized treatments. From the initial understanding of insulin's role to the development of insulin sensitizers like TZDs, incretin mimetics, SGLT2 inhibitors, and novel insulins, each discovery has significantly improved the management of this widespread chronic disease. The ongoing pursuit aims to address unmet needs, such as preventing complications, achieving sustained remission, and ultimately, finding a cure, highlighting a dynamic field driven by a profound patient imperative

1.2. Diabetes Mellitus

In this modernized industrial world and changing lifestyles and lack of physical activity have led to various lifestyle disorders, like diabetes, which has become a noteworthy health issue in present century, affecting large portion of society (29). Diabetes mellitus (DM) is a metabolic disorder that impacts carbohydrate like glucose and lipid metabolism (30). It is characterized by high blood glucose levels over prolonged periods, accompanied by symptoms such as over thirst (Polydipsia), increased hunger (Polyphagia), recurrent urination (Polyuria) and weight loss (31). Untreated symptoms can lead to chronic complications, which are long-term issues that require immediate attention and treatment (32).

1.2.1 Prevalence of diabetes mellitus

World Health Organization (WHO) reports a steady increase in the number and prevalence of diabetes over the past few decades (33).

- Diabetes was responsible for 3.4 million deaths in 2024
- Type 2 diabetes (T2DM) prevalence has significantly increased in all income-level countries over the past three decades.
- Predicting almost 540 million people already live with diabetes and by 2045, it's estimated over 780 million people will have the condition.
- DM is a major cause of various health issues including blindness, kidney and heart failure, stroke, and limb amputation.
- Maintaining a healthy diet, regular physical activity, and avoiding tobacco use can potentially prevent or delay the onset of DM

According to the latest IDF diabetes atlas (2025), the prevalence of DM is (34):

- 11.1% (or 1 in 9) of the adult population (20-79 years) worldwide is living with diabetes.
- This translates to approximately 589 million adults globally.
- A significant concern is that over 4 in 10 (or 252 million) of these individuals are unaware they have the condition.

1.2.2 Classification

Diabetes mellitus is commonly classified under four conditions (Figure 3):

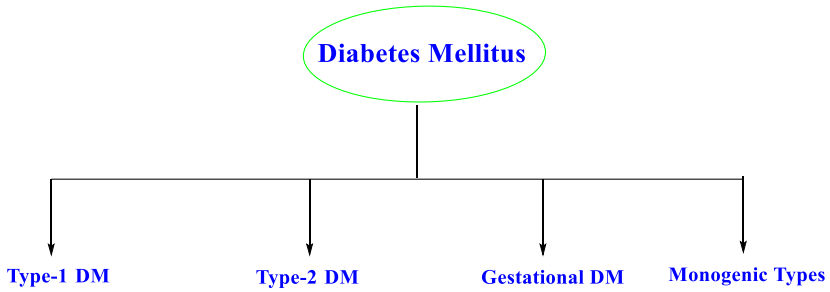

Figure 3: Common types of diabetes

Type-I diabetes mellitus (T1DM), also known as juvenile onset diabetes mellitus, is a global condition resulting from the destruction of pancreatic β (beta) cells helps in insulin synthesis in the human body (35). β cells destruction can be two types: Type IA (with detectable autoimmune antibodies) or type IB (idiopathic-no detectable antibodies in blood). Due to complete destruction of β cells, the patient needs to be dependent on exogenous insulin (36). Type 2 diabetes mellitus (T2DM), is also called non-insulin dependent diabetes mellitus (NIDDM) or maturity onset diabetes mellitus, impacts the human body's ability (β cells) to produce proinsulin or insulin (37). It accounts approximately 90% of all global diabetic cases and arise due to (a) It is primarily caused by obesity-related insulin resistance (impaired insulin response in target tissues) and inadequate insulin production (diminished insulin secretion by β-cells) (38); (b) The pancreatic β cells are responding to an increase in glucose levels in the blood (39); and (c) Excessive release of hyperglycemic hormones (40).Gestational diabetes mellitus (GDM), similar to T2DM, is a condition that typically develops in pregnant women. The prevalence of GDM affects 1-14% of all pregnancies, with an increasing threat for T2DM in the future. Regrettably, this condition leads to a substantial rise in the occurrence of macrosomia delivery.

Diabetes is treatable and preventable through lifestyle modifications. Pregnancy necessitates medical procurement, frequent blood glucose monitoring, insulin, and dietary changes, with occasional insulin and dietary changes required (41,42).The other type of diabetes is Monogenic type of diabetes caused by a single gene mutation, accounting for 1-5% of DM (43). It encompasses early-onset conditions like, maturity-

onset diabetes of the young (MODY), neonatal diabetes (NDM) and various syndromic diabetes, which are typically characterized by DM (44). Over 40 monogenic diabetes subtypes have been identified, with MODY, the most common form, likely underdiagnosed due to insufficient genetic testing due to mutations in *HNF1A*, *HNF4A*, and *HNF1B* genes (45,46).

1.2.3 Causes for diabetes mellitus

Beta-cell dysfunction involves different dysregulated processes like glucose sensing, insulin production, and exocytosis. Genetic defects in β-cells can affect the structural (β-cell mass) or functional (secretion of insulin) fate of the β-cell (47).

(a) Mutation in Insulin gene: Mutations in the insulin gene can cause hyper(pro)insulinemia, resulting from defective receptor binding and longer half-life. Replacement of amino acid is necessary for proinsulin processing results in hyper pro insulinemia (48).Three mutant insulin gene have been identified: (i) insulin Chicago (F49L or PheB25Leu); (ii) insulin Los Angeles (F48S or PheB24Ser), and (iii) insulin Wakayama (V92L or ValA3Leu) (49).Four mutant proinsulin gene have been identified: (i) proinsulin Providence (H34D); (ii) proinsulin Tokyo (R89H); (iii) proinsulin Kyoto (R89L); and (iv) proinsulin Oxford (R89P) (50).

(b) Mutations in mitochondrial DNA: it is a type of diabetes that is inherited from the mother due to a mutation in mitochondrial tRNA. This mutation leads to a β-cell defect, causing diabetes due to reduced insulin secretion, and is frequently linked to neurosensory deafness (51).

(c) Mutations of Insulin receptor gene (INSR): INSR can cause wide range of conditions, characterized by insulin resistance, like type A insulin resistance syndrome, Leprechaunism and Rabson-Mendenhall syndrome (52).

1.2.4 Signs and symptoms of diabetes mellitus

Diabetes symptoms often go unnoticed due to patients' inability to recognize warning signs or attribution to other causes. The disease may be diagnosed years after onset, causing complications, making it crucial to be aware of risk factors (53). Diabetes is

likely to affect various systems including the central, respiratory, ophthalmic, gastric, systemic, and urinary system (54) (Figure 4).

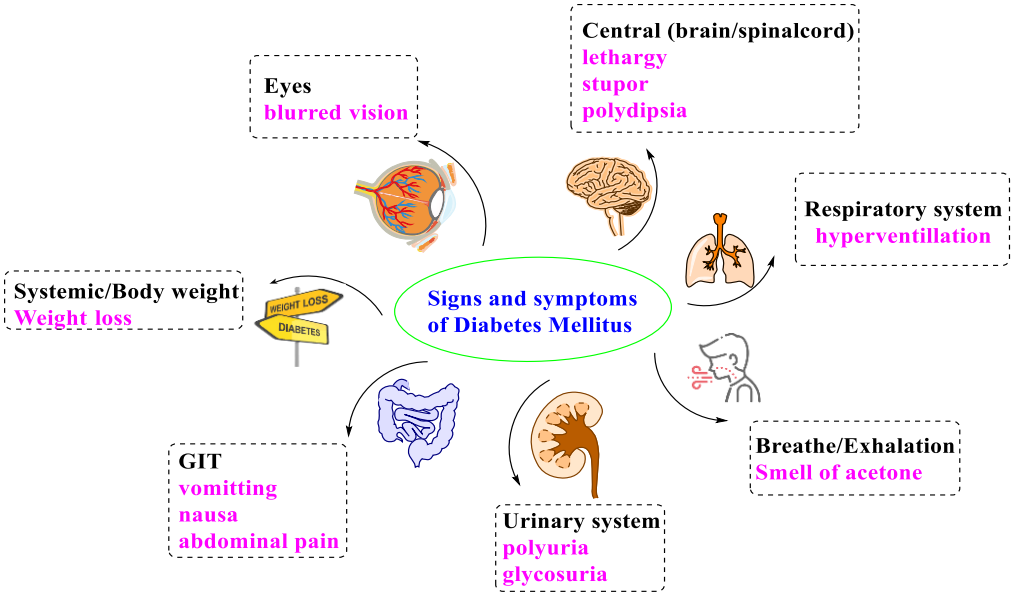

Figure 4: Signs and symptoms of diabetes

Prolonged high blood glucose levels can cause glucose absorption in the eye's lens, resulting in a change in its shape (55). Diabetic dermadromes are a group of skin rashes that can occur in individuals with diabetes (56). Moderate hypoglycemia, often mistaken for drunkenness, is characterized by rapid breathing, sweating, cold, and pale skin, but is not definitive (57). Mild to moderate cases can be self-treated by consuming or drinking low-sugar foods or beverages (58). Severe cases can cause unconsciousness and require treatment with intravenous glucose or injection with glucagon (59). People with T2DM may also experience diabetic ketoacidosis, a metabolic disturbance characterized by nausea, vomiting, abdominal pain, acetone smell, deep breathing (Kussumaul breathing), and in severe cases, decreased consciousness (60,61).

1.2.5 Complications of diabetes mellitus

Untreated diabetes can lead to acute complications, which can progress into chronic or serious issues over time (Figure 5**)**

(a) Acute complications

- **Diabetic ketoacidosis:** Ketoacidosis, a common symptom in T1DM patients and insulin dependent diabetics, is less common in T2DM. Precipitating factors include infection, stroke, stress, and pancreatitis (62)
- **Nonketotic hyperosmolar coma:** Nonketotic hyperosmolar coma, primarily affecting elderly T2DM patients, is influenced by factors like ketoacidosis, particularly dehydration, and its cause remains uncertain (63).

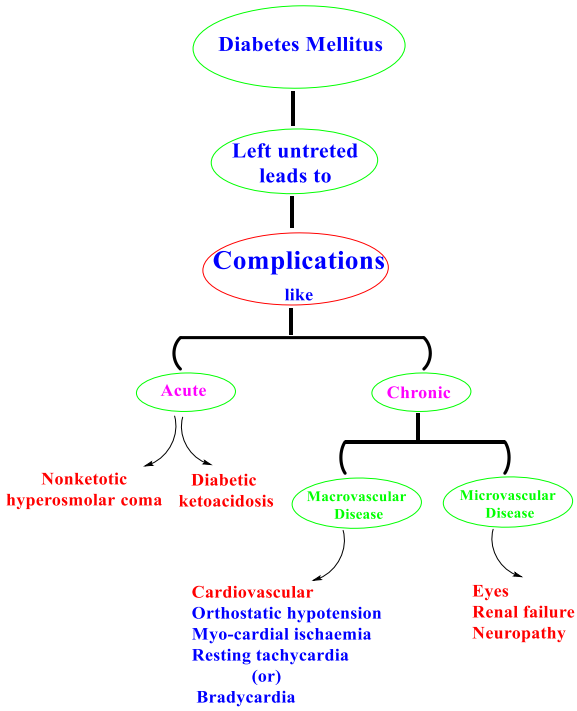

Figure 5: Major late-stage complications of diabetes

(b) Chronic complications

- **Macrovascular diseases:** Diabetes increases the risk of atherosclerotic vascular disease, orthostatic hypotension, myocardial ischaemia, resting tachycardia (or) bradycardia with factors like hyperglycemia, lipid abnormalities and increased proinflammatory and prothrombotic factors contributing to the development of macrovascular disease (64,65).
- **Microvascular diseases:** diabetic condition will damage the body's microvascular circulation, leading to tissue damage and organ damage, resulting in retinal damage, chronic kidney failure and neuropathy (66).

The detail association of diabetes complications with different body parts or organs were listed in the Table 1.1

Table 1.1: Classification of diabetic complications

S.no	Types of complication	Complications	References
1.	Cardiovascular Complications	Atherosclerosis, Peripheral Artery Disease, Stroke, Cardiomyopathy, Myocardial infarction, Coronary Artery Disease, Dyslipidemia	(67)
2.	Kidney Complications	End-Stage Renal Disease, Hypertension, Diabetic Nephropathy, Proteinuria	(68)
3.	Eye Complications	Macular oedema, Blindness, Diabetic Retinopathy (Retinal capillary microaneurysms [background retinopathy], Neovascularisation [proliferative retinopathy], non-proliferative retinopathy, Cataracts, Glaucoma	(69)
4.	Nerve Complications (Neuropathy)	Proximal neuropathy, Focal Neuropathy, Autonomic Neuropathy, Symmetric polyneuropathy, Radiculopathy, Cranial neuropathy, Mononeuropathy, Peripheral neuropathy	(70)
5.	Foot Complications	Charcot Foot, Diabetic Foot Ulcers, Gangrene, Amputations	(71)
6.	Skin Complications	Xanthelasma, Necrobiosis Lipoidica, Bullosis diabeticorum, Diabetic Dermopathy, Granuloma annulare, Acanthosis nigricans, Carotenoderma	(72)
7.	Sexual and Reproductive Complications	Gestational Diabetes, Erectile Dysfunction, Vaginal and Urinary Tract Infections (balanitis, vaginitis, male accessory gland infection etc)	(73)

8.	Liver Complications	Non-alcoholic fatty liver disease (NAFLD) and Non-alcoholic steatohepatitis (NASH), cirrhosis, chronic liver diasease, fibrosis	(74)
9.	Cancer Complications	Pancreatic Cancer, Hepatocellular carcinoma, Endometrial Cancer, colorectal Cancer, Breast Cancer, Ovarian Cancer, Prostate Cancer	(75)
10.	Bone Complications	Osteoporosis, Osteomyelitis	(76)
11.	Metabolic and Hormonal Complications	Hypoglycaemia, Hyperosmolar, Hyperglycaemic state (HHS), Polycystic Ovarian Syndrome, Diabetic Ketoacidosis	(77)
12.	Infections	Cellulitis, oral and vaginal candidiasis, pyelonephritis, emphysematous cholecystitis, malignant otitis externa, rhinocerebral mucormycosis	(78)
13.	Dental Complications	Gingivitis, Periodontitis	(79)
14.	Mental Health	Alzheimer's disease, Depression, Dementia	(75)
15.	Musculoskeletal disorders	Muscle infarction, Carpal tunnel syndrome, Dupuytren contracture, adhesive capsulitis, sclerodactyly etc	(80)
16.	Gastrointestinal complications	Gastroparesis, GERD (Gastroesophageal reflux disease), Diabetic enteropathy	(74)

1.2.6 Treatment of DM

1.2.6.1 Lifestyle change

The pharmacological approach to diabetes treatment is only partially effective in long-term management, requiring significant lifestyle modifications and pharmacological interventions for optimal results (81).These include modifying physical activity, diet adjustment, stress management and enhancing sleep patterns.

- **Physical activity:** Physical activity including walking, gardening, and household chores, is linked to manage glycemic levels in T2DM patients, particularly walking, which offers significant glycemic control with minimal physical burden (82). In addition, Regular aerobic exercise improves HbA1c levels in diabetes patients through increased mitochondrial densities, improved insulin sensitivity, improved blood vessel compliance, and enhanced lung functions with enhanced cardiac output (83).
- **Diet adjustment:** Insulin resistance and subsequent occurrence of T2DM are closely linked with high intake of sugars, fried food, and red meat (84) and also, vegetables having high content of antioxidants, fibre, and other nutrients (85). Diabetic patients should limit refined sugar intake and replace saturated fats and cholesterol with polysaturated fats (86). In addition, Changes in eating patterns, like dividing meals into smaller portions, can prevent postprandial peaks in blood glucose levels (87). Adherence to a controlled diet and regular physical activity is linked to a lower diabetes incidence, and the use of nutritional therapy is also recommended (88).
- **Stress management:** Excess stress levels are linked to poor treatment adherence and glycemic control in diabetic patients (89). Chronic stress exposure causes dysregulated glucose metabolism and low-grade inflammation. Moreover, psychological stress and constant exposure to stress will worsen the condition to treat the diabetes further (90). Apparently, treatment strategies, including stress management interventions, are a promising approach in effectively preventing or controlling the incidence diabetes (91).

- **Enhancing sleep pattern**: Sleep is a lifestyle behaviour that significantly impacts metabolic health and energy status in the diabetic patients (92). Studies states that short sleep and imparts the insulin resistance and HbA1c levels in T2DM patients.so, making optimizing sleeping patterns crucial for diabetes control (93).

1.2.6.2 Weight management

Around 60% of people with T1DM and 85% of people with T2DM are carrying extra weight or are living with obesity (94). Sears *et.al.* study states excess weight leads to increased adipose tissue mass and secretion of adipokines, which can be dysregulated, resulting in the development of T2DM.Excess body weight is associated with the risk of cardiometabolic complications, which are major causes of morbidity and mortality in T2DM (95). The potential to prevent or delay the onset of T2DM in high-risk individuals through lifestyle interventions such as diet modification, weight reduction and increased physical activity has been established in several clinical trials (96).

1.2.6.3 Hormonal therapy

Insulin is still considered the most appropriate pharmacologic agent for effectively controlling and maintaining glycemic control (97). Insulin is the oldest and most effective hormonal treatment currently available for all types of DM. Insulin is a crucial component for T1DM, and many patients with T2DM will eventually require insulin due to declining beta-cell function (98). New hormonal treatments for T2DM include incretin mimetic, including GLP-1 and amylin analogues. Amylin-like medications, like pramlintide, mimic the action of amylin, a pancreatic hormone, regulating blood glucose levels after eating by suppressing glucagon secretion (99).

1.2.6.4 Pharmacological treatment of T2DM

Pharmacological therapy is recommended for patients who cannot alter their lifestyle through a hypocaloric diet, increased physical activity, weight loss, or who continue to have high glycemia (100). Diabetes medications, apart from insulin, are often taken orally and are referred to as oral hypoglycaemic or antihyperglycemic drugs (Table 1.2).

They are categorized based on various factors including age, health condition, and type of diabetes. Typically, more effective for T2DM, these drugs are often combined for enhanced efficacy, with the FDA approving 23 distinct combinations as of 2020 (101). In 2019, the first oral triple combination (dapagliflozin, saxagliptin, and metformin) was approved, followed by a second combination (linagliptin, empagliflozin, and metformin) in 2020 (102).

Table 1.2: FDA approved antidiabetic agents to treat diabetes (103)

S. No.	Antidiabetic agents	Drugs/ example/structures (Figure 6 and 7)
1	Insulin and its analogs	Regular Insulin, NPH Insulin, insulin Glulisine, Lispro, Aspart, Detemir and Glargine.
2	Sulfonylureas	First generation: Tolbutamide, tolazamide and chlorpropamide. Second generation: Glimepiride, Glipizide, Gliclazide and Glibenclamide.
3	Biguanides	Metformin and Phenformin
4	PAA and IAG inhibitors	Acarbose, Voglibose and Miglitol
5	Meglitinide analogues	Nateglinide and Repaglinide
6	TZDs (or) Glitazones	Rosiglitazone and Pioglitazone
7	DPP4 Inhibitors (or) Phenylalanine Analogues	Sitagliptine, Saxagliptine, Linagliptine and Alogliptine
8	Bile acid Sequestrant	Colesevelam, Colestipol and Cholestyramine
9	Dopamine receptor agonist	Bromocriptine, Cabergoline, Pergolide and Lisuride
10	SGLT2 Inhibitors	Dapagliflozin, Ipragliflozin, Empagliflozin and Canagliflozin
11	GLP-1 analogs	Dulaglutide and semaglutide
12	Amylinomimetics	Pramlintide acetate

DPP4: Dipeptidyl peptidase-4; GLP-1: Glucagon like peptide-1; IAG: Intestinal α-glucosidase; PAA: Pancreatic α-amylase; SGLT2: Sodium-glucose transport protein 2; TZDs: Thiazolidinediones.

Insulin sensitizing agents (Biguanides):

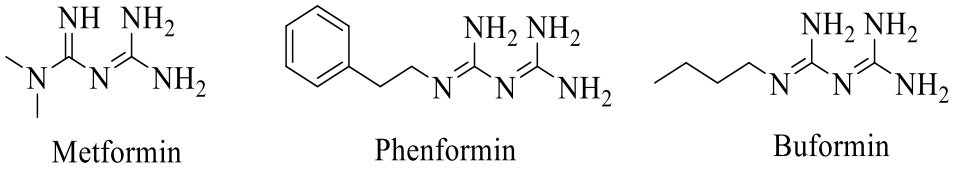

Metformin Phenformin Buformin

Sulfonylureas (Secretagogues):

First generation

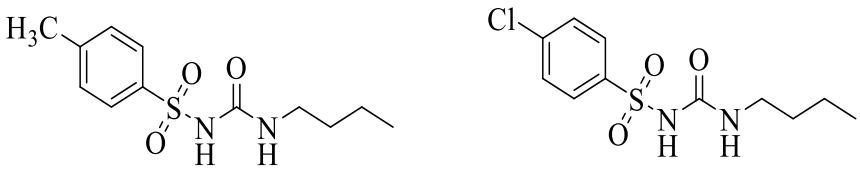

Tolbutamide Chlorpropamide

Second generation

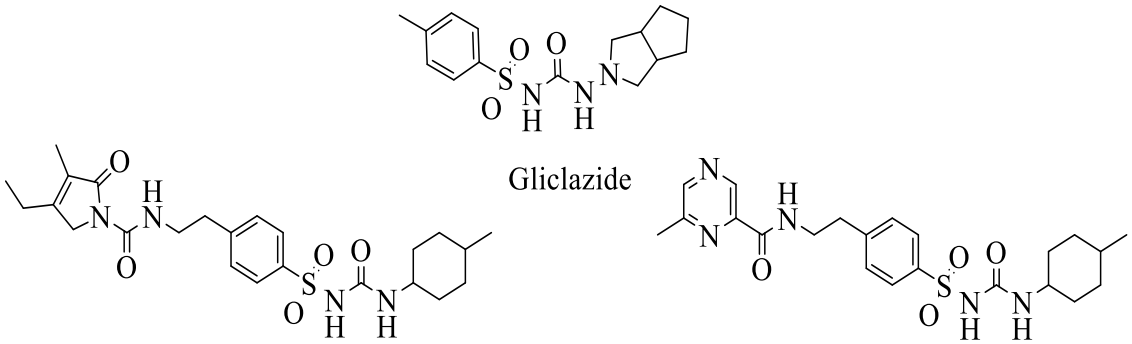

Gliclazide

Glimepiride Glipizide

Figure 6: Structure of biguanide and sulfonylureas agents to treat T2DM

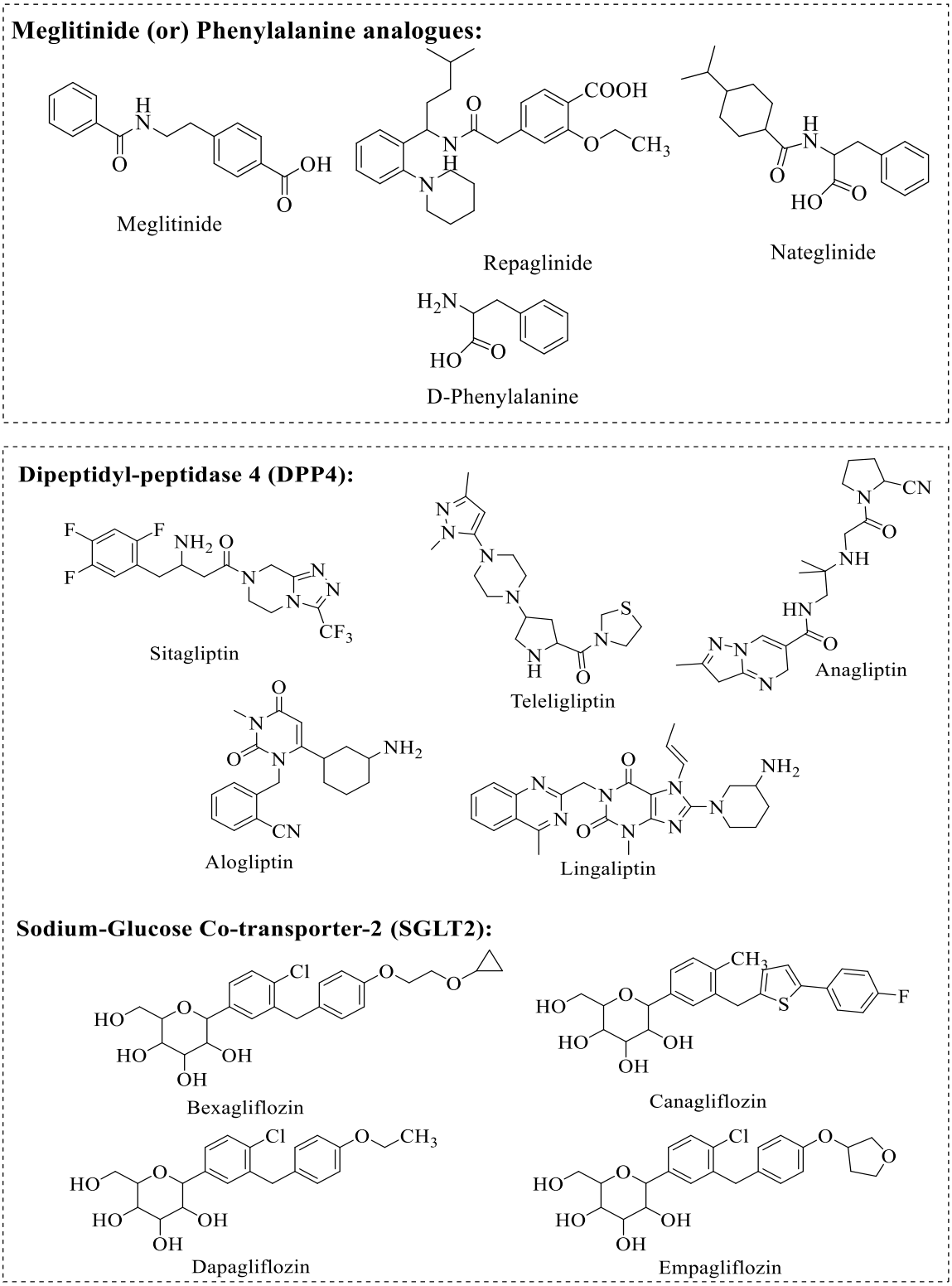

Figure 7: Structures of meglitinide, DPP-4 and SGLT2 drugs to treat T2DM

1.3 Thiazole

In 1987 Hantzch and Weber was first, to prepare thiazole in synthetic method and its structure was confirmed by the Prop in the year 1889 (104). Thiazole is a five-membered heterocyclic compound containing both sulphur (S) and nitrogen (N) atoms (Molecular formula: C_3H_3NS) as structural framework. Thiazoles and its derivatives play a significant role in both organic and medicinal chemistry due to their interesting chemical properties and biological activities (105). The thiazole ring system is aromatic, which means that the electrons in the conjugated π-system are delocalized over the ring, contributing to its stability and making it less reactive than non-aromatic analogues (106). Thiazole exhibits a number of distinct chemical properties due to the presence electronegative atoms like sulphur and nitrogen in its ring structure which affects the electronic distribution, making the compound relatively reactive. The nitrogen atom in thiazole can donate electron density, making the molecule relatively basic and capable of forming salts with acids. Thiazoles can participate in electrophilic substitution reactions where the sulphur or nitrogen atoms serve as sites for electrophilic attack (107).

Thiazole and its derivatives have always annoyed the interest of medicinal chemists due to their various pharmacological properties were listed in the Figure 8. Thiazole, as a single nucleus or fused ring, is a key component of natural penicillin-like drugs known as antibiotics (108). Additionally, vitamin B1 (thiamine) chemically thiazole-ring containing water-soluble vitamin, helps in the facilitating the formation of acetylcholine, supports in working of the neurological system in the human body (109). Pramipexole (Dopamine analogue) is dopamine D2 agonist, which contains 2-amino-thiazole is linked with cyclohexane ring are effective drug in treating Parkinson's disease (110). Amiphenazole is a diamino thiazole, employed in treating barbiturate or opiate poisoning (111). Ritonavir is a thiazole ring containing antiretroviral drug, effective towards control HIV infection by suppressing the protease enzyme (112). Nizatidine and Famotidine is a histamine-2 (H_2) receptor blocker, used to control peptic ulcers by reducing the acid (HCl) secretion in the stomach (113). Abafungin is a sterol 24-C-methyltransderase inhibitor, containing thiazole based tetrahydro pyrimidine ring used in the treatment of fungal infections (114).

Thiabendazole, thiazole based benzimidazole ring, inhibits the helminth-specific enzyme, fumarate reductase in the tricarboxylic acid cycle (TCA cycle) leads to helminth's death by reducing the adenosine triphosphate (ATP) production (115). Voreloxin, chemically a thiazole-based quinolone group, is presently used in treating various neoplasms, that intercalates DNA and inhibits Topoisomerase II (116). The substitution of the thiazole ring at different positions resulted in the creation of novel compounds with diverse biological activities (117).

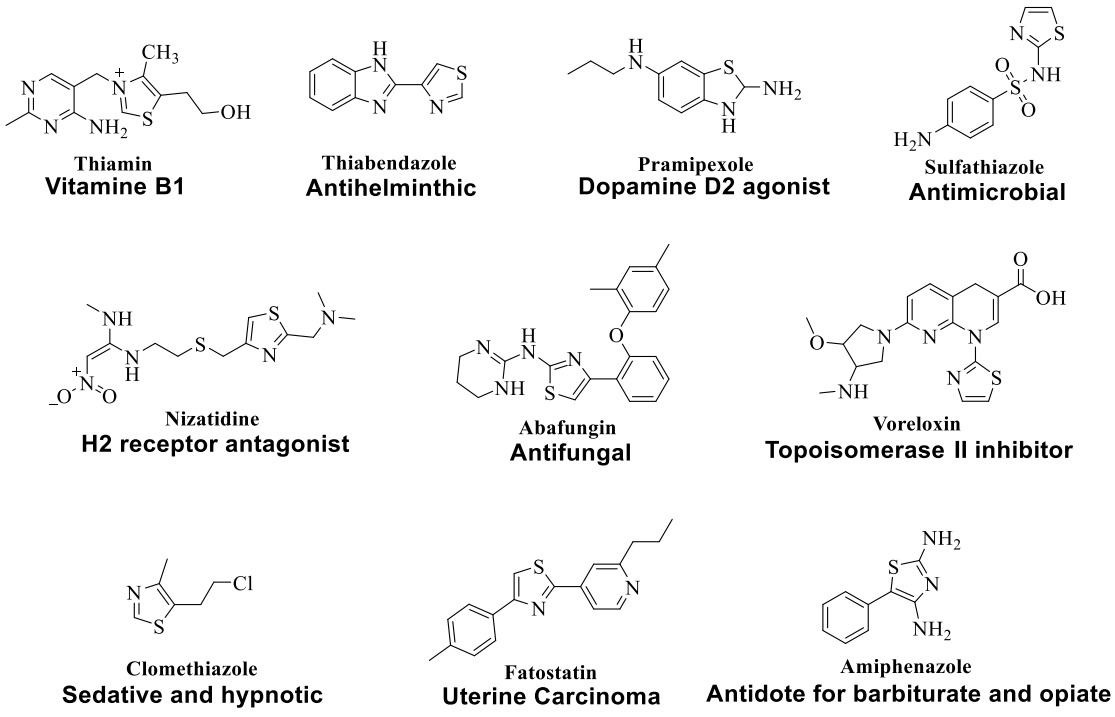

Figure 8: Structure of thiazole-containing drugs

1.3.1 Thiazole as antidiabetic agents

Thiazole derivatives exhibit significant potential as antidiabetic agents due to their diverse mechanisms of action, including the inhibition of α-glucosidase, enhancement of insulin sensitivity, modulation of glucose transporter activity and antioxidant activity. In the recent past various thiazole-based benzamide, coumarin and imidazopyridine derivatives (Figure 9) have been identified as potent antidiabetic agents

In 2023, Fan and his co-workers synthesized thiazole-benzamide derivatives and tested their antidiabetic activity against α-glucosidase enzyme. The compound **1**

exhibited potent oral hypoglycemic activity against α-glucosidase enzyme (118). Recently, compound **2** as reported by Ichale *et al*, has shown antidiabetic activity by inhibiting the enzyme α-glucosidase. In 2023, Hussain and his co-workers developed some Imidazopyridine-based thiazole derivatives, among the all compounds, **3** shown strong inhibitory activity against enzyme α-glucosidase (119).Ullah and co-workers synthesized some thiazole bearing biphenyl substituted moieties. These derivatives showed antidiabetic activity against α- amylase and α-glucosidase. The compounds **4** shown strong inhibitory activity against on both enzymes (120).

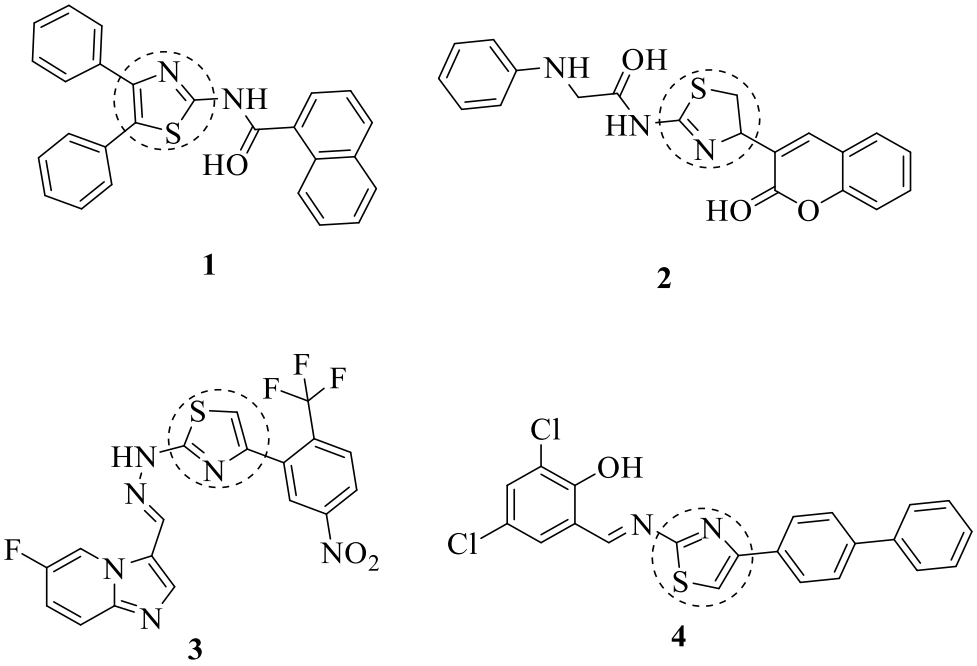

Figure 9: Thiazole ring containing antidiabetic agents

Thiazolidinedione (TZD) core is a specific structural motif that is directly derived from the broader family of thiazole-containing compounds. While the thiazole ring itself is aromatic, the thiazolidinedione ring is saturated and contains two critical carbonyl groups. It is this particular thiazolidinedione structure that imbues the compounds belonging to this class with their distinctive pharmacological properties, most notably their role as insulin sensitizers and glucose lowering agent during the treatment of T2DM

1.3.2. Thiazolidinedione as antidiabetic agents (Glitazones)

Thiazolidinedione (TZD) ring containing drugs also called Glitazones, are the new class of insulin sensitizing agents approved by US FDA in late 1990s as anti-diabetic agents. Thiazolidinedione is a globally recognized anti-diabetic agent known for its effective anti-hyperglycemic properties without causing hypoglycaemia (121). It is a five-membered heterocyclic with a thiazole or thiazolidine skeleton, consisting of one sulphur (S), one nitrogen (N), and two carbonyl (C=O) groups with the molecular formula $C_3H_3NO_2S$ (Figure 10).

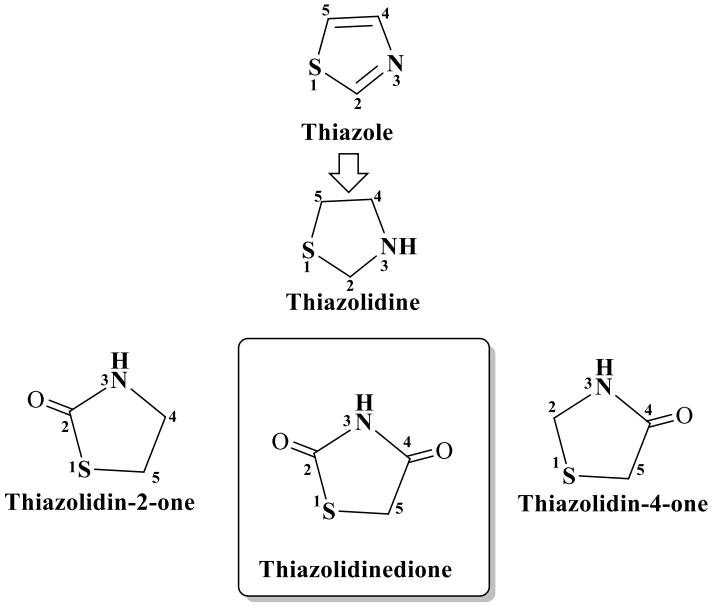

Figure 10: Structures of thiazole and its derivatives

Thiazolidinedione and their derivatives are crucial bioactive scaffolds in medicinal chemistry, with various biological activities including antibacterial (122), antiviral (123), analgesic (124), anticancer (125), antitubercular (126), and anticonvulsant (127) properties. Their versatility and use in clinically used drugs underscore their importance in medicinal chemistry (128). The Journey of thiazolidinedione started with the appearance of first representative drug i.e. ciglitazone, which was discovered in 1982, soon followed by the discovery of troglitazone, englitazone, pioglitazone, rosiglitazone etc. which are mentioned in figure 11. Extensive research is still under pipeline to improve their potential and to lessen their adverse effects (129).

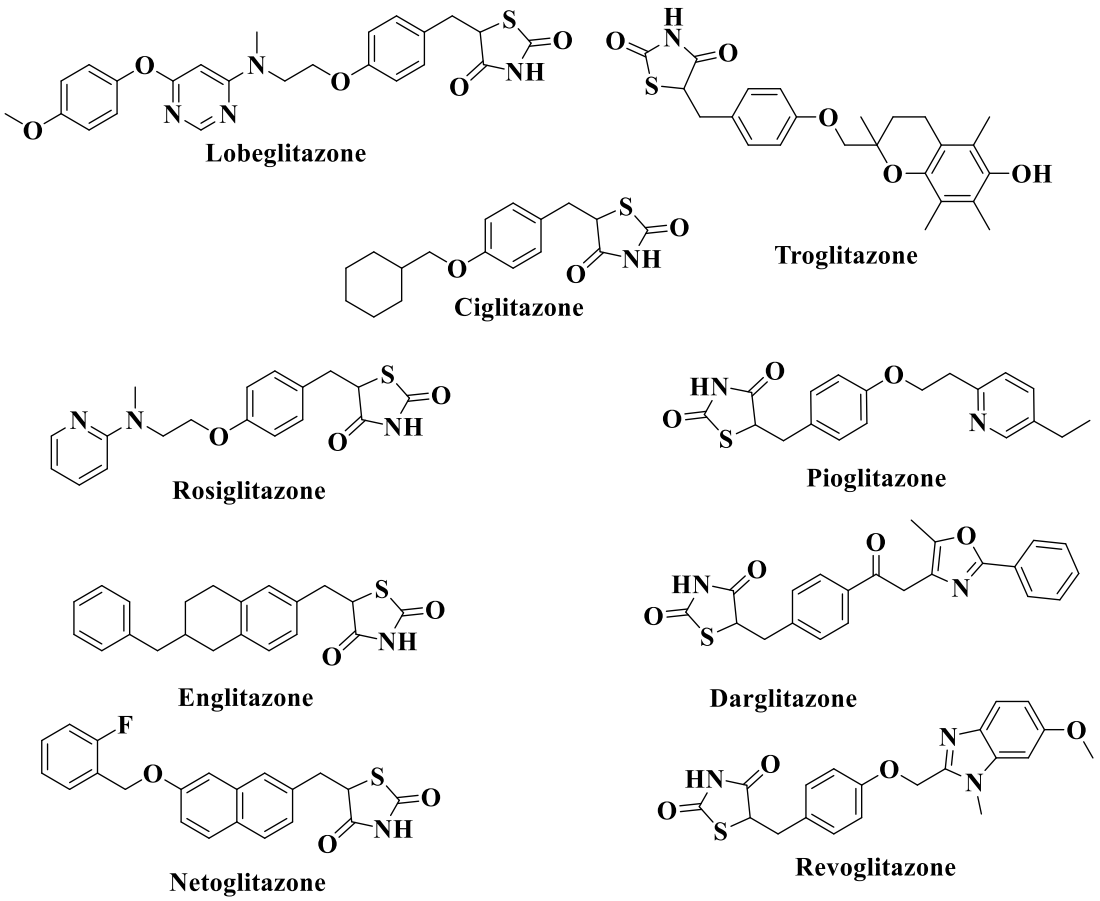

Figure 11: Thiazolidinedione ring containing antidiabetic drugs (glitazones)

1.3.3. Synthetic methods for Thiazolidinediones core

In 1923 the Sten kallenberg, first reported synthetic methodology for generating the thiazolidinedione core ring. During Kallenberg condensation, it is synthesized by reacting compound **5** (carbonyl sulphide) with ammonia leads to the formation of compound **6** (thiocarbamate) in the presence of potassium hydroxide (KOH). Later, thiocarbamate is cyclised in acidic conditions, in the presence of compound **7** called 2-chloroacetic acid (α-halogenated carboxylic acid) to yield the desired compound called thiazolidinedione core ring (130). The reaction was shown in scheme 1.1 in figure 12.

Using more recent methodology, thiazolidinedione was synthesized from the simple compound **8** (thiourea). Heating of thiourea with in presence of 2-chloroacetic acid (**7**), water as solvent for 12h at 100-110 ^{o}C, later Liberman *et al.* proposed the reaction mechanism (Scheme 1.2 in Figure 12) (131).

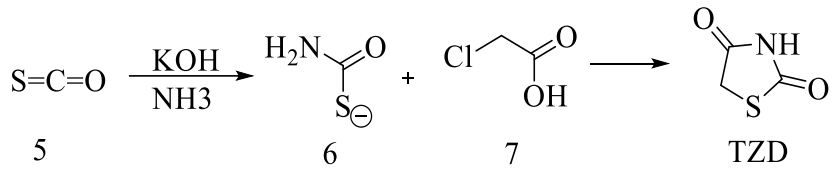

Scheme 1.1: Synthesis of TZD using carbonyl sulphide and 2-chloroacetic acid

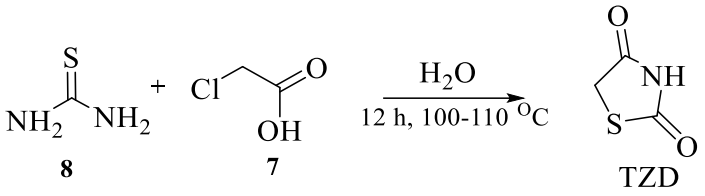

Scheme 1.2: Synthesis of TZD using ethyl chloroacetate and thiourea

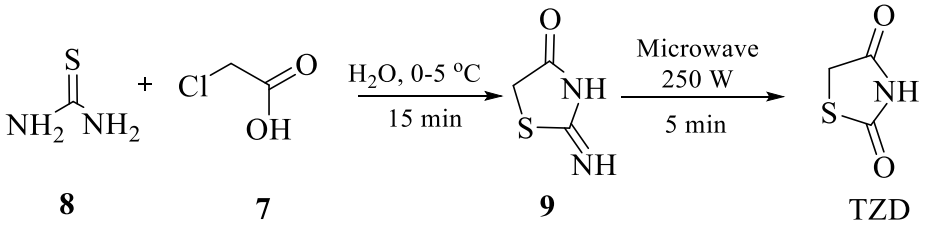

Scheme 1.3: Microwave-induced synthesis of TZD.

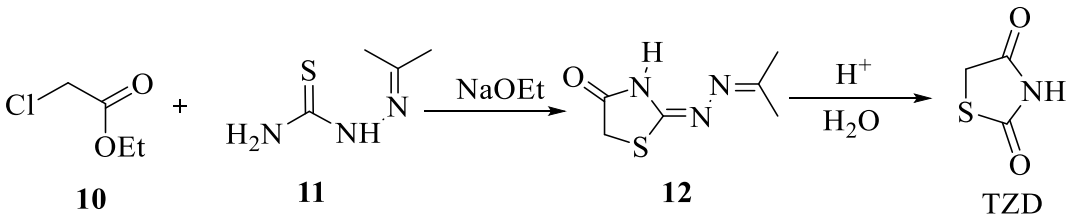

Scheme 1.4: Synthesis of TZD using ethyl chloroacetate and thiosemicarbazone

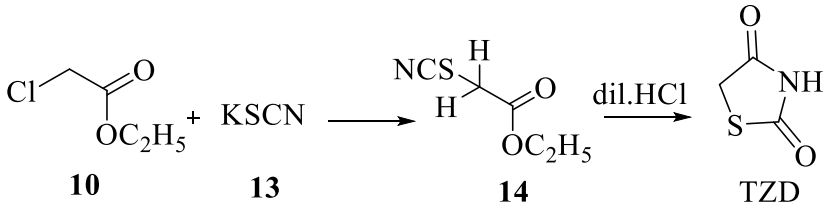

Scheme 1.5: Synthesis of TZD using ethyl chloroacetate and potassium thiocyanate.

Figure 12: Synthetic methods for thiazolidinedione core

Kumar and his research team assessed the use of microwave-induced synthesis to produce a thiazolidinedione core ring, which can withstand prolonged heating at high temperatures (100-110 °C). In this process, the two-step reaction can be completed in

less than 0.5 h. Both compounds, thiourea (**8**) and 2-chloroacetic acid (**7**) were dissolve in water and stirred under ice-cold condition for 15 min leads to the formation of intermediate compound **9** (2-imino-4-thiazolidinone), and it is further subjected to microwave initiation at 250 W for a period of 5 min. The desired thiazolidinedione core was successfully isolated after cooling and vacuum filtration, yielding 82-83% without the need for further purification (Scheme 1.3 in Figure 12) (132).

The fourth common synthetic protocol involves reacting compound **10** (ethyl chloroacetate) with compound **11** (thiosemicarbazone), in the presence of sodium ethoxide (NaOEt), generates the intermediate **12** (2-hydrazino-4-thiazolidinone). Further refluxed in dill HCl to give the thiazolidinedione core ring (Scheme 1.4 in Figure 12) (133).Recently proposed method to prepare thiazolidinedione ring is using compound **10** reacting with compound **12** (potassium thiocyanate) in acidic condition covering intermediate compound **14**. However, caution is required due to the release of toxic HCN gas as a by-product (134).The novel methodologies have been stated in figure 12, are most widely used synthetic pathway to produce the thiazolidinedione ring. Notably, reaction using hydrochloric acid and heating for 7-8 hours resulted in the highest yield of thiazolidinedione about 94% (135,136).

1.3.4. Thiazolidinedione derivatives

Thiazolidinediones (so called Glitazones) are a class of drugs used primarily in the treatment of T2DM, which elicit the activation peroxisome proliferator-activated receptor gamma (PPAR-γ) (137) in adipose cells (lipid metabolism and adipogenesis). Numerous alterations on the core thiazolidinedione frame have the ability to change chemical characteristics, the generation of novel molecules and potentially bioactive candidates. The most commonly used protocols for structural modification of the thiazolidinedione core involve two major sites i.e. Substitutions at the nitrogen position N-3 and C-5 position (methylene group). The carbonyl group at C-4 is highly unreactive (138). At first, the main methodology used to introduce substituents onto the N-3 atom involves deprotonation with an appropriate base, followed by substitution with alkyl or benzyl halides (139).Thiazolidinedione framework can be further functionalized by substituting at the methylene C-5 position. The most commonly used method is

Knoevenagel condensation (KC), which involves adding an aldehyde to an activated methylene unit and dehydrating it to produce a new olefin (arylidene derivatives) (140).

1.3.4.1. *N*-3 substituted thiazolidinedione derivatives

There are numerous synthetic methodologies are available for the synthesis of N-substituted thiazolidinedione derivatives. The main method for introducing substituents onto the nitrogen atom is deprotonation with a suitable base, followed by substitution with alkyl or benzyl halides**.**

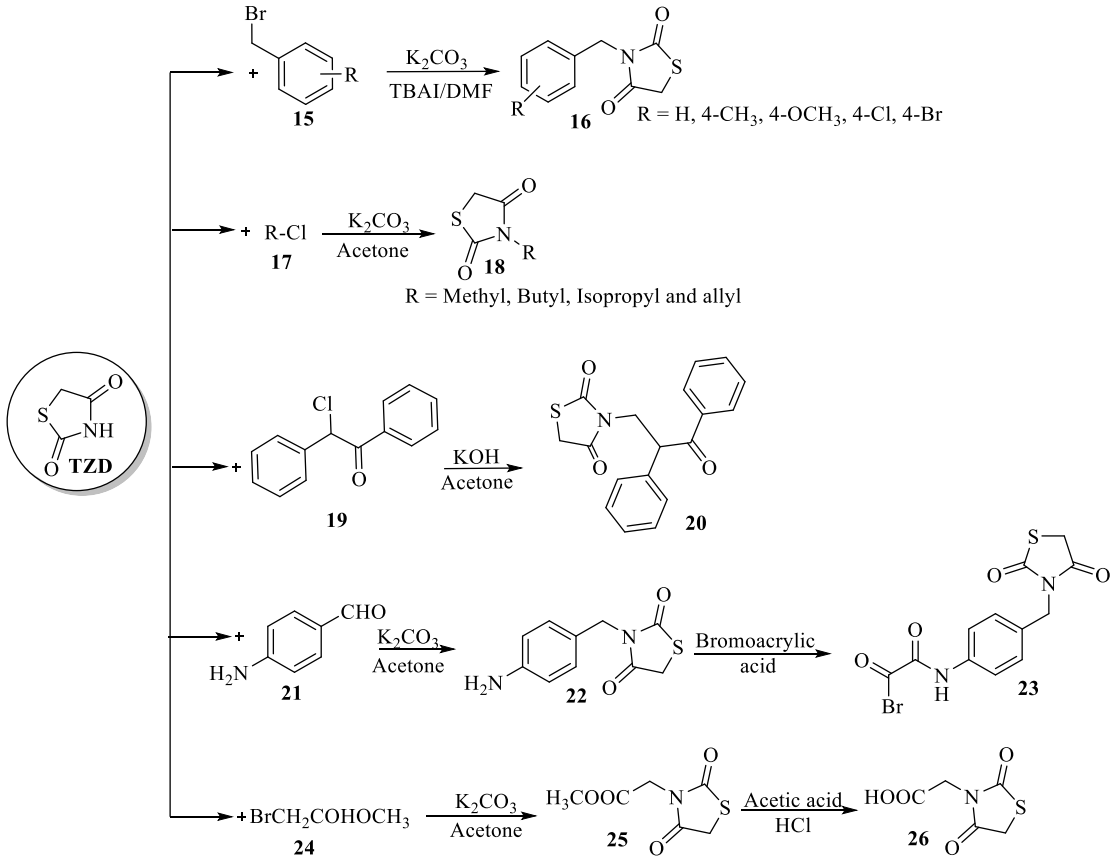

Figure 13: Reported *N*-substituted thiazolidinediones (141,142)

Most commonly used bases, such as potassium carbonate (143), tetrabutylammonium iodide (144), Triethylamine (145) and also sodium hydride (146) using dichloromethane (DCM), dimethyl formamide (DMF) and acetone solvent

source. Figure 13 lists the various derivatives that can be produced by substituting free –NH of the TZD core.

1.3.4.2. Substitution at methylene carbon or Knoevenagel condensation

The thiazolidinedione framework can be further functionalized by substituting at the methylene carbon (C-5) so, called Arylidene derivatives. Knoevenagel condensation (KC) is a widely used method for synthesizing thiazolidinedione core arylidene derivatives by substituting methylene with aldehydes or ketones, followed by a dehydration reaction to generate a new olefine. It is widely employed to achieve the synthesis of 5-arylidene derivatives (REF). During knoevenagel condensation on thiazolidinedione used varity of aldehydes and reactions condition, mainly like:

(i) ethanol or methanol as a solvent with few drops of piperidine (147) and Pyrrolidine under reflux (148)

(ii) treating the mixture of thiazolidinedione and aldehyde in glacial acetic acid in the presence of sodium acetate.

The various thiazolidinedione derivatives reported by the knoevenagel reaction condensation on free carbon (-CH_2) on TZD core were listed in the figure 14. Recently, observed that various type of ketones has been condensed with TZD, in the presence of different reagent like piperidinium acetate or ammonium acetate in toluene or ethyl acetate solvents (149). Moreover, eco-friendly reactions for KC have been explored recent days, such as L-tyrosine in water (150), β-alanine in acid (acetic acid) (151), and baker's yeast in alcohol (ethanol) (152). And also, unconventional technics, like microwave and ultra-sound assisted synthesis have been used to improve yield and enhance the rate of reaction (132).

In summary, the synthesis of thiazolidinediones primarily revolves around the cyclization of precursors to form the core five-membered ring, followed by diverse derivatization strategies at the N-3 and C-5 positions to create a wide array of pharmacologically active compounds.

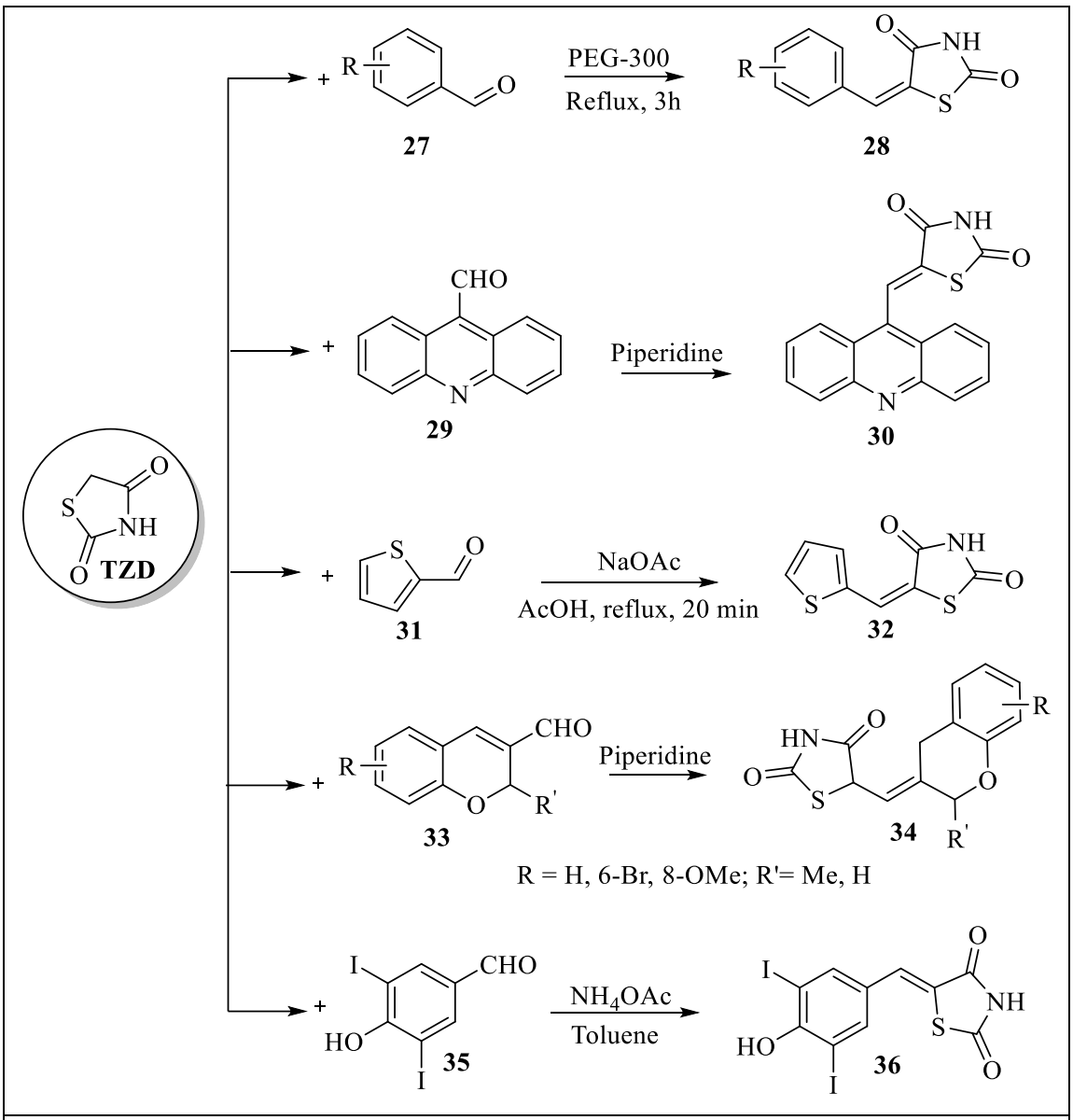

Figure 14: Reported methylene substituted thiazolidinediones (153,154)

1.4. Role of enzymes in glucose management

Pancreatic α-amylase (PAA) and intestinal α-glucosidase (IAG) are both key enzymes involved carbohydrate metabolism and in regulating blood glucose levels (155). Pancreatic α-amylase is an enzyme secreted by the pancreas into the small intestine, which initiates the breakdown of dietary starches into smaller carbohydrate molecules, such as maltose (disaccharide) and oligosaccharides (156). PAA hydrolyses (break down) α-1,4-glycosidic bonds present in starch and glycogen (link glucose molecules) were broken down into maltose and simple sugars (156).

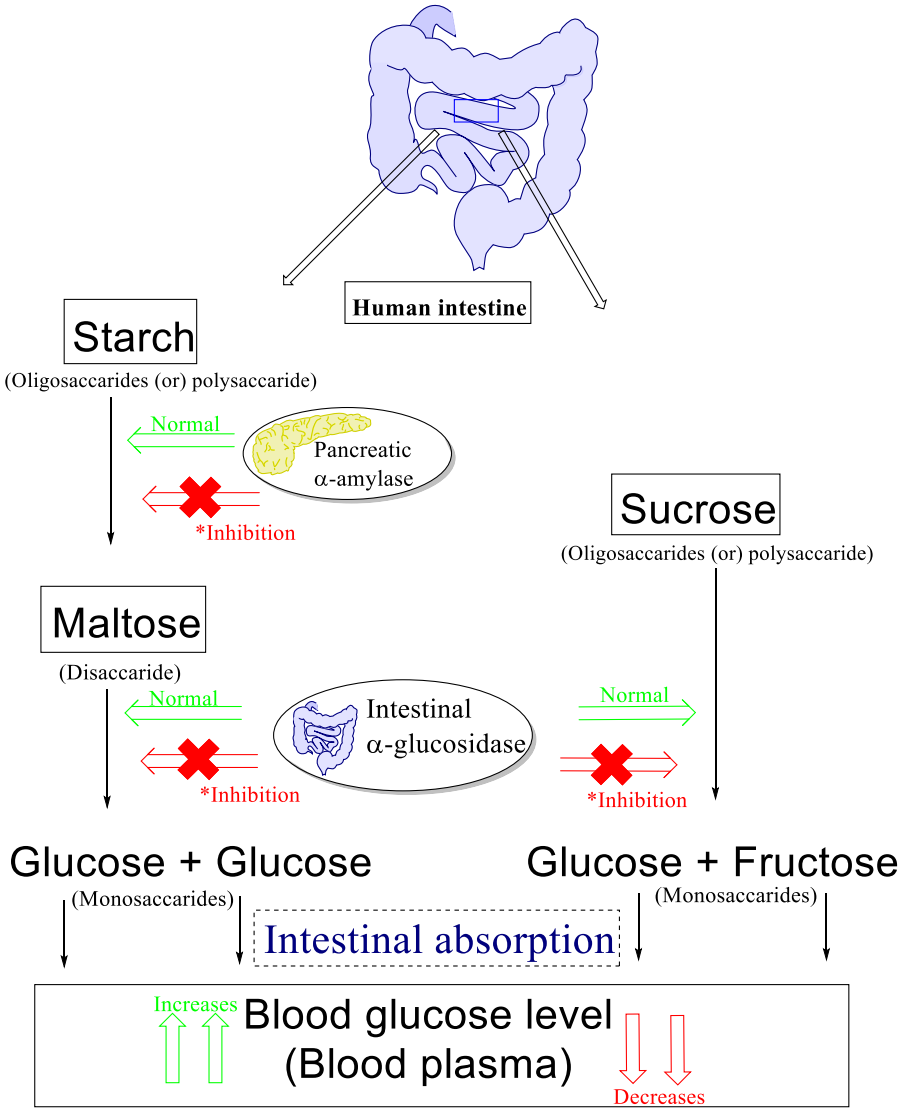

Figure 15: Role of enzymes in glucose management

Intestinal α-glucosidases are a group of enzymes such as isomaltose or sucrase, and glucoamylase are located on the surface of enterocytes (intestinal cells), primarily in the brush border of the small intestine (157). These enzymes play a crucial role in the final stages of carbohydrate digestion, by hydrolyzing disaccharides and oligosaccharides produced by the action of PAA and other enzymes (158). PAA and IAG are prominent targets in the treating diabetes due to their role in digestion of carbohydrates and its absorption into human body (159). By Restricting the activity of these two enzymes can lower the risk of developing diabetes and postprandial hyperglycaemia (160). Thus, IAG and PAA inhibitors are helpful in the management of hyperglycaemia by delaying the digestion of carbohydrates (Figure 15). Among all the targets pancreatic α-amylase (PAA) and intestinal α-glucosidase (IAG) is well known therapeutic targets for the treatment and maintenance of T2DM, because they play significant role in the elevation of glucose levels in blood plasma (161) and also, both the enzymes are involved in the metabolism of various sources of glucose like carbohydrates, proteins and fats (162). Inhibiting the activity of these enzymes (PAA and IAG) can lower the risk of developing T2DM.

CHAPTER-2

LITERATURE REVIEW

CHAPTER-2
LITERATURE REVIEW

2. Literature review

Over the past decade, numerous literature reports have highlighted the biological potential of thiazolidinedione derivatives in various disease conditions like diabetes and cancer (163).Thiazolidinedione derivatives exhibit diverse biological activities in screening parameters and directed experiments, making them valuable candidate for designing and developing new compounds with impressive biological profiles (164). Additionally, significant progress in synthetic chemistry for thiazolidinedione has not only improved the efficiency and safety of their synthesis but also opened new avenues for therapeutic applications. Also, the exploration of thiazolidinediones combined with aromatic or heterocyclic moieties represents a promising pathway in drug design for diabetes and related metabolic disorders (165). The extensive research on the synthesis, optimization, and biological evaluation of these hybrids may lead to the development of novel therapeutic agents with enhanced efficacy and safety profiles (166).The continued innovation in this field holds promise for developing next-generation thiazolidinedione or thiazolidinedione-based compounds with better clinical outcomes and safety profiles (167).

Substitution positions on thiazolidinedione core (NH and -CH2) are being strategically modified to create various derivatives, to enhancing biological activities and optimizing structure-activity relationships. Arylidene derivatives have been widely recognized as a wonderful class in the field of medicinal chemistry due to its ability to accommodate a wide variety of bioactive motifs in its unique structural framework. Recent literature also suggests the, various reactions were succussed in allowing linkage between TZD with benzylidene derivatives and other heterocyclic ring moieties, including chalcones (168) chromone (169), pyrazole (170), phenothiazine (171), benzofuran (172), flavones (173) and acridines (174) etc.

benzylidene derivatives, and also other heterocyclic ring moieties such as

2.1. Furan and thiophene based TZDs as antidiabetic agents

Mahapatra and his colleagues were design, synthesized the novel furan-based thiazolidinedione derivatives and evaluated for antidiabetic activity (Figure 16**)**. The alkyl and haloalkyl moiety were added to amidic nitrogen of thiazolidinedione ring to improve its anti-hyperglycaemic activity, tested *in vivo* on alloxan-induced diabetic Laca mice. Molecular docking studies were also supported out for complementing the *in vivo* results. The *in vivo* antidiabetic results revealed that compound **37** and **38** confirmed the highest activity among the tested compounds. Molecular docking simulation studies, clarify the compound **1** and **2** bind well in the active site of Protein tyrosine phosphatase 1B (**PDB ID: 2NT7**), and were aligned well in the active sit of PPAR-γ (**PDB ID: 2XKW**) with the best docking scores (175).

Gowdru srinivasa and team were designed fifteen novel thiophene based thiazolidine-2,4-diones derivatives and predicted the anti-diabetic activity targeting the PPAR-γ (**PDB ID: 2PRG**). The based on the molecular docking, molecular dynamic (MD) simulation and ADMET results, top three lead ligands were synthesized and characterized by spectral data. The *in vivo* anti-diabetic study (Dexamethasone-induced Wistar strain rat model) indicated that compounds **3**, **4**, and **5** were more effective in reducing blood glucose levels than Pioglitazone (176).

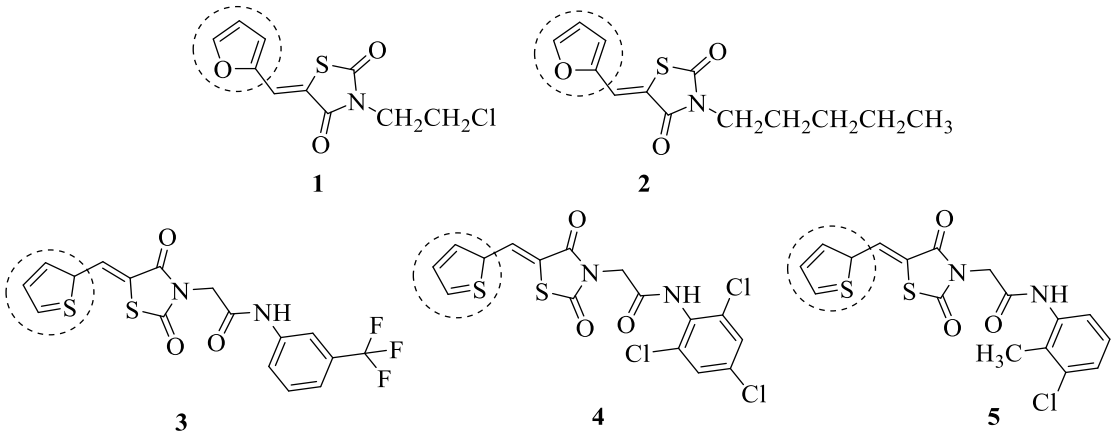

Figure 16: Furan and thiophene based thiazolidinediones as antidiabetic agents

2.2. Pyridine based TZDs as antidiabetic agents

Patel and coworkers were synthesized the seven novel thiazolidinedione derivatives and evaluated for the antidiabetic agents. The *in vitro* results confirmed that the compound **5** and **6** containing pyridine ring is highly active as compared to Rosiglitazone as standard drug (Figure 17). Finally, it was concluded that result obtained from *in vivo* biological activity on rat are significant, compound **5** and **6** can serve as a potential lead molecule for the development of a more potent analogue (177).

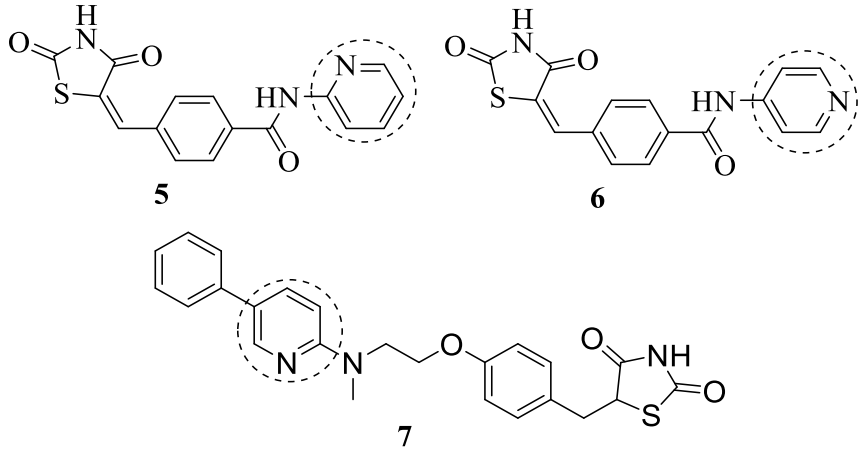

Figure 17: Pyridine clubbed thiazolidinediones as antidiabetic agents.

Kim and his team members were design and synthesized pyridine-based thiazolidinedione derivatives. The synthesized compounds were tested *in vitro* on 3T3-L1 cell lines (triglyceride accumulation). *In vivo* hypoglycemic (blood sugar-lowering) and lipid-lowering effect is assessed by using diabetic KK-Ay mice (obese, hyperglycemic and insulin resistance mice). The compound **7** (Figure 17) shows more potential with effective dose 25 % (ED_{25}) of 0.02 mg/kg towards blood glucose and 2.51 mg/Kg towards triglyceride per day. It is compared with standard drugs called Rosiglitazone (178).

2.3. Pyrazole and imidazole based TZDs as antidiabetic agents

Bansal and coworkers explored the pyrazole-based thiazolidinedione derivatives and assessed the *in vivo* and *in vitro* antidiabetic activity. Additionally, also studied the anti-inflammatory and antioxidant potential. The results suggested that the all the synthesized compounds are effective and potential against as antidiabetic, anti-

inflammatory, and antioxidant. The *in vitro* antidiabetic screening results (α-amylase assay) showed that the benzylated thiazolidinediones along with NO_2 group (**8**) with IC_{50} value of 4.08 µg/mL and OCH_3 (**9**) with IC_{50} value of 7.59 µg/mL and exhibited the highest potency as compared with standard acarbose (IC_{50}: 8.0 µg/mL) (Figure 18).

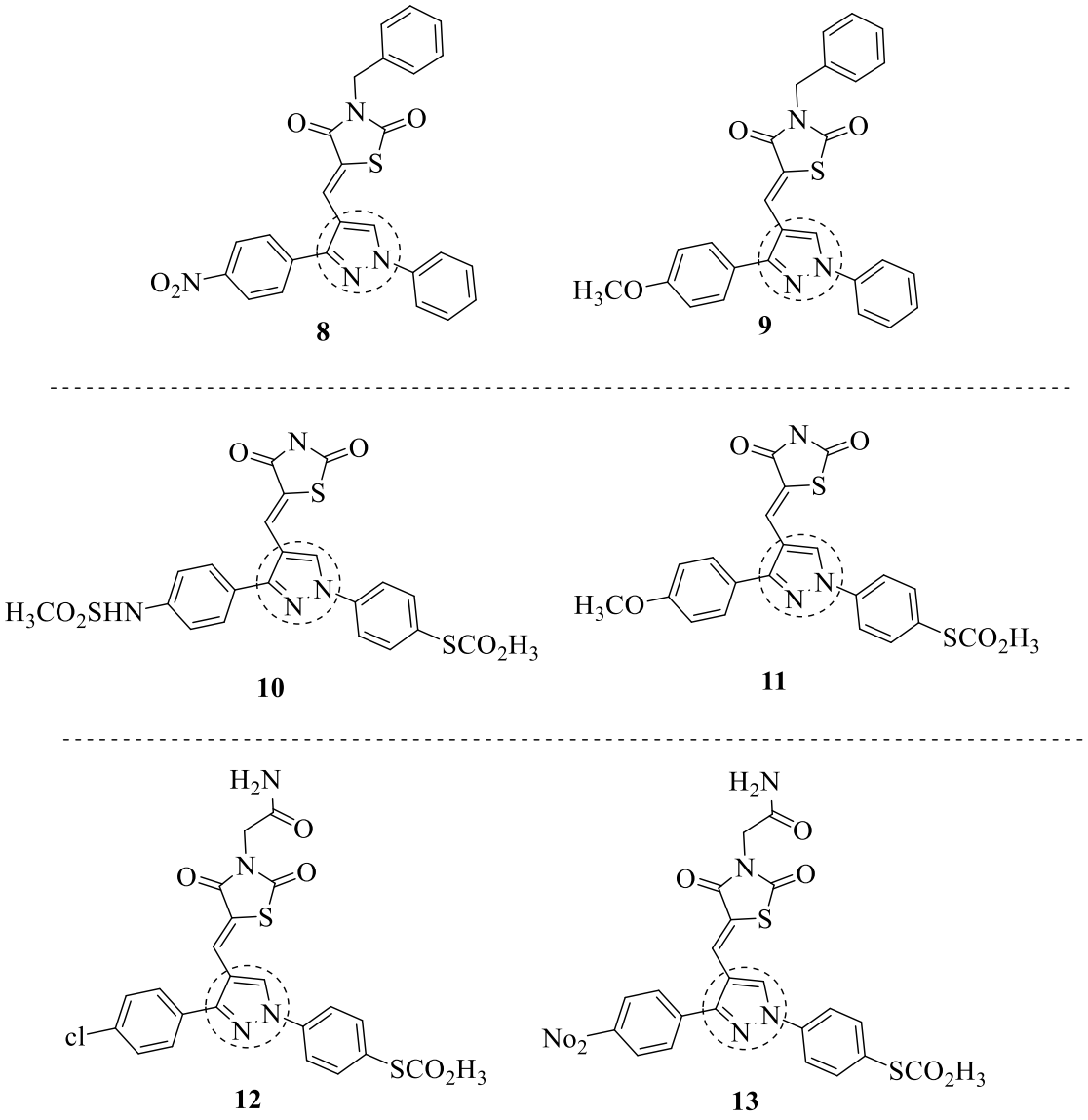

Figure 18: Pyrazole clubbed TZDs as antidiabetic agents

Molecular docking studies states the all the compounds are well binded to PPAR-γ's active site, and also align well with α-amylase's active site. Additionally, compounds were also evaluated the anti-inflammatory and antioxidant screening. The

study found that benzylated thiazolidinediones and NO_2 group showed the highest potency in anti-inflammatory screening and antioxidant activity (179).

Abdellatifa and colleagues were designed and synthesized the two new series of diaryl substituted pyrazole with thiazolidinedione or thiazolidinone derivatives were screened for antidiabetic (α-glucosidase/β-glucosidase) and anti-inflammatory potential. *In vitro* Anti-diabetic potential thiazolidinedione derivatives displayed higher inhibitory activities against *α*- and *β*-glucosidase than the reference compounds (Acarbose and *D*-Saccharic acid 1,4-lactone monohydrate, % inhibitory activity of about 65.37 %, 59.08 % for α-glucosidase and 58.19 %, 66.90 % for β-glucosidase respectively). Among all the standard drugs, the compound **10** and **11** exhibited good PPAR-γ trans activation (52.11 % and 59.63 %) and significant *in vivo* hypoglycemic activity as compared to the standard drugs pioglitazone and rosiglitazone. Further, docking studies with PPARγ receptor revealed satisfactory binding affinity within the active site of receptor (**PDB ID: 4O8F**) (180).

Naim and team were exploring the substituted diaryl pyrazole with thiazolidinedione derivatives on the bases of virtual screening (molecular docking). Finally, about eleven designed compounds were prepared and characterized. Later, all the synthesized compounds were tested *in vivo* antidiabetic using rats (streptozotocin induced diabetic rat). Among all synthesized analogues, compound **12** and compound **13 (**142.4 ± 7.45 and 145.4 ± 5.57) showed good antidiabetic activity as compared to the reference drug Pioglitazone (134.8 ± 4.85) and Rosiglitazone (144.6 ± 6.56)(181).

Shakour and co-workers were designed and synthesized thirteen analogues containing imidazolyl and thiazolidinediones (Figure 19), and evaluated the *in vitro* and *in vivo* antidiabetic activity (182). Molecular docking and molecular dynamics simulations assessed the binding affinity and stability of these compounds with the PPAR-γ receptor. The toxicity of the compounds was tested in 3T3 cells. The in vitro and in vivo testing results suggest compound **14** showed a notable glucose-lowering effect (HepG2 cells) without significant toxicity. *In silico* validation techniques like protein ligand docking and molecular dynamic (MD) simulations were used to assesses

the binding affinity and protein ligand stability with in the PPAR-γ receptor (**PDB ID: 5Y2O**) active site.

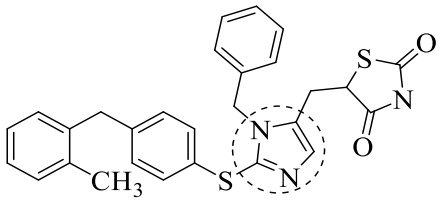

14

Figure 19: Imidazolyl clubbed TZD as antidiabetic agents

2.4. Isoxazoline and oxadiazole based TZDs as antidiabetic agents

Fettach *et al*., are reported the biological evaluation, molecular docking, toxicological studies of novel isoxazoline clubbed thiazolidinedione derivatives (Figure 20). One-pot four components synthesis methodology is used to synthesize and reported the three novel compound **15**, **16** and **17** (Figure 20), later three compounds were evaluated for antidiabetic activity targeting α-amylase and α-glucosidase protein inhibition. *In vitro* enzymatic evaluation revealed that compound **16** shows significant inhibitory activity against α-glucosidase with IC_{50}: 40.67 µM, and α-amylase with IC_{50}: 07.01 µM to standard drug Acarbose (IC_{50}: 97.12 µM, α-glucosidase and IC_{50}: 2.97 µM, α-amylase**).** Furthermore, molecular homology and docking studies reveals, all compounds are allied well at the binding site of pancreatic α-amylase (**PDB ID: IUA3**) and isomaltase (**PDB ID: 3AXH**) enzymes (183).

Iqbal and coworkers were designed and synthesized the different series (thiazole, triazole and oxadiazole) of thiazolidinediones derivatives and were explored to determine the antidiabetic effect by *in vivo* hypoglycemic and hyperlipidemic activities in male Wistar rates (184). Compound **18** showed best antidiabetic effect, lowering plasglucose levels by 50.08 % and plasma triglyceride levels by 72.32 % at a dose of 100 mg/kg body weight, as compared with standard drug Pioglitazone, reduced plasma glucose by 45.89 % and plasma triglycerides by 75.43 % at the same dose.

Nazreen and team synthesized aryl oxadiazole based thiazolidinedione derivatives and analysed by *in vitro* PPAR-γ transactivation (185) studies to estimate the antidiabetic activity. PPAR-γ is a nuclear receptor plays a key role in glucose metabolism and insulin sensitivity. *In vitro* PPAR-γ transactivation assays are used to determine whether a synthesized compound can activate PPAR-γ, which may advise antidiabetic potential. Compound **19** demonstrated PPAR-γ transactivation of 64.67 % of inhibition. The study compared the effectiveness of Pioglitazone (PPAR-γ transactivation of 71.94%) and Rosiglitazone (PPAR-γ transactivation of 85.22%).

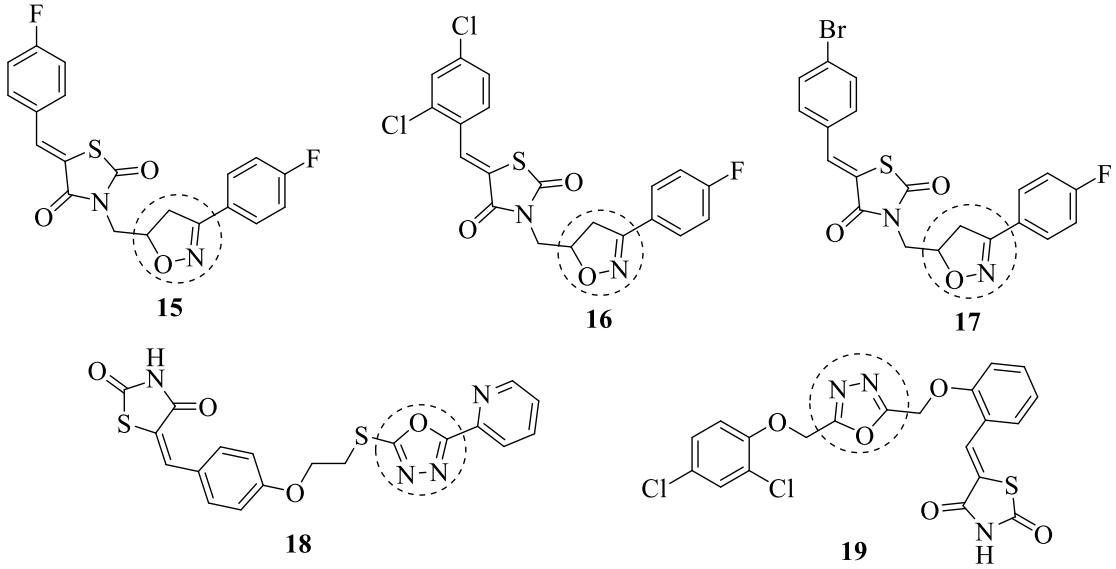

Figure 20: Isooxazoline and oxadiazole based TZDs as antidiabetic agents

2.5. Indole based TZDs as antidiabetic agents

Kumar and his research and team were design, synthesized a series of twelve novel indole clubbed thiazolidinedione derivatives and evaluated the *in vivo* antidiabetic (alloxan-induced tail tipping diabetic model of Wistar albino rats) and *in vitro* anti-microbial and antioxidant activities. The *in vivo* antidiabetic results suggest that, compound **20** and **21** (Figure 21**)** exhibited significant antidiabetic activity as compared with standard drug Glibenclamide. The docking procedure was applied on a set of designed ligands within the region of PPARα active site (**PDB ID: 2PRG**) using AutoDock 4.2.6 software. The compound **20** shown promising binding affinity i.e. -9.65 kcal/mol and forms two H-bonds with Ser289 and Gln286 at active site of PPARα

protein. Additionally, compounds were also evaluated for antioxidant activity by DPPH and hydrogen peroxide assay (H_2O_2). DPPH assay results states that, the compound **20** (IC_{50}: 52.36 µg/mL) were found to be shown significant antioxidant activity (186).

Verma and co-workers were designed and synthesised the indolyl linked benzylidene-based thiazolidinedione (**22 and 23**), diethyl malonate and methyl acetoacetate derivatives. The synthesised indolyl linked benzylidene-based thiazolidinedione (Figure 20), predicted the antidiabetic activity, using *In-silico* docking tool Surflex-dock module using crystal structures of PPARα (**PDB ID: 1I7G**) and PPARγ (**PDB ID: 1I7I**) complexed with Tesaglitazar as internal co-crystal ligand and as standard. The compound **22** and **23** (indolyl linked benzylidene-based thiazolidinedione derivatives), were promising binding affinity at active site of both PPARα and PPARγ protein as compared to diethyl malonate and methyl acetoacetate derivatives (187).

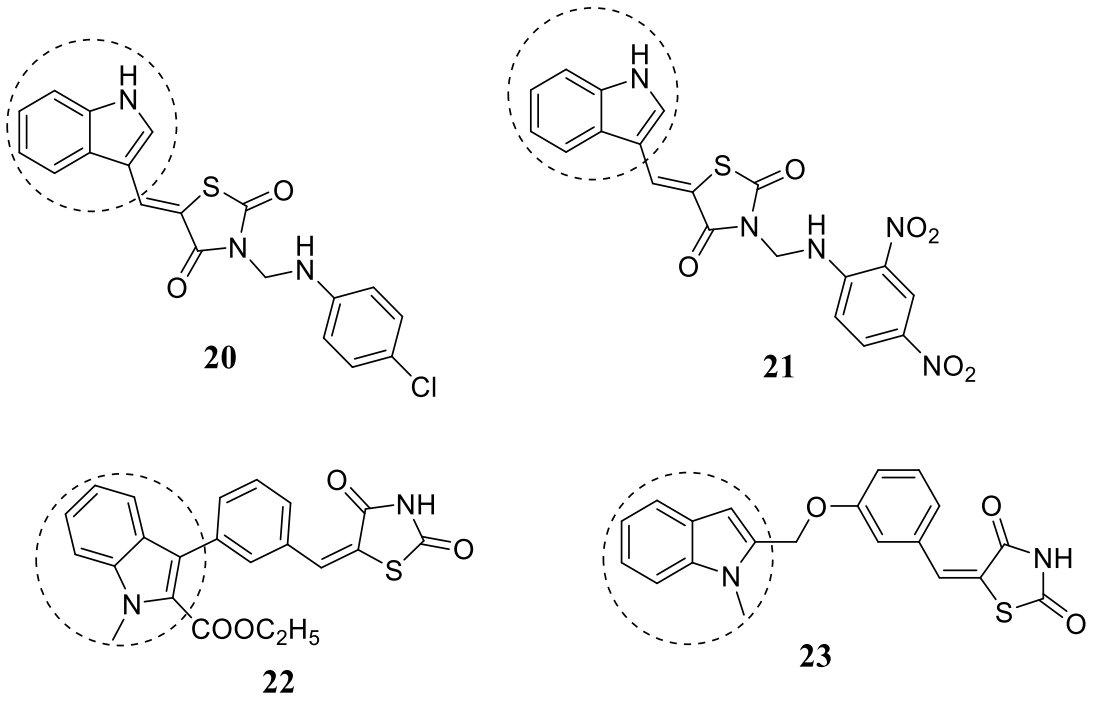

Figure 21: Indole based TZDs as antidiabetic agents

2.6. Benzodioxole and benzoxazole based thiazolidinediones

Sameeh and the research team were designed and synthesized a four novel (5-(benzo [1,3] dioxol-5-ylmethylene) thiazolidinedione (Figure 22) and evaluated there *in vivo* and *in vitro* antidiabetic and in vitro antioxidant activities (188). *In vitro* alpha-amylase

study suggested that Compounds **24** (IC_{50}: 11.8 µg/mL) and **25** (IC_{50}: 11.8 µg/mL) showed higher inhibitory potential as compared with standard acarbose (IC_{50}: 24.1 µg/mL). Additionally, compounds were also evaluated for antioxidant activity by DPPH method, effect of the scavenging is rising in the trend **24** > **25** > **26** > STD > **27**.

Compounds (**24–27**) possess antioxidant activity higher than standard ascorbic acid, while **27** has lower scavenging activity than standard ascorbic acid. *In vivo*, oral anti-hyperglycemic activity was evaluated for compounds by an alloxan induced diabetic rat model. Diabetes was successfully induced in the rats, blood glucose level for each tested compound at three different doses (50, 100 and 250 mg/Kg) and for five experimental period durations (0, 2, 4, 15, 30 days). The compounds were docked to study the ligand protein interactions of designed compounds with PPAR-γ (**PDB ID: 2PRG**) and alpha-amylase (**PDB ID: 2QV4**) using gold score function in MOE.2019. Compounds **24** (-8.25 Kcal/mol), **25** (-8.43 Kcal/mol) and **26** (-6.59 Kcal/mol) bind well in the active site of PPAR-γ, while **24** (-7.32 Kcal/mol), **25** (-7.46 Kcal/mol) and **26** (-6.74 Kcal/mol) aligned well in the active site of alpha-amylase with the best docking scores (189).

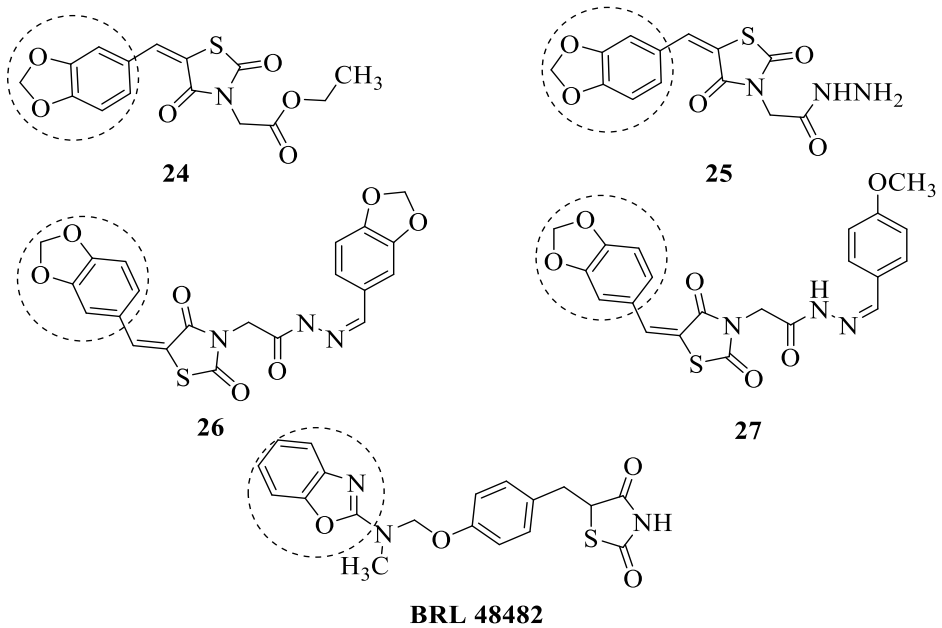

Figure 22: Benzodioxole, benzoxazole and benzothiazole based TZDs

Jeon and research group have designed, synthesized the benzoxazole based thiazolidinediones and evaluate the potency of compounds for PPAR-γ transactivation using PPAR-GAL4 chimeric receptors (expressed in CV-1 cells) (190). Compound **BRL48482** (Figure 22) demonstrated PPAR- γ transactivation in range 51.0 - 75.2% of inhibition (191). Similarly, the compound **BRL48482** demonstrated PPAR- γ transactivation in range 54 -74 % of inhibition.

2.7. Quinoline clubbed TZDs as antidiabetic agents

Kumar and co-workers were designed and synthesised eight novel 2-chloro- quinoline clubbed thiazolidinedione derivatives (Figure 23) and evaluated the *in vivo* hypoglycemic potentials by streptozotocin-induced diabetic Wistar albino rat model using dose of 30 mg/kg. The *in vivo* antidiabetic results suggest that, among all the synthesized derivatives, compounds **28** and **29** exhibited significant antidiabetic activity as compared with standard drug Pioglitazone.

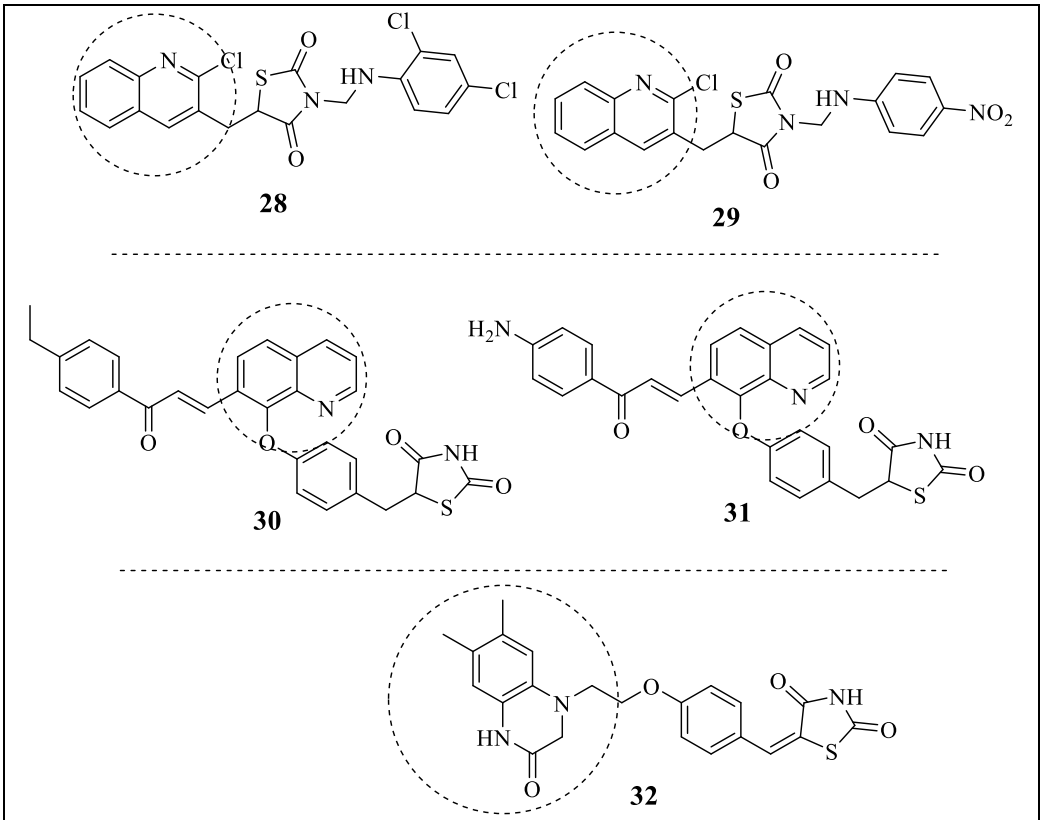

Figure 23: Quinoline based TZDs as antidiabetic agents

Srikanth and team were synthesised a nine new series of quinoline based thiazolidinedione derivatives (Figure 23) and evaluated the for their *in vivo* antidiabetic activity by Wister strain albino rat's species by tail vein method. Among all nine synthesized compounds five were used for *in vivo* hypoglycemic activity, the compounds **30** and **31** showed significant activity as compared to the reference drug Rosiglitazone (192).

Gupta and research team designed, synthesized, and characterized the tetrahydroquinoline-based thiazolidinedione derivatives and evaluated their antidiabetic activity. The *in vivo* euglycemic (blood glucose-normalizing) and hypolipidemic (lipid lowering) activities were evaluated in male Wistar rats. All the compounds (100 mg/kg body weight) were tested and compared with standard drug Rosiglitazone. The results demonstrate the compound **32** (Figure 23) is potent as normalising blood glucose levels (81.25 %) and lowering the lipid levels (54.95 %) in the blood plasma (193).

2.8. Coumarin based TZDs as antidiabetic agents

Mishra and colleagues were synthesized novel Coumarin based thiazolidinedione derivatives and assessed them for their *in vivo* antidiabetic activity in Wistar rats (male) weighing 150–250 gm, using the alloxan-induced diabetic model and considering pioglitazone as a standard. The antidiabetic screening revealed that all synthesized derivatives exhibited promising glucose-reducing potential. Compounds **33**, **34**, and **35** (Figure 24) were found to be nearly identical to the standard (194).

Nazreen and research team was synthesized a series of chromone-based thiazolidinediones and assessed their antihyperglycemic potential, including an *in vitro* PPAR-γ transactivation activity. Among all five derivatives analysed, compound **36** (Figure 24) shows PPAR-γ transactivation of 48.71 % inhibition in contrast to standard drugs Rosiglitazone (85.27 %) and Pioglitazone (62.48 %) (195).

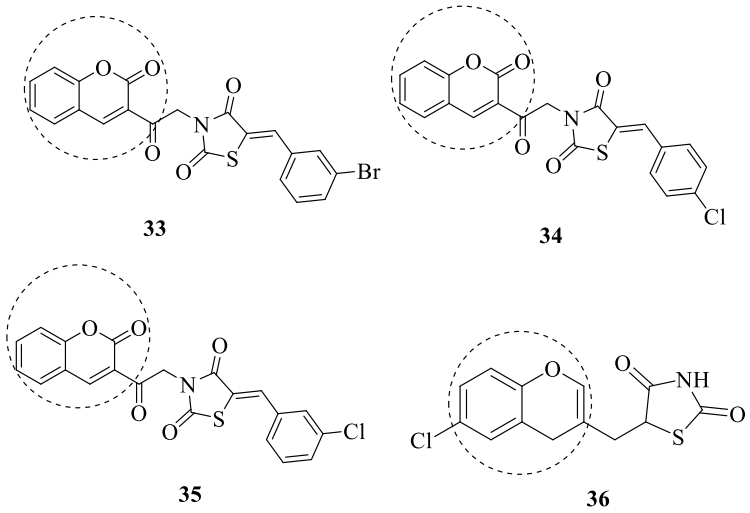

Figure 24: Coumarin clubbed TZDs as antidiabetic agents

2.9. Phthalazinone, pyrimidine and pyrimidinone based thiazolidinediones

Madhavan and his research team synthesized a series of phthalazinone and benzoxazineone-based thiazolidinediones and tested their effectiveness in lowering plasma glucose and triglyceride levels in diabetic db/db mice (196). Additionally, *in vitro* PPARγ transactivation assay was also evaluated by using HEK293T cell lines. Results states, among all the synthesised analogues, compound **36** (Figure 25) shows more potent with good *in vitro* PPAR-γ transactivation inhibition activity as compared to standard drugs called Pioglitazone and Troglitazone.

Later in 2002, same team were designed and synthesized pyrimidinone-based thiazolidinedione derivatives. All prepared compounds were analysed for their hypoglycemic and hypolipidemic activity in diabetic mice (db/db type) and also estimated the *in vitro* PPARγ transactivation assay using HEK293T cell lines. The compound **38** (Figure 25) shows 73 % and 85 % decrease (30 mg/kg/day) in glucose and triglyceride level in blood plasma respectively. Rosiglitazone is used as reference compound, which shows 65 % decrease in glucose and 41 % decrease (30 mg/kg/day) in triglyceride level in the blood plasma (197).Another research team, Lee *et al*., were designed and synthesized the pyrimidine-based thiazolidinedione derivatives and analysed the glucose and lipide lowering potential in the KK-Ay mice model using standard drugs like Pioglitazone and rosiglitazone. Among all the prepared analogues,

compound **39** (Figure 25) exhibited potent antidiabetic activity having ED_{25} values of 1.7 mg/kg/day in plasma glucose and 3.4 mg/kg/day as triglyceride level (198). Compound **39** showed significant antidiabetic activity, with ED_{25} values of 1.7 mg/kg in plasma glucose per day and 3.4 mg/kg in triglyceride levels per day among all prepared compounds.

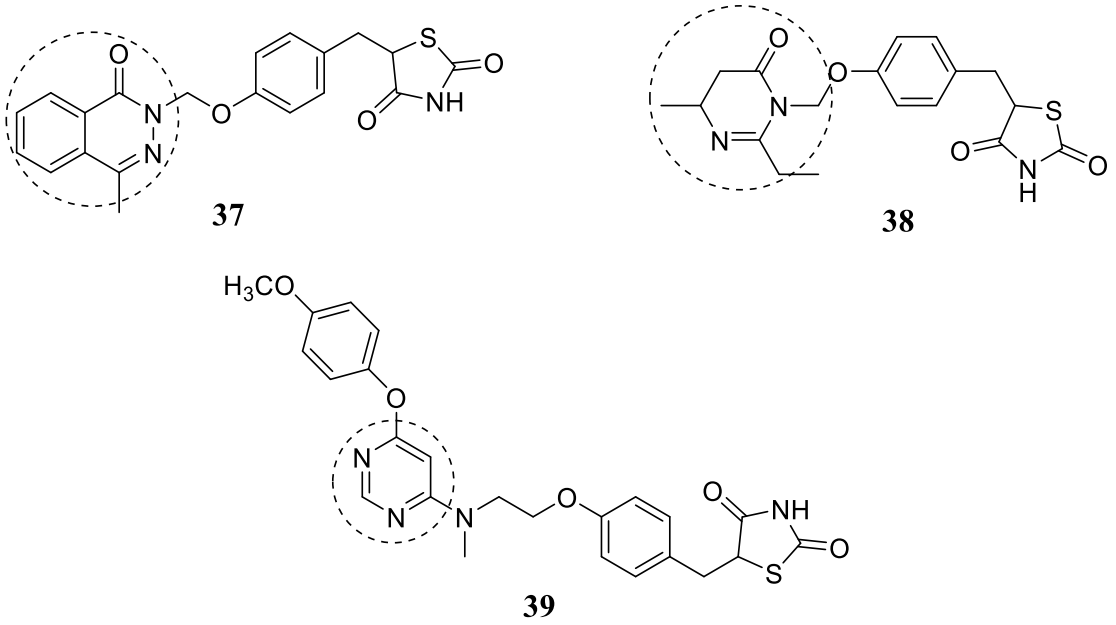

Figure 25: Phthalazinone, pyrimidine and pyrimidinone based TZDs

2.10. Naphthalene clubbed TZDs as antidiabetic agents

Besides thiazolidinediones, naphthalene ring containing compounds were also showed good antidiabetic properties. Zask and his coworkers were first to report the Naphthalene based thiazolidinedione derivatives as antidiabetic agent.

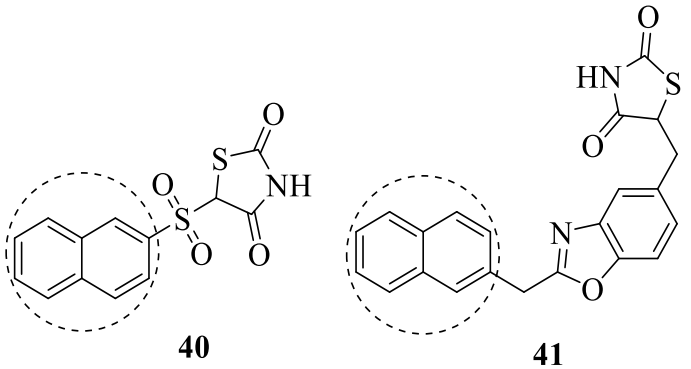

Figure 26: Naphthalene based thiazolidinediones as antidiabetic agents

Series of 5-(naphthalenylsulfonyl) thiazolidinediones were synthesized and evaluated for antihyperglycemic activity. Within this series, compound **74** (Figure 26) was found to be superior to other groups for eliciting antihyperglycemic activity. Later, Hulin and team reported that naphthalene moiety with glitazones showed greater antihyperglycaemic effect than only glitazones. The compound **75** showed 10 times greater potency than that of Ciglitazone (199). Benzoxazole derivative with a 2-naphthylmethyl chain was considered to be responsible for the enhanced activity.

2.11. Phenothiazine clubbed TZDs as antidiabetic agents

Doddagaddavalli *et al*., evaluated the new thiazolidinedione with phenothiazine molecular hybrids, and screened for antidiabetic activity like glucose uptake assay and α -amylase enzyme inhibition. Most substances significantly to moderately inhibited α-amylase and glucose uptake activity.The compound **42** (Figure 27) shows potent inhibitor of α-amylase having IC_{50} value 130.6 µM and glucose uptake assay exhibits IC_{50} value 459.3 µM. the results are compared with the reference called acarbose (IC_{50}: 101.8 µM) and metronidazole (IC_{50}: 441.2 µM) Additionally, computational studies confirmed the interactions of all compounds are well align in α-amylases (**PDB ID: 2QV4**) active site (171).

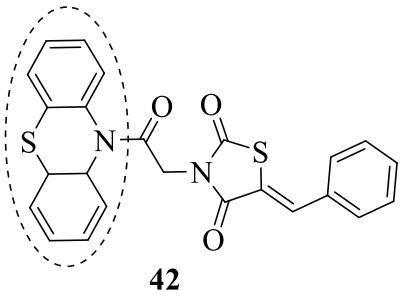

42

Figure 27: Phenothiazine based TZD as antidiabetic agent

2.12. Arylidene based thiazolidinediones as antidiabetic agents

Nazreen and collegues desiged and synthesized a series of phenoxy acetic acid-based thiazolidinedione conjugates. Antidiabetic activity evaluation is measured by *in vitro* PPAR-γ transactivation assay. Results states, compound **43a** and **43b** were more potent at activating PPAR-γ leads to lipid and glucose metabolism. Compound **43a** shows

54.51 % and compound **43b shows** 55.41 % of activating PPAR-γ as compared to reference drug Pioglitazone (65.94 %) and Rosiglitazone (82.21 %). The authors concluded that these compounds as promising for the treatment of T2DM (200).

Leite and co-workers was designed and synthesized the novel diaryl substituted thiazolidinediones and analysed the hypoglycemic and hypolipidemic activities by *in vivo* studies using mice (alloxan induced diabetic). (201). Among all the tested analogues, compound **44** (Figure 28), shows the potent antidiabetic activity. It shows 21.80 % and 40 % of lowering (10 mg/kg body weight) the glucose and triglyceride level in the blood plasma of alloxan induced diabetic mice. Rosiglitazone is used as standard compound, shows 36.7 % of glucose and 43.3 % of triglyceride decrease in blood plasma.

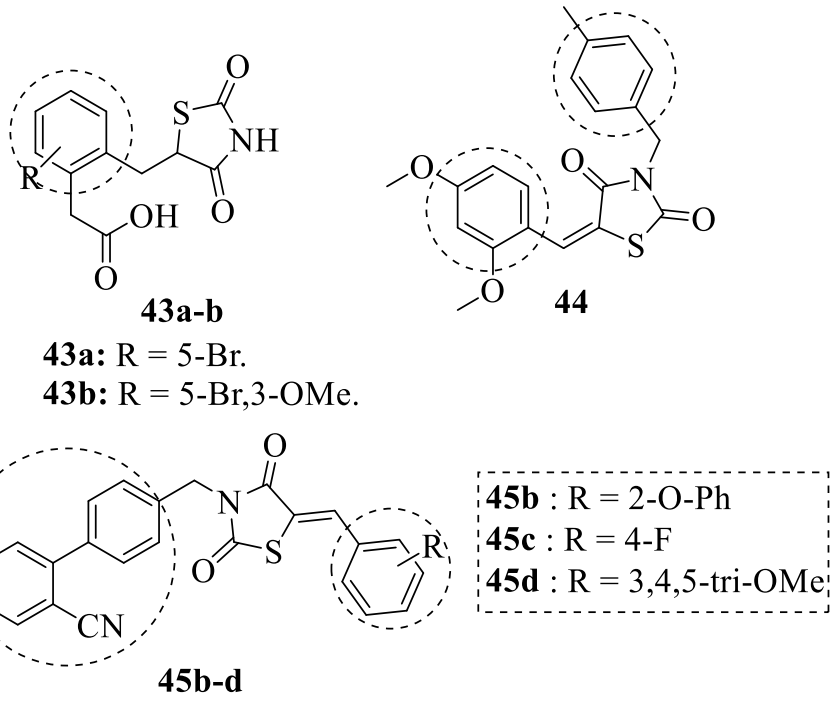

Figure 28: Arylidene based thiazolidinediones as antidiabetic agents

Rathod and his team desinged, synthesized and *in vitro* therapeutic potentials of new biphenyl carbonitrile clubbed thiazolidinediones as antidiabetic agents (202). The all newly synthesized compounds were tested for their in vitro α-amylase activity using Acarbose as a positive control at varying concentrations (50-150 µg/mL). Results of

antidiabetic evaluation shows that all good inhibitors activity against α-amylase enzyme, off these, compounds **45b**, **45c** and **45d** (Figure 28) exhibited excellent antidiabetic activity with IC_{50} values 0.13 Mm, 0.15 μM and 0.13 μM respectively. Furthermore, docking study demonstrated that biphenyl carbonitrile unit and thiazolidinediones core of all compounds shows strong interactions aligned well within active site residues of barley (malt) α-amylase (**PDB ID: 1RPK**). while **45b**, **45c** and **45d** associated well in the active sit of barley (malt) α-amylase with the best docking scores.

In summary, the existing literature provides a comprehensive foundation for thiazolidinedione derivatives as antidiabetic agents as provided the clear rationale for the current study. The literature reveals that the -NH and -CH_2 moieties of the thiazolidinedione core have been key substitution sites, extensively explored to generate diverse derivatives with improved biological activity and therapeutic potential. Studies consistently demonstrate that modifications at the -NH and -CH_2 positions of the thiazolidinedione scaffold have led to a broad spectrum of derivatives, underlining their significance in drug development and structure–activity relationship (SAR) studies. The broad range of successful thiazolidinedione conjugations with heterocyclic ring such as pyrazole, phenothiazine, benzofuran, chromones and quinoline underscores its value in scaffold hybridization strategies, providing a strong rationale for further development of multifunctional therapeutic agents

CHAPTER-3

RATIONALE, AIM, OBJECTIVES AND WORK PLAN

CHAPTER-3

RATIONALE, AIM, OBJECTIVES AND WORK PLAN

3.1. Rationale

In current investigation, we employed a pharmacophore-based strategy to facilitate the development of thiazolidinedione based novel compounds. The most commonly used protocols for structural modification of the thiazolidinedione core involve two major sites, such as substitutions at the nitrogen position (N-3 group) and the methylene carbon (C-5 group).The rational design of 3,5-disubstituted thiazolidinediones for diabetes treatment involves optimizing substitutions to enhance their binding affinity and pharmacokinetic properties while minimizing side effects (Figure 29).To verify this suggestion, we have done an extensive review of existing literature, which illuminated an excess of compounds characterized as 3,5-disubstituted thiazolidinedione system.

In this context, Bansal and co-authors has synthesized diaryl pyrazolyl thiazolidinedione compound **1**. It is synthesized through Knoevenagel condensation tailed by N-substitution using bromoacetic acid and benzyl bromide and evaluated as a potent antidiabetic agent acting *via* inhibition of α-amylase enzyme with IC_{50} value of 4.08 µg/Ml (179). Additionally, Rathod and colleagues has also synthesized novel N-3 and C-5 disubstituted thiazolidinedione derivative based compound **2** demonstrating promising antidiabetic activity with IC_{50} value of 0.13µM (202). Fortified by the above-cited literature and our continuous efforts to identify thiazolidinediones based potential anti-diabetic agents, we decided to synthesize 3,5-disubstituetd thiazolidinedione derivatives as potential antidiabetic agents acting *via* inhibition of pancreatic α-amylase (PAA) and Intestinal α-glucosidase (IAG).

In this context, Initially, we have explored the molecular structure of Netoglitazone also called MCC-555 as oral hypoglycemic agents containing thiazolidinedione core glitazone class drug available in the market. This analysis unveiled a distinctive structural motif consisting of aromatic naphthalene ring linked to thiazolidinedione at C-5 position (methylene group) within the Netoglitazone molecule.

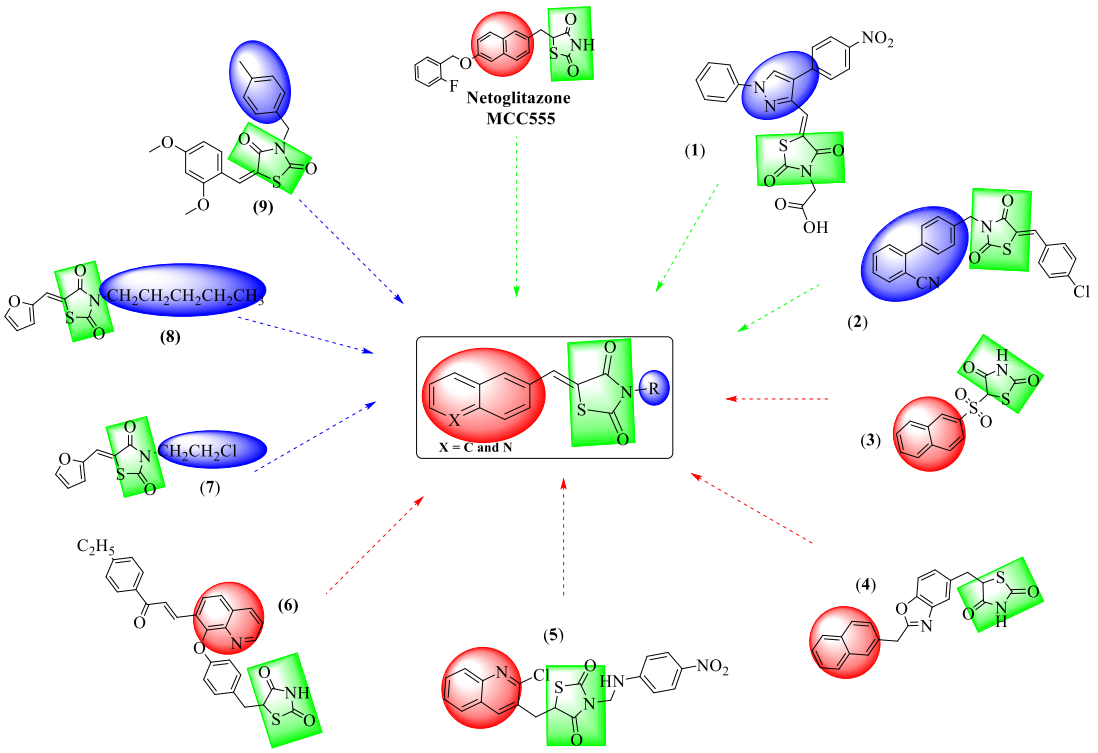

Figure 29: Designing of proposed molecules

Additionally, we emphasized the example of the 5-(naphthalenyl sulfonyl) thiazolidinediones based compound **3** (203) This compound was designed, synthesized, evaluated as a potent antidiabetic agent by Zask *et al*., (1990). Later, Hulin *et al*., (1996) naphthalene moiety with glitazones showed greater antihyperglycemic effect than only glitazones. The compound **4** showed 10 times greater potency than that of Ciglitazone (199). Benzoxazole derivative with a 2-naphthylmethyl chain was considered to be responsible for the enhanced activity. Moreover, Kumar *et al*., (2021) and colleagues reported the quinoline based thiazolidinedione derivatives, compound **5** is efficacious as antidiabetic agents (204). Furthermore, Srikanth *et al*., (2010) and his group reported a novel series of quinoline based thiazolidinedione derivatives, compound **6** demonstrating promising antidiabetic activity as compared with Rosiglitazone (192). In all the aforementioned studies reveals that the presence of naphthalene and quinoline substituted leads to improve the selectivity and enhance the antidiabetic activity.

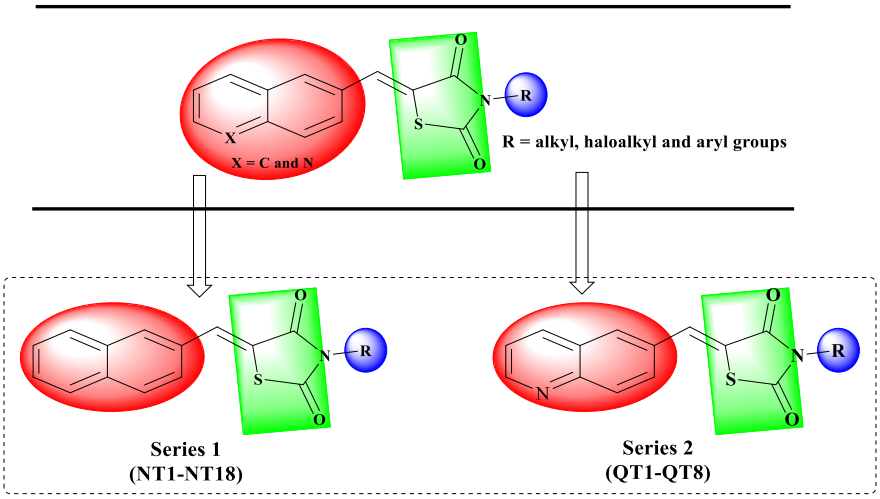

Figure 30: Basic structure of the designed **Series 1** and **2**

Moreover, we have also observed that compound **7**, **8** and **9** feature an aliphatic and aromatic hydrophobic group on the amidic nitrogen (N-3 Substitution) of thiazolidinedione ring to improve its anti-hyperglycaemic activity. Compounds **7** and **8** exhibits an alkyl/haloalkyl moiety are directly attached to the amidic nitrogen of thiazolidinedione ring (143) and compound **9** showcased the aryl group such as biphenyl carbonitrile (205).Introducing the hydrophobic group other than hydrogen on the amidic nitrogen of thiazolidinedione ring enhance the insulin releasing activity (206).This rationale leads to design of two series, namely naphthalene-based thiazolidinedione (**NT1-NT18**) and quinoline-based thiazolidinedione **(QT1-QT8)** (**Figure 30**).

3.2. Aim

Synthesis and Antidiabetic Investigation on Thiazole Derivatives

3.3. Objectives

- Designing of novel thiazole derivatives as potential antidiabetic agent.
- Synthesis and Characterization of selected designed thiazole derivatives.
- In-vitro screening of synthesized derivatives for their antidiabetic potential

3.4. Plan of work

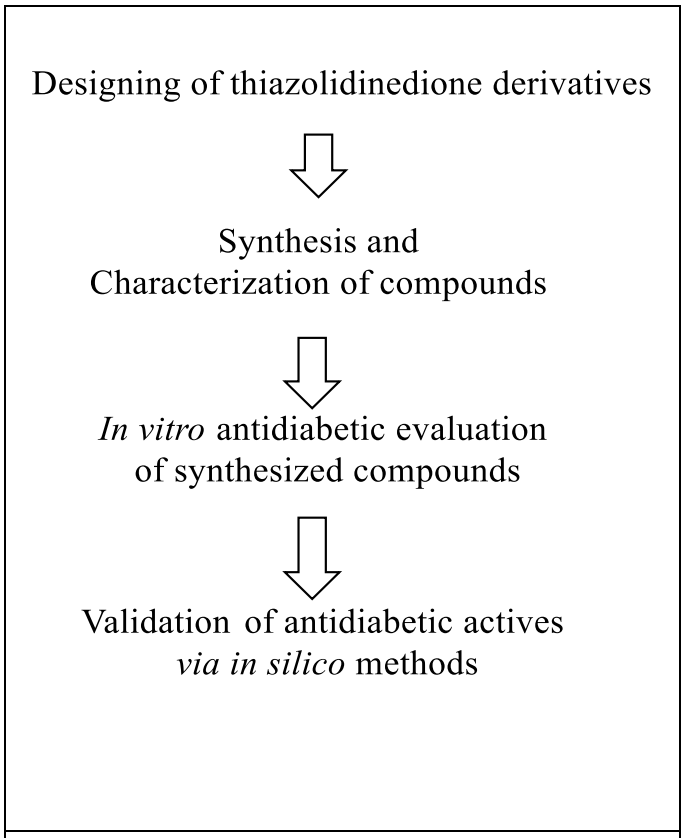

Figure 31: Present work plan

CHAPTER-4

MATERIALS AND METHODS

CHAPTER-4
MATERIALS AND METHODS

The present work consists of several aspects, like pharmacophore-based strategy to facilitate the development of thiazolidinedione based novel compounds, the synthesis of novel thiazolidinedione derivatives, as well as screening the synthesized compounds for their inhibitory activities against the potential target enzymes crucial for glucose homeostasis. e.g., α-amylase and α-glucosidase. A Further step was to perform molecular docking and molecular dynamics (MD) simulations, with the targeted receptors to correlate *in silico* predictions with *in vitro* experimental results to gain deeper mechanistic understanding.

4.1. Materials

All the chemicals, solvents and reagents used in this study were of analytical grade and procured form reputable suppliers. Key compounds like thiazolidinedione (TZD), naphthaldehyde, 5-methoxy naphthaldehyde and quinoline-6-carbaldehyde were specifically procured from BLD Pharma. Additionally, chemicals like various alkyl bromides, solvents and reagents were obtained from Sigma-Aldrich, Merck India and Loba Chemie. The solvents were purified using standard laboratory procedures as needed during the work. Deionized water was used for all aqueous solutions. The reaction progress was monitored by using pre-coated thin layer chromatographic (TLC) plates. Aluminum TLC silica gel 60 with fluorescent indicator F_{254} (Merck, India) using Hexane: Ethyl acetate (8:2) as eluent and TLC spot visualization was done by using UV cabinet (Lab line, LSC-130) and self-prepared iodine chamber (central instrumentation lab, school of pharmaceutical sciences, LPU).

Synthesized compounds were characterised using melting point, FT-IR, MS, ^{1}H NMR and ^{13}C NMR spectroscopy. Fourier Transform Infra-Red (FT-IR) spectra were recorded using a Perkin-Elmer Spectrum 2 at central instrumentation facility (CIF) of Lovely Professional University (LPU). The ^{1}H (400 MHz) and ^{13}C NMR (100 MHz) spectra were obtained using the FT NMR Spectrometer model Avance-II (Bruker) at SAIF, Panjab University and Innatura scientific Pvt Ltd. The chemical shifts were recorded in δ (ppm) and DMSO-d_6 and $CDCl_3$ was used a s solvent and tetramethyl

silane (TMS) as internal standard for calibrating chemical shifts. Mass spectra (ESI-MS) were recorded using a GC-MS/MS, specifically Shimadzu TQ8040 (CIF, LPU) within the range of 0 to 700 m/z.

The melting points were observed using the Droplet RSW 138 B (central instrumentation lab, school of pharmaceutical sciences, LPU) melting point device, with the caveat that the reported melting points were uncorrected. Additionally, HPLC chromatograms were recorded on Shimadzu LC2030 Plus using PDA as detector (CIF, LPU). The mobile phase used was a mixture of methanol and water (60:40 v/v), with a flow rate of 1.0 mL/min at 25 ºC column temperature (Autosampler).

In Silico validation techniques, like molecular docking and molecular dynamic simulations were used to predict the binding affinity and stability of synthesized compounds against the target enzyme. AutoDock Vina 4.2.6 (freeware version by Scripps Research Institute, USA) was used to predict the binding orientation and affinity (binding energy score) of a ligand (synthesized compounds) towards target protein (PAA and IAG) so called docking, into the protein's active site. Desmond module (version: Desmond/2020.4 by Schrödinger LLC) is employed to perform molecular dynamic study at JSS academy of higher education and research, Mysore.

All structures were drawn and designed (2D and 3D) using ChemBioDraw Ultra 14.0 software. Target proteins used for the docking and MD investigation is pancreatic α-amylase and intestinal α-glucosidase, were retrieved from RCSB (www.rcsb.org) protein data bank (PDB) with the **PDB ID: 4W93** and **PDB ID: 3A4A** respectively. Discovery studio visualizer software (https://discover.3ds.com/discovery-studio-visualizer-download) was used to analyzing the molecular structures, sequences and alignment with in the binding pocket with various amino acid.

Molecular mechanics generalized born surface area (MM-GBSA) tool is used to predict the binding free energies of protein- ligand complex. Finally, study incorporated, *in silico* ADME (Absorption, Distribution, Metabolism, Excretion) and toxicity studies, using Molsoft portal (https://molsoft.com/mprop), SwissADME web tool (http://www.swissadme.ch) and OSIRIS property explorer (https://www.organic-chemistry.org/prog/peo/) to assess physicochemical properties and durglikeness.

4.2. Methods

The experimental work methodology was categorized into three parts for the better understanding:

Part-I: Synthesis and characterization of designed compounds

Part-II: *In vitro* antidiabetic and antioxidant studies

Part-III: *In silico* validation

4.2.1. Part-I: Synthesis and characterization of designed compounds

In the current investigation, we employed a pharmacophore-based strategy to facilitate the development of novel thiazolidinedione-based compounds. Review of literature revealed that, thiazolidinedione core is a well-established scaffold in medicinal chemistry, particularly in the context of diabetes treatment. Structural modifications to this core are commonly undertaken at two major sites: Nitrogen Position (N-3 Group) and Methylene Carbon (C-5 Group). Our rational design of 3,5-disubstituted thiazolidinediones for diabetes treatment specifically involved optimizing substitutions at these two sites.

4.2.1.1. Synthesis

We initiated our work with two different types of thiazolidinediones such as naphthalene and quinoline-based thiazolidinedione. The synthetic protocols of the target compounds were categorized into **Scheme-1 (series-I)** and **Scheme-2** (**series-2**).

4.2.1.1.1. Preparation of series-1 compounds (Scheme-1)

Scheme-1: compounds **NT1-NT18** were synthesized in two steps. Initially thiazolidinedione (**2**) was used to synthesis the naphthalen-2-yl-methylene thiazolidinedione (**3a**) and 5-methoxy naphthalen-2-ylmethylene thiazolidinedione (**3b**) in the presence of naphthaldehyde (**1a**) and 5-methoxy naphthaldehyde (**1b**) respectively. Subsequently, alkyl/haloalkyl or aryl bromides were reacted with naphthalen-2-ylmethylene thiazolidinedione and 5-methoxy naphthalen-2-ylmethylene yield final analogs (**NT1-NT18**) shown in the **scheme-1.**

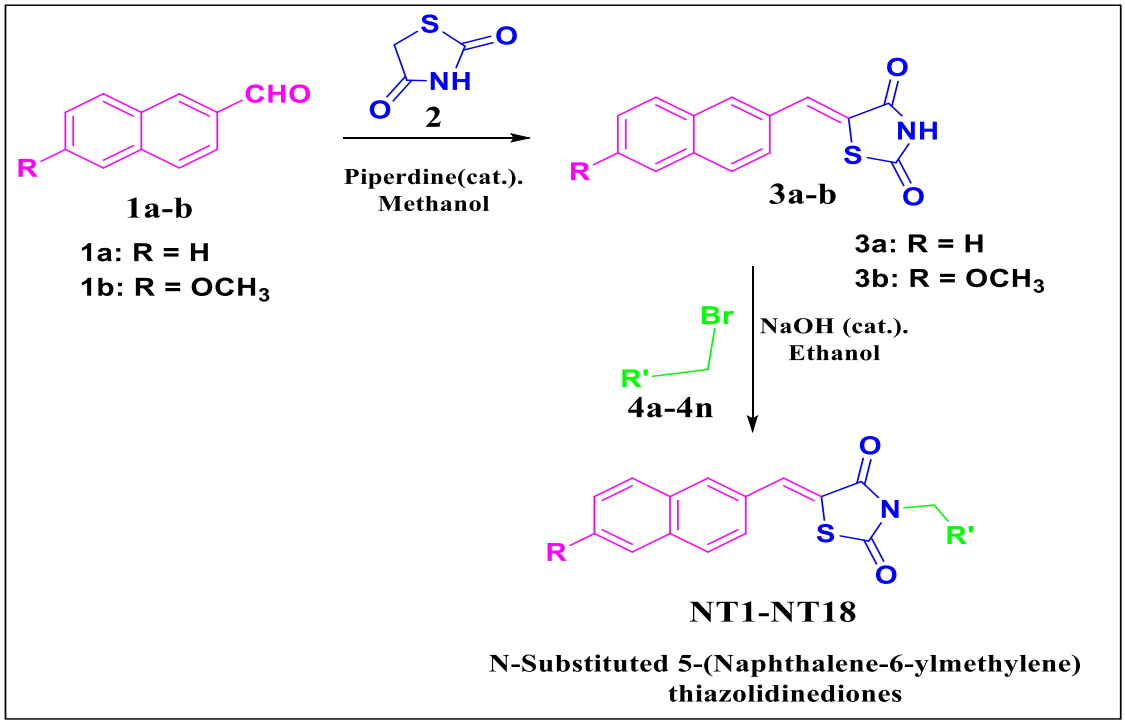

Scheme 1: Synthesis of naphthalene based thiazolidinediones

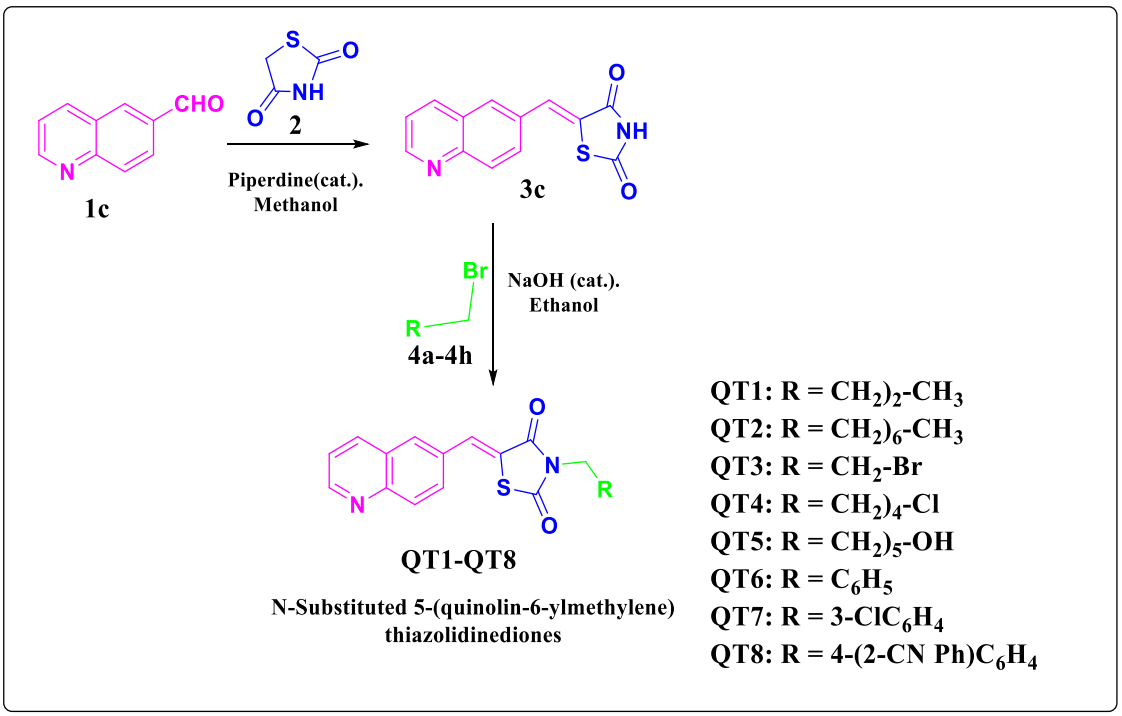

Scheme 2: Synthesis of quinoline based thiazolidinediones

4.2.1.1.1.1. Preparation of naphthalen-2-ylmethylene thiazolidinedione (3a)

In a 100 mL of round bottom flask, 2-naphthaldehyde **1a** (3.2 mmol) was added to 20 mL of methanol along with the thiazolidinedione **2** (3.2 mmol), and stirred at normal room temperature for 2-3 minutes. To the above reaction mixture, about 0.4 mL of piperidine was added and refluxed for 18 hrs over an oil bath. The reaction progress is verified through thin layer chromatography (TLC) Method. The mixture was cooled at room temperature, and the resulting precipitate was collected by filtration, then washed with dichloromethane and diethyl ether. The resulting solid compound was further purified by the column chromatography (Eluent: 80:20 hexane: ethyl acetate). As the result, product is separated by vacuum filtration and then purified through recrystallization using ethanol and kept in a desiccator at room temperature (207).

4.2.1.1.1.2. Preparation of 5-methoxy naphthalen-2-yl methylene thiazolidinedione (3b)

In a 100 mL of round bottom flask, 6-methoxy-2-naphthaldehyde **1b**, (3.2 mmol) and thiazolidinedione **2** (3.2 mmol) were added to 20 mL of methanol, stirred at room temperature for 2-3 minutes. Later, to above reaction mixture, 0.4 mL of piperidine was added and refluxed for 18 hrs over an oil bath. The reaction progress is verified through TLC method. Finally, after cooling the content at normal room temperature, precipitate is formed and washed it with diethyl ether and dichloromethane. The reaction mixture was cooled to room temperature, and the precipitate was filtered and washed with dichloromethane and diethyl ether. The resulting solid compound was further purified by the column chromatography (Eluent: 80:20 hexane: ethyl acetate). As the result, product is separated by vacuum filtration and then purified through recrystallization using ethanol and kept in a desiccator at room temperature.

4.2.1.1.1.3. Preparation of naphthalene-based thiazolidinediones derivatives (NT1-NT18)

A suspension was prepared by stirring 12.5 mmol of sodium hydroxide in 10 mL of aqueous ethanolic solution. To the above suspension, naphthalen-2-yl methylene thiazolidinedione **3a** (2.0 mmol) or 5-methoxy naphthalen-2-yl methylene

thiazolidinedione **3b** (2.0 mmol) was added respectively. Suitable alkyl/haloalkyl/aryl derivatives (10.5 mmol) were added to the content and refluxed for 10-12 h with continuous monitoring of the reaction progress using TLC (eluent: 80:20 hexane: ethyl acetate; developer: Iodine chamber and ultraviolet light). The solvent was evaporated at low pressure to produce desired analogues, which were then washed with water to form naphthalene-based thiazolidinedione derivatives (**NT1-NT18**). Further purification was achieved by recrystallization using suitable solvents. After successful synthesis of naphthalene-based thiazolidinediones derivatives, structure of compounds was assigned on the basis of their analytical and spectroscopic data (FTIR, Mass ^{1}H & ^{13}C NMR).

4.2.1.1.2. Preparation of series-2 compounds (Scheme-2)

Scheme-2: compounds **QT1-QT8** were also synthesized in two steps. Initially, thiazolidinedione (**2**) was treated with quinoline-6-carbaldehyde (**1c**) in the presence of piperidine, ethanol and acetic acid give quinolin-6-ylmethylene thiazolidinedione (**3c**). Further, quinolin-6-ylmethylene thiazolidinedione is reacted with eight different alkyl and benzyl bromides (**4a-4h**) to afford final compounds called quinoline based thiazolidinediones (**QT1-QT8**) shown in the **scheme-2**.

4.2.1.1.2.1. Preparation of N'-(quinolin-6-ylmethylene) thiazolidinedione (3c)

In a 100 mL round bottom flask, a reaction mixture was prepared by mixing 3.2 mmol of quinoline-6-carbaldehyde (**1**) and 3.2 mmol of thiazolidinedione (**2**) are taken in to 20 mL methanol and stirred 2-3 minutes. To the above reaction content, about 0.4 mL of piperidine was added and refluxed for 18 hrs over an oil bath. The reaction progress is verified through TLC. Later, resulting mixture was cooled at normal room temperature, precipitate is formed and washed with dichloromethane and diethyl ether. The resulting solid compound was further purified by the column chromatography (Eluent: 80:20 hexane: ethyl acetate). As the result, product is separated by vacuum filtration and then purified through recrystallization using ethanol and kept in a desiccator at room temperature.

4.2.1.1.2.2. Preparation of quinoline based thiazolidinediones (QT1-QT8)

The compounds **QT1-QT8** was synthesized by refluxing the aqueous ethanolic solution (ethanol: water 1:1) containing 2.0 mmol of 5-(quinoline-6-ylmethylene) thiazolidinedione (**3c**) and 2.0 mmol of various substituted alkyl and benzyl chloride analogues (**4a-4h**) in the presence of sodium hydroxide (NaOH) as a catalyst **(Scheme 2)**.The reaction time is varied from 10-12 hr and reaction progress was monitored using TLC (eluent: 80:20 hexane: ethyl acetate; developer: Iodine chamber and ultraviolet light). The solvent was evaporated at low pressure to produce desired analogues, which were then washed with water to form substituted quinoline-based thiazolidinedione hybrids.

4.2.1.2. Characterization

After successful synthesis of desired compounds, solubility followed by purification (recrystallization and column chromatography) is performed for all compound by using suitable solvents. After purification, melting point range is observed for all novel compounds. FT-IR, MS, ^{1}H NMR and ^{13}C NMR spectroscopy are used to elucidate the structure of all desired compound as per the designed studies.

4.2.2. Part-II: In vitro antidiabetic and antioxidant studies

4.2.2.1 *In vitro* PAA inhibition activity

The PAA inhibitory activity of all synthetic compounds evaluated out by reported method of Telagari & Hullatti *et al.,* The different concentration of all compounds was prepared in DMSO (0, 2.5, 10, 25, 50, 100, 250 µg/mL). 500 µg/mL α-amylase solutions were prepared in 0.02M sodium phosphate buffer (pH 6.8) and incubated for 15 minutes at 25 ºC to obtain unique concentrations of compounds. After 10 minutes, 500 µg/mL of 1 % starch solution in 0.02M sodium phosphate buffer was added to each tube and incubated at 25 ºC for 10 min. Then the reaction was terminated by adding 0.5 mL of 2 N sodium hydroxide (NaOH). Later one mL of 3,5-dinitro salicylic acid (DNS) reagent was added and whole content is warmed on water bath for 2-4 min and measure the absorbance (540 nm). Acarbose was used as control/standard. Anti-diabetic efficacy of the all compounds were estimated by the inhibition of PAA. The percentage inhibition was determined using equation-1 (208).

$$\textbf{Pecentage inhibition} = \frac{\boldsymbol{Abs\ of\ the\ control - Abs\ of\ the\ sample}}{\boldsymbol{Abs\ of\ the\ control}}\ \boldsymbol{X\ 100} \quad (\textbf{equation} - \textbf{1})$$

4.2.2.2. *In vitro* IAG inhibition activity

The IAG inhibitory activity of all synthetic compounds evaluated out by reported method of Telagari & Hullatti *et al.,* (209)**.** At first, the reaction mixture containing 20 µg/mL of varying concentration of all compounds (0, 2.5, 10, 25, 50, 100, 250 µg/mL), 50 µg/mL phosphate buffer (100 Mm, p^H = 6.8) and 10 µg/mL of IAG is taken into a 96-well pate, and preincubated for 15 min at 37 °C. Then, 20 µg/mL of P-nitrophenol glycol (P-NPG) was added (5 % v/v) as substrate and incubated for 20 min at 37 °C. About 0.1M sodium carbonate (Na_2CO_3) was added to stop the reaction. Acarbose was used as control/standard. The absorbance of free P-NPG is measured at 404 nM. The percentage inhibition was determined using equation-2.

$$\textbf{Percentage inhibition} = \frac{\boldsymbol{1 - Abs\ of\ the\ sample}}{\boldsymbol{Abs\ of\ the\ control}}\ \boldsymbol{X\ 100} \quad (\textbf{equation} - \textbf{2})$$

4.2.2.3 *In-vitro* antioxidant activity

The 2,2-Diphenyl-1-picrylhydrazyl (DPPH) free radical scavenging assay was carried out using Blois et al.'s methodology with some modifications (210). The assay was carried out by taking 100 µg/mL of the standard (ascorbic acid) or all synthetic compounds with different concentrations (0, 2.5, 10, 25, 50, 100, 250 µg/mL) in a 96-well plate. Analyses were performed with a UV-vis spectrophotometer in 1 mL or 3 mL cuvettes. DPPH radical solution absorbance was measured spectrophotometrically at 517 nm. To prepare the DPPH solution, 3 mL of the stock solution was diluted to 50 mL with methanol in a volumetric flask and protected from light with aluminum foil. Then, 3 mL of DPPH working solution was transferred to the 0.5 mL all synthetic compounds with different concentrations, mixed, and left in the dark for 30 min (incubation period). All analyses were carried out in four replicates, and absorbance was recorded. Lower absorbance states the higher antioxidant activity for a given content. Finally, the radical scavenging activity was calculated as percentage of DPPH

discoloration as per the equation-1. The IC_{50} values were determined from the logarithmic plot of the all-synthesis compound's concentration vs the percentage inhibition at that concentration (211).

4.2.2.4. Statistical analysis

Statistical analysis was performed using Graph pad prism ver. 5.0 and results were expressed as mean ± S.D. ANOVA (analysis of variance) was performed using Dunnett's t-test and the values $p < 0.05$ were regarded statistically significant.

4.2.3. Part-III: *In silico* validation

Artificial intelligence (AI) is gaining potential, while molecular modelling is being used as an investigative technique to discover potential molecules (212).computational techniques in drug designing and development includes, molecular docking approach, which includes virtual screening of large compound libraries to find molecules that bind effectively to a target (213). Additionally, Molecular dynamics (MD) simulations studies are used to estimate the stability of a drug-protein complex, helps refine docking results, and informs structural changes (214). During the drug designing, predicting the pharmacokinetic parameters so called absorption, distribution, metabolism and excretion (ADME) results of all the designed compound important to address the challenging due to complex physiological mechanisms. Unfavourable ADME properties contribute to 40% of drug failures, and early ADME prediction is crucial for improving compound success in discovery and development stages (215). Toxicity determination is a complex process *in vivo* system. Toxicity determination is important during the drug development process, because it's a leading causes of drug withdrawals at the preclinical or clinical phase (216).

4.2.3.1. Molecular Docking Studies

Molecular docking (DC) study was carried out to assess the interaction and binding modes of synthesized potential derivatives with target receptor using Auto dock tool vina 1.5.6 software (217). The process involves selection and procuring the target protein, ligand preparation (synthesised compounds), receptor grid generation and

docking it to the receptor binding pocket. The target protein used for the present study is PAA and IAG crystal structure is downloaded from the RCSB online portal (www.rcsb.org), with the **PDB ID: 4W93** (218) and **PDB ID: 3A4A** (219) respectively. Target protein preparation involved removal of ligand (co-crystal ligands), water atoms and heteroatoms. Later, polar hydrogen atoms and Kollam charges were added, and saved as pdb.qt extension at workplace. The receptor grid is a fixed binding pocket (area at which protein interacts with the ligand) within the receptor target, determined by the reference drug or co-crystal ligand validation of the protein.

All the synthetic compound structure were designed (2D and 3D) on ChemBioDraw Ultra 14.0 software. Later, energy minimization is performed and saved at the workplace. Finally, prepared protein with fixed grid and ligand were imported into the Auto dock vina interface and docking protocol was executed. The binding affinity (Kcal/mol) or docking score was included in the output file is saved the folder (workstation).Using discovery studio visualizer software (https://discover.3ds.com/discovery-studio-visualizer-download), was used to analyzing molecular structures, sequences, and alignment with in the binding pocket with amino acid of receptor.

4.2.3.1.1 Validation of protein for docking

The method's (docking methodology) reproducibility and its validation were assessed using the Root mean square deviation (RMSD) value in the redocked binding sites with crystallographic conformations (**Table 4.1**) or with synthetic compounds.

Table 4.1: Details of PAA and IAG protein crystal structure

Protein	Methods source	Resolution (A^o)	R-value	Amino acid number	Co-crystallized ligands	Binding affinity
PAA (4W93)	X-ray diffraction method	1.32	0.194	495	Montbretine A	-6.5
IGA (3A4A)	X-ray diffraction method	1.58	0.153	586	α-D-Glucose	-8.5

This crucial process can enhance the accuracy and reliability of an *in silico* docking experiment. The co-crystallographic ligand structure was derived from their PAA (Montbretine A) and IAG (α-D-Glucose) (.pdb) files i.e. **4W93** and **3A4A** respectively and subsequently re-docked into the corresponding binding site for several times **(Figure 32**). The value of RMSD calculated was less than 2 Å making the protein validated and appropriate to proceed with docking studies.

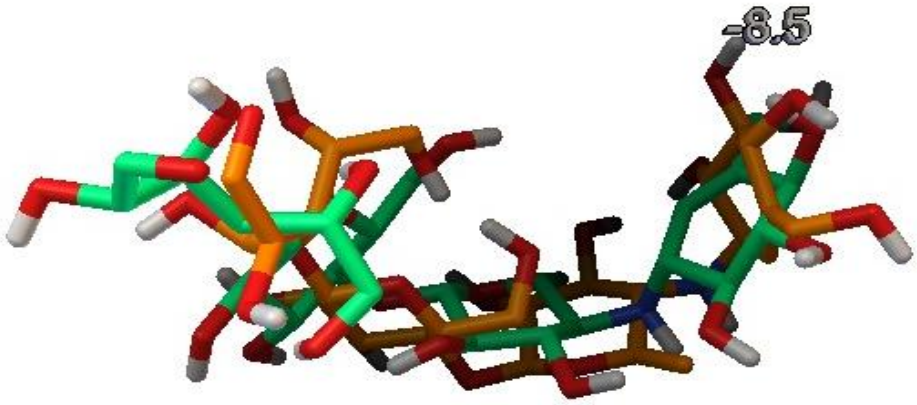

Figure 32: Co-crystallized ligand before (green) and after (orange colour) docking

4.2.3.2. MM-GSBA binding free energy prediction

The MM-GSBA assay is used to predict the binding free energies of protein- ligand complex. This analysis is performed using the schrodinger Suite 2020-2 Prime module(https://www.schrodinger.com/platform/products/prime/), which employs the OPLS3 force field and the VSGB solvation model. This is done through the Molecular Mechanics Generalized Born Surface Area (MM-GBSA) method (220).

4.2.3.3 Molecular dynamics (MD) simulation studies

Molecular Dynamic simulations were executed on both PAA (**PDB ID: 4W93**) and IAG (**PDB ID: 3A4A**) receptors with the lead compounds utilizing the Desmond software, a molecular dynamics simulation tool for a duration of 200 nanoseconds Desmond is a highly advanced tool, which contains temperature, pressure, and volume system, making it ideal for studying protein-ligand interactions. Maestro program's system builder tool is used to construct the protein ligand complex i.e. **4W93**, **3A4A**-

ligand complex system. After, constructing the complex(s) are enclosed into a cubic box containing water molecules, were exposed to the simple point charge (SPC) model, which is characterized by three-point water molecules. Later, the sodium ions (Na+) are added to the complex(s) to neutralize the total charge of the entire solvent system, facilitating periodic boundary conditions. A crucial step in MD simulations studies is applying the steepest descent method (SDM), used to achieve energy minimization. In the fixed system, a cubic box with 10 Å dimensions is apply to achieve periodic boundary conditions and alleviate edge effects, with all atoms placed in a space-filling box surrounded by translated copies of itself. Finally, to characterizing the potential energy of the system, OPLS3e force field parameter is specifically designed for molecular dynamics simulations of proteins (221).

4.2.3.4. Prediction of physicochemical properties

Lipinski's Rule-5 (LR5) was utilized to assess the drug-likeness of all newly synthesized compounds (222). The drug's lipophilicity (Log P), polar surface area, rotatable bonds, H-bond acceptors and donors was determined using freely availed web server Molsoft portal (https://molsoft.com/mprop).

4.2.3.5. ADME Prediction

The SwissADME web tool (http://www.swissadme.ch) was utilized to predict various pharmacokinetic aspects such as absorption, distribution, metabolism, and excretion (ADME) (223). The input for this analysis involved the SMILES representations of all synthesised compounds. The assessment included factors affecting absorption, P-glycoprotein substrate (P-gp substrate) potential, gastrointestinal (GI) absorption, and membrane permeability. Additionally, we considered the blood-brain barrier (BBB) for its impact on drug delivery. Furthermore, cytochrome (CYP) P450 is a family of enzymes that are responsible for about 72% of all metabolic reactions. Notably, among 57 CYP enzymes encoded in the human genome, mainly CYP1A2, CYP2C9, CYP2C19, CYP2D6, and CYP3A4 participate in the metabolism of most drugs and mediate many adverse drug reactions (224).

4.2.3.6. Toxicity prediction

Absorption, distribution, metabolism, and elimination (ADME) predication for all synthesized compounds were analysed. Later, toxicity was analysed using OSIRIS property explorer (https://www.organic-chemistry.org/prog/peo/).It is an essential that non-toxic oral drugs depend on their solubility in the gastrointestinal tract (GIT), which is a critical factor in their effectiveness.The characteristics of the selected compounds

CHAPTER-5

RESULTS AND DISCUSSION

CHAPTER-5
RESULTS AND DISCUSSION

The results and discussion were divided into three parts as per series-I and series-II for the better understanding:

Part-I: Synthesis and characterization of designed compounds

Part-II: *In vitro* antidiabetic and antioxidant studies

Part-III: *In silico* validation

5.1 Series-I (Results and discussion)

5.1.1. Part-I: Synthesis and characterization of designed compounds

5.1.1.1. Synthesis

The synthetic route of title compounds, naphthalene based thiazolidinediones outlined in **Scheme 1**. **NT1-NT18** were synthesized in two steps. Initially thiazolidinedione (**2**) was used to synthesis the *N*′-naphthalen-2-ylmethylene thiazolidinedione (**3a**) and 5-methoxy naphthalen-2-ylmethylene thiazolidinedione (**3b**) in the presence of naphthaldehyde (**1a**) and 5-methoxy naphthaldehyde (**1b**) respectively. Subsequently, alkyl/haloalkyl or aryl bromides were reacted with naphthalen-2-ylmethylene thiazolidinedione and 5-methoxy naphthalen-2-ylmethylene yield final analogs (**NT1-NT18**). Initially the melting points of the synthesized compounds were compared with the similar compounds containing the thiazolidinedione as their basic moiety in the literature. Initially, melting point, molecular weight (mass spectroscopy) and percentage yield of the synthesis compounds were observed (Table 5.1), are crucial in characterization processes. Later, spectral characterization of all compounds, were performed by instrumental techniques like FT-IR, and NMR (^{1}H and ^{13}C).

Table 5.1: The physical data of compound **NT1-NT18**

Compound Name	Molecular formula	MW	Melting Point (°C)	Yield (%)
NT1	$C_{22}H_{14}F_3NO_2S$	413.07	225-228	84
NT2	$C_{22}H_{14}F_3NO_2S$	413.07	220-222	82
NT3	$C_{23}H_{19}NO_4S$	405.47	234-236	85

NT4	$C_{26}H_{23}NO_4S$	445.53	250-255	81
NT5	$C_{28}H_{18}N_2O_2S$	446.11	248-250	82
NT6	$C_{20}H_{14}N_2O_2S$	346.40	231-234	87
NT7	$C_{24}H_{15}NO_4S$	413.45	265-269	84
NT8	$C_{19}H_{19}NO_3S$	341.11	292-295	80
NT9	$C_{20}H_{21}NO_3S$	355.12	297-298	75
NT10	$C_{23}H_{27}NO_3S$	397.17	310-315	64
NT11	$C_{18}H_{13}NO_3S$	323.06	272-275	82
NT12	$C_{19}H_{17}NO_5S$	371.08	295-298	79
NT13	$C_{22}H_{16}ClNO_3S$	409.88	261-265	88
NT14	$C_{22}H_{16}ClNO_3S$	409.05	282-285	82
NT15	$C_{23}H_{16}F_3NO_3S$	443.44	271-272	79
NT16	$C_{24}H_{21}NO_5S$	435.49	282-285	84
NT17	$C_{29}H_{20}N_2O_3S$	476.55	290-294	87
NT18	$C_{21}H_{16}N_2O_3S$	376.43	264-265	78

5.1.1.2. Characterization

5.1.1.2.1. 5-(naphthalen-2-ylmethylene)-3-(2-(trifluoromethyl) benzyl) thiazolidinedione (NT1)

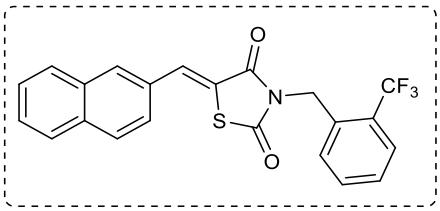

Yield: 84%; Yellow Solid Powder; M.P : 225-228 °C, **FT-IR (KBr)** $\bar{\nu}$/cm^{-1}: 3381, 2920, 1743, 1683; **^{1}H NMR** ($CDCl_3$, 500 MHz), δ (ppm): 8.08 (s, 1H), 8.00 (s, 1H), 7.91 (dd, *J* = 8.7, 4.6 Hz, 2H), 7.87 – 7.84 (m, 1H), 7.72 (s, 1H), 7.65 (d, *J* = 7.7 Hz, 1H), 7.60 – 7.54 (m, 4H), 7.49 (d, *J* = 7.8 Hz, 1H), 4.97 (s, 2H); **^{13}C NMR** (at 100 MHz, using $CDCl_3$), δ ppm: 167.79, 166.03, 136.02, 134.73, 133.96, 133.13, 132.33, 131.61, 130.60, 129.33, 129.14, 128.82, 128.14, 127.83, 127.17, 125.90, 125.80, 125.77, 125.25, 125.22, 125.20, 44.73.; **MS** m/z (ES^+): 413.01.

5.1.1.2.2. 5-(naphthalen-2-ylmethylene)-3-(3-(trifluoromethyl) benzyl) thiazolidinedione (NT2)

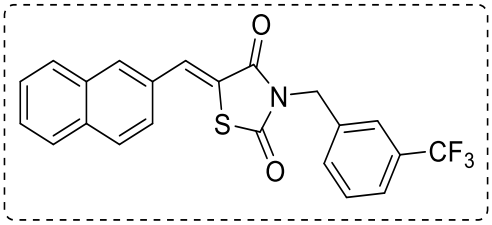

Yield: 82 %; Pale Yellow Powder; M.P :220-223 °C; **FT-IR (KBr)** $\bar{\nu}/cm^{-1}$: 3381, 2920, 1743, 1683; **^{1}H NMR** (at 500 MHz, using $CDCl_3$), δ ppm: 8.08 (s, J = 8.0Hz, 1H), 8.00 (s, 1H), 7.90 (m, J =7.8Hz, 2H),7.86 (m, J=7.7Hz, 1H), 7.72 (s, J=7.6Hz, 1H), 7.65 (d, J =7.59Hz, 1H),7.57 (m, J=7.35Hz, 4H) 7.48 (t, 1H), 4.97 (s, 2H); **^{13}C NMR** (at 100 MHz, using $CDCl_3$), δ ppm: 166.06, 161.01, 137.25, 134.24, 133.89, 131.45, 129.09, 128.80, 128.04, 127.90, 125.14, 121.66 100.29, 55.39, 45.34; **MS** m/z (ES^+): 413.41.

5.1.1.2.3. 3-(3,5-dimethoxybenzyl)-5-(naphthalen-2-ylmethylene) thiazolidinedione (NT3)

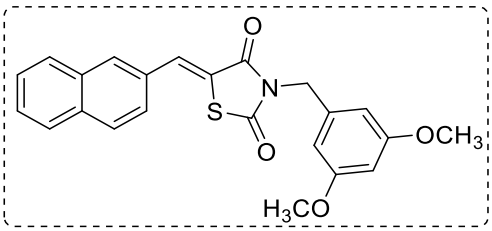

Yield: 85 %; White Powder; M.P :234-236 °C; **FT-IR** (KBr) $\bar{\nu}/cm^{-1}$: 3381, 2920, 1743, 1683; **^{1}H NMR** (at 500 MHz, using $CDCl_3$), δ ppm: 8.07 (s, 1H): 8.00 (s, 1H), 7.89 (m, 3H), 7.56 (m, 3H), 6.60 (d, *J* = 2.3 Hz, 2H), 6.40 (t, *J* = 2.3 Hz, 1H), 4.86 (s, 2H), 3.79 (s, 6H); **^{13}C NMR** (at 100 MHz, using $CDCl_3$), δ ppm: 166.06, 161.01, 137.25, 134.24, 133.15, 131.45, 130.75, 129.09, 128.04, 127.52, 127.42, 121.66, 106.69, 100.29, 55.39, 45.34; **MS** m/z (ES^+): 405.10.

5.1.1.2.4. Ethyl -2-(4-((5-(naphthalen-2-ylmethylene)-2,4-dioxothiazolidin-3-yl) methyl) phenyl) propanoate (NT4)

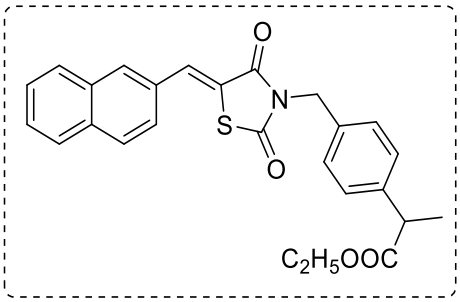

Yield: 81%; White Powder; M.P: 250-255 °C, **FT-IR** (KBr) $\bar{\nu}$/cm^{-1}: 2918, 2853, 1678, 1542, 1301; **^{1}H NMR** (at 500 MHz, using $CDCl_3$), δ ppm: 8.06 (s, 1H), 7.99 (s, 1H), 7.88 (dd, J = 7.94 Hz, 3H), 7.56 (ddd, J = 7.63 Hz, 3H), 7.41 (d, 2H), 7.28 (d, 2H), 4.90 (s, 1H), 4.11 (m, 1H), 3.69 (q, 1H), 1.48 (t, J = 1.52, 3H) 1.22 (dd, 2H), 1.20 (t, 1H); **^{13}C NMR** (at 100 MHz, using $CDCl_3$) δ ppm : 183.64, 174.33, 167.77, 162.78, 147.19, 134.26, 131.66, 129.95, 128.97, 126.97, 121.67, 42.93; **MS** m/z (ES^+): 445.13.

5.1.1.2.5. 4'-((5-(naphthalen-2-ylmethylene)-2,4-dioxothiazolidin-3-yl) methyl)-[1,1'-biphenyl]-2-carbonitrile (NT5)

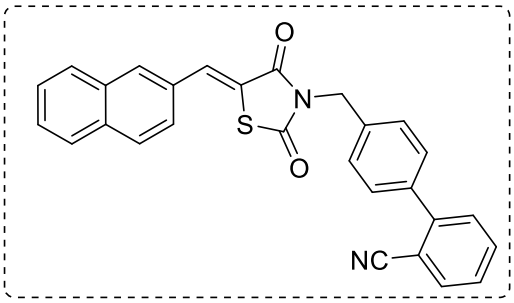

Yield: 82 %; Dark Brown Powder, M.P: 248-250 °C; **FT-IR** (KBr) $\bar{\nu}$/cm^{-1}: 3502, 3116, 1670, 1607; **^{1}H NMR** (at 500 MHz, using $CDCl_3$), δ ppm: 8.09 (s, 1H), 8.01 (s, 1H), 7.90 (m, J =7.89Hz, 2H),7.86 (m, J=8.85Hz, 1H), 7.76 (dd, J=7.74Hz, 1H), 7.64 (t, J =7.62Hz, 1H),7.56 (m, J=7.55Hz, 7H) 7.45 (m, J=7.43Hz, 2H), 4.99 (s, 2H); **^{13}C NMR** (at 100 MHz, using $CDCl_3$) δ ppm: 168.09, 166.06, 153.15, 144.88, 138.22, 137.93, 135.63, 134.66, 130.63, 128.97, 126.54, 121.66, 111.46, 44.82; **MS** m/z (ES^+): 466.11.

5.1.1.2.6. 5-(naphthalen-2-ylmethylene)-3-(pyridin-3-ylmethyl) thiazolidinedione (NT6)

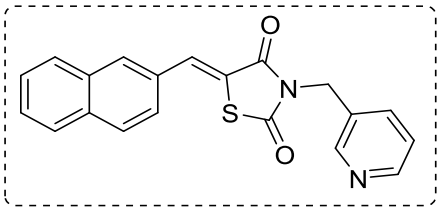

Yield:87 %; Pale yellow Powder; M.P: 231-234 °C; **FT-IR** (KBr) $\bar{\nu}$/cm^{-1}: 2925, 1740, 1685, 1142; **^{1}H NMR** (at 500 MHz, using $CDCl_3$), δ ppm: 8.74 (d, J = 2.3 Hz, 1H), 8.58 (dd, J = 4.9, 1.6 Hz, 1H), 8.08 (s, 1H), 8.00 (s, 1H), 7.91 (dd, J = 7.90 Hz, 1H), 7.85 (d, J = 7.85 Hz, 1H), 7.80 (d, J = 7.79 Hz, 3H), 7.57 (m, J = 7.56 Hz, 2H), 7.30 (m, J=7.28Hz, 3H), 4.94 (s, 2H); **^{13}C NMR** (at 100 MHz, using $CDCl_3$) δ ppm: 167.77, 165.77, 150.38, 149.84, 136.77, 134.80, 133.15, 130.96, 129.15, 128.82, 128.16, 127.18, 125.83, 123.69, 42.93; **MS** m/z (ES^+): 346.08.

5.1.1.2.7. 3-((1,3-dioxo-2,3-dihydro-1H-inden-2-yl) methyl)-5-(naphthalen-2-yl methylene) thiazolidinedione (NT7)

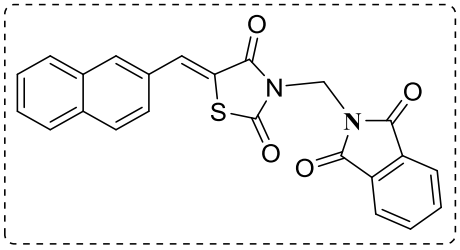

Yield: 84 %; Pale Brown Powder; M.P: 265-269 °C; **FT-IR** (KBr) $\bar{\nu}$/cm^{-1}: 2925, 1740, 1685, 1142; **^{1}H NMR** (at 500 MHz, using $CDCl_3$), δ ppm: 8.08 (s, 1H), 7.98 (s, 1H), 7.91 (s, 3H), 7.77 – 7.75 (m, 4H), 7.56 (d, *J* = 7.8 Hz, 3H), 5.70 (s, 2H); **^{13}C NMR** (at 100 MHz, using $CDCl_3$) δ ppm: 170.69, 166.73, 165.11, 162.11, 149.87, 145.84, 135.25, 134.65, 131.96, 128.32, 127.34, 126.03, 124.00, 120.70, 43.55; **MS** m/z (ES^+): 414.07.

5.1.1.2.8. 3-butyl-5-((6-methoxynaphthalen-2-yl) methylene) thiazolidinedione (NT8)

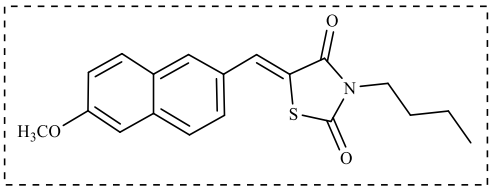

Yield: 80 %; White Colour Powder; M.P: 292-295 °C; **FT-IR** (KBr) $\bar{\nu}/cm^{-1}$: 3545, 3016, 1698, 1617; **^{1}H NMR** (at 500 MHz, using $CDCl_3$), δ ppm: 8.0 (s, 1H), 7.92 (s, 1H), 7.78 (t, *J* = 7.7 Hz, 2H), 7.56 (m, 1H), 7.21 (s, 1H), 7.13 (d, *J* = 7.1 Hz, 1H), 3.95 (s, 3H), 3.79 (t, *J* = 7.7 Hz, 2H), 1.64 – 1.62 (m, 2H), 1.39 – 1.35 (m, 2H), 0.98 (t, *J* = 7.7 Hz, 3H); **^{13}C NMR** (at 100 MHz, using $CDCl_3$) δ ppm: 165.11, 164.58, 158.47, 135.46, 134.05, 133.39, 131.41, 130.42, 128.62, 127.79, 126.79, 120.30, 105.84, 55.49, 41.81, 27.52, 22.28, 13.95; **MS** m/z (ES^+): 341.11.

5.1.1.2.9. 5-((6-methoxynaphthalen-2-yl) methylene)-3-pentylthiazolidinedione (NT9)

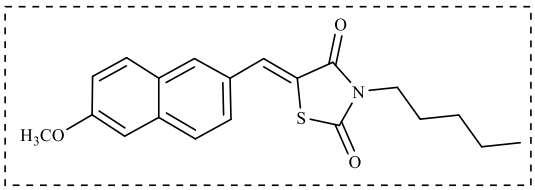

Yield: 75 %; White Colour Powder; M.P: 297-298 °C, **FT-IR** (KBr) $\bar{\nu}/cm^{-1}$: 3512, 3056, 1870, 1620; **^{1}H NMR** (at 500 MHz, using $CDCl_3$), δ ppm: 8.1 (s, 1H), 7.92 (s, 1H), 7.80 (t, *J* = 7.7 Hz, 2H), 7.56-7.54 (m, 1H), 7.21 (s, 1H), 7.13 (d, *J* = 7.1 Hz, 1H), 3.95 (s, 3H), 3.76 (t, *J* = 7.7 Hz, 2H), 1.72 – 1.67 (m, 2H), 1.36 – 1.34 (m, 4H), 0.91 (t, *J* = 7.7 Hz, 3H); **^{13}C NMR** (at 100 MHz, using $CDCl_3$) δ ppm: 167.11, 165.58, 158.47, 135.46, 134.05, 133.39, 131.41, 130.42, 128.62, 127.79, 126.79, 120.30, 105.84, 55.49, 41.81, 27.52, 22.28, 13.95; **MS** m/z (ES^+):355.12.

5.1.1.2.10. 5-((6-methoxynaphthalen-2-yl) methylene)-3-octyl thiazolidinedione (NT10)

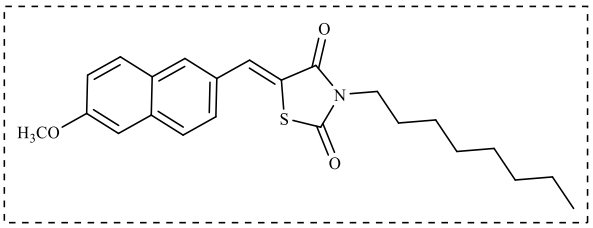

Yield: 64 %; White Colour Powder; M.P: 310-315 °C, **FT-IR** (KBr) $\bar{\nu}$/cm^{-1}: 3502, 3006, 1670, 1607; **^{1}H NMR** (at 500 MHz, using $CDCl_3$), δ ppm: 8.1 (s, 1H), 7.92 (s, 1H), 7.80 (t, *J* = 7.7 Hz, 2H), 7.56-7.54 (m, 1H), 7.21 (s, 1H), 7.13 (d, *J* = 7.1 Hz, 1H), 3.94 (s, 3H), 3.77 (t, *J* = 7.7 Hz, 2H), 1.69 – 1.66 (m, 2H), 1.33 – 1.27 (m, 12H), 0.89 (t, *J* = 7.7 Hz, 3H); **^{13}C NMR** (at 100 MHz, using $CDCl_3$) δ ppm: 168.11, 166.58, 159.47, 135.46, 134.05, 133.39, 131.41, 130.42, 128.62, 127.79, 126.79, 120.30, 105.84, 55.49, 42.09, 41.81, 28.86, 27.52, 22.28, 13.95; **MS** m/z (ES^+): 397.17.

5.1.1.2.11. 5-((6-methoxynaphthalen-2-yl) methylene)-3-(prop-2-yn-1-yl) thiazolidinedione (NT11)

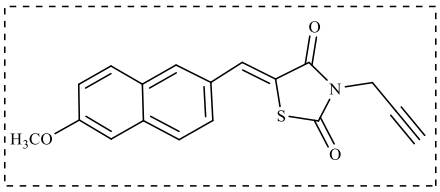

Yield: 82 %; White Colour Powder, M.P: 272-275 °C; **FT-IR** (KBr) $\bar{\nu}$/cm^{-1}: 3412, 3154, 2154, 1789, 1577; **^{1}H NMR** (at 500 MHz, using $CDCl_3$), δ ppm: 8.07 (s, 1H), 7.93 (s, 1H), 7.81 (d, J =7.8 Hz, 2H), 7.79 (dd, *J* = 7.7 Hz, 1H), 7.56-7.54 (m, 1H), 7.22 (t, *J* = 7.0 Hz, 1H), 4.53 (s 2H), 3.95 (s 3H), 3.0 (s 1H); **^{13}C NMR** (at 100 MHz, using $CDCl_3$) δ ppm: 173.31, 164.23, 157.12, 143.21, 138.90, 131.31, 129.34, 127.51, 126.26, 119.27, 116.44, 78.21, 73.24, 55.23, 32.71; **MS** m/z (ES^+): 323.06.

5.1.1.2.12. Ethyl-2-(5-((6-methoxynaphthalen-2-yl) methylene)-2,4-dioxothiazolidin-3-yl) acetate (NT12)

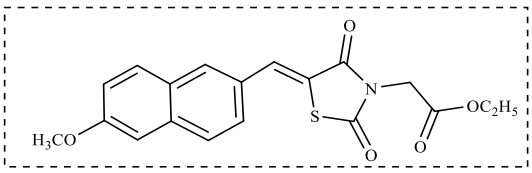

Yield: 79 %; White Colour Powder; M.P: 295-298 °C; **FT-IR** (KBr) $\bar{\nu}$/cm^{-1}: 3402, 3126, 1801, 1577, 1421; **^{1}H NMR** (at 500 MHz, using $CDCl_3$), δ ppm: 8.07 (s, 1H), 8.02 (s, 1H), 7.94 (d, J =7.8 Hz, 2H), 7.57-7.55 (m, 2H), 7.22 (dd, J = 7.2, 3.2 Hz, 1H), 7.15 (s, 1H), 4.50 (s, 1H), 1.28-1.23 (m, 2H), 3.95 (s, 3H), 1.30 (t, *J* = 7.1 Hz, 3H); **^{13}C NMR** (at 100 MHz, using $CDCl_3$) δ ppm:173.21, 167.41, 167.58, 157.01, 143.23, 138.91, 131.21, 129.3, 127.52, 126.2, 119.11, 116.25, 105.34, 61.02, 55.81, 45.70, 14.19; **MS** m/z (ES^+): 371.08

5.1.1.2.13. 3-benzyl-5-((6-methoxynaphthalen-2-yl) methylene) thiazolidinedione (NT13)

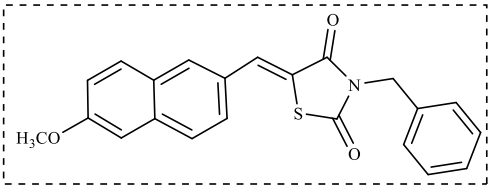

Yield: 88 %; Light white Powder; M.P: 261-265 °C; **FT-IR** (KBr) $\bar{\nu}$/cm^{-1}: 3512, 3186, 1678, 1689; **^{1}H NMR** (at 500 MHz, using $CDCl_3$), δ ppm: 8.03 (s, 1H), 7.91 (s, 1H), 7.80 (d, *J* = 7.8 Hz, 2H), 7.77 (dd, *J* = 8.8, 3.4 Hz, 1H), 7.52 (d, *J* = 7.7 Hz, 2H), 7.32 (dd, *J* = 19.2, 9.1 Hz, 3H), 7.19 (t, *J* = 7.8 Hz, 1H), 7.13 (d, *J* = 7.1 Hz, 1H), 4.92 (s, 2H), 3.94 (s, 3H); **^{13}C NMR** (at 100 MHz, using $CDCl_3$) δ ppm: 167.97, 166.32, 165.56, 159.52, 141.70 134.54, 131.50, 130.44, 128.90, 127.87, 120.07, 105.85, 55.49, 45.29; **MS** m/z (ES^+): 375.09.

5.1.1.2.14. 3-(3-chlorobenzyl)-5-((6-methoxynaphthalen-2-yl) methylene) thiazolidinedione (NT14)

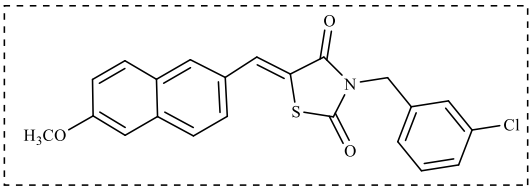

Yield: 82 %; White Colour Powder; M.P: 282-285 °C; **FT-IR** (KBr) $\bar{\nu}$/cm^{-1}: 3517, 3126, 1650, 1590; **^{1}H NMR** (at 500 MHz, using $CDCl_3$), δ ppm: 8.05 (s, 1H), 7.94 – 7.90 (m, 1H), 7.79 (dd, J = 8.7, 3.9 Hz, 2H), 7.54 (dd, J = 8.6, 1.9 Hz, 1H), 7.44 (d, J = 2.1 Hz, 1H), 7.37 – 7.31 (m, 1H), 7.31 – 7.25 (m, 3H), 7.21 (dd, J = 9.0, 2.5 Hz, 1H), 7.14 (d, J = 2.5 Hz, 1H), 4.88 (s, 2H), 3.95 (s, 3H); **^{13}C NMR** (at 100 MHz, using

$CDCl_3$) δ ppm: 173.31, 164.45, 157.09, 143.01, 138.95, 134.21, 131.52, 129.68, 127.02, 127.54, 126.11, 125.11, 119.01, 116.25, 115.11, 55.84, 46.74 ; **MS** m/z (ES^+): 409.05 **MS** m/z (ES^+): 375.09.

5.1.1.2.15. 5-((6-methoxynaphthalen-2-yl) methylene)-3-(3-(trifluoromethyl) benzyl) thiazolidinedione (NT15)

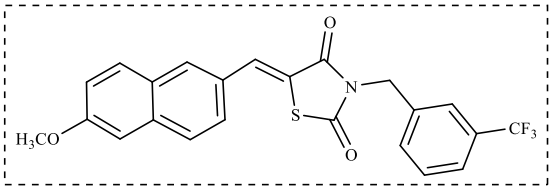

Yield: 79 %; White Colour Powder; M.P: 271-272 °C; **FT-IR** (KBr) $\bar{\nu}/cm^{-1}$: 3502, 3116, 1670, 1607; **^{1}H NMR** (at 500 MHz, using $CDCl_3$), δ ppm: 8.05 (s, 1H), 7.92 (s, 1H), 7.79 (dd, *J* = 8.8, 3.4 Hz, 3H), 7.65 (d, *J* = 7.7 Hz, 1H), 7.56 (dd, *J* = 19.2, 9.1 Hz, 2H), 7.47 (t, *J* = 7.8 Hz, 1H), 7.24 – 7.10 (m, 2H), 4.96 (s, 2H), 3.95 (s, 3H); **^{13}C NMR** (at 100 MHz, using $CDCl_3$) δ ppm: 167.77, 166.06, 161.01, 137.25, 134.24, 133.89, 131.45, 129.09, 128.80, 128.04, 127.90, 125.14, 121.66 100.29, 55.39, 45.34, 21.31; **MS** m/z (ES^+): 443.08

5.1.1.2.16. 3-(3,5-dimethoxybenzyl)-5-((6-methoxynaphthalen-2-yl) methylene) thiazolidinedione (NT16)

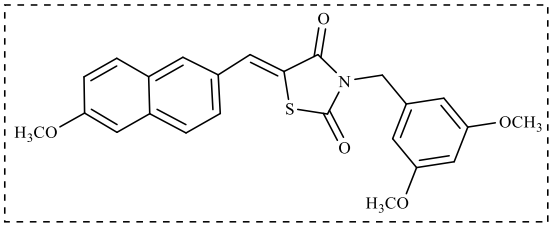

Yield: 84 %; Pale Yellow Colour Powder ; M.P: 282-285 °C; **FT-IR** (KBr) $\bar{\nu}/cm^{-1}$: 3454, 3256, 3084, 1692, 1611; **^{1}H NMR** (at 500 MHz, using $CDCl_3$), δ ppm: 8.0 (s, 1H), 7.92 (s, 1H), 7.81 (s, 1H), 7.78 (m, 2H), 7.55 (t, *J* = 7.5 Hz, 1H), 7.19 (s, 1H), 7.14 (d, *J* = 7.1 Hz, 1H), 6.59 (d, *J* = 6.5 Hz, 2H), 6.35 (t, *J* = 6 Hz, 1H), 4.85 (s, 2H), 3.95 (s, 3H), 3.78 (s, 6H); **^{13}C NMR** (at 100 MHz, using $CDCl_3$) δ ppm: 173.24, 164.45, 161.42, 161.42, 157.92, 143.65, 138.95, 131.45, 129.35, 127.51, 126.52, 161.42, 119.25, 116.25, 105.52, 103.25, 98.41, 55.84, 47.82.**MS** m/z (ES^+): 435.11.

5.1.1.2.17. 4'-((5-((6-methoxynaphthalen-2-yl) methylene)-2,4-dioxothiazolidin-3-yl) methyl)-[1,1'-biphenyl]-2-carbonitrile (NT17)

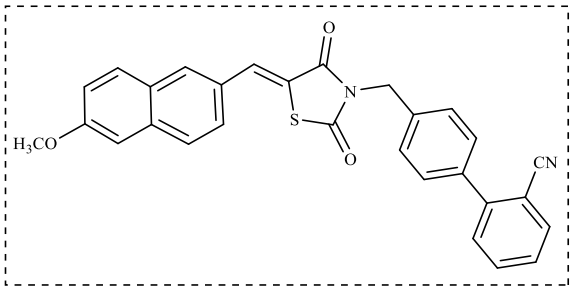

Yield: 87 %; Brown Colour Powder; MP: 290-294 °C; **FT-IR** (KBr) $\bar{\nu}$/cm^{-1}: 3502, 3116, 2054, 1610, 1598; **^{1}H NMR** (at 500 MHz, using $CDCl_3$), δ ppm: 8.06 (s, 1H), 7.93 (d, J = 1.8 Hz, 1H), 7.82 – 7.74 (m, 3H), 7.63 (td, J = 7.7, 1.4 Hz, 1H), 7.61 – 7.51 (m, 5H), 7.46 (ddd, J = 16.5, 7.8, 1.2 Hz, 2H), 7.21 (dd, J = 9.0, 2.5 Hz, 1H), 7.14 (d, J = 2.5 Hz, 1H), 4.98 (s, 2H), 3.95 (s, 3H); **^{13}C NMR** (at 100 MHz, using $CDCl_3$) δ ppm: 176.33, 162.67, 159.03, 133.86, 132.73, 130.46, 129.05, 127.56, 125.77, 120.14, 119.01, 106.82, 105.69, 55.42, 50.28; **MS** m/z (ES^+): 476.12.

5.1.1.2.18. 5-((6-methoxynaphthalen-2-yl) methylene)-3-(pyridin-3-ylmethyl) thiazolidinedione (NT18)

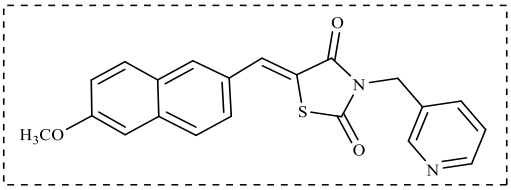

Yield: 78 %; Pale Yellow Powder; M.P: 264-265 °C, **FT-IR** (KBr) $\bar{\nu}$/cm^{-1}: 3502, 3116, 1670; **^{1}H NMR** (at 500 MHz, using $CDCl_3$), δ ppm: 8.74 (dd, *J* = 2.3, 0.9 Hz, 1H), 8.57 (dd, *J* = 4.8, 1.6 Hz, 1H), 8.05 (s, 1H), 7.92 (d, *J* = 1.8 Hz, 1H), 7.79 (ddd, *J* = 8.5, 3.7, 1.5 Hz, 3H), 7.54 (dd, *J* = 8.6, 1.9 Hz, 1H), 7.28 (ddd, *J* = 7.9, 4.8, 0.9 Hz, 1H), 7.21 (dd, *J* = 9.0, 2.5 Hz, 1H), 7.14 (d, *J* = 2.5 Hz, 1H), 4.93 (s, 2H), 3.95 (s, 3H); **^{13}C NMR** (at 100 MHz, using $CDCl_3$) δ ppm: 173.32, 164.47, 157.01, 148.71, 147.32, 143.38, 138.92, 135.52, 132.52, 131.32, 129.62, 127.52, 123.02, 119.12, 105.21, 55.82, 47.21; **MS** m/z (ES^+): 376.09.

5.1.2. Part-II: *In vitro* antidiabetic and antioxidant studies

5.1.2.1 *In vitro* antidiabetic activity

We further evaluated all the synthesized naphthalene-based thiazolidinediones derivatives (**NT1-NT18**) for the screening of antidiabetic activity. The intestinal α-glucosidase (IAG) and pancreatic α-amylase (PAA) are significant targets in the treatment of diabetes due to its involvement in digestion of carbohydrates and its absorption into human body. By restricting the activity of these two enzymes can lower the risk of developing diabetes and postprandial hyperglycaemia (159,225).

Table 5.2: *In-vitro* PAA and IAG inhibition activity of compounds (**NT1-NT18**)

Compound	PAA Percentage inhibition (%)	PAA inhibition activity IC_{50} (µM)	IAG Percentage inhibition (%)	IAG inhibition activity IC_{50} (µM)
NT1	87.22	9.22 ± 0. 11	85.74	11.715 ± 0. 17
NT2	91.12	8.14 ± 0. 17	86.25	10.158 ± 0. 11
NT3	86.24	10.23 ± 0. 10	80.17	14.258 ± 0. 17
NT4	83.65	13.45 ± 0. 13	94.23	5.245 ± 0. 18
NT5	90.78	8.84 ± 0. 14	88.58	9.582 ± 0. 12
NT6	84.21	11.12 ± 0. 16	84.12	12.251 ± 0. 08
NT7	94.58%	5.156 ± 0. 10	96.78	3.148 ± 0. 16
NT8	75.25	20.121 ± 0. 03	76.69	18.151 ± 0. 06
NT9	71.12	22.104 ± 0. 04	73.74	19.196 ± 0. 02
NT10	68.52	24.152 ± 0. 05	60.15	22.178 ± 0. 07
NT11	78.32	16.785 ± 0. 07	79.58	15.105 ± 0. 07
NT12	73.39	21.878 ± 0. 06	71.65	20.985 ± 0. 07
NT13	92.24	7.456 ± 0. 10	90.14	6.148 ± 0. 01
NT14	91.89	7.683 ± 0. 06	89.24	6.683 ± 0. 06

NT 15	93.45	6.432 ± 0. 10	91.75	5.432 ± 0. 10
NT16	80.44	15.421 ± 0. 02	81.54	13.421 ± 0. 02
NT17	96.47	4.488 ± 0. 10	98.12	2.145 ± 0. 16
NT18	76.56	18.124 ± 0. 05	78.25	16.124 ± 0. 05
Acarbose	88.45	12.455 ± 0. 06	90.15	9.145 ± 0. 14

5.1.2.1.1. *In vitro* PAA inhibition activity

To assess the antidiabetic effect of **NT1-NT18**, the PAA inhibition assay was performed by using acarbose as the standard. The newly synthesized compounds were evaluated for their *in vitro* PAA activity using acarbose as a positive control at various concentrations (0, 2.5, 10, 25, 50, 100, 250, 500 µg/mL) and IC_{50} valves were calculated and listed in the table 5.2. The results of the PAA assay conducted to determine the antidiabetic activity, using as series of compounds **NT1-NT18**, revealed a remarkable inhibitory effect on PAA enzyme. The percentage inhibition ranged up to 96.47 % with in the series, with corresponding IC_{50} values spanning from 4.48 µM to 24.15 µM against PAA enzyme. In comparison, the reference compound acarbose exhibited an IC_{50} value 12.45 µM and a percentage inhibition of 88.45 %. As results states that all tested compounds shown significant PAA enzyme inhibition activity at the dose of 50 (µg/mL). Among the all compounds, **NT17** (96.47 %, 4.48 µM) and **NT7** (94.58 %, 5.15 µM) were found to be the most potent compared to standard Acarbose (Figure 33).

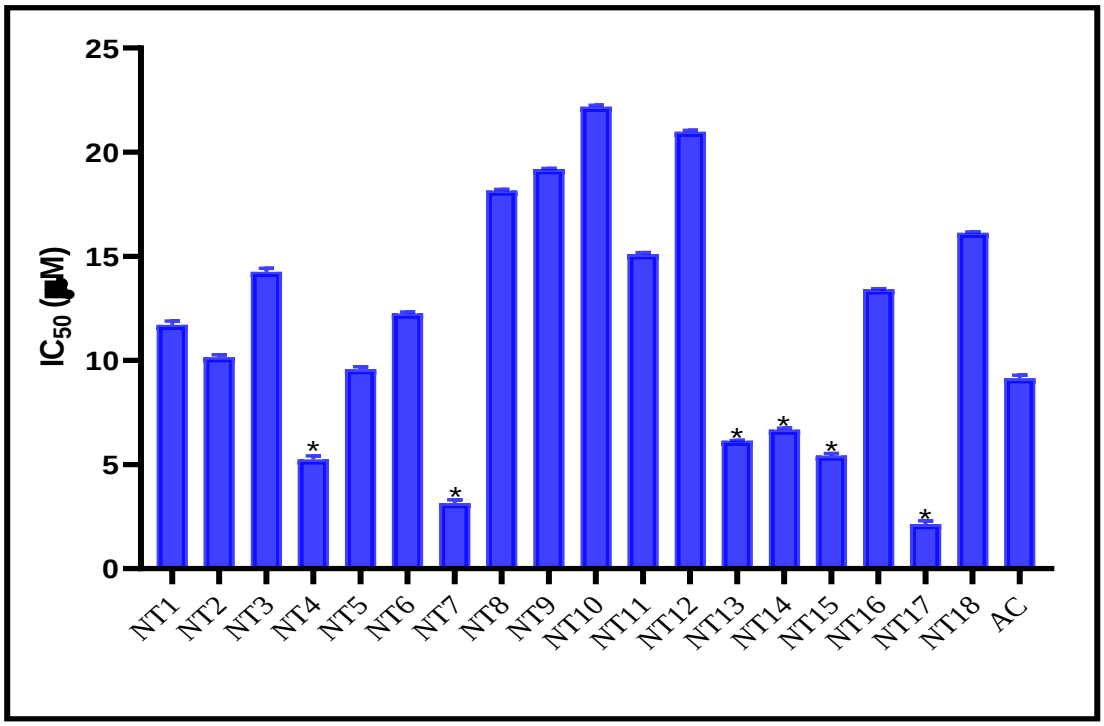

*p < 0.05 as compared with acarbose (AC), statistical one-way ANOVA followed by Dunnett's 't' test.

Figure 33: *In-vitro* PAA inhibition activity of compounds (**NT1-NT18**).

5.1.2.1.2. *In vitro* IAG inhibition activity

To assess the antidiabetic activity of synthesised naphthalene-based thiazolidinedione derivatives (**NT1-NT18**), the IAG inhibition assay is performed using the acarbose. The inhibition profile of each synthesized compounds was tested for their ability to inhibit IAG enzyme, percentage of inhibition and IC_{50} values presented in table 5.2. The percentage inhibition arranged up to 98.12 % within the series, with corresponding IC_{50} values spanning from 2.145 µM to 20.98 µM against IAG enzyme. In comparison, the reference compound Acarbose exhibited an IC_{50} value 9.14 µM and a percentage inhibition of 98 %. As results states that all tested compounds shown significant IAG enzyme inhibition activity at the dose of 50 (µg/mL). Among the all compounds, **NT17** (98.12 %, 2.14 µM) and **NT7** (96.78 %, 3.14 µM) were found to be the most potent compared to standard Acarbose and followed by compounds **NT4**, **NT15** and **NT13** with IC_{50} value 3.148, 5.245, and 5.432 µM respectively (Figure 34).

Generally, it was abridged based on the above-mentioned observation that PAA inhibition activity of thiazolidinedione-naphthalene analogues (**NT1-NT18**) was largely affected by the introduction of substituents, the group type and position with respect to the phenyl ring can vary. Moreover, the inhibitory potential was also impacted by the introducing methoxy (-OCH_3 at 5th position) on naphthalene ring (**NT8-NT18**).

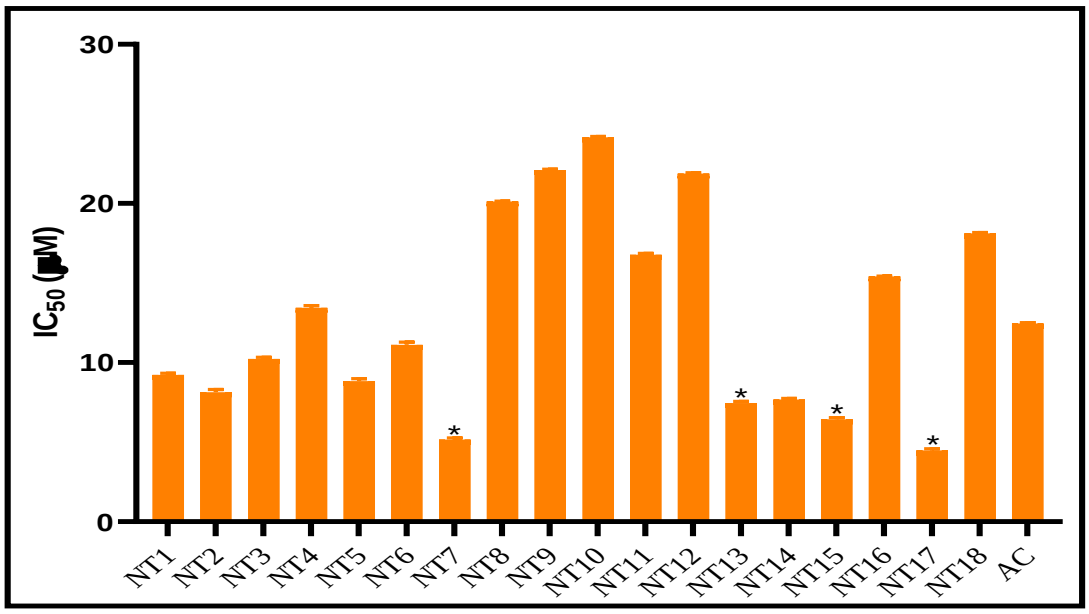

*p < 0.05 as compared with acarbose (AC), statistical one-way ANOVA followed by Dunnett's 't' test

Figure 34: *In-vitro* IAG inhibition activity of compounds (**NT1-NT18**)

5.1.2.2. *In vitro* antioxidant activity

Antioxidant agents safeguard cells from reactive oxygen species (ROS), thereby preventing diabetes caused by ROS and oxidative stress. ROS cause protein glycation, lipid peroxidation, DNA damage and enzyme inactivation which can be neutralized by endogenous or exogenous antioxidant systems (Alminderej et al., 2020).

Table 5.3: *In-vitro* Antioxidant activity of compounds (**NT1-NT18**)

Compound	Antioxidant activity IC_{50} (µM)
NT1	21.894 ± 0.42
NT2	19.472 ± 0.45
NT3	25.174 ± 0.18
NT4	31.274 ± 0.19

NT5	13.012 ± 0.64
NT6	29.134 ± 0.12
NT7	8.014 ± 0.21
NT8	30.144 ± 0.19
NT9	28.174 ± 0.15
NT10	37.24 ± 0.18
NT11	30.371 ± 0.11
NT12	32.385 ± 0.18
NT13	23.844 ± 0.15
NT14	16.218 ± 0.14
NT15	14.419 ± 0.17
NT16	35.185 ± 0.08
NT17	6.376 ± 0.12
NT18	19.917 ± 0.65
Ascorbic acid (AA)	8.98 ± 0.061

The antioxidant activity was studied for the **NT1-NT18**, using the stable DPPH assay. The antioxidant result was graphically represented in the figure 35. As per the observation, free radical scavenging effect is rising as such like **NT17 > NT7 > NT5 > NT15 > STD >NT13 > NT18 > NT2 > NT1**. Few compounds like **NT6**, **NT4** and **NT16,** all the remaining compounds possess good to moderate antioxidant activity than standard (ascorbic acid) compound (Table 5.3).

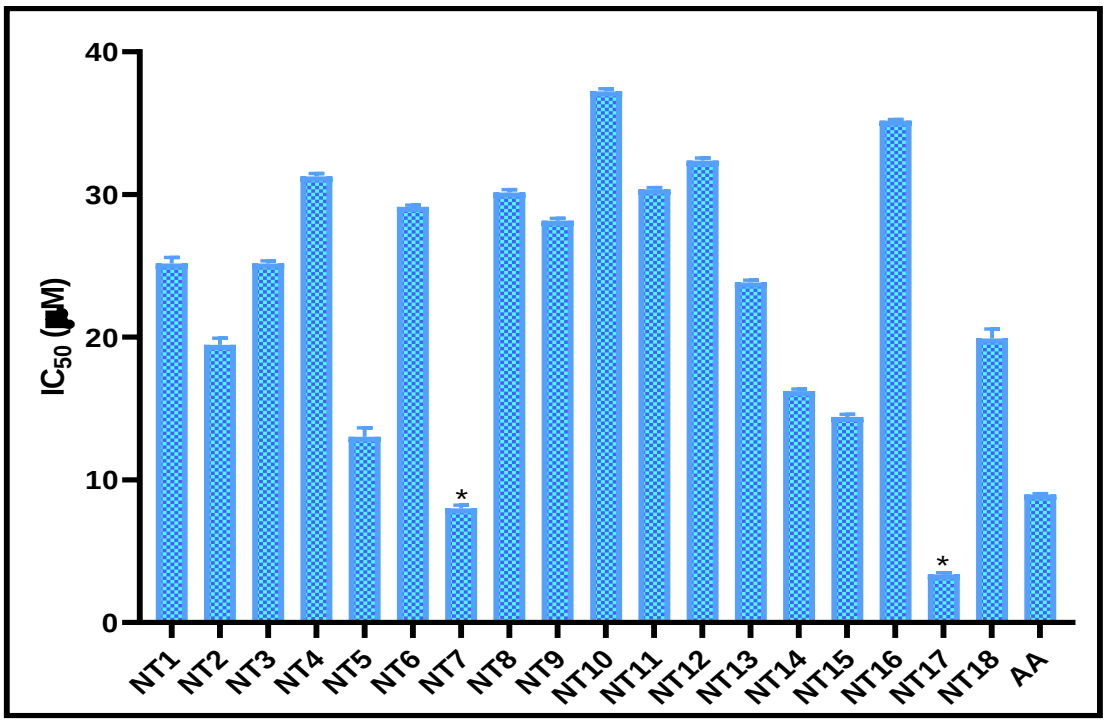

*p < 0.05 as compared with ascorbic acid (AA), statistical one-way ANOVA followed by Dunnett's 't' test

Figure 35: *In-vitro* antioxidant activity of compounds (**NT1-NT18**).

5.1.3. *In silico* validation

5.1.3.1. Molecular Docking Studies

After conducting *in vitro* analysis of synthesized compounds molecular docking studies were performed using autodock Vina 1.5.4. The PAA (**PDB ID: 4W93**) and IAG (**PDB ID: 3A4A**) protein was downloaded from the PDB portal and subsequent docking analysis results present in the Table 5.4 Table 5.5. Subsequently, BIOVIA discovery studio visualizer was exploited to authenticate the 2D and 3D interactions of the docked ligands (Figure 36 and Figure 37).

Table 5.4: Molecular docking interaction of compounds (**NT1-NT8**) with PAA (**4W93**)

Compounds	**Binding affinity (Kcal/mol)**	***H*-Bond**	**π – π T Shaped**	**π- alkyl/alkyl**	**π – σ Bond**	**π- Sulphur**
NT1	-9.3	--	Trp59	Ile235	Trp59, Try62, Ile235	Trp58, Tyr62, His299
NT2	-9.6	--	--	Trp58, Tyr62, Ala198, His299	Trp59, Try62	--
NT3	-9.2	Arg195	--	Leu165, Ala198, His201, Lys200, Ile235	Thr163, Leu54	Trp58, Tyr62, His299
NT4	-9.3	Arg195	Trp59, Tyr62	Leu165, Ala198	Leu162, Thr163	Trp58 Tyr62, His299
NT5	-10.1	--	His20, Trp59	Leu165, Lys200	Ile235	--
NT6	-9.2	Arg195	Trp59	Leu165, Ala198	--	Trp58, Tyr62, His299
NT7	-10.3	--	Trp59, His201	Ile235, Leu162	Leu162	Trp58
NT8	-8.0	--	Trp59	Leu165, Ala198, His201, Ile235, Leu162	Thr163	Trp58, Tyr62, His299
NT9	-8.2	Thr163, Arg195	Trp59	Leu59, Ile235, Lys200, Ala198, His201, Leu162	Thr163	Trp58, Tyr62, His299
NT10	-7.6	--	Trp59	Leu162, Ala198	--	Trp58, Tyr62, His299

NT11	-8.1	Gln63	Trp59	Leu165, Ile235, His201	--	Trp58
NT12	-8.0	Arg195	Trp59, Tyr62	Leu165, Lys200, His201, Ile235	Thr163	Trp58, Tyr62, His299
NT13	-9.1	Thr163, Arg195	Trp59, His201	Tyr62, Leu165, Ala198	Leu162	Trp58, Tyr62, His299
NT14	-9.4	Thr163, Arg195	Trp59, Tyr62, His201	Ala198, Lys200, His201, Ile235	Leu162	Trp58, Tyr62, His299
NT15	-10.0	Arg195	Trp59, Tyr62, His201	Lys200, Ile235	Leu162, Thr163	Trp58, Tyr62, His299
NT16	-9.2	Thr163, Arg195	Trp59, Tyr62, His201	Lys200 Ile235, Ala198	Leu162	Trp58, Tyr62, His299
NT17	-10.7	Thr163, Arg195	Trp59, Tyr62, His201	Leu165, Ala198	Thr163, Leu162, Ile235	Trp58, Tyr62, His299
NT18	-9.1	Thr163, Arg195	Trp59, Tyr62	Leu165, Ala198	Leu162	Trp58, Tyr62, His299
Co crystal ligand	-8.7	Tyr151, Arg195, Glu240, Lys233, Lys200, Ile235	Tyr62, His299	--	--	--
Acarbose	-6.7	Thr163, Glu233, Asp300		--	--	--

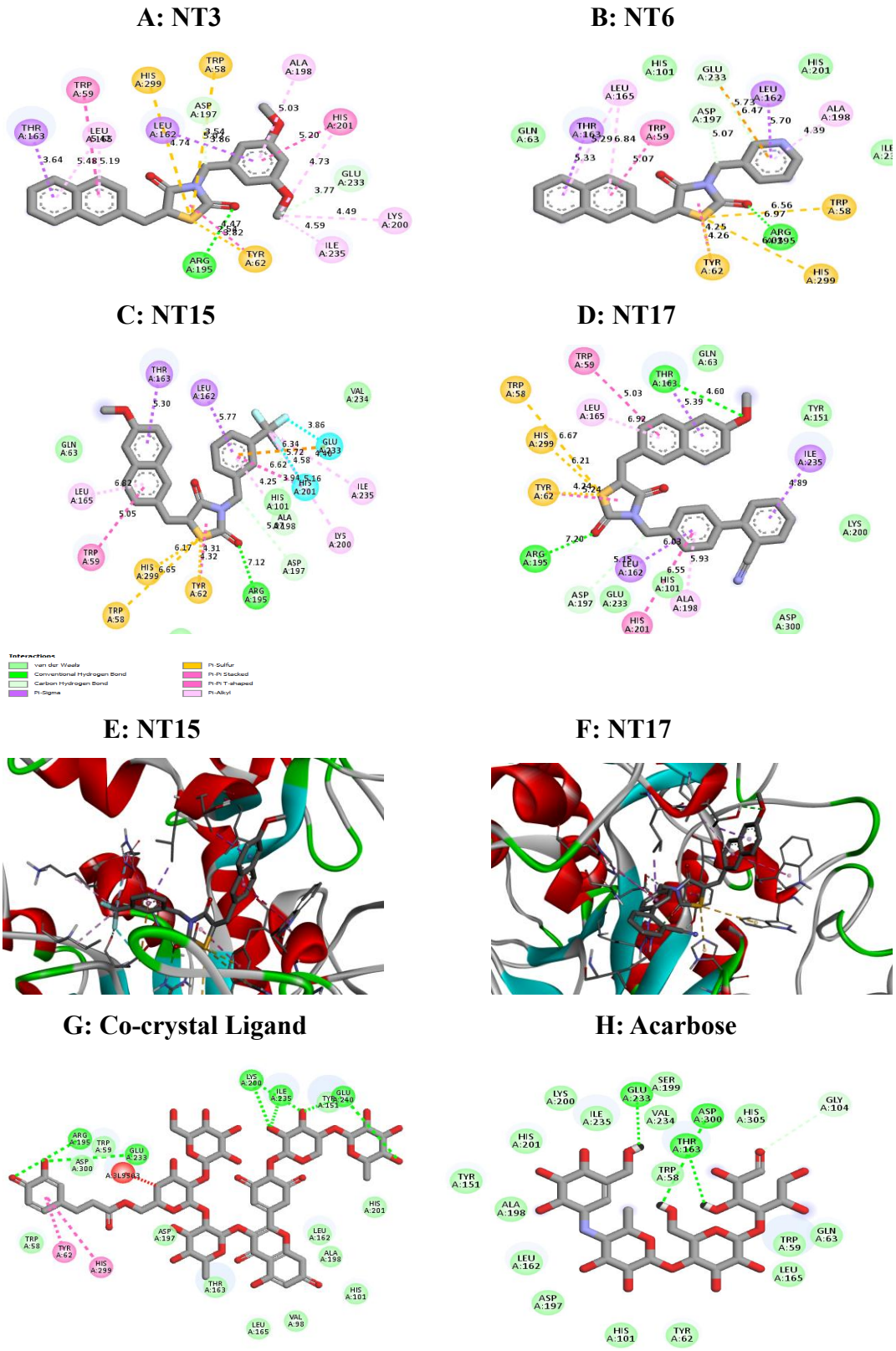

Figure 36: 2D and 3D structure of the series **NT1-NT18** with PAA (**4W93**)

Table 5.5: Molecular docking interaction of compounds (**NT1-NT8**) with IAG (**3A4A**)

Compounds	Binding affinity (Kcal/mol)	*H*-Bond	π – π T Shaped	π- alkyl/alkyl	π – σ Bond	π- Sulphur
NT1	-10.1	--	Tyr158	Lys156	Arg315	His280
NT2	-10.3	Arg315	Ser157	Lys156, Phe303	Arg315	His280
NT3	-9.7	--	His280	Lys158, Phe303, Val308, Pro312	Arg315	His280
NT4	-9.0	--	--	Val266, Arg263	Ala292	--
NT5	-10.3	Arg315	His280, Phe303	Pro312, Arg315	--	--
NT6	-9.9	--	--	Lys156	Tyr158	His280
NT7	-10.6	--	Trp15	Lys13, Arg263	Ala292	--
NT8	-8.5	Arg315	Tyr158	Lys156, Tyr158, Phe178, Val216	Tyr158	Phe314
NT9	-8.5	Gln279, Arg442	His280	Tyr158, Phe303, Pro312, Arg315	--	Tyr158, Phe159
NT10	-6.2	Thr274, Ser298	Ile262	Trp15, Arg263, Val266, Ala292	--	--
NT11	-8.4	Arg315	Tyr158	Phe178, Val216, Arg315	--	--
NT12	-8.8	Ser298, Thr274	--	Trp15, Val266, Ala292	Arg263	--
NT13	-9.9	Arg442, Arg315	Phe303	Lys156, Phe178	Arg315	--
NT14	-10.3	Arg315, Arg442	Phe303	Lys156, Tyr158	Arg315	His280

NT15	-9.5	Ser240, Ser241, Arg315, Arg442	Phe303	Lys156, Lyr158	Arg315	His280
NT16	-8.3	--	Tyr158	Lys156, Phe178	--	His280
NT17	-10.9	Arg315	His280, Phe303, Arg315	Val308, Pro312	--	---
NT18	-9.9	Arg315, Arg442	Phe303	Lys156	Arg315	His280
Co-crystal ligand	-6.9	Arg442, His112, Asp69, Asp215, Glu277, His351, Asp352, Arg213	--	--	--	--
Acarbose	-8.5	Glu271, Ser298, Thr274, Ile272, Glu296, Asn259	--	--	--	--

A: NT2

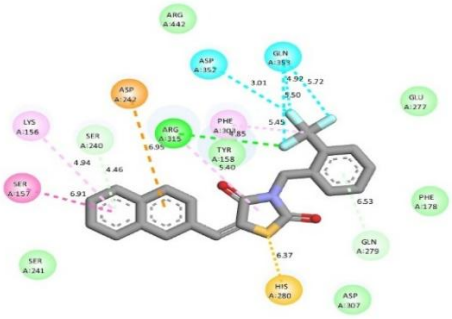

B: NT7

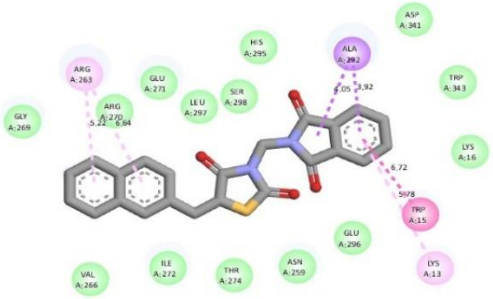

C: NT9

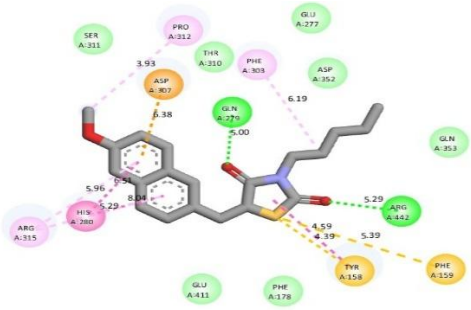

D: NT14

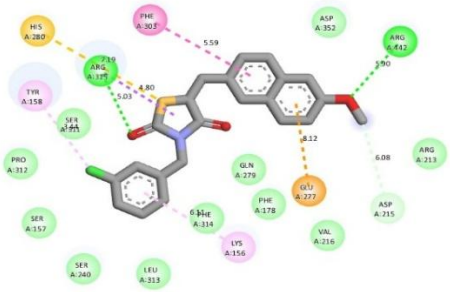

E: NT17

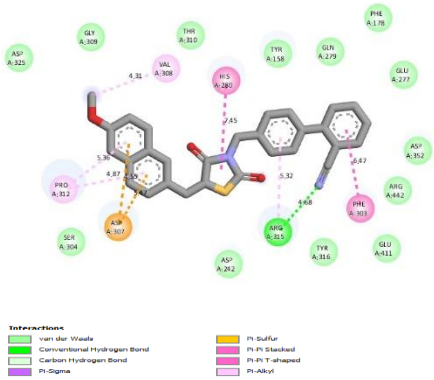

F: NT17

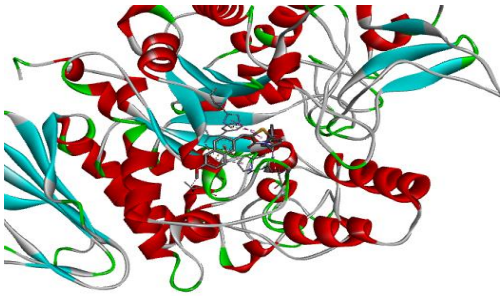

G: Co-Crystal structure

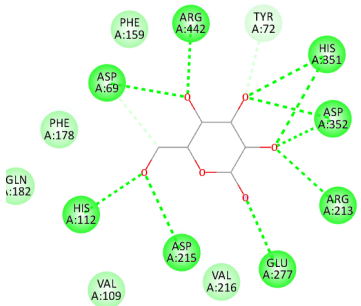

H: Acarbose

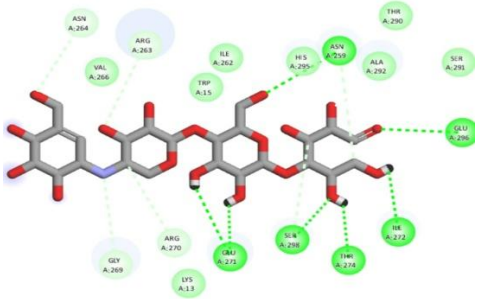

Figure 37: 2D and 3D structure of the series **NT1-NT18** with IAG (**3A4A**)

5.1.3.2. MM-GBSA validation

The MM-GBSA validation provides insight into the relative binding strengths of set of synthesized compounds with PAA (**PDBID-4W93**) and IAG (**PDBID-3A4A**) protein. These interactions include, such as coulomb interactions, hydrophobic contacts, and also hydrogen, covalent bonds. This method is reliable for assessing the how well the compounds bind to their target proteins. The overall binding free energy values for all compounds fall within the range of -21.43 to -42.59 kcal/mol with PAA and -32.23 to -62.64 kcal/mol with IAG protein. Notably, the standard drug acarbose shows ΔG binding energy of -27.58 kcal/mol and -52.83 kcal/mol with PAA and IAG respectively, but compound **NT10** exceeds this valve of -42.59 kcal/mol with PAA receptor and -62.64 kcal/mol with IAG receptor. Conversely, other energy like ΔG bind covalent (covalent energy) do not significantly contributed to targets. Additionally, compounds **NT7**, **NT1** and **NT5** display good binding energies of -40.69, -40.68, -40.65 kcal/mol with PAA protein. Ans also compounds **NT7**, **NT5**, **NT14** and **NT12** displays good binding energies of -53.46, -53.07, -51.20 and -50.07 kcal/mol with IAG receptor (Table 5.6 and Table 5.7).

Table 5.6: Calculation of binding free energy using the Prime/MM-GBSA method for **PDB ID: 4W93**

Compounds	ΔG bind (Kcal/ mol)	ΔG bind Coulomb	ΔG bind covalent	ΔG bind H Bond	ΔG bind vdW	ΔG bind Lipophilic
NT1	-40.68	-40.84	-0.65	-2.91	-25.28	-10.97
NT2	-42.58	-20.11	6.08	-3.42	-30.61	-13.90
NT3	-40.65	-23.14	2.29	-2.02	-23.86	-13.59
NT4	-29.39	-10.98	1.26	-0.65	-31.63	-12.77
NT5	-40.65	-23.14	2.29	-2.02	-23.86	-13.59
NT6	-25.28	-13.00	-0.71	-1.46	-28.04	-9.85
NT7	-40.69	-40.84	-0.65	-2.91	-25.28	-10.97
NT8	-31.15	-10.45	-0.97	-0.75	-28.99	-13.46
NT9	-26.51	-8.53	0.02	-0.72	-31.20	-13.37
NT10	-42.59	-20.11	6.08	-3.42	-30.61	-13.90
NT11	-30.88	-10.05	0.66	-0.68	-25.21	-9.68
NT12	-22.01	-18.18	1.11	-1.09	-20.54	-7.23
NT13	-30.63	-9.09	1.11	-0.66	-26.15	-10.86
NT14	-38.53	-14.54	-0.73	-0.75	-32.25	-13.02
NT15	-27.45	-8.62	-0.09	-0.73	-29.68	-13.60
NT16	-21.43	-18.40	4.13	-1.84	-24.80	-8.07
NT17	-24.25	-12.89	0.86	-0.97	-22.50	-10.01
NT18	-25.97	-5.34	-1.05	-0.75	-28.75	-16.13
Acarbose	-27.58	-16.97	-0.77	-0.73	-22.67	-10.15

Δ G bind: free energy of binding; ΔG bind Coulomb: Coulomb free energy; ΔG bind covalent: internal or covalent energy; ΔG bind vdW: van der Waal force or energy; ΔG bind H Bond: free hydrogen bonding energy; ΔG bind Lipophilic: hydrophobic energy.

Table 5.7: Calculation of binding free energy using the Prime/MM-GBSA method for **PDB ID: 3A4A**

Compounds	ΔG bind (Kcal/ mol)	ΔG bind Coulomb	ΔG bind covalent	ΔG bind H Bond	ΔG bind vdW	ΔG bind Lipophilic
NT1	-41.64	-18.97	6.75	-3.17	-25.37	-31.78
NT2	-32.23	-28.29	4.83	-4.91	-54.75	-36.39
NT3	-46.59	-26.94	10.90	-1.61	-28.49	-30.52
NT4	-37.30	-10.37	5.13	-0.90	-47.33	-27.43
NT5	-53.07	0.33	2.88	-0.36	-50.33	-26.57
NT6	-33.55	-23.48	3.51	-1.37	-39.87	-26.16
NT4	-37.30	-10.37	5.13	-0.90	-47.33	-27.43
NT7	-53.46	-20.69	4.01	-0.72	-43.10	-25.33
NT8	-37.05	-10.26	0.95	-0.62	-46.35	-30.27
NT9	-38.67	-11.78	0.93	-0.62	-45.62	-31.23
NT10	-62.64	-99.97	6.75	-5.17	-54.37	-37.78
NT11	-24.46	-8.54	7.21	-0.70	-47.76	-34.66
NT12	-50.07	0.33	2.88	-0.36	-50.33	-26.57
NT13	-39.65	-12.18	2.77	-0.62	-49.23	-33.39
NT14	-51.20	-7.74	1.67	-0.13	-45.42	-27.40
NT15	-37.99	-20.37	3.13	-0.98	-43.35	-28.06
NT16	-39.75	-11.65	0.90	-0.62	-45.05	-31.13
NT17	-40.74	-9.30	2.45	-0.60	-51.53	-34.45
NT18	-48.58	-9.65	2.47	-0.21	-44.11	-29.51
Acarbose	-52.83	-8.02	2.93	-0.21	-46.24	-29.92

Δ G bind: free energy of binding; ΔG bind Coulomb: Coulomb free energy; ΔG bind covalent: internal or covalent energy; ΔG bind vdW: van der Waal force or energy; ΔG bind H Bond: free hydrogen bonding energy; ΔG bind Lipophilic: hydrophobic energy

5.1.3.3. Molecular properties

The drug-like properties were assessed using Lipinski's rule of five (LR5), which states the oral bioavailable drugs as small molecules, must have a molecular weight (MW) of equal or less than 500 Daltons, hydrogen bonds (donor) are not more than 5, the hydrogen bond (acceptors) are equal or less than 10, and a partition coefficient (LogP) should not greater than 5 or 6.5.These parameters are crucial in evaluating their suitability for oral bioavailability and drug-likeness. The results demonstrate that all the compounds (**NT1-NT18**) as desired physicochemical properties without any deviations from the established standard ranges, as outlined in table 5.8.

5.1.3.4. Absorption, distribution, metabolism, and excretion and toxicity prediction

The study evaluated the pharmacokinetics properties of synthesized compounds (**NT1-NT18**) using Swiss ADME online server and toxicity report using OSIRIS property explorer, results were summarized in table 5.9. In general evaluation of

absorption, distribution, metabolism, excretion and toxicity (ADMET), properties of all compounds demonstrated high oral absorption characteristics. However, when it comes to their ability to enter the central nervous system (CNS), as indicated by their blood/brain coefficients (BBB), majority of the compounds displayed less permeability. Additionally, the results show that none of the synthetic compounds are P-glycoprotein (P-gp) substrates. The metabolic distribution properties of compounds are predicted by the behaviour of cytochrome P450 and its isoform enzymes. Lower pharmacokinetic drug interactions were seen for certain of the drugs with specific isoenzyme inhibitors, including CYP2C19, CYP1A2, CYP2C9, and CYP3A4. The OSIRIS tool is used to evaluate the possible toxicity of these produced chemicals. It contains mutagenicity, irritation, effects on reproduction, and tumorigenicity. In table 5.9 a green tone indicates a lack of mutagenic, tumorigenic, reproductive and irritant toxicity, suggesting that the compounds have favourable drug-related qualities.

Table 5.8: Prediction of drug likeness of compounds (**NT1-NT18**)

Compound	MW (g/mol)	HB(D)	HB (A)	LogP	MR	RB	TPSA (A)	No. Rings	No. Carbons	No. HA	Drug likeness					BV Score
Acceptable range	**≤ 500**	**≤ 5**	**≤ 10**	**-2.0 to 6.5**	**40-130**	**≤ 15**	**≤ 140**	**≤ 7**	**> 4**	**> 1**	**LR-5**	**Ghose**	**Veber**	**Egan**	**Muegge**	**0.55**
NT1	413.41	0	5	5.22	111.0	4	62.68	4	22	2	N	N	Y	N	N	0.55
NT2	413.41	0	5	5.23	111.0	4	62.68	4	22	2	N	N	Y	N	N	0.55
NT3	405.47	0	4	4.19	119.0	5	81.14	4	23	2	Y	Y	Y	Y	N	0.55
NT4	445.53	0	4	4.86	131.5	7	88.98	3	26	2	Y	N	Y	Y	N	0.55
NT5	446.52	0	3	5.29	136.1	4	86.47	4	28	2	Y	N	Y	N	N	0.55
NT6	346.40	0	3	3.47	103.8	3	75.57	3	20	3	Y	Y	Y	Y	Y	0.55
NT7	413.45	0	4	3.77	121.3	3	100.0	4	23	3	Y	Y	Y	Y	Y	0.55
NT8	341.11	0	3	3.95	102.4	5	71.91	3	19	2	Y	Y	Y	Y	Y	0.55
NT9	355.12	0	3	4.30	107.2	6	71.91	3	20	2	Y	Y	Y	Y	N	0.55
NT10	397.53	0	3	5.38	121.6	9	71.91	3	23	3	Y	N	Y	Y	N	0.55
NT11	323.06	0	3	3.24	95.81	3	71.91	3	18	2	Y	Y	Y	Y	Y	0.55
NT12	371.08	0	5	3.04	103.7	6	98.21	3	19	2	Y	Y	Y	Y	Y	0.55
NT13	375.44	0	3	4.19	112.5	4	71.91	3	22	2	Y	Y	Y	Y	N	0.55
NT14	409.05	0	3	4.73	117.2	4	71.91	4	22	2	Y	Y	Y	Y	N	0.55
NT15	443.44	0	6	5.22	117.5	5	71.91	3	23	2	Y	N	Y	N	N	0.55
NT16	435.49	0	5	4.19	125.5	6	90.37	4	24	2	Y	Y	Y	Y	N	0.55
NT17	476.55	0	4	5.27	142.6	5	95.70	5	29	2	Y	N	Y	N	N	0.55
NT18	376.43	0	4	3.44	110.3	4	84.80	4	21	2	Y	Y	Y	Y	Y	0.55
Acarbose	645.60	14	19	6.41	136.6	9	321.17	4	25	-	N	N	N	N	N	0.17

MW: Molecular weights; **HB(D)**: Hydrogen bond donor; **HB(A)**: Hydrogen bond acceptor; **QplogPo/w**: partition coefficient; **MR**: Molar refractivity; **RB**: Rotatable bonds; **tPSA**: Total polar surface area; **No. HA**: Number of heterocyclic atoms; **BV Score**: Bioavailability score

Table 5.9: Absorption, distribution, metabolism and toxicity properties of synthesized compounds (**NT1-NT18**)

Compound	% of Human oral absorption	HI Absorption	BBB Permeation	CYP1A2 Inhibitors	CYP2C19 Inhibitors	CYP2C9 Inhibitors	CYP2D6 Inhibitors	CYP3A4 Inhibitors	P-gp substrate	Mutagenic	Tumorigenic	Reproductive effect	Irritant
NT1	94	High	No	Yes	No	Yes	No	No	No	G	G	G	G
NT2	97	High	No	Yes	No	Yes	No	No	No	G	G	G	R
NT3	93	High	Yes	Yes	Yes	Yes	No	Yes	No	G	G	G	G
NT4	94	High	No	No	No	Yes	No	Yes	No	G	G	G	G
NT5	93	High	No	No	No	Yes	No	Yes	No	G	G	G	R
NT6	93	High	No	Yes	Yes	Yes	No	Yes	No	G	G	G	G
NT7	98	High	No	Yes	Yes	Yes	No	Yes	No	G	G	Y	G
NT8	95	High	No	Yes	Yes	Yes	No	Yes	No	G	G	G	G
NT9	98	High	No	Yes	Yes	Yes	No	Yes	No	G	G	G	G
NT10	92	High	No	Yes	Yes	Yes	No	Yes	No	G	G	G	G
NT11	97	High	No	Yes	Yes	Yes	No	Yes	No	G	G	G	G
NT12	98	High	No	Yes	Yes	Yes	No	Yes	No	G	G	G	G
NT13	92	High	No	Yes	Yes	Yes	No	Yes	No	G	G	G	G
NT14	95	High	No	Yes	Yes	Yes	No	Yes	No	G	G	G	G
NT15	92	High	No	Yes	Yes	Yes	No	Yes	No	G	G	G	G
NT16	90	High	No	Yes	Yes	Yes	No	Yes	No	G	G	G	G
NT17	95	High	No	Yes	No	Yes	No	Yes	No	G	G	G	G
NT18	93	High	No	Yes	Yes	Yes	No	Yes	No	G	G	G	G
Acarbose	68	High	No	No	No	No	No	No	Yes	G	G	Y	G

HI: human intestinal absorption; **BBB**: blood brain barrier; **Red (R) colour**: illustrates high toxicity tendency; **Yellow (Y) colour**: illustrates moderate toxicity tendency; **Green (G) colour**: illustrates low toxicity tendency

5.1.3.5. Discussion

The choice of substituents and groups like aliphatic and aromatic rings on the amidic nitrogen (N-3 Substitution) of thiazolidinedione core to improve its anti-hyperglycaemic activity. The synthesised N-Substituted naphthalene and methoxy thiazolidinedione derivatives (**NT1-NT17**) were substituted with aliphatic and aromatic groups exhibited different anti-hyperglycaemic activity targeting PAA and IAG enzymes. The results of *in vitro* assay and biological properties of **NT1-NT17** have shown percentage inhibition up to 96 % and 98 % and IC_{50} values in the range from 4.48 µM to 24.15 µM and 2.14 µM to 20.98 µM against PAA enzyme and IAG enzyme (Table 5.2) respectively. The compounds **NT1-NT17** exhibits different binding affinities, ranging from -7.6 to -10.7 kcal/mol with in active site of **PDB ID: 4W93** and -6.2 to -10.9 kcal/mol with in active site of **PDB ID: 3A4A** (Table 5.4 and Table 5.5). In contrast, the reference compound acarbose, displaying the IC_{50} values of 12.45 µM and 9.14 µM robust binding affinity of -6.5 kcal/mol with receptor PAA and -7.4 kcal/mol with receptors IAG receptor respectively. The strong binding was attributed to the formation of three hydrogen bonds with amino acids Thr163, Glu233 and Asp300 with in active site of **PDB ID: 4W93** (Table 5.4, Figure 36) and six hydrogen bonds with amino acids Glu271, Ser298, Thr274, Ile272, Glu296 and Asn259 with in active site of **PDB ID: 3A4A** (Table 5.5, Figure 37).

The first synthesized compounds **NT1-NT7**, features a naphthalene ring on methylene carbon and various aryl groups on nitrogen connected by an TZD central core were prepared. The FT-IR spectra of compound **NT1** demarcated absorption bands at 3381 cm^{-1} for C-H-aromatic, 2920 cm^{-1} for CH-aliphatic and the appearance of the two carbonyl (C=O) groups at 1743 cm^{-1}, 1683 cm^{-1} clearly conforms the thiazolidinedione ring in the compound.

The ^{1}H NMR spectral data of compound **NT1** confirmed two singlet peaks at δ: 4.97 ppm, consistent to -CH_2 protons attached to (-NH substituted) thiazolidinedione ring. The eleven aromatic protons were observed as multiplet in the region δ 8.08 - 7.55 and also sharp singlet peak at δ: 7.48 ppm was attributed to the -CH (double bond) proton in the compound. The ^{13}C NMR spectrum of compound **NT1** revealed distinctive peaks that correspond to its molecular structure. The two carbonyl (C=O)

carbons of the thiazolidinedione are denoted by peaks at δ: 167.79 and 166.03 ppm. The peak at δ: 135.98 ppm clear states the -CH carbon between naphthalene and thiazolidinedione ring. The ten carbons originating from the naphthalene ring were discerned by five peaks at δ: 132.33, 131.58, 130.60, 129.33, 128.85, 128.14 ppm. Additionally, a peak at δ: 44.73 ppm, clarify the identity of -CH_2 carbon. Notably, ^{1}H NMR spectral data of 5-methoxynaphthalene based thiazolidinediones (**NT8-NT18**) compounds confirmed singlet peaks at region δ: 3.46 -3.14 ppm attributed to methoxy (-OCH_3) protons attached to naphthene ring at 5th position. Moreover, mass spectrum revealed a molecular ion peak (M^+H peak) at 413.07 (m/z) and 341.11 (m/z) confirming the molecular mass of compound **NT1** and **NT8** respectively.

Remarkably, all seven compounds exhibited a substantial inhibitory effect on both PAA and IAG enzymes. All the seven compounds are shows effectively high binding affinities towards IAG enzyme ranging from -9.9 to -10.4 kcal/mol except compound **NT4**. Notably, the central core TZD carbonyl (2C=O) oxygen is engaged a strong hydrogen bond interaction at the binding pocket of both PAA (Arg195) and IAG (Arg315) enzymes. Additionally, the sulphur atom of TZD linker formed a π-Sulphur type interaction with the amino acid Trp58, Tyr62 and His299 with PAA protein and His280 with IAG protein respectively. **NT7** demonstrated a significant inhibitor effect on PAA with an IC_{50} value of 5.15 μM and IAG with an IC_{50} value of 3.14 μM diminishing antidiabetic activity among the series.

Further, to explore the impact of structural modifications on compounds **NT1-NT7**, in the pursuit of enhancing their potential against PAA and IAG proteins, eleven new analogues such as **NT8-NT18**, were synthesized via incorporating electron donating methoxy group on naphthene ring at fifth positions and various alkyl and aryl groups are substituted to an amide nitrogen on the TZD central core. The *in vitro* PAA and IAG inhibitory results, indicate the all the compounds **NT8-NT18** having a significant inhibitory impact on antidiabetic activity, achieving the remarkable IC_{50} values of 4.48 μM and 2.14 μM against PAA and IAG enzyme respectively. Out of eleven compounds, it was observed that compounds from **NT8**-**NT12** Exhibited the least activity. This could be attributed to the presence of aliphatic alkyl chain (**NT8-NT10**), propynyl (**NT11**) and ethyl acetate (**NT12**) groups substituted to an amide

nitrogen on the TZD linkage, potentially impending the molecule's optimal binding to the target PAA and IAG enzyme and consequently diminishing the antidiabetic activity.

Upon substituting the aryl groups to an amidic nitrogen on the TZD linkage along with electron donating methoxy group on naphthene ring at fifth position (**NT13-NT18**) contributed to the maximum activity, yielding an IC_{50} values of 4.48 μM and 2.14 μM (**NT17**) against PAA and IAG enzyme respectively.

Notably, compound **NT17** unveiled the highest binding affinity at -10.7 kcal/mol with receptors PAA in the series, and engaging in two hydrogen bond interactions with Thr163 and Arg195 and also shows π – π T-shaped and π- alkyl/alkyl connections with Trp59, Tyr62, Ala198 and His201 amino acid residues (226). Figure 5.3 (D) and 5.3 (F) demonstrates the 2D and 3D docking interactions of compound **NT17** with the receptor **4W93** respectively. Additionally, compound **NT17** unveiled the highest binding affinity at affinity at -10.9 kcal/mol with receptors IAG in the series, and engaging in one hydrogen bond interactions with Arg315 and also shows π – π T-shaped, π- alkyl/alkyl connections with His280, Phe303, Val 308, Pro312 and Arg315 amino acid residues. Figure 5.4 (E) and 5.4 (F) demonstrates the 2D and 3D docking interactions of compound **NT17** with the receptor **3A4A** respectively.

In summary, compound **NT17** emerged as the standout analogue in the series, featuring diphenyl carbonitrile group to the amidic nitrogen on the TZD core along with electron donating methoxy group on naphthene ring at fifth position.

5.1.3.6. Structure activity relationship (SAR)

The results of *in vitro* PAA and IAG inhibition assay and *in silico* evaluation studies revealed that the SAR of all the compounds (thiazolidinedione-naphthalene and methoxy naphthalene analogues) shown good antidiabetic activity, upright drug-likeness as well as best pharmacokinetic properties. The compound bearing diphenyl carbonitrile exhibited higher percentage of inhibition (**NT17**), followed by **NT7**. It was observed that there was no significant change in the anti-diabetic activity after introducing the alkyl chain on the nitrogen of thiazolidinedione (**NT8-NT12**). The compounds (**NT8-NT18**), with a methoxy group at the 5^{th} position on the naphthalene ring, showed an improvement in their antidiabetic activity.

5.2 Series-2 (Results and discussion)

5.2.1. Part-I: Synthesis and characterization of designed compounds

5.2.1.1. Synthesis

The proposed compounds (**QT1-QT8**) were synthesized in two steps (Scheme 2, chapter 4). Firstly, thiazolidinedione was treated with quinoline-6-carbaldehyde in the presence of piperidine, ethanol and acetic acid (Knoevenagel condensation) to give quinolin-6-ylmethylene thiazolidinedione. Further, various substituted alkyl and benzyl bromides derivatives were reacted quinolin-6-ylmethylene thiazolidinedione (-NH Substitution on to the thiazolidinedione ring) leads to formation of quinoline based thiazolidinediones (**QT1-QT8**). Initially the melting points of the synthesized compounds were compared with the similar compounds containing the thiazolidinedione as their basic moiety in the literature (227,228). Initially, melting point, molecular weight (mass spectroscopy) and percentage yield of the synthesis compounds were observed (Table 5.10), are crucial in characterization processes. Later, spectral characterization of all compounds, were performed by FT-IR, and NMR (^{1}H and ^{13}C).

Table 5.10: The physical data of compound **QT1-QT8**.

Compound	Molecular formula	MW	Melting Point (°C)	Yield (%)
QT1	$C_{17}H_{16}N_2O_2S$	312.09	134-137	68
QT2	$C_{21}H_{24}N_2O_2S$	368.16	198-200	79
QT3	$C_{18}H_{17}ClN_2O_2S$	360.07	142-146	64
QT4	$C_{15}H_{11}BrN_2O_2S$	361.97	158-159	75
QT5	$C_{19}H_{20}N_2O_3S$	356.12	162-165	78
QT6	$C_{20}H_{14}N_2O_2S$	346.08	212-214	72
QT7	$C_{20}H_{15}ClN_2O_2S$	380.04	236-238	75
QT8	$C_{27}H_{17}N_3O_2S$	447.10	264-268	84

5.2.1.2 Characterization

5.2.1.2.1. 3-butyl-5-(quinolin-6-ylmethylene) thiazolidinedione (QT1)

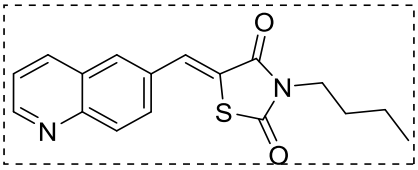

Yield 68%; Yellow powder; m.p.134-137 ºC; HPLC T_R = 7.71 min; **FT-IR** (KBr): 2954 (CH-Ar), 2871 (CH-aliphatic), 1735, 1667 (C=O), 1346 (CN-Ar); **^{1}H NMR** (at 500 MHz, using $CDCl_3$), δ ppm: 8.98 (dd, *J* = 4.2, 1.7 Hz, 1H, Ar-H), 8.25 – 8.15 (m, 2H, Ar-H), 8.05 (s, 1H, CH), 7.97 (d, *J* = 2.0 Hz, 1H, Ar-H), 7.83 (dd, *J* = 8.7, 2.1 Hz, 1H, Ar-H), 7.48 (dd, *J* = 8.3, 4.2 Hz, 1H, Ar-H), 3.79 (t, *J* = 7.4 Hz, 2H, CH_2), 1.73 – 1.63 (m, 2H, CH_2), 1.40 (dt, *J* = 15.1, 7.5 Hz, 2H, CH_2), 0.97 (t, *J* = 7.4 Hz, 3H, CH_3); **^{13}C NMR** (at 100 MHz, using $CDCl_3$) δ ppm: 167.57, 166.25, 152.09, 148.45, 136.61, 132.58, 131.61,130.67-130.61, 129.81, 128.20, 122.19, 41.99, 29.81, 19.98, 13.62; **MS** m/z(ES^+): 312.0945 (HRMS M^+ = 313.0995); Anal. Calculated for $C_{17}H_{16}N_2O_2S$: C = 65.36; H = 5.16; N = 8.97, Found: C = 65.21; H = 5.03; N = 8.71 %.

5.2.1.2.2. 3-octyl-5-(quinolin-6-ylmethylene) thiazolidinedione (QT2)

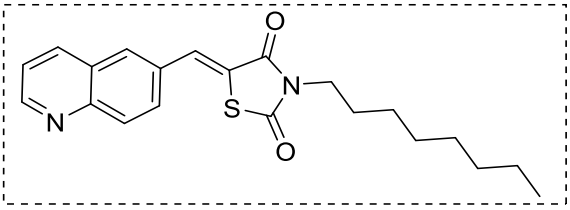

Yield 79 %; Yellow powder; m.p.198-200 ºC; HPLC T_R = 6.20 min; **FT-IR** (KBr): 3056 (CH-Ar), 2847 (CH-aliphatic), 1731, 1658 (C=O), 1335 (CN-Ar TZD core); **^{1}H NMR** (at 500 MHz, using $CDCl_3$), δ ppm: 9.00 – 8.97 (m, 1H), 8.20 (dd, J = 21.4, 8.4 Hz, 2H), 8.05 (s, 1H), 7.98 (d, J = 1.5 Hz, 1H), 7.83 (dd, J = 8.8, 1.9 Hz, 1H), 7.48 (dd, J = 8.3, 4.2 Hz, 1H), 3.82 – 3.73 (t, 2H), 1.72 – 1.67 (m, 2H), 1.31 (m, 8.3 Hz, 9H), 0.87 (t, J = 7.0 Hz, 3H); **^{13}C NMR** (at 100 MHz, using $CDCl_3$) δ ppm:167.57, 166.26, 152.10, 148.47, 136.61, 132.58, 131.63, 130.64, 129.82, 128.21, 123.06, 122.19, 42.27, 39.24, 31.78 29.42 – 28.92, 28.54, 27.77, 26.73, 22.62, 14.08; **MS** m/z(ES^+): 368.1639

(HRMS M^+ = 369.1638); Anal. Calculated for $C_{21}H_{24}N_2O_2S$: C = 68.45; H = 6.57; N = 7.60, found C = 68.21; H = 6.19; N = 7.42 %.

5.2.1.2.3. 3-(5-chloropentyl)-5-(quinolin-6-ylmethylene) thiazolidinedione (QT3)

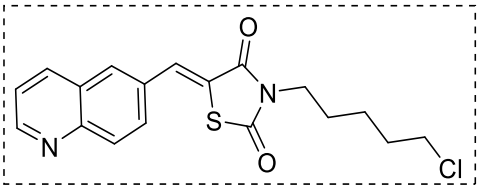

Yield 64%; Brown powder; m.p.142-146 ºC; HPLC T_R = 9.42 min; **FT-IR** (KBr): 3044 (CH-Ar), 2841 (CH-aliphatic), 1732, 1658 (C=O), 1328 (CN-Ar TZD core) and 721 (CH-Br); **^{1}H NMR** (at 500 MHz, using $CDCl_3$), δ ppm: 8.96 (d, *J* = 4.6 Hz, 1H), 8.14 (t, *J* = 7.9 Hz, 2H), 8.01 (s, 1H), 7.87 – 7.74 (m, 2H), 7.47 (ddd, *J* = 16.3, 8.2, 4.2 Hz, 2H), 3.80 (td, *J* = 7.3, 3.3 Hz, 2H), 2.88 (d, *J* = 4.1 Hz, 2H), 1.99 – 1.59 (m, 2H), 1.50 – 1.37 (m, 4H); **^{13}C NMR** (at 100 MHz, using $CDCl_3$) δ ppm: 166.60, 166.24, 152.06, 148.35, 136.63, 132.77, 131.52, 130.61 129.76, 128.14, 122.90, 122.19, 42.04, 41.72, 36.49, 33.28, 32.11, 27.21, 26.84 – 26.62, 25.22, 23.71, 22.97; **MS** m/z(ES^+): 360.0786 (HRMS M^+ = 361.1074); Anal. Calculated for $C_{18}H_{17}ClN_2O_2S$: C = 59.91; H = 4.75; N = 7.76, Found: C = 59.55; H = 4.54; N = 7.52 %.

5.2.1.2.4. 3-(2-bromoethyl)-5-(quinolin-6-ylmethylene) thiazolidinedione (QT4)

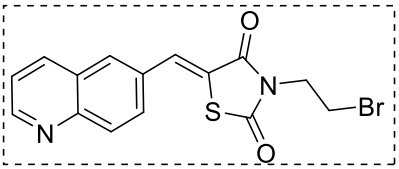

Yield 75%; Pale yellow powder; m.p.158-159 ºC; HPLC T_R = 6.45 min; **FT-IR** (KBr): 3034 (CH-Ar), 2851 (CH-aliphatic), 1731, 1674 (C=O), 1321 (CN-Ar TZD core) and 731 (CH-Br); **^{1}H NMR** (at 500 MHz, using $CDCl_3$), δ ppm: 9.00 (dd, *J* = 4.2, 1.7 Hz, 1H, Ar-H), 8.28 – 8.16 (m, 2H, Ar-H), 8.09 (s, 1H, CH), 8.00 (d, *J* = 2.1 Hz, 1H, Ar-H), 7.84 (dd, *J* = 8.7, 2.1 Hz, 1H, Ar-H), 7.50 (dd, *J* = 8.3, 4.2 Hz, 1H, Ar-H), 4.21 (t, *J* = 6.7 Hz, 2H, CH_2), 3.63 (t, *J* = 6.7 Hz, 2H, CH_2); **^{13}C NMR** (at 100 MHz, using $CDCl_3$) δ ppm: 152.25, 136.68, 133.60, 130.89-130.79, 129.74, 122.29, 42.80, 26.83; **MS** m/z(ES^+): 361.9701 (HRMS M^+ = 362.9462); Anal. Calculated for $C_{15}H_{11}BrN_2O_2S$: C = 49.60; H = 3.05; N = 7.71, Found: C = 49.41; H = 3.01; N = 7.54 %.

5.2.1.2.5. 3-(6-hydroxyhexyl)-5-(quinolin-6-ylmethylene) thiazolidinedione (QT5)

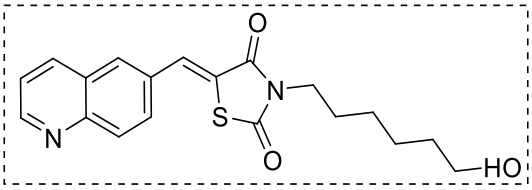

Yield 78%; Brown powder; m.p.162-165 ^{o}C; HPLC T_R = 10.67 min; **FT-IR** (KBr): 3274 (C-OH), 3035 (C-H-Ar), 2861 (C-H-aliphatic), 1721, 1687 (C=O), 1354 (C-N-Ar); **^{1}H NMR** (at 500 MHz, using $CDCl_3$), δ ppm: 8.98 (dd, J = 4.1, 1.5 Hz, 1H), 8.21 (dd, J = 22.3, 8.5 Hz, 2H), 8.05 (s, 1H), 7.98 (s, 1H), 7.83 (dd, J = 8.8, 1.8 Hz, 1H), 7.49 (dd, J = 8.3, 4.2 Hz, 1H), 3.79 (t, J = 7.3 Hz, 2H), 3.65 (t, J = 7.4 Hz, 2H), 1.72 (dt, J = 14.5, 7.4 Hz, 2H), 1.62 – 1.57 (m, 2H), 1.46 – 1.37 (m, 4H); **^{13}C NMR** (at 100 MHz, using $CDCl_3$) δ ppm: 167.60, 168.24, 149.06, 148.35, 141.63, 132.77, 133.52, 132.61, 128.77, 128.27, 122.90, 121.19, 43.04, 42.72, 35.49, 31.28, 30.11, 29.21, 28.84 – 26.62 22.22, 21.71, 21.38; **MS** m/z(ES^+): 356.1242 (HRMS M^+ = 357.1246); Anal. Calculated for $C_{19}H_{20}N_2O_3S$: C = 64.12; H = 5.66; N = 7.86, Found: C = 64.02; H = 5.45; N = 7.57 %

5.2.1.2.6. 3-benzyl-5-(quinolin-6-ylmethylene) thiazolidinedione (QT6)

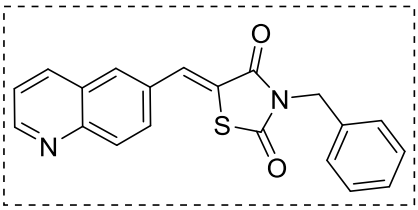

Yield 72 %; Pale yellow powder; m.p.212-214 ^{o}C; HPLC T_R = 7.00 min; **FT-IR** (KBr): 3049 (CH-Ar), 2841 (CH-aliphatic), 1722, 1678 (C=O), 1214 (CN-Ar TZD core); **^{1}H NMR** (at 500 MHz, using $CDCl_3$), δ ppm: 8.98 (dd, J = 4.2, 1.6 Hz, 1H, Ar-H), 8.19 (dd, J = 21.6, 8.5 Hz, 2H, Ar-H), 8.06 (s, 1H, CH), 7.96 (d, J = 1.7 Hz, 1H, Ar-H), 7.81 (dd, J = 8.8, 2.0 Hz, 1H, Ar-H), 7.51 – 7.42 (m, 4H, Ar-H), 7.38 – 7.30 (m, 4H, Ar-H), 4.93 (s, 2H, CH2); **^{13}C NMR** (at 100 MHz, using $CDCl_3$) δ ppm: 167.19, 165.77, 152.22, 136.83-136.65, 133.45, 131.43, 130.80-130.77, 129.73, 128.99-128.21, 127.10,122.25, 77.27-77.02, 44.75; **MS** m/z(ES^+): 346.0842 (HRMS M^+ = 347.0841); Anal. Calculated for $C_{20}H_{14}N_2O_2S$: C = 69.35; H = 4.07; N = 8.09, found C = 69.18; H = 4.01; N = 8.02 %.

5.2.1.2.7. 3-(3-chlorobenzyl)-5-(quinolin-6-ylmethylene) thiazolidinedione (QT7)

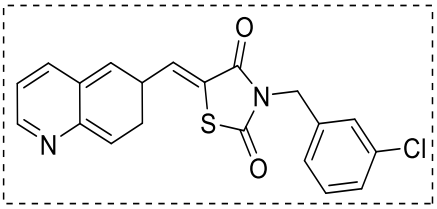

Yield 75 %; Pale yellow powder; m.p.236-238 ºC; HPLC T_R = 6.84 min; **FT-IR** (KBr): 3049 (CH-Ar), 2841 (CH-aliphatic), 1722, 1668 (C=O), 1214 (CN-Ar TZD core); **^{1}H NMR** (at 500 MHz, using $CDCl_3$), δ ppm: 8.98 (dd, J = 4.2, 1.6 Hz, 1H, Ar-H), 8.20 (dd, J = 20.5, 8.3 Hz, 2H, Ar-H), 8.08 (s, 1H, CH), 7.97 (d, J = 1.8 Hz, 1H), 7.82 (dd, J = 8.8, 2.0 Hz, 1H, Ar-H), 7.50 – 7.43 (m, 2H, Ar-H), 7.38 – 7.19 (m, 3H, Ar-H), 4.89 (s, 2H, CH_2); **^{13}C NMR** (at 100 MHz, using $CDCl_3$) δ ppm: 167.19, 165.77, 152.22, 136.83-136.65, 133.45, 131.43, 130.80-130.77, 129.73, 128.99-128.21, 127.10,122.25, 77.27-77.02, 44.75; **MS** m/z(ES^+): 380.0439 (HRMS M^+ = 381.0443); Anal. Calculated for $C_{20}H_{13}ClN_2O_2S$: C = 63.08; H = 3.44; N = 7.36, found C = 63.02; H = 3.22; N = 7.20 %.

5.2.1.2.8. 4'-((2,4-dioxo-5-(quinolin-6-ylmethylene) thiazolidin-3-yl) methyl)-[1,1' biphenyl]-2-carbonitrile (QT8)

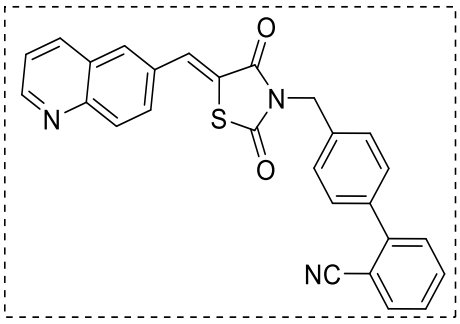

Yield 84 %; Pale yellow powder; m.p.264-268 ºC; HPLC T_R = 14.22 min; **FT-IR** (KBr): 3076 (C-H-Ar), 2897 (C-H-aliphatic), 2245 (-C=N), 1711, 1662 (C=O), 1255 (C-N-Ar); **^{1}H NMR** (at 500 MHz, using $CDCl_3$), δ ppm: 8.98 (d, *J* = 4.1 Hz, 1H), 8.20 (dd, *J* = 22.7, 8.6 Hz, 2H), 8.09 (s, 1H), 7.98 (s, 1H), 7.90 – 7.71 (m, 3H), 7.66 – 7.42 (m, 7H), 4.99 (s, 2H); **^{13}C NMR** (at 100 MHz, using $CDCl_3$) δ ppm: 164.97, 152.14, 147.48, 144.83, 138.22, 136.69, 135.55, 133.81,132.89, 131.53, 130.68, 129.79, 128.21,127.75, 122.23, 118.60, 45.01; **MS** m/z(ES^+): 447.1024 (HRMS M^+ = 448.1026); Anal.

Calculated for $C_{27}H_{17}N_3O_2S$: C = 72.47; H = 3.83; N = 9.39, found C = 72.12; H = 3.22; N = 9.21 %.

5.2.2. Part-II: *In vitro* antidiabetic and antioxidant studies

5.2.2.1. *In-vitro* antidiabetic activity (QT1-QT8)

We further evaluated all the synthesized quinoline-based thiazolidinediones derivatives (**QT1-QT8**) for the screening of antidiabetic activity. The intestinal α-glucosidase (IAG) and pancreatic α-amylase (PAA) are important targets in the treatment of diabetes due to its involvement in digestion of carbohydrates and its absorption into human body. By restricting the activity of these two enzymes can lower the risk of developing diabetes and postprandial hyperglycaemia (159,225).

Table 5.11: *In vitro* PAA and IAG inhibition activity of compounds (**QT1-QT8**)

Compound	PAA Percentage inhibition (%)	PAA inhibition activity IC_{50} (µM)	IAG Percentage inhibition (%)	IAG inhibition activity IC_{50} (µM)
QT 1	92.16	5.54 ± 0. 17	90.68	7.15 ± 0. 11
QT2	90.07	8.12 ± 0. 16	92.26	6.25 ± 0. 08
QT3	83.49	10.23 ± 0. 10	91.58	8.25 ± 0. 17
QT4	85.49	11.22 ± 0. 11	87.32	10.71 ± 0. 17
QT5	87.01	9.84 ± 0. 14	89.01	9.58 ± 0. 12
QT6	91.22	7.45 ± 0. 13	93.57	5.24 ± 0. 18
QT7	93.87	5.48 ± 0. 10	94.01	3.14 ± 0. 16
QT8	95.36	4.68 ± 0.06	96.56	2.45 ± 0. 07
Acarbose (AC)	90.19	10.15 ± 0. 09	89.21	8.24 ± 0. 16

*IC_{50} values were determined by regression analyses and expressed as means ± SD of four replicates.

5.2.2.1.1. *In-vitro* PAA inhibition activity

To assess the antidiabetic effect of **QT1-QT8**, the PAA inhibition assay was performed by using acarbose as the standard. The newly synthesized compounds were evaluated for their *in vitro* PAA activity using acarbose as a positive control at various concentrations (0, 2.5, 10, 25, 50, 100, 250, 500 µg/mL) and IC_{50} valves were calculated. The results of the PAA assay conducted to determine the antidiabetic activity, using as series of compounds **QT1-QT8**, revealed a remarkable inhibitory effect on PAA enzyme, and the findings were graphically represented in figure 5.11. The percentage inhibition ranged up to 95.36 % with in the series, with corresponding IC_{50} values spanning from 4.68 µM to 11.22 µM against PAA enzyme. In comparison, the reference compound acarbose exhibited an IC_{50} value 12.45 µM and a percentage inhibition of 90.19 %.

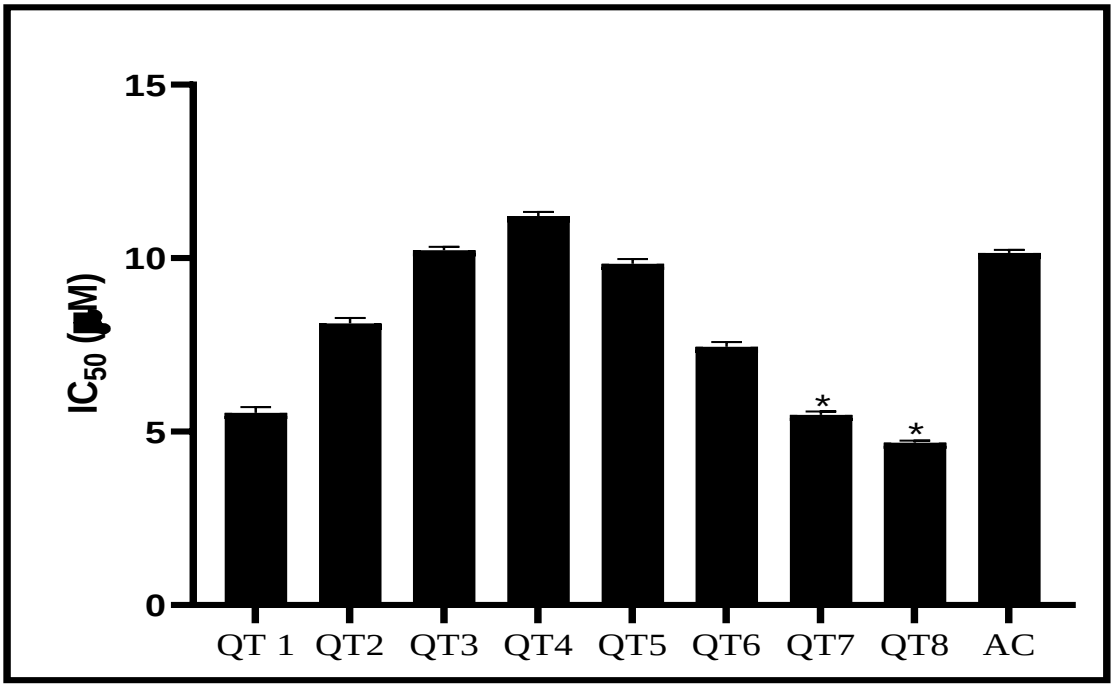

*p < 0.05 as compared with acarbose (AC), statistical one-way ANOVA followed by Dunnet's 't' test

Figure 38: *In-vitro* PAA inhibition activity of compounds (**QT1-QT8**)

As results states that all tested compounds shown significant PAA enzyme inhibition activity at the dose of 50 (µg/mL). Among the all compounds, **QT8** (95.36 %, 4.68 µM) and **QT7** (93.87 %, 5.48 µM) were found to be the most potent compared

to standard Acarbose. The results suggested that the compounds **QT8** and **QT7** were considered as promising antidiabetic candidates among all other compounds due to their functional group diversity. PAA inhibition activity of all synthesized derivatives were graphically represented in the figure 38.

5.2.2.1.2. *In-vitro* IAG inhibition activity

Newly synthesized compounds **QT1-QT8**, were tested for their ability to inhibit IAG enzyme by using Acarbose as the standard and IC_{50} valves were calculated. The results of the IAG assay conducted to determine the antidiabetic activity, using as series of compounds **QT1-QT8**, revealed a remarkable inhibitory effect on PAA enzyme, and the findings were graphically represented in Figure 39. The percentage inhibition ranged up to 96.56 % with in the series, with consistent IC_{50} values spanning from 2.45 µM to 10.71 µM against IAG enzyme.

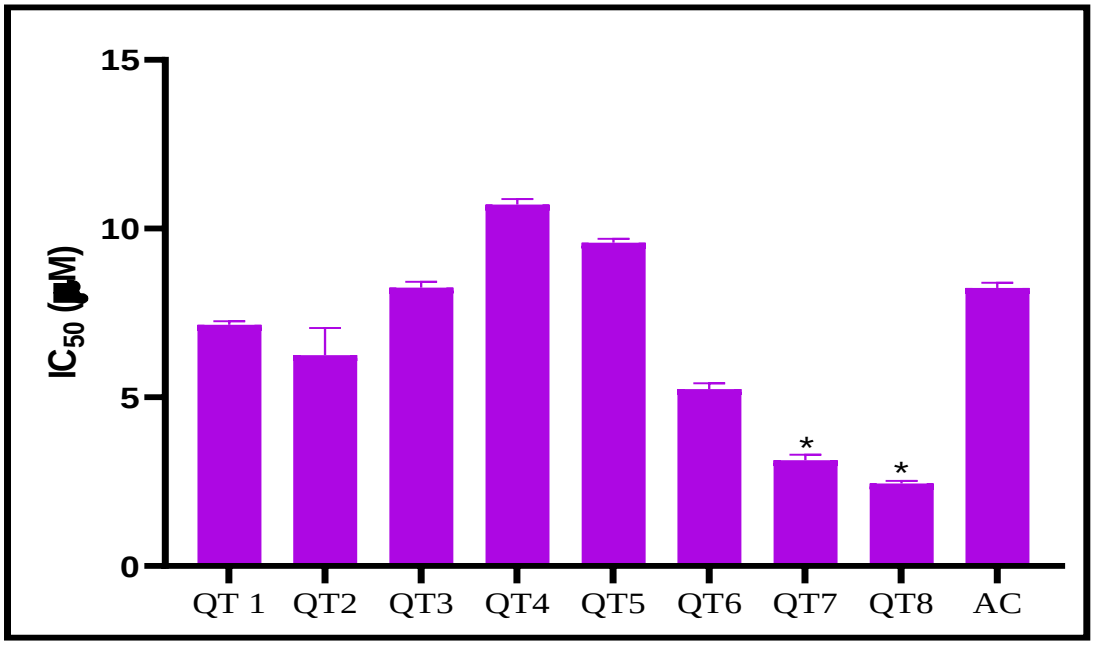

*p < 0.05 as compared with acarbose (AC), statistical one-way ANOVA followed by Dunnet's 't' test

Figure 39: *In-vitro* IAG inhibition activity of compounds (**QT1-QT8**)

In comparison, the reference compound acarbose exhibited an IC_{50} value 8.24 µM and a percentage inhibition of 89.21 %. As results states that all tested compounds shown significant PAA enzyme inhibition activity at the dose of 50 (µg/mL). Among

the all compounds, **T8** (96.56 %, 2.45 µM) and **QT7** (94.01 %, 3.14 µM) were found to be the most potent compared to standard Acarbose. The results suggested that the compounds **QT8** and **QT7** were considered as promising antidiabetic candidates among all other compounds due to their functional group diversity. The IAG percentage inhibition and corresponding IC_{50} value are shown in table 5.11.

5.2.2.2 *In vitro* antioxidant activity

The antioxidant activity was studied for the all newly synthesized quinoline-based thiazolidinediones derivatives (**QT1-QT8**) using the Diphenyl picrylhydrazine (DPPH) assay. Antioxidant agents safeguard cells from reactive oxygen species (ROS), thereby preventing diabetes caused by ROS and oxidative stress. The reactive oxygen species can cause protein glycation, lipid peroxidation, DNA damage and enzyme inactivation which can be neutralized by endogenous or exogenous antioxidant systems (189,229). The screening results (Table 5.12) showed that all synthesized compounds demonstrated excellent to moderate antioxidant activity, with IC_{50} values ranging from 5.04 µM to 13.84 µM.

Table 5.12: *In vitro* antioxidant activity of compounds (**QT1-QT8**)

Compound codes	**Antioxidant activity IC_{50} (µM)**
QT1	8.84 ± 0.056
QT2	9.84 ± 0.015
QT3	10.84 ± 0.083
QT4	6.84 ± 0.017
QT5	13.84 ± 0.021
QT6	6.65 ± 0.051
QT7	5.84 ± 0.043
QT8	5.04 ± 0.054
Ascorbic acid (AA)	7.028 ± 0.061

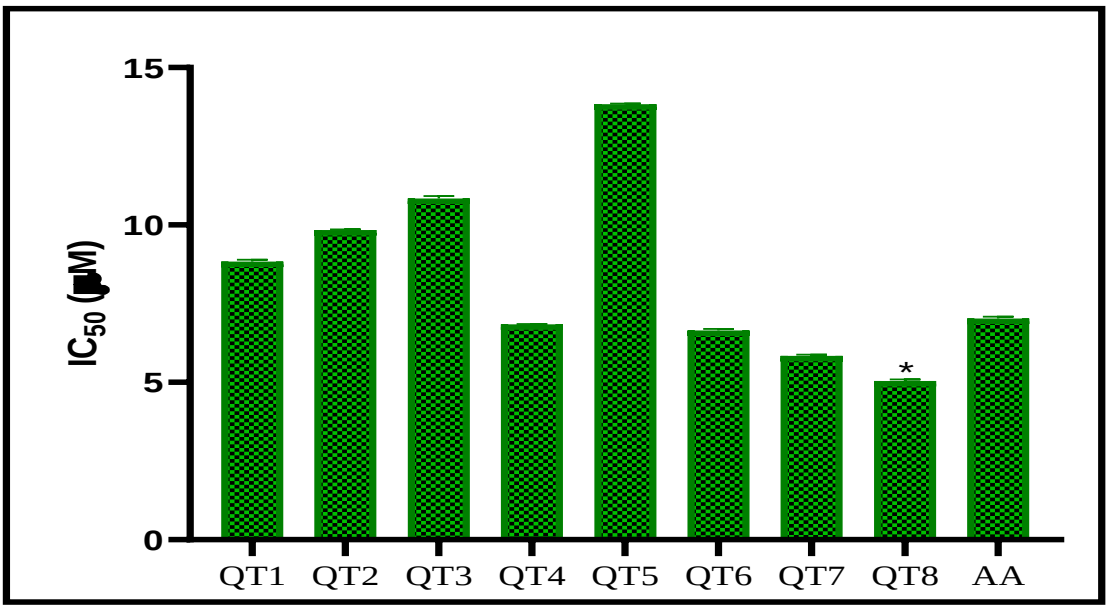

*p < 0.05 as compared with ascorbic acid (AA), statistical one-way ANOVA followed by Dunnet's 't' test

Figure 40: *In-vitro* antioxidant activity of compounds (**QT1-QT8**)

Except compounds **QT3** and **QT4**, all the remaining compounds possess good antioxidant activity. Overall, the antioxidant assay results state that compounds **QT6**, **QT7** and **QT8** are potential towards scavenge the stable free radical DPPH.

5.2.3. Part-III: *In silico* validation

5.2.3.1. Molecular docking studies

After conducting *in vitro* analysis of synthesized compounds molecular docking studies were performed using Autodock Vina 1.5.4. The *in silico* molecular docking was conducted to investigate the binding interactions between a set of synthesized compounds (quinoline-based thiazolidinediones) with PAA and IAG receptors. The PAA (**PDBID: 4W93**) and IAG (**PDBID: 3A4A**) protein was downloaded from the protein data bank. Subsequently, BIOVIA discovery studio visualizer was exploited to authenticate the 2D and 3D interactions of the docked ligands (**QT1-QT8**). Table 5.13 presents the affinity of these compounds for PAA in terms of their binding affinity, which ranged from -11.3 to -7.3 kcal/mol. Table 5.14 presents the affinity of these compounds for IAG in terms of their binding affinity, which ranged from -10.6 to -7.5 kcal/mol. In contrast, standard compounds acarbose (-6.7 kcal/mol) with PAA and

acarbose (-8.5 kcal/mol) with IGA displayed considerably lower docking scores when compared to the synthesized compounds. Synthesized compounds have shown hydrogen bonding, π-π T shaped, π- alkyl/alkyl, π – σ and π- Sulphur type of binding interactions at active site the PAA (Table 5.13) and IAG (Table 5.14) receptors.

Table 5.13: Molecular docking interaction of compounds (**QT1-QT8**) with **4W93**

Compounds	**Binding affinity Kcal/mol**	***H*-Bond**	**π – π T Shaped**	**π- alkyl/alkyl**	**π – σ Bond**	**π- Sulphur**
QT1	-7.7	Arg195	Tyr62, Trp59	Ile235, his201, Ala198, leu163	Thr163	Trp58, His299, Tyr62
QT2	-7.9	-	Tyr62, Trp59	Trp59, Leu165	-	Asp300
QT3	-8.1	-	Trp59	Ile235, His201, Ala198, leu162	-	-
QT4	-7.3	-	Tyr62, Trp59	Tyr62, His201, Leu165, Ala198	Thr163	Trp58, His299, Tyr62, Asp197
QT5	-7.4	Arg195, Glu233	Trp29	Leu165	Leu162	His101
QT6	-8.8	Arg195	His201, Trp59, Tyr62, Trp59	Ala198, leu165	Thr163, Leu162	Trp58, His299, Tyr62 Asp197
QT7	-9.1	Arg195	Trp59, Tyr62	Leu162, Ile235	-	Trp58, His299, Tyr62 Asp300
QT8	-11.3	Gln63, His299	Trp59, Tyr62	Lys200, Ala198	Ile235	Glu233, His201
Co crystal ligand	-8.7	Tyr151, Arg195, Glu240, Lys233, Lys200, Ile235	Tyr62, His299	--	--	--
Acarbose	-6.7	Thr163, Glu233, Asp300	-	-	-	-

Table 5.14: Molecular docking interaction of compounds (**QT1-QT8**) with **3A4A**

Compounds	**Binding affinity Kcal/mol**	***H*-Bond**	**π – π T Shaped**	**π- alkyl/alkyl**	**π – σ Bond**	**π- Sulphur**
QT1	-8.0	-	Tyr158, Arg315	Lys156, Tyr158	Tyr158	Phe314, Tyr316
QT2	-8.7	-	Tyr158	His112, Val216, Phe178, Lys156	Phe178, Tyr158	-
QT3	-7.5	Arg315	Phe303	Lys156, Tyr158	Arg315	His280, Glu277
QT4	-8.3	-	Phe303	Arg315, Lys156, Phe314	-	His280
QT5	-8.5	-	Tyr158	Phe158, Lys156	Tyr158	-
QT6	-9.4	Arg315	Tyr158, Phe303	Lys156, Arg315	-	-
QT7	-9.2	Arg315	Phe303	Tyr158, Lys156	Arg315	-
QT8	-10.6	Ser162, Arg176	-	Ala418, Ile150	-	-
Co-crystal ligand	-6.9	Arg442, His112, Asp69, Asp215, Glu277, His351, Asp352, Arg213	--	--	--	--
Acarbose	-8.5	Glu271, Ser298, Thr274 Ile272, Glu296, Asn259	--	--	--	--

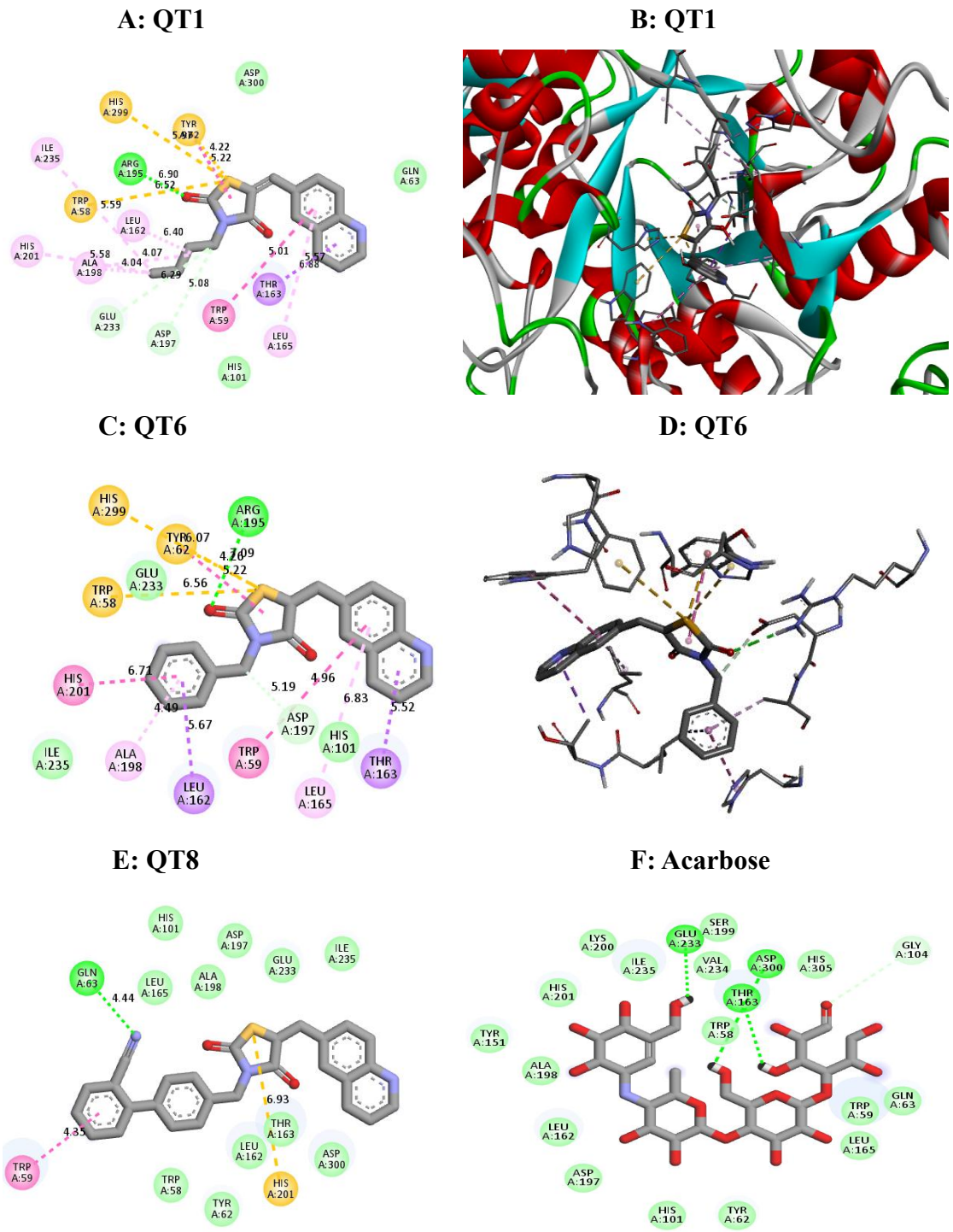

Figure 41: 2D and 3D structure of the series QT**1-QT18** with PAA (**4W93**)

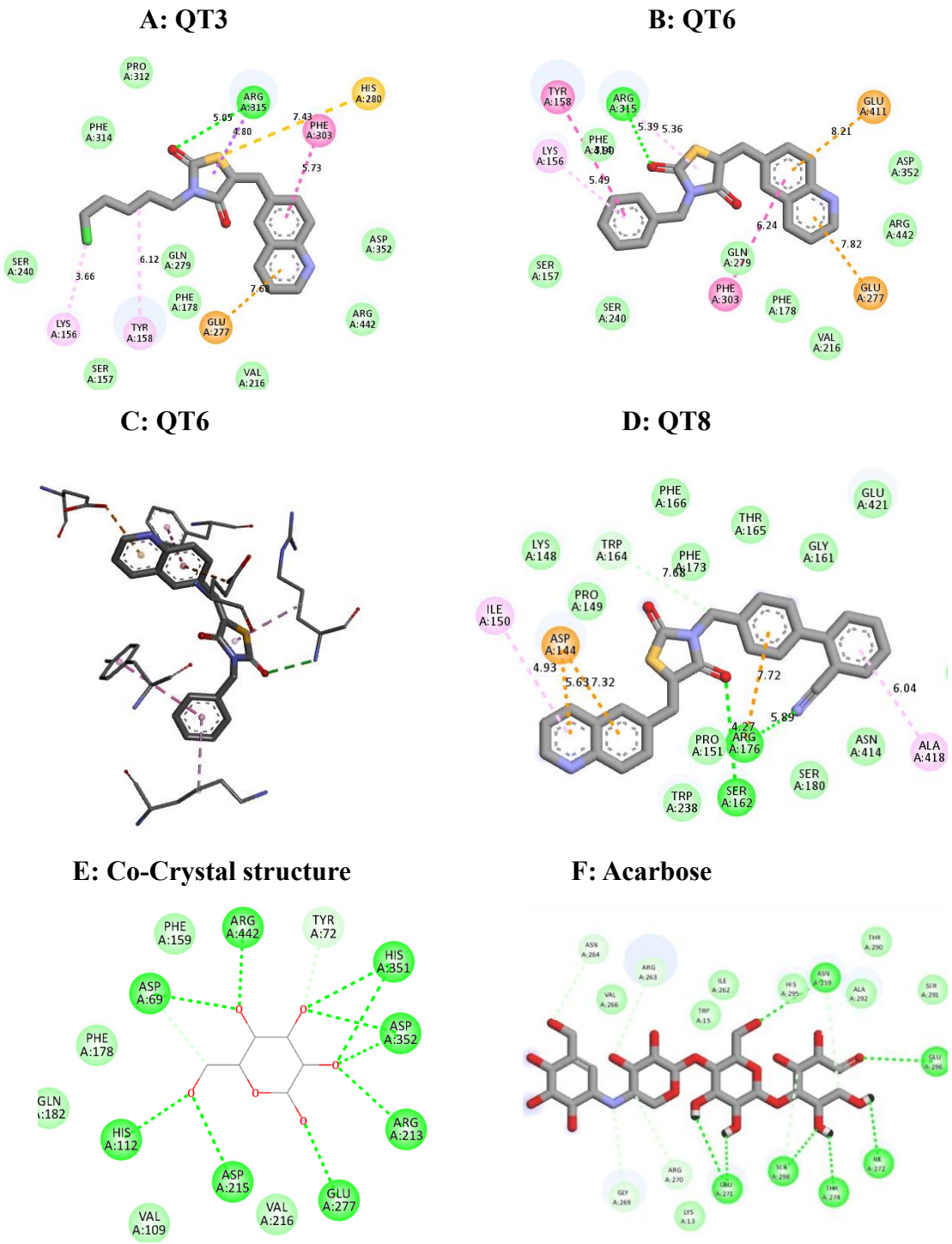

Figure 42: 2D and 3D structure of the series QT**1-QT18** with IAG (**3A4A**)

5.2.3.2. MM-GBSA validation

The MM-GBSA validation provides insight into the relative binding strengths of set of synthesized compounds with PAA (PDB: **3W93**) and IAG (PDB: **3A4A**) enzyme. These interactions include, such as coulomb interactions, hydrophobic contacts, hydrogen bonds and also covalent bonds. The overall binding free energy values for all compounds fall within the range of -24.21 to -42.55 kcal/mol with PAA enzyme and -32.23 to -62.64 kcal/mol with IAG enzyme. Notably, the standard drug acarbose shows ΔG binding energy of -27.58 kcal/mol and -52.83 kcal/mol with PAA and IAG respectively, but compound **QT8** exceeds this valve of -42.59 kcal/mol with PAA receptor and -62.64 kcal/mol with IAG receptor. Conversely, other energy like ΔG bind covalent (covalent energy) do not significantly contributed to targets. This method is reliable for assessing the how well the compounds bind to their target proteins. Additionally, compounds **QT7**, **QT4** and **QT6** display good binding energies of -40.69, -40.65, -38.53 kcal/mol with PAA and -53.46, -53.07, -51.20 kcal/mol with IAG receptor (Table 5.15 and Table 5.16).

Table 5.15: Calculation of binding free energy using the Prime/MM-GBSA method for **PDB ID: 3W93**

Compounds	ΔG bind (Kcal/ mol)	ΔG bind Coulomb	ΔG bind covalent	ΔG bind H Bond	ΔG bind vdW	ΔG bind Lipophilic
QT1	-41.56	-21.11	5.08	-3.52	-31.61	-12.90
QT2	-26.21	-14.00	-0.81	-1.36	-28.04	-10.85
QT3	-41.64	-24.14	3.29	-2.22	-24.86	-11.49
QT4	-38.47	-38.84	-0.75	-3.81	-23.28	-11.97
QT5	-42.55	-25.14	2.28	-2.52	-22.86	-12.39
QT6	-31.88	-11.05	0.56	-0.68	-26.21	-9.28
QT7	-26.39	-13.98	-0.56	-0.56	-38.63	-11.77
QT8	-24.21	-12.00	-0.62	-1.27	-25.04	-9.67
Acarbose	-27.58	-16.97	-0.77	-0.73	-22.67	-10.15

Δ G bind: free energy of binding; ΔG bind Coulomb: Coulomb free energy; ΔG bind covalent: internal or covalent energy; ΔG bind vdW: van der Waal force or energy; ΔG bind H Bond: free hydrogen bonding energy; ΔG bind Lipophilic: hydrophobic energy

Table 5.16: Calculation of binding free energy using the Prime/MM-GBSA method for **PDB ID: 3A4A**

Compounds	ΔG bind (Kcal/ mol)	ΔG bind Coulomb	ΔG bind covalent	ΔG bind H Bond	ΔG bind vdW	ΔG bind Lipophilic
QT1	-32.23	-28.29	4.83	-4.91	-54.75	-36.39
QT2	-33.55	-23.48	3.51	-1.37	-39.87	-26.16
QT3	-46.59	-26.94	10.90	-1.61	-28.49	-30.52
QT4	-41.64	-18.97	6.75	-3.17	-25.37	-31.78
QT5	-53.07	0.33	2.88	-0.36	-50.33	-26.57
QT6	-37.30	-10.37	5.13	-0.90	-47.33	-27.43
QT7	-53.46	-20.69	4.01	-0.72	-43.10	-25.33
QT8	-39.65	-12.18	2.77	-0.62	-49.23	-33.39
Acarbose	-52.83	-8.02	2.93	-0.21	-46.24	-29.92

Δ G bind: free energy of binding; ΔG bind Coulomb: Coulomb free energy; ΔG bind covalent: internal or covalent energy; ΔG bind vdW: van der Waal force or energy; ΔG bind H Bond: free hydrogen bonding energy; ΔG bind Lipophilic: hydrophobic energy

5.2.3.3. Molecular dynamics (MD) simulation analysis

The main goal of MD investigations to assess ligand binding strength within receptor binding pocket. MD simulations were used to determine forces and understand atomic motions. The conformational change analysis of the protein-ligand complex(s) conducted during various MD production runs (10, 20, 50, 100, 120, 150, 180 and 200 nanosecond), with the minimum change observed at 10 ns, maximum at 120 ns, and slight changes from 180 to 200 ns (figure 43).

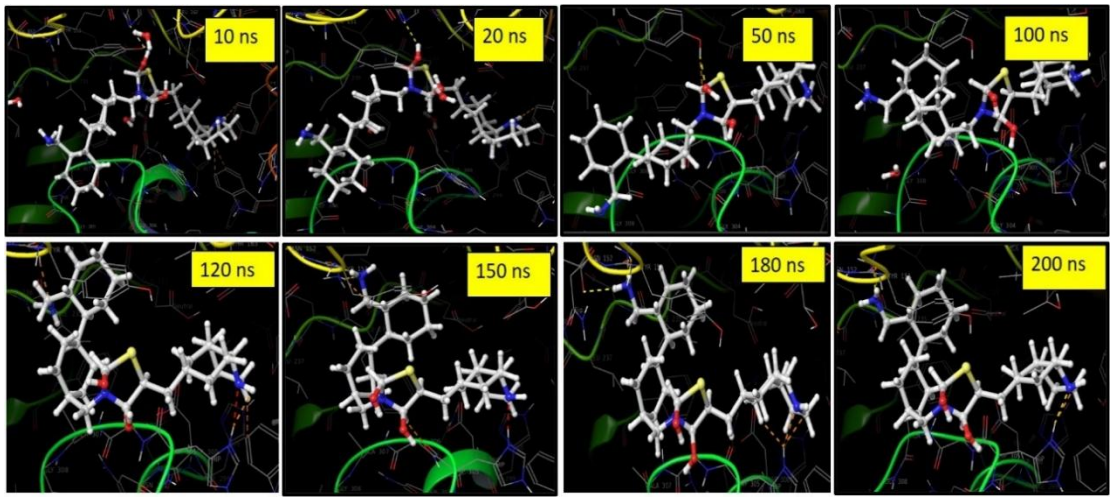

Figure 43: Compound **QT8** with complex **3A4A** receptor at different ns (MD run).

5.2.3.3.1. Root mean square deviation (RMSD)

The stability of the selected ligand-protein complex was evaluated by examining the RMSD. The main objective of this analysis is to measure the difference between the backbone atoms of the receptor and the crystal structure of the protein. The initial conformation of the structure was carefully observed and tracked until its final position throughout this investigation. Consequently, any changes observed during this simulation study can offer valuable information about the stability of the protein in relation to its confirmation. Figure 44a illustrates the RMSD plots for the complex **QT8** with protein **4W93**.Evidently, the RMSD metric for this specific complex was consistently maintained at levels below 2 Å throughout the simulation period, signifying a remarkably high degree of stability. In figure 44b, RMSD analysis is presented for compound **QT7** in conjunction with protein **4W93**.The complex established stability, as reflected in an RMSD value consistently below 1Å over the entire simulation period. In figure 44c, the RMSD analysis is presented for compound Acarbose interacting with protein **4W93**.The complex adopts very stable conformations with negligible deviation in the observed value. The figure 44d pertaining to the interaction between compound **QT8** and protein **3A4A**. The complex unveiled constant stability throughout the trajectory of the simulation (200 ns) period, with a RMSD value less than 2Å. The complex exhibits a highly dynamic nature, with a narrow fluctuation in backbone RMSD ranging from 150 to 200nm. However, in between 50-150ns, the complex adopts very stable conformations with negligible deviation in the observed value.

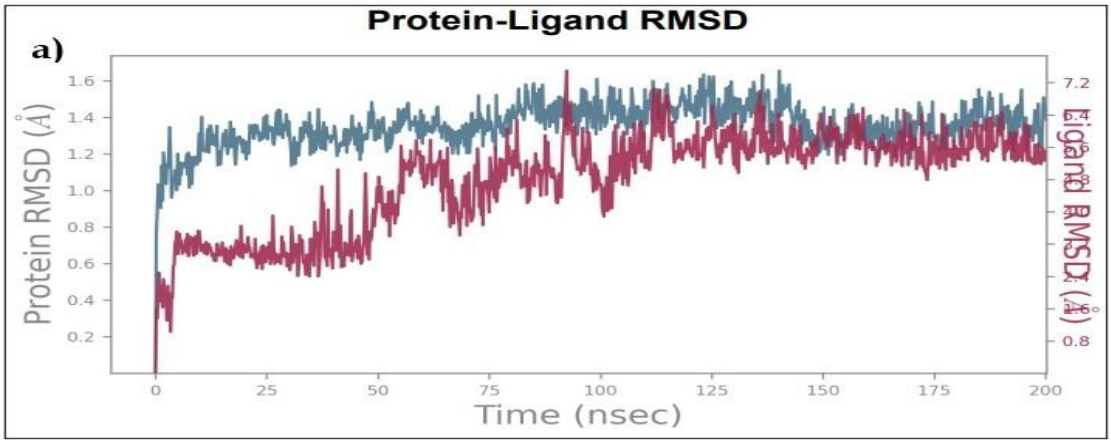

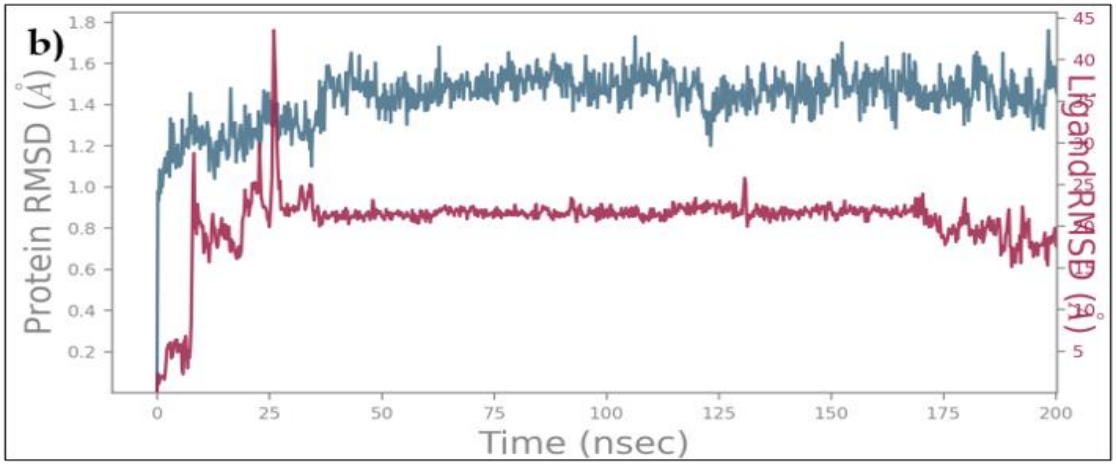
b)
Protein RMSD (Å)
Ligand RMSD (Å)
Time (nsec)

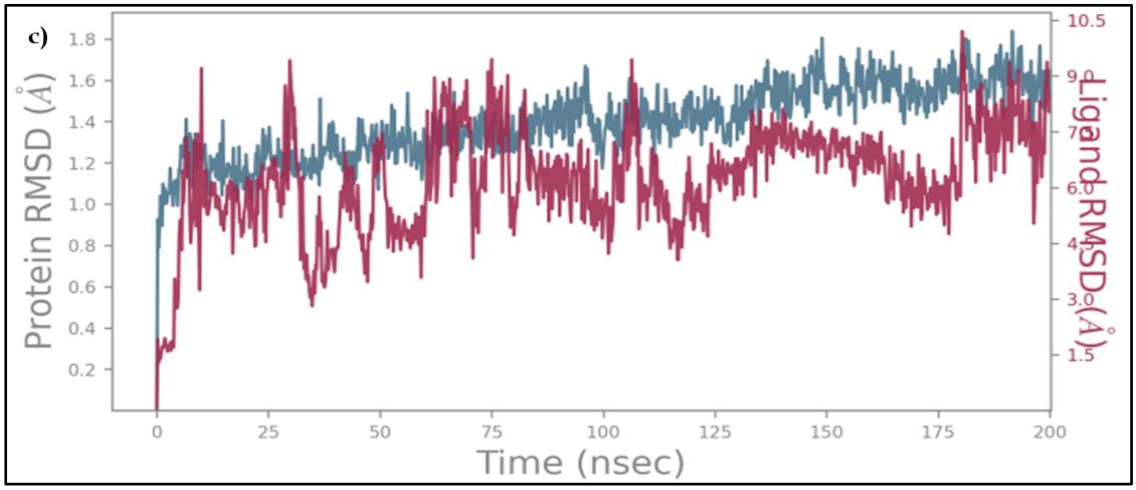
c)
Protein RMSD (Å)
Ligand RMSD (Å)
Time (nsec)

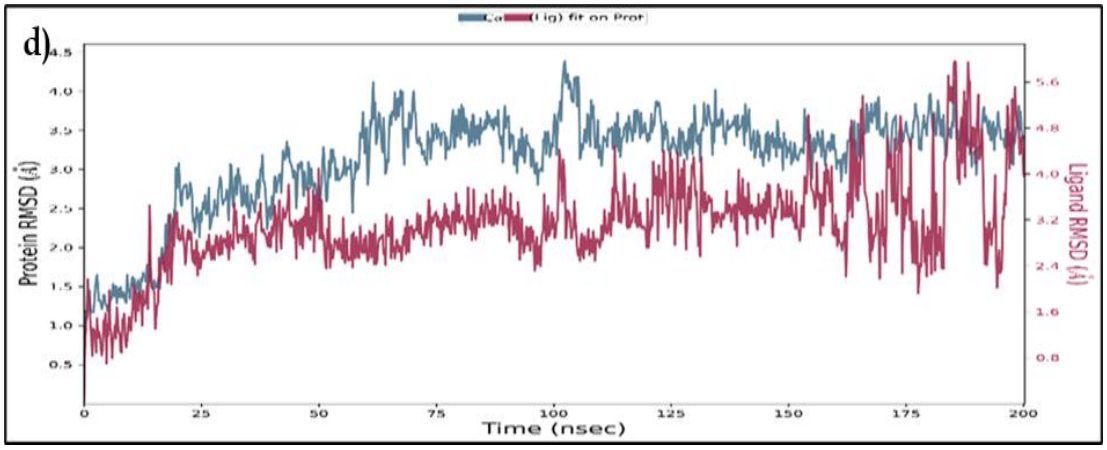
d)
Protein RMSD (Å)
Ligand RMSD (Å)
Time (nsec)

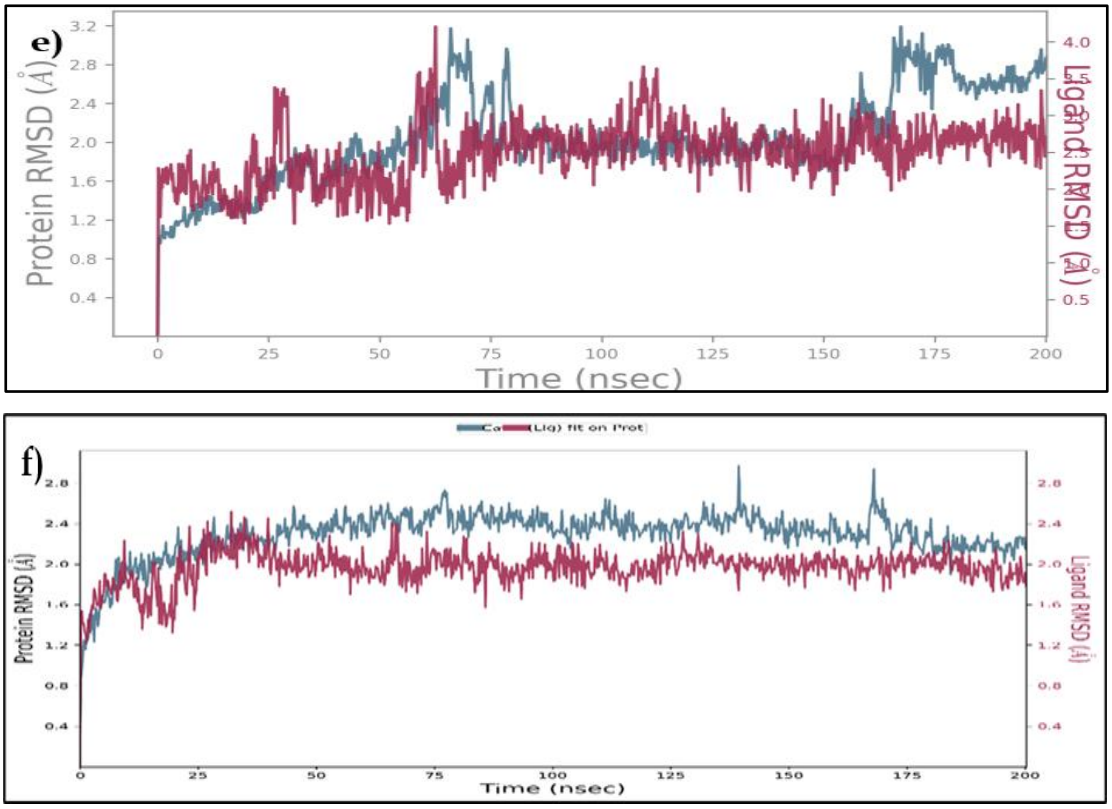

Figure 44: The RMSD Vs time plot for **4W93** protein docked with compound. a) **QT8**, b) **QT7**, c) Acarbose (Standard) and **3A4A** protein docked with compound d) **QT8**, e) **QT7**, f) Acarbose (Standard).

In figure 44d, the RMSD analysis is presented for standard compound Acarbose interacting with protein **3A4A**. The complex (**3A4A-Acarbose**) complex exhibited sustained stability throughout the 200 ns simulation period, with an RMSD value consistently below 2Å. Although a marginal deviation in ligand RMSD was observed between 10-40 ns and 180-185 ns, subsequent stabilization ensued. Cumulatively, the RMSD examination across all studied complexes affirms the persistent stability of the ligand-protein complexes during the simulation.

5.2.3.3.2 Root mean square fluctuation (RMSF) analysis

The evaluation of the adaptability and robustness of the intricate system in the MDS investigation includes carrying out RMSF on the top docked compound **QT8** and **QT7**. Furthermore, the RMSF examinations are executed to assess the variations in the actions of amino acid residues of the objective protein upon binding with the top compounds. In figure 45a, 45b, 45c and 45e, 45f, 45g 45h intricately portray the comprehensive residue-wise fluctuations inherent in the protein when in association

with compounds **QT8**, **QT7**, acarbose with **4W93** receptor and **QT8**, **QT7**, acarbose with 3**A4A** receptor respectively.

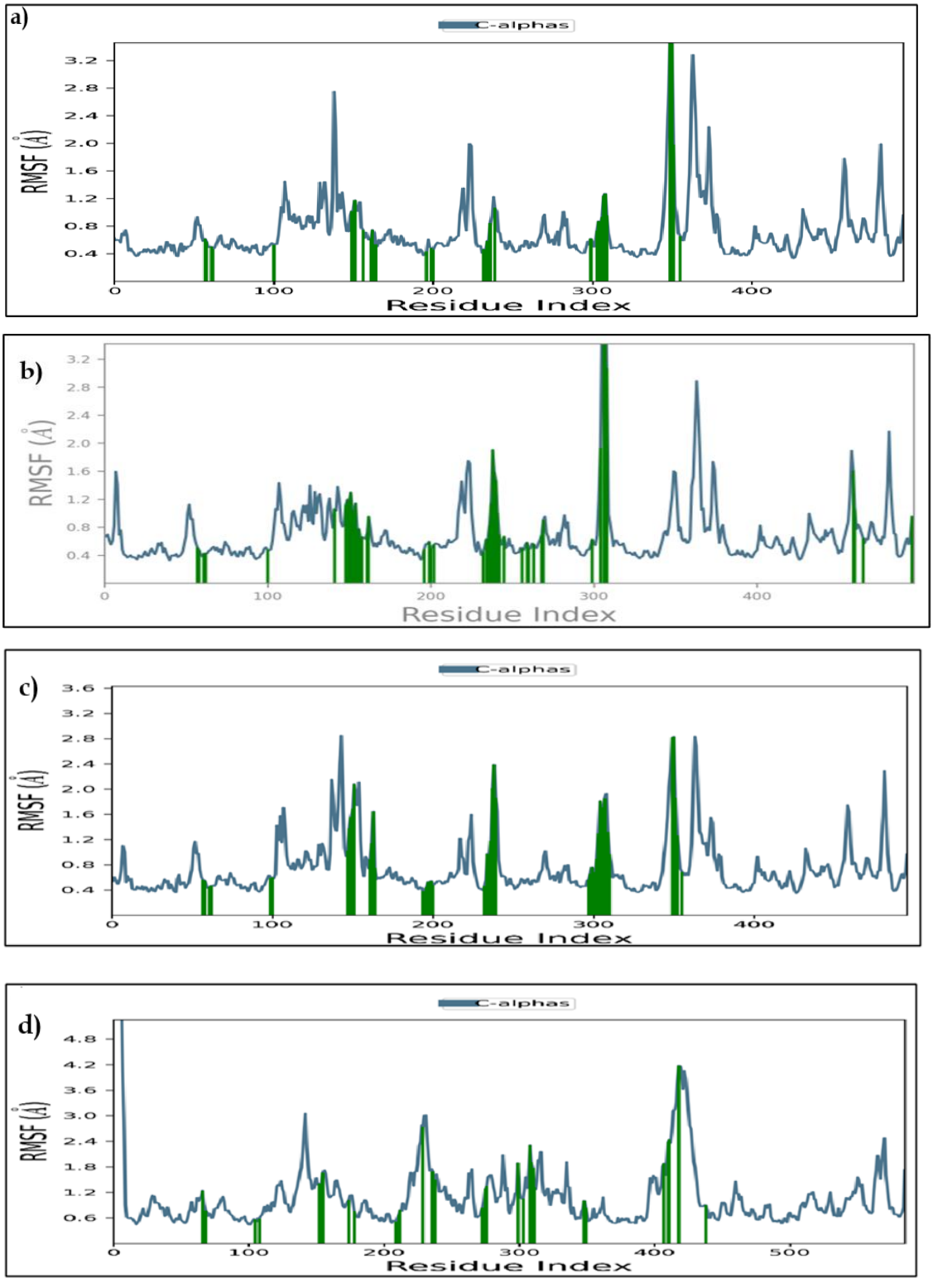

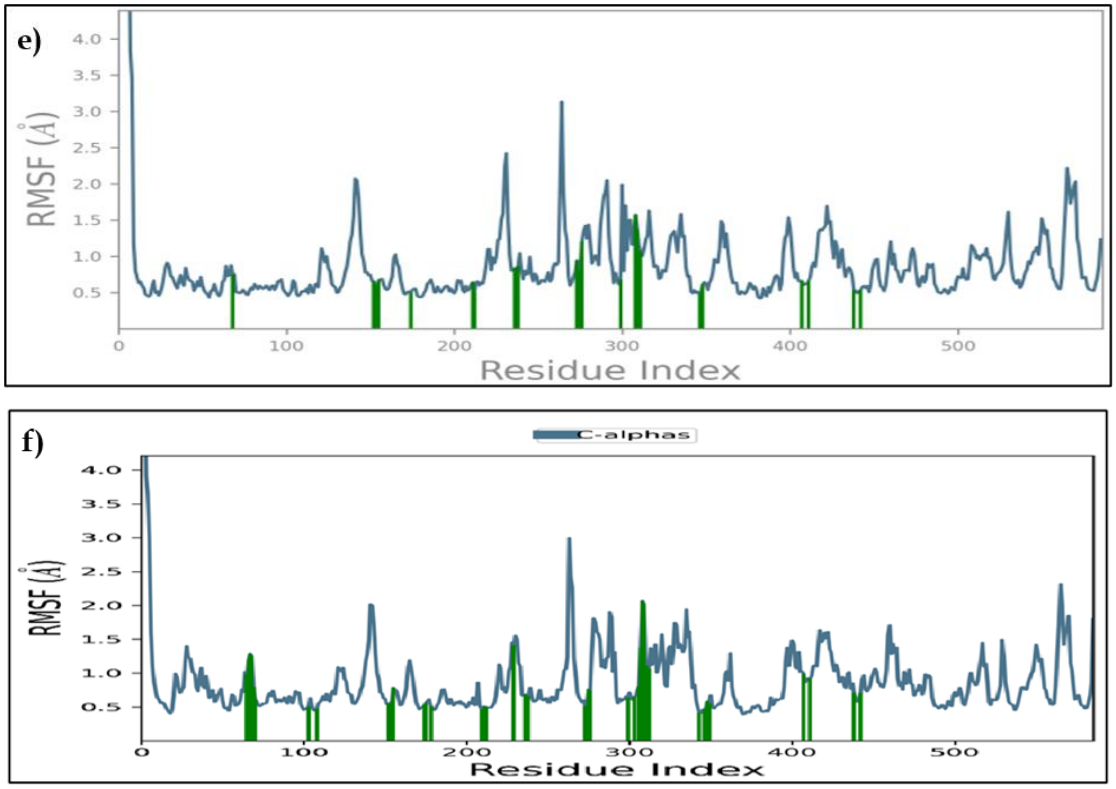

Figure 45: The RMSF plot for **4W93** protein coded by compound. a) **QT8**, b) **QT7**, c) Acarbose (Standard) and **3A4A** protein coded with compound d) **QT8**, e) **QT7**, f) Acarbose (Standard).

The RMSF studies' visual representation indicates a consistent absence of significant deviations across the simulation trajectory. Each complex exhibits a distinct level of enhanced stability, underscoring the robust interactions sustained during the simulation duration. This comprehensive portrayal underscores the persistent strength of the ligand-protein complexes, validating the enduring stability observed throughout the simulations.

5.2.3.3.3. Radius of gyration (Rg) analysis

The compactness of the protein can be comprehended through an analysis of the radius of gyration (Rg). Greater radius of gyration values implies reduced flexibility and compactness, whereas lower values signify increased rigidity and compactness. The results showed a decrease in Rg for the protein-ligand complex over the simulation time, indicating an increase in the structure's compactness (Figure 46).

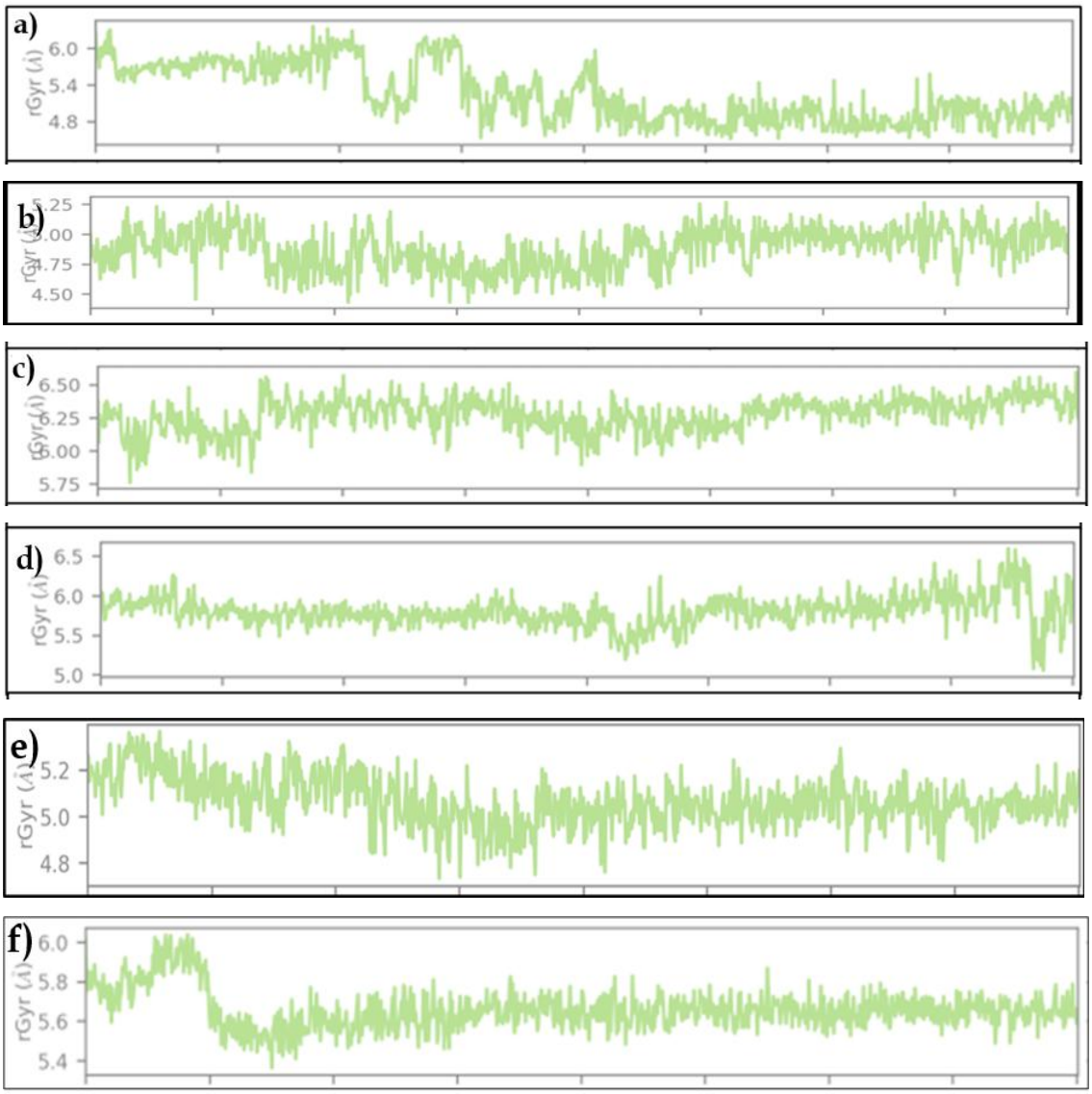

Figure 46: Radius of gyration (Rg) of protein–ligand complex(s). a) **4W93-QT8**, b) **4W93- QT7** c) Acarbose and d) **3A4A- QT8**, c) **3A4A- QT7**, f) Acarbose during 200 ns simulation time.

5.2.3.3.4 Protein ligand interactions

During the simulation process, we closely monitored the interactions between proteins and ligands. These interactions were categorized into hydrophobic bonds, hydrogen bonds, water bridges, and ionic bridges. The protein-ligand complex(s) stability is influenced by the specific amino acid residues present in the active site of the target protein. Throughout the 200 nanoseconds MD simulation study, we observed Various interactions between the complex(s) **4W93-QT8**, **QT7**, acarbose and **3A4A- QT8**,

QT7, acarbose as illustrated in figure 47a, 47b, 47c and 47d, 47e, 47f respectively. For instance, in figure 47a interaction with compound **QT8** with **4W93** receptor include hydrophobic interactions with Trp58,59, Tyr62,151, Leu162, Ile235 and Ala307. Additionally, H-bonds interactions were seen with Tyr151, Lys200, His201, Glu240 and His305. Also showed water bridges and ionic interaction with Trp59, Tyr62, Asn152, Asp197, Lys200, His201, Glu240, Gly304, His305, Gly306 Gly304 and Gly306 respectively. Moreover, in figure 47b interaction with compound **QT8** with **4W93** receptor shows hydrophobic interactions with Trp58,59, His101, Lys142, Tyr151, Ala154, Trp203, Pro241 and Lys243,257. Furthermore, H-bonds interactions were seen with Lys142, Asn150, Tyr151, Asn152, Ala154, Gly239, Asn270 and His305. Also showed water bridges with Tyr62, Gln63, Lys142, Asn150, Tyr151, Asn152, Asp153, Arg158, Lys243, Asp246, Asp300 and Asn461.

Similarly, compound **QT8** with **3A4A** receptor (**Figure 47c**) shows hydrophobic interactions with Tyr72, Val109, Tyr158, Phe178, Val216, Phe303, Pro312 and leu313. Furthermore, H-bonds interactions were seen with His112, Lys156, Tyr158, Asp215, Gln279, Pro312, Leu312, Arg315 and Glu353.Also showed water bridges and ionic interaction with Lys156, Tyr158, Phe159, Asp215, Glu277, Pro312, Leu313, Arg315, Asp352, Glu411, Asn414, Arg442 and Leu313, Asp352, Glu411 respectively. Moreover, in figure 47d interaction with compound **QT7** with **3A4A** receptor shows hydrophobic interactions with Tyr72,158, Phe178, Val216, Phe303 and Arg442.Furthermore, H-bonds interactions were seen with Gln279, Leu313 and Arg442.The hydrogen-bonded protein-ligand interactions mediated by a water molecule (water bridges) showed with Tyr62, Gln63, Lys142, Asn150, Tyr151, Asn152, Asp153, Arg158, Lys243, Asp246, Asp300 and Asn461.The investigation demonstrates hydrogen-bonded protein-ligand interactions mediated by a water molecule (water bridges), such as Tyr72,158, Asp215,242, Gln279, Pro312, Leu313, Arg315, His351 and Arg442.The MD simulation results were demonstrated the protein-ligand complex's stability over 200 nanoseconds, highlighting strong and permanent binding interactions among all amino acids at the active site.

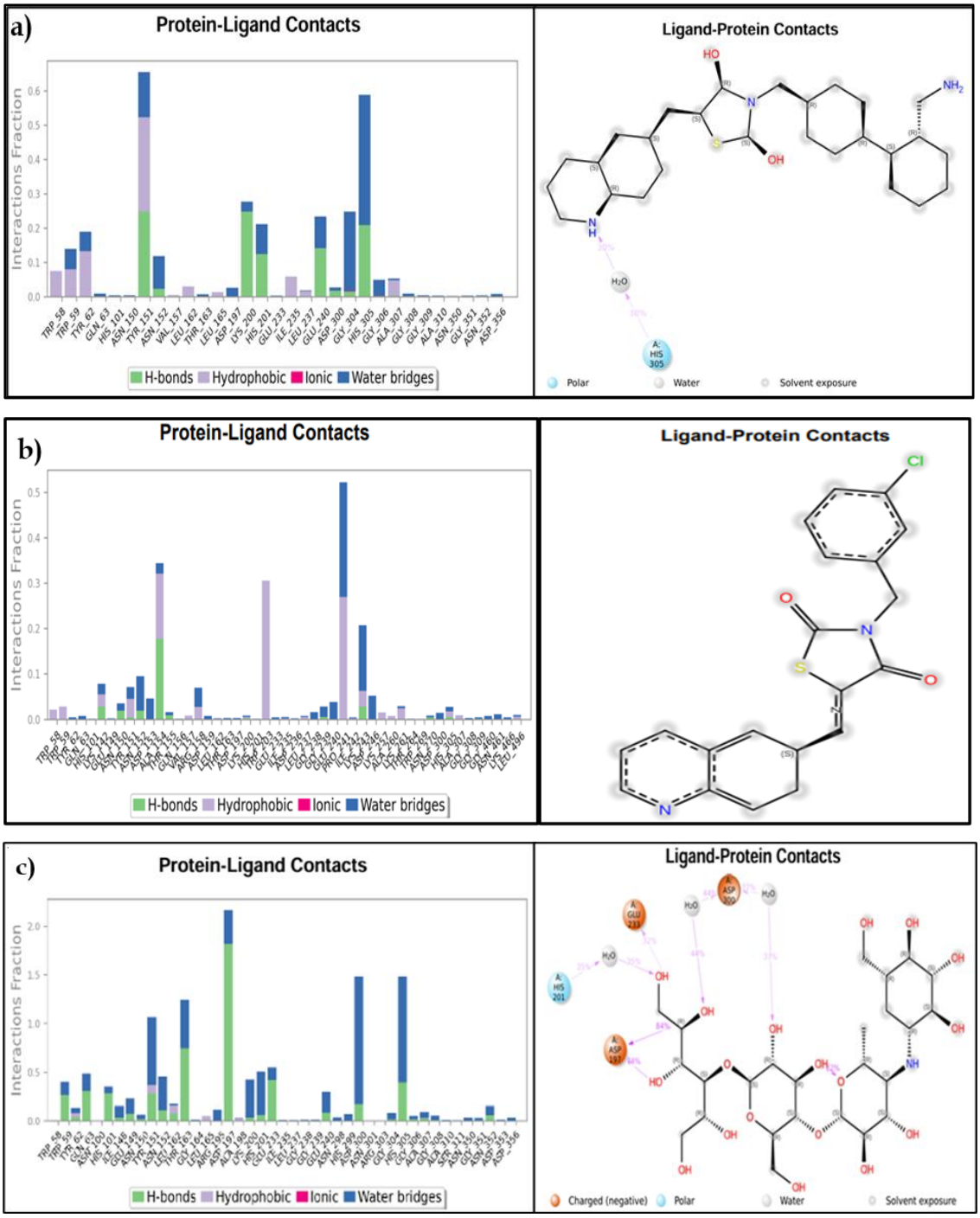
a)
Protein-Ligand Contacts
Interactions Fraction
H-bonds
Hydrophobic
Ionic
Water bridges
Ligand-Protein Contacts
Polar
Water
Solvent exposure
b)
Protein-Ligand Contacts
Interactions Fraction
H-bonds
Hydrophobic
Ionic
Water bridges
Ligand-Protein Contacts
c)
Protein-Ligand Contacts
Interactions Fraction
H-bonds
Hydrophobic
Ionic
Water bridges
Ligand-Protein Contacts
Charged (negative)
Polar
Water
Solvent exposure

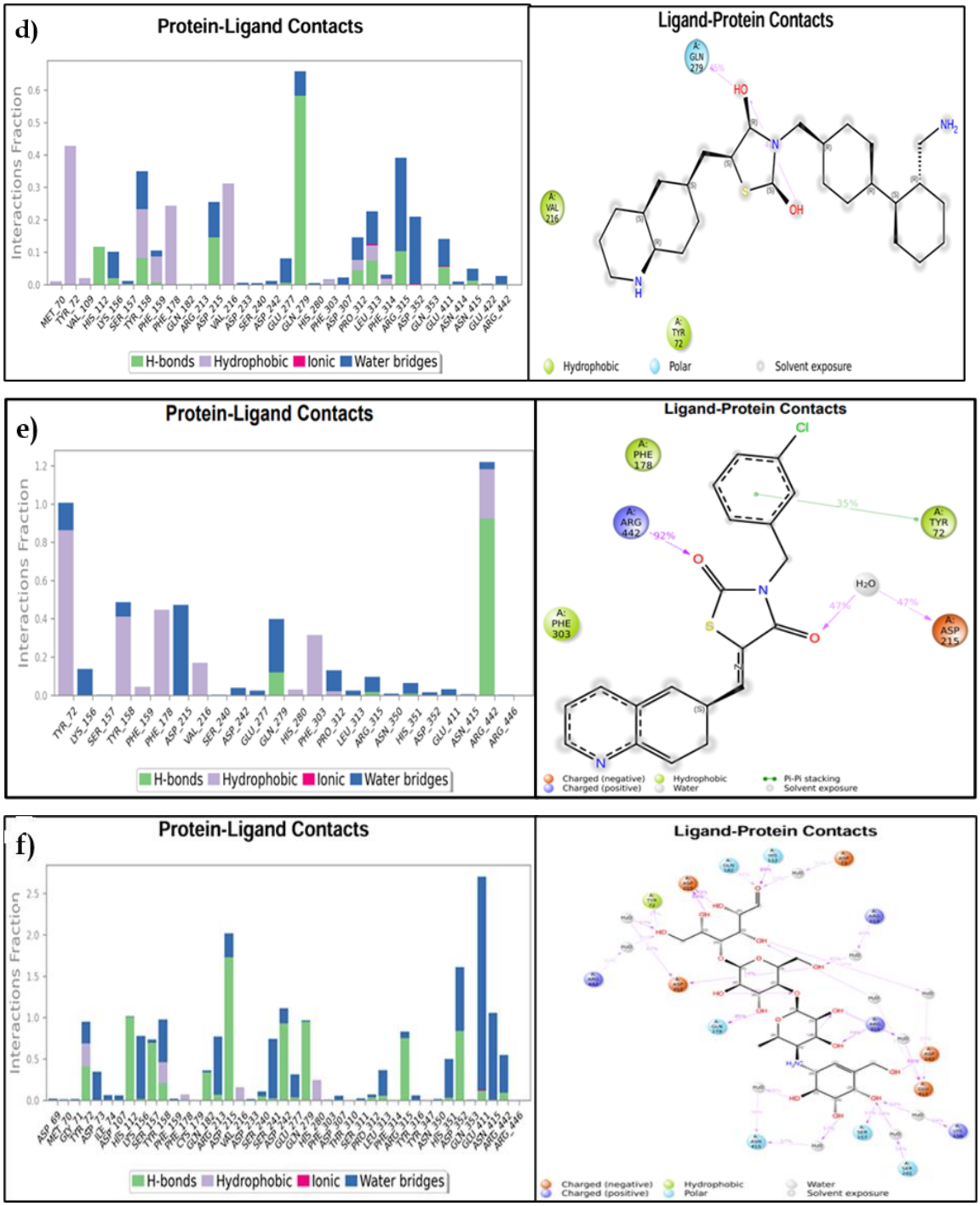

Figure 47: Interactions of receptor **4W93** with a) **QT8**, b) **QT7**, c) Acarbose and receptor **3A4A** with d) **QT8**, e) **QT7** f) Acarbose

5.2.3.4. Molecular properties

All synthesized compounds (**QT1-QT8**) meet the desired physicochemical properties without any deviations from the established standard ranges, as outlined in table 5.16. Lipinski rule of five (LR5), the drug likeness rule states compounds must have a molecular weight (MW) of ≤ 500, the number of hydrogen bond donors (HBD) is ≤ 5, the number of hydrogen bond acceptors are ≤ 10, and a partition coefficient of ≤ 6.5, and a Total Polar Surface Area (TPSA) value of ≤ 140.These characteristics values are crucial in evaluating their suitability for oral bioavailability and drug-likeness. The bioavailability of all synthesized compounds, including acarbose, was found to be 0.55, which is considered the optimal value. Bioavailability is a crucial factor in determining the percentage of a drug's dose that remains unchanged in the systemic circulation, ensuring effective drug delivery. The results demonstrate that all the compounds adhere to LR5 and exert good oral bioavailability.

Table 5.17: Physicochemical and drug likeness score of compounds (**QT1-QT8**)

Compound	MW	RB	QP Log $P_{O/W}$	HBD	HBA	TPSA	Bioavailability score	Drug likeness Score
Acceptable range	**≤ 500**	**≤ 10**	**-2.0 to 6.5**	**≤ 5**	**≤ 10**	**≤ 140**	**0.55**	**-**
QT1	312.09	4	3.84	0	4	75.58	0.55	-0.74
QT2	368.16	8	5.99	0	4	75.35	0.55	-0.81
QT3	360.07	6	4.19	0	4	75.54	0.55	-0.82
QT4	361.97	3	3.25	0	4	75.57	0.55	-0.84
QT5	356.12	7	3.25	1	5	95.85	0.55	-0.77
QT6	346.08	3	4.24	0	4	75.57	0.55	-0.70
QT7	382.05	3	4.85	0	4	75.57	0.55	-0.72
QT8	447.10	4	5.25	0	5	99.36	0.55	-0.80
Acarbose	645.25	9	-4.58	14	19	321.12	0.55	0.40

MW: Molecular weight; **RB**: Rotatable bonds; **QP Log $P_{o/w}$**: Predicated octanal/water partition coefficient; **HBD**: Hydrogen bond donor; **HBA**: Hydrogen bond acceptor; **TSPA**: Total polar surface area

5.2.3.5. Absorption, distribution, metabolism, and excretion and toxicity prediction

The development of a novel drug molecule heavily relies on its pharmacokinetic properties. The drug molecule requires excellent pharmacokinetic and medicinal properties.To evaluate the ADME (absorption, distribution, metabolism, and excretion) and toxicity properties of the synthesized compounds and acarbose, data was analysed using Swiss ADME online server and OSIRIS tools respectively. The ADME and toxicity results were summarized in table 5.18.

The results revealed that all the synthesized compounds exhibited high GI absorption, indicating their beneficial uptake within the gastrointestinal tract, except for acarbose. Moreover, except compound **QT8**, **QT7**, **QT5** and acarbose have shown no permeation for the blood-brain barrier (BBB), and apart from that, other compounds have demonstrated the strong potential to permeate the BBB, implying their capacity to traverse this crucial physiological barrier. Lower pharmacokinetic drug interactions were seen for certain of the drugs with specific isoenzyme inhibitors, including CYP2C19, CYP1A2, CYP2D6, CYP2C9, and CYP3A4. Additionally, the results show that none of the synthetic compounds are P-glycoprotein (P-gp) substrates. Furthermore, the possible toxicity profile of the synthesized compounds predicted based on the multiple parameters, which includes mutagenic, tumorigenic, reproductive effect and irritant. In table 5.18, a green tone indicates low toxicity tendency, where yellow tone illustrates moderate toxicity and red tone states high toxicity towards mutagenic, tumorigenic, reproductive and irritant toxicity. However, all the synthesized compounds demonstrated low toxicity tendency. Notably, the compound **QT2** and **QT4** shows high (red tone) irritant toxicity and compound **QT8** shows moderate toxicity towards reproductive system.

Table 5.18: ADME and Toxicity properties of compounds (**QT1-QT8**)

Compound	HI Absorption	BBB Permeation	CYP1A2 Inhibitors	CYP2C19 Inhibitors	CYP2C9 Inhibitors	CYP2D6 Inhibitors	CYP3A4 Inhibitors	P-gp substrate	Mutagenic	Tumorigenic	Reproductive effect	Irritant
QT1	High	Yes	Yes	Yes	Yes	No	Yes	No	G	G	G	R
QT2	High	No	Yes	Yes	Yes	No	Yes	No	G	G	G	G
QT3	High	Yes	Yes	Yes	Yes	No	Yes	No	G	G	G	G
QT4	High	Yes	Yes	Yes	Yes	No	No	No	G	G	G	G
QT5	High	Yes	Yes	Yes	Yes	No	Yes	No	G	G	G	R
QT6	High	Yes	Yes	Yes	Yes	No	Yes	No	G	G	G	G
QT7	High	No	Yes	Yes	Yes	No	Yes	No	G	G	Y	G
QT8	High	No	Yes	Yes	Yes	No	Yes	No	G	G	G	G
Acarbose	Low	No	No	No	No	No	No	Yes	G	G	Y	G

HI: human intestinal absorption; **BBB**: blood brain barrier; Red (R)colour: illustrates high toxicity tendency; Yellow (Y) colour: illustrates moderate toxicity tendency; Green (G) colour: illustrates low toxicity tendency.

5.2.3.6. Discussion

In the present study, both naphthalene and quinoline-based thiazolidinedione derivatives exhibited notable antidiabetic potential; however, distinct differences were observed in their inhibitory effects on carbohydrate-hydrolysing enzymes like PAA and IAG enzymes. The first series of naphthalene-based thiazolidinedione derivatives (**NT1-NT18**), demonstrated good to moderate inhibition of PAA and IAG (Table 5.11), likely due to favorable hydrophobic and π–π stacking interactions with the enzyme's active site (Table 5.13 and Table 5.14). Compound **NT17**, with a diphenyl carbonitrile substituent, was particularly potent. In the present series, quinoline-based thiazolidinedione derivatives (**QT1-QT8**) were synthesised with alkyl, haloalkyl and aromatic groups are strategically placed on amidic nitrogen of central thiazolidinedione core while a quinoline ring is introduced, attributed to the presence of the heterocyclic nitrogen, which facilitates additional hydrogen bonding and polar interactions. Which enhance the enzymes inhibition with superior control of postprandial glucose levels. Here acarbose, was also used as standard compound. In contrast, the acarbose, displaying the IC_{50} values of 10.15 µM against PAA and 8.24 µM against IAG enzymes, robust binding affinity of -6.7 kcal/mol with PAA and -8.5 kcal/mol with IAG receptors respectively.

Initially, alkyl substituted compounds **QT1** and **QT2** was synthesized, and *in vitro* results states that both compounds are effectively inhibiting the PAA and IAG enzymes. Compound **QT1** exhibiting the IC_{50} values of 5.54 µM against PAA and 7.15 µM against IAG enzymes. The binding affinity of compound **QT1** was -7.7 kcal/mol with in active site of PAA (**PDB ID: 4W93)** and -8.0 kcal/mol with in active site of IAG (**PDB ID: 3A4A)** receptor. Similarly, compound **QT2** exhibiting the IC_{50} values of 8.12 µM against PAA and 6.25 µM against IAG enzymes. The binding affinity of compound **QT1** was -7.9 kcal/mol with in active site of PAA and -8.7 kcal/mol with in active site of IAG receptor. Figure 41(A) and 41(B) demonstrates the 2D and 3D docking interactions of compound **NT17** with the receptor **4W93** respectively. It was found to show π – π T Shaped interaction with amino acid Trp59 by quinoline ring and Trp59 by thiazolidinedione central core. Whereas alkyl chain (butyl) present attached to the amidic nitrogen to the thiazolidinedione central core showed π- alkyl/ alkyl type of

interactions with the leu163, Ala198, His201 and Ile235 in the active site of receptor. Conspicuously, one of the carbonyl oxygens (C=O) of thiazolidinedione ring of the compound **QT1** has shown hydrogen bonding with Arg195 amino acid within active site of PAA (**PDB ID: 4W93)**.

The FT-IR of compound **QT1** demarcated absorption bands at 2954 cm^{-1} for C-H-aromatic, 2871 cm^{-1} for CH-aliphatic, 1346 cm^{-1} for CN-aromatic (quinoline ring) very clearly. The appearance of the carbonyl (-C=O) group at 1735, 1167 cm^{-1} clearly conforms the thiazolidinedione ring in the compound.

^{1}H NMR spectral data of compound **QT1** confirmed, a singlet peak at δ: 3.79 ppm, is conforms the -CH_2 protons attached to (-NH substituted) thiazolidinedione ring. The six aromatic protons (naphthalene ring) were observed in the region δ 7.48-8.21 and also sharp singlet peak at δ: 8.98 ppm was attributed to the -CH proton (benzylidene proton) conjugated with the thiazolidinedione ring. The ^{13}C NMR spectrum of compound **QT1** revealed distinctive peaks that correspond to its molecular structure. The two carbonyl (-C=O) carbons of the thiazolidinedione are denoted by peaks at δ: 167.57 and 166.25 pp. The Nine carbons originating from the quinoline ring were discerned by nine peaks at δ: 152.09, 148.45, 136.61, 132.58, 131.61, 130.63, 129.81 128.20 and 121.19 ppm. Additionally, a peak at δ: 42.99, 29.81, 19.98, 13.62 ppm clarify the identity of four alkyl carbons in the structure attached to the nitrogen group on the thiazolidinedione ring. Initially the purity of the synthesized compounds is analyzed by the melting point apparatus (Table 5.10). Moreover, mass spectrum revealed a molecular ion peak (M^+ peak) at 312.0945 (m/z), confirming the molecular mass of compound **QT1**.

Further, introduction of haloalkyl groups on the thiazolidinedione ring, halogens like chlorine (compound **QT3**) and bromine (compound **QT4**) resulted in the low to moderate PAA Inhibition activity as compared with on IAG receptor. This diminished activity could be attributed to its lower electronegativity, steric hindrance and due to absence of H-bond interactions with in the PAA binding site. Remarkably, the compound **QT3** shows H-bond interactions with in the IAG binding site, boasting the binding affinity of 8.25 μM against IAG enzyme. Notably, compound **QT5**, featuring

hydroxy alkyl exhibits good PAA Inhibition activity (9.84 μM) as compared with on IAG receptor (9.84 μM).

Upon substituting the aryl groups to an amidic nitrogen on the thiazolidinedione ring along with quinoline ring like compound **QT6-QT8** contributed to the maximum activity, yielding an IC_{50} values of 4.68 μM and 2.45 μM (**NT17**) against PAA and IAG enzyme respectively. Notably, compound **QT8** unveiled the highest binding affinity at -11.1 kcal/mol with receptors PAA in the series, and engaging in two hydrogen bond interactions with Gln63 and His299 and also shows π – π T-shaped and π- alkyl/alkyl connections with Trp59, Tyr62, Ala198 and Lys200 amino acid residues (226). Figure 42 (E) demonstrates the 2D docking interactions of compound **QT8** with the active site of receptor **4W93**. Similarly, same compound **QT8** shown the highest binding affinity at affinity at -10.6 kcal/mol with receptors IAG in the series, and engaging in two hydrogen bond interactions with Ser162 and Arg176 and also shows π – π T-shaped, connections with Ile150 and Ala418 amino acid residues. Figure 42 (D) demonstrates the 2D docking interactions of compound **QT8** with the receptor **3A4A** respectively.

In summary, compound **QT8** emerged as the standout analogue in the present series, featuring diphenyl carbonitrile amidic nitrogen on the TZD core along with quinoline ring.

5.2.3.7. Structure activity relationship (SAR)

The results from both the *in vitro* PAA and IAG inhibition assays, as well as the *in silico* evaluation studies, demonstrated that the SAR of all the synthesized quinoline-based thiazolidinedione analogues exhibited promising antidiabetic potential. **QT1-QT8** showed favorable drug-likeness profiles and optimal pharmacokinetic properties, indicating their suitability as potential therapeutic agents for diabetes management. compound **QT8** (biphenyl carbonitrile) and **QT7 (**Chloro benzene**)** shows higher percentage of inhibition against both PAA and IAG enzymes. It was observed that there was no significant change in the anti-diabetic activity after introducing the alkyl chain on the nitrogen of thiazolidinedione (**QT1 and QT2**).

CHAPTER-6

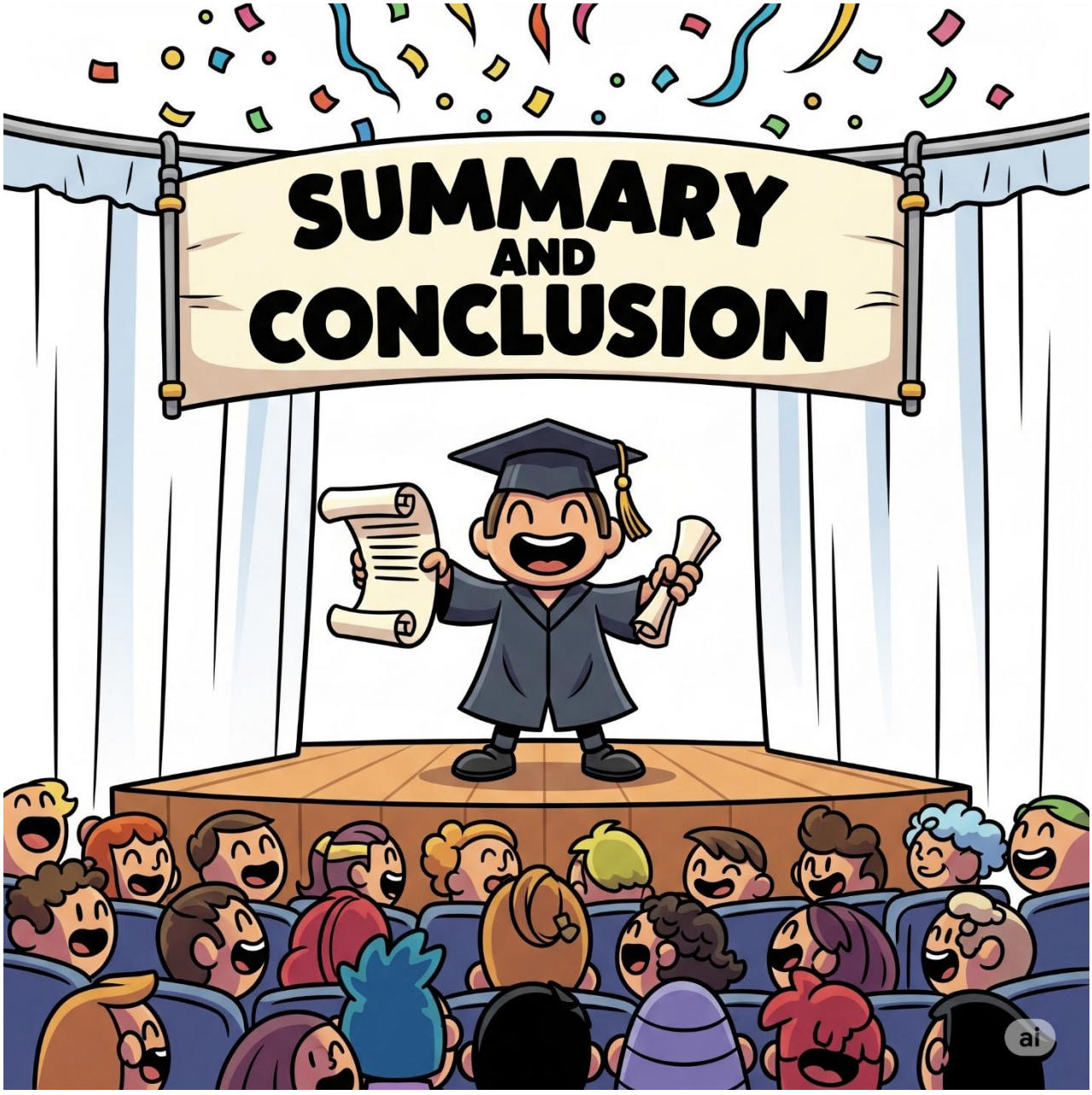

CHAPTER-6
SUMMARY AND CONCLUSION

The scope of the present study is to explore new bioactive molecules for the treatment of DM. An ideal drug molecule should have potent activity against selected targets as well as optimum pharmacokinetic properties for the purpose of good bioavailability and low toxicity. The study was conducted to find suitable pharmacological drugs through an easy and cost-effective synthetic pathway for the treatment of T2DM. we have tested antidiabetic activity of synthesized molecules against pancreatic α-amylase (PAA) and intestinal α-glucosidase (IAG). Additionally, studied antioxidant activity of synthesized molecules indicating the effectiveness in able to reduce the reactive oxygen species (ROS) induced DM. PAA and IAG are both key enzymes involved carbohydrate metabolism and in regulating blood glucose levels. PAA hydrolyses α-1,4-glycosidic bonds in starch and glycogen, breaking them down into maltose and other oligosaccharides and IAG enzymes play a crucial role in the final stages of carbohydrate digestion, by hydrolysing disaccharides and oligosaccharides produced by the action of PAA and other enzymes. As a result, restricting the activity of these two enzymes can lower the risk of developing diabetes and postprandial hyperglycaemia. Thus, while PAA and IAG inhibitors like acarbose, voglibose and miglitol offer substantial benefits in managing diabetes, their limitations underscore the ongoing need for further research and the development of alternative strategies to improve patient outcomes.

Designing antidiabetic agents, specifically thiazolidinediones analogues, are effective in managing the blood glucose levels (reduced postprandial blood glucose) and improving the insulin sensitivity. Thiazolidinedione analogues offer a promising alternative due to their unique structural features, which allow for precise interactions with the PAA and IAG binding pocket. Therefore, we have selected thiazolidinedione and naphthalene conjugate as our main scaffold in the present research based on the existed therapeutic potential of molecule (Netaglitazone) having this unique combination. Furthermore, various alkyl (or) aryl halides and methoxy group were attached on to the ‘Nitrogen’ group of TZD and on 5^{th} position of naphthalene respectively and evaluated the potency of the new molecules against PAA and IAG to

treat T2DM and also to reduce the limitations of already existed pharmacophore. After successful synthesis and characterization of **NT1-NT18** series, comprised of 18 molecules were evaluated the antidiabetic activity.

Furthermore, all the synthesised compounds were screened for *In vitro* antidiabetic activity against PAA and IAG enzymes (Table 5.2, Chapter 5), revealed that compound **NT7** and **NT17** having naphthalene and N-substituted dioxoisoindolin and biphenyl carbonitrile groups on TZD ring respectively was found to be the most potent exhibited high potency compared to acarbose. Notably, compound **NT17 s**hows IC_{50} value of 4.48 µM and 2.14 µM as compared with acarbose against PAA and IAG enzymes respectively. Subsequently, DPPH antioxidant assay demonstrates that the compound **NT7** and **NT17** are effective against ascorbic acid, indicating the effectiveness in able to reduce the reactive oxygen species (ROS) induced DM. A molecular docking and MM-GSBA studies provided insights into the interaction patterns of these compounds with PAA and IAG receptors. Compound **NT17** emerged as the most potent compound in the series (**NT1-NT18**), displaying an increased binding affinity of -10.7 kcal/mol with PAA receptor and -10.9 kcal/mol with receptors IGA receptor and engaging in hydrogen bond interactions with Thr163 and Arg195 amino acids within the PAA active binding pocket (Table 5.4, Chapter 5) and Arg315 and Arg442 amino acids within IAG active binding pocket (Table 5.5, Chapter 5) respectively. Molecular properties, Pharmacokinetic (ADME) and toxicity analysis revealed favourable physicochemical properties leads to durglikeness and manageable toxicity profiles of all compounds including compound **NT7** and **NT17**.

Novel thiazolidinedione-based quinoline compounds (**QT1-QT8**) were synthesized by a facile method. These chemical entities were well characterized by FT-IR, Mass and NMR (^{1}H & ^{13}C) spectroscopic methods. Furthermore, these compounds were screened for *In vitro* antidiabetic activity against PAA and IAG enzymes (Table 5.11 Chapter 5). As results states that all tested compounds shown significant PAA enzyme inhibition activity at the dose of 50 (µg/mL). Among the all compounds **QT8** (IC_{50} = 4.68 µM) and **QT7** (IC_{50} = 5.48 µM) was found to be the most potent as compared with standard acarbose with IC_{50} value of 10.15 µM. Additionally,

synthesized compounds were tested for their ability to inhibit IAG enzyme. The results suggest, compound **QT8** (IC_{50} = 2.45 µM) shown best results as followed by the compounds **QT7**, **QT6** and **QT5** with IC_{50} value 3.14 µM, 5.24 µM and 6.25 µM respectively. Acarbose was used as a positive control, showing prominent enzyme inhibition activity with IC_{50} value 8.245 µM. Furthermore, *in vitro* antioxidant activity was performed for all compounds using the DPPH assay, the results demonstrated that the except compounds **QT1 and QT3,** all the remaining compounds possess good antioxidant activity than standard (ascorbic acid) compound. The molecular docking studies exhibited significant information on biochemical and structural features of the molecules. The biochemically active moieties of the compound **QT8** are the carbonyl group (-C=O) of the thiazolidinedione ring, the nitrogen of the quinoline ring and the cyano (-CN) groups that are involved in the formation of strong conventional hydrogen bonds with Gln63 and His299 amino acids with PAA receptor (Figure 41, Chapter 5) and Arg213, Gln279, Arg315 and His351 amino acids with IAG receptor (Figure 42, Chapter 5). The molecular dynamic simulation studies states, RMSD, RMSF, Rg and protein ligand contacts, confirmed the stable binding of compound **QT7** and **QT8** with the both PAA and IAG proteins. Further, the results of molecular and pharmacokinetic properties of all the synthesised compounds states, they may show good oral absorption as well as optimum distribution properties and metabolic properties.

The study concludes that the designed novel thiazolidinedione-based naphthalene and quinoline derivatives may go for pre-clinical and clinical trials as they are showing good antidiabetic activity along with ideal molecular and pharmacokinetic properties. We have found out that the molecules **NT17** and **QT8** are showing potent antidiabetic activity via inhibition PAA and IAG enzymes that leads management of hyperglycaemia by delaying the digestion of carbohydrates. All the results suggested that the potential drug molecules **NT17** and **QT8** are suitable for further analysis studies to develop as novel antidiabetic drug candidate.

CHAPTER-7

REFERENCES

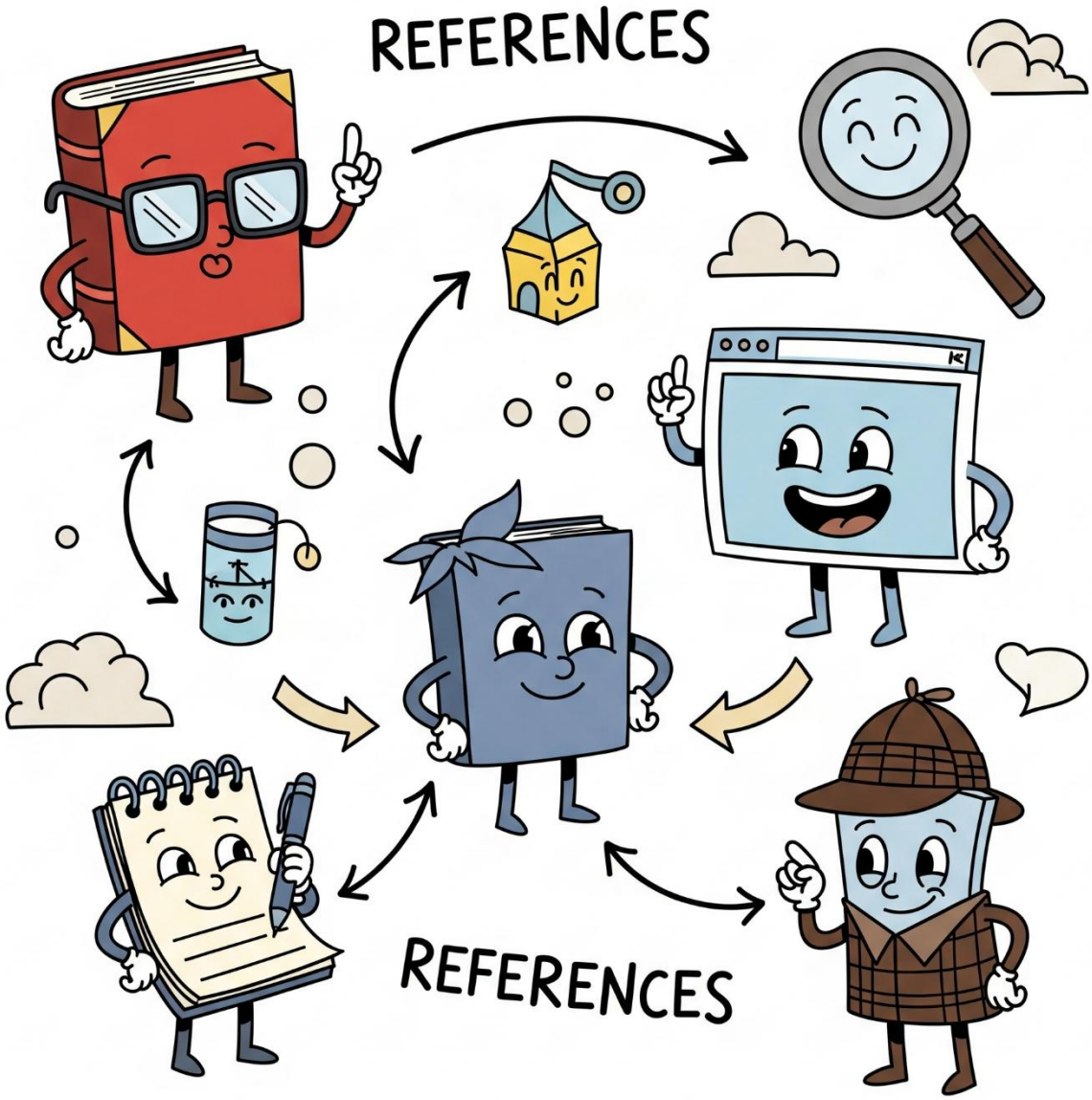

CHAPTER-7

REFERENCES

1. Pore A V, Bais SK, Shahnawaz SM. Review on Pharmaceutical Sales and Marketing. International Journal of Pharmacy and Herbal Technology2023. 2023;1(2):239–48.
2. Vangala S, Saxena U, Satish Chandran C. Building Human In Vitro 3D Models to Replace Animal Studies During Drug Discovery Research: Scientific, Ethical and Regulatory Considerations. In: Microfluidics and multi organs on chip. Springer; 2022. p. 695–717.
3. Sarkar B, Chakraborty S, Rakshit G, Singh RP. Fundamental approaches of drug discovery. In: Biochemical and Molecular Pharmacology in Drug Discovery. Elsevier; 2024. p. 251–82.
4. Palmer ME, Andrews LJ, Abbey TC, Dahlquist AE, Wenzler E. The importance of pharmacokinetics and pharmacodynamics in antimicrobial drug development and their influence on the success of agents developed to combat resistant gram-negative pathogens: A review. Front Pharmacol. 2022; 13:888079.
5. Pinzi L, Bisi N, Rastelli G. How drug repurposing can advance drug discovery: challenges and opportunities. Frontiers in Drug Discovery. 2024; 4:1460100.
6. Patton EE, Zon LI, Langenau DM. Zebrafish disease models in drug discovery: from preclinical modelling to clinical trials. Nat Rev Drug Discov. 2021;20(8):611–28.
7. Prajapati RN, Bhushan B, Singh K, Chopra H, Kumar S, Agrawal M, et al. Recent Advances in Pharmaceutical Design: Unleashing the Potential of Novel Therapeutics. Curr Pharm Biotechnol. 2024;25(16):2060–77.
8. Brogi S, Ramalho TC, Kuca K, Medina-Franco JL, Valko M. In silico methods for drug design and discovery. Vol. 8, Frontiers in chemistry. Frontiers Media SA; 2020. p. 612.
9. Martinez-Mayorga K, Madariaga-Mazon A, Medina-Franco JL, Maggiora G. The impact of chemoinformatics on drug discovery in the pharmaceutical industry. Expert Opin Drug Discov. 2020;15(3):293–306.
10. Wu K, Karapetyan E, Schloss J, Vadgama J, Wu Y. Advancements in small molecule drug design: A structural perspective. Drug Discov Today. 2023;103730.

11. Tiwari PC, Pal R, Chaudhary MJ, Nath R. Artificial intelligence revolutionizing drug development: Exploring opportunities and challenges. Drug Dev Res. 2023;84(8):1652–63.

12. Swinney DC, Anthony J. How were new medicines discovered? Nat Rev Drug Discov. 2011;10(7):507–19.

13. Adelusi TI, Oyedele AQK, Boyenle ID, Ogunlana AT, Adeyemi RO, Ukachi CD, et al. Molecular modeling in drug discovery. Inform Med Unlocked. 2022; 29:100880.

14. Sadybekov A V, Katritch V. Computational approaches streamlining drug discovery. Nature. 2023;616(7958):673–85.

15. Kiriiri GK, Njogu PM, Mwangi AN. Exploring different approaches to improve the success of drug discovery and development projects: a review. Futur J Pharm Sci [Internet]. 2020 Dec 23;6(1):27. Available from: https://fjps.springeropen.com/articles/10.1186/s43094-020-00047-9

16. Bharatam P V. Computer-aided drug design. Drug Discovery and Development: From Targets and Molecules to Medicines. 2021;137–210.

17. Zeng W, Guo L, Xu S, Chen J, Zhou J. High-throughput screening technology in industrial biotechnology. Trends Biotechnol. 2020;38(8):888–906.

18. Badrinarayan P, Narahari Sastry G. Virtual high throughput screening in new lead identification. Comb Chem High Throughput Screen. 2011;14(10):840–60.

19. Lipinski CA. Lead-and drug-like compounds: the rule-of-five revolution. Drug Discov Today Technol. 2004;1(4):337–41.

20. Jia CY, Li JY, Hao GF, Yang GF. A drug-likeness toolbox facilitates ADMET study in drug discovery. Drug Discov Today. 2020;25(1):248–58.

21. Fang Y. Ligand–receptor interaction platforms and their applications for drug discovery. Expert Opin Drug Discov. 2012;7(10):969–88.

22. Kitchen DB, Decornez H, Furr JR, Bajorath J. Docking and scoring in virtual screening for drug discovery: methods and applications. Nat Rev Drug Discov. 2004;3(11):935–49.

23. Wang A, Zhang Y, Chu H, Liao C, Zhang Z, Li G. Higher accuracy achieved for protein–ligand binding pose prediction by elastic network model-based ensemble docking. J Chem Inf Model. 2020;60(6):2939–50.

24. Vyas VK, Ukawala RD, Ghate M, Chintha C. Homology modeling a fast tool for drug discovery: Current perspectives. Indian J Pharm Sci. 2012;74(1):1–17.

25. Pradeepkiran JA, Sainath SB, Shrikanya KVL. In silico validation and ADMET analysis for the best lead molecules. In: Brucella Melitensis. Elsevier; 2021. p. 133–76.

26. Osmaniye D, Ahmad I, Sağlık BN, Levent S, Patel HM, Ozkay Y, et al. Design, synthesis and molecular docking and ADME studies of novel hydrazone derivatives for AChE inhibitory, BBB permeability and antioxidant effects. J Biomol Struct Dyn. 2023;41(18):9022–38.

27. Kawsar SMA, Hosen MA, Chowdhury TS, Rana KM, Fujii Y, Ozeki Y. Thermochemical, PASS, molecular docking, drug-likeness and in silico ADMET prediction of cytidine derivatives against HIV-1 reverse transcriptase. Revista de Chimie. 2021;72(3):159–78.

28. Raju B, Verma H, Narendra G, Sapra B, Silakari O. Multiple machine learning, molecular docking, and ADMET screening approach for identification of selective inhibitors of CYP1B1. J Biomol Struct Dyn. 2022;40(17):7975–90.

29. Arena R, McNeil A, Sagner M, Hills AP. The current global state of key lifestyle characteristics: health and economic implications. Prog Cardiovasc Dis. 2017;59(5):422–9.

30. Mohajan D, Mohajan HK. Basic Concepts of Diabetics Mellitus for the Welfare of General Patients. Studies in Social Science & Humanities. 2023;2(6):23–31.

31. Zakir M, Ahuja N, Surksha MA, Sachdev R, Kalariya Y, Nasir M, et al. Cardiovascular complications of diabetes: from microvascular to macrovascular pathways. Cureus. 2023;15(9).

32. Lotfy M, Adeghate J, Kalasz H, Singh J, Adeghate E. Chronic complications of diabetes mellitus: a mini review. Curr Diabetes Rev. 2017;13(1):3–10.

33. world health organisation [Internet]. [cited 2023 Mar 28]. Available from: https://www.who.int/news-room/fact-sheets/detail/diabetes

34. IDF Diabetes Atlas 2025. million [Internet]. [cited 2025 Jun 2]. Available from: https://diabetesatlas.org/resources/idf-diabetes-atlas-2025/

35. Rojas J, Bermudez V, Palmar J, Martínez MS, Olivar LC, Nava M, et al. Pancreatic beta cell death: novel potential mechanisms in diabetes therapy. J Diabetes Res. 2018;2018(1):9601801.

36. Roep BO, Thomaidou S, van Tienhoven R, Zaldumbide A. Type 1 diabetes mellitus as a disease of the β-cell (do not blame the immune system?). Nat Rev Endocrinol. 2021;17(3):150–61.

37. mukhtar y, galalain a, yunusa ujej. a modern overview on diabetes mellitus: a chronic endocrine disorder. european journal of biology. 2020 nov 23;5(2):1–14.

38. Das B, Das M, Kalita A, Baro MR. The role of Wnt pathway in obesity induced inflammation and diabetes: a review. J Diabetes Metab Disord. 2021;1–12.

39. Benninger RKP, Kravets V. The physiological role of β-cell heterogeneity in pancreatic islet function. Nat Rev Endocrinol. 2022;18(1):9–22.

40. Antar SA, Ashour NA, Sharaky M, Khattab M, Ashour NA, Zaid RT, et al. Diabetes mellitus: Classification, mediators, and complications; A gate to identify potential targets for the development of new effective treatments. Biomedicine and Pharmacotherapy

41. Saravanan P, Magee LA, Banerjee A, Coleman MA, Von Dadelszen P, Denison F, et al. Gestational diabetes: opportunities for improving maternal and child health. Lancet Diabetes Endocrinol. 2020;8(9):793–800.

42. Bernea EG, Uyy E, Mihai DA, Ceausu I, Ionescu-Tirgoviste C, Suica VI, et al. New born macrosomia in gestational diabetes mellitus. Exp Ther Med. 2022;24(6):1–12.

43. Gaál Z, Balogh I. Monogenic forms of diabetes mellitus. Genetics of Endocrine Diseases and Syndromes. 2019;385–416.

44. Bhattacharya S, Pappachan JM. Monogenic diabetes in children: An underdiagnosed and poorly managed clinical dilemma. World J Diabetes. 2024;15(6):1051.

45. Zhang H, Colclough K, Gloyn AL, Pollin TI. Monogenic diabetes: a gateway to precision medicine in diabetes. J Clin Invest. 2021;131(3).

46. Bonnefond A, Unnikrishnan R, Doria A, Vaxillaire M, Kulkarni RN, Mohan V, et al. Monogenic diabetes. Nat Rev Dis Primers. 2023;9(1):12.

47. Davison LJ. Diabetes mellitus and pancreatitis–cause or effect? Journal of Small Animal Practice. 2015;56(1):50–9.

48. Nishi M, Nanjo K. Insulin gene mutations and diabetes. J Diabetes Investig. 2011;2(2):92–100.

49. Arneth B. Insulin gene mutations and posttranslational and translocation defects: associations with diabetes. Endocrine. 2020;70(3):488–97.

50. Ataie-Ashtiani S, Forbes B. A review of the biosynthesis and structural implications of insulin gene mutations linked to human disease. Cells. 2023;12(7):1008.

51. Reardon W, Pembrey ME, Trembath RC, Ross RJM, Sweeney MG, Harding AE, et al. Diabetes mellitus associated with a pathogenic point mutation in mitochondrial DNA. The Lancet. 1992;340(8832):1376–9.

52. Harouch B, Klar A, TC FZ. INSR-related severe syndromic insulin resistance. 2018;

53. Alam S, Hasan MK, Neaz S, Hussain N, Hossain MF, Rahman T. Diabetes Mellitus: insights from epidemiology, biochemistry, risk factors, diagnosis, complications and comprehensive management. Diabetology. 2021;2(2):36–50.

54. Khanam A, Hithamani G, Naveen J, Pradeep SR, Barman S, Srinivasan K. Management of invasive infections in diabetes mellitus: A comprehensive review. Biologics. 2023;3(1):40–71.

55. Balaji R, Duraisamy R, Kumar MP. Complications of diabetes mellitus: A review. Drug Invention Today. 2019;12(1).

56. Hiraoka S, Kawasumi M. A case of diabetic ketoacidosis with prurigo pigmentosa as a dermadrome. Diabetol Int. 2024;15(3):594–9.

57. Paluchamy T. Hypoglycemia: essential clinical guidelines. In: Blood glucose levels. IntechOpen; 2019.

58. Imamura F, O'Connor L, Ye Z, Mursu J, Hayashino Y, Bhupathiraju SN, et al. Consumption of sugar sweetened beverages, artificially sweetened beverages, and fruit juice and incidence of type 2 diabetes: systematic review, meta-analysis, and estimation of population attributable fraction. Bmj. 2015;351.

59. La Sala L, Pontiroli AE. New fast acting glucagon for recovery from hypoglycemia, a life-threatening situation: nasal powder and injected stable solutions. Int J Mol Sci. 2021;22(19):10643.

60. Dhatariya KK, Glaser NS, Codner E, Umpierrez GE. Diabetic ketoacidosis. Nat Rev Dis Primers. 2020;6(1):40.

61. Karrar HR, Nouh MI, Alhendi RSA. Diabetic ketoacidosis: a review article. World Family Medicine. 2022;20(6):66–71.

62. Aramovna DZ, Obloqulov J, Norova E, Xudoyberdiyev B. Diabetic Ketoacidosis, Pathophysiology, Diagnosis and Treatment. Central Asian Journal of Medical and Natural Science. 2023;4(3):116–20.

63. Zahran NA, Jadidi S. Pediatric Hyperglycemic Hyperosmolar Syndrome: A Comprehensive Approach to Diagnosis, Management, and Complications Utilizing Novel Summarizing Acronyms. Children. 2023;10(11):1773.

64. Fettach S, Thari FZ, Hafidi Z, Tachallait H, Karrouchi K, El achouri M, et al. Synthesis, α-glucosidase and α-amylase inhibitory activities, acute toxicity and molecular docking studies of thiazolidine-2,4-diones derivatives. J Biomol Struct Dyn. 2022;40(18):8340–51.

65. Katsarou A, Gudbjörnsdottir S, Rawshani A, Dabelea D, Bonifacio E, Anderson BJ, et al. Type 1 diabetes mellitus. Nat Rev Dis Primers. 2017; 3:1–18.

66. Mezil SA, Abed BA. Complication of diabetes mellitus. Ann Rom Soc Cell Biol. 2021;1546–56.

67. Dal Canto E, Ceriello A, Rydén L, Ferrini M, Hansen TB, Schnell O, et al. Diabetes as a cardiovascular risk factor: An overview of global trends of macro and micro vascular complications. Eur J Prev Cardiol. 2019 Dec;26(2_suppl):25–32.

68. Bolignano D, Zoccali C. Non-proteinuric rather than proteinuric renal diseases are the leading cause of end-stage kidney disease. Nephrology Dialysis Transplantation. 2017;32(suppl_2): ii194–9.

69. Nentwich MM. Diabetic retinopathy - ocular complications of diabetes mellitus. World J Diabetes. 2015;6(3):489.

70. Bril V, Breiner A, Perkins BA, Zochodne D, Committee DCCPGE. Neuropathy. Can J Diabetes. 2018;42: S217–21.

71. Boulton AJM, Armstrong DG, Kirsner RS, Attinger CE, Lavery LA, Lipsky BA, et al. Diagnosis and management of diabetic foot complications. 2018;

72. Leal JM, de Souza GH, Marsillac PF de, Gripp AC. Skin manifestations associated with systemic diseases–Part II. An Bras Dermatol. 2022; 96:672–87.

73. La Vignera S, Condorelli RA, Cannarella R, Giacone F, Mongioi' LM, Cimino L, et al. Urogenital infections in patients with diabetes mellitus: Beyond the conventional aspects. Int J Immunopathol Pharmacol. 2019; 33:2058738419866582.

74. Mare R, Sporea I. Gastrointestinal and liver complications in patients with diabetes mellitus—A review of the literature. J Clin Med. 2022;11(17):5223.

75. Tomic D, Shaw JE, Magliano DJ. The burden and risks of emerging complications of diabetes mellitus. Nat Rev Endocrinol. 2022;18(9):525–39.

76. Huang JF, Wu QN, Zheng XQ, Sun XL, Wu CY, Wang XB, et al. The characteristics and mortality of osteoporosis, osteomyelitis, or rheumatoid arthritis in the diabetes population: a Retrospective Study. Int J Endocrinol. 2020; 2020:1–13.

77. Galway U, Chahar P, Schmidt MT, Araujo-Duran JA, Shivakumar J, Turan A, et al. Perioperative challenges in management of diabetic patients undergoing non-cardiac surgery. World J Diabetes. 2021;12(8):1255.

78. Egede LE, Hull BJ, Williams JS. Infections associated with diabetes. 2021;

79. Nguyen ATM, Akhter R, Garde S, Scott C, Twigg SM, Colagiuri S, et al. The association of periodontal disease with the complications of diabetes mellitus. A systematic review. Diabetes Res Clin Pract. 2020; 165:108244.

80. Kermani ZH, Bazzaz SMM, Farahmand SK, Raoof AA. The comparison of frequency of the upper limb musculoskeletal disorders among patients with diabetes type II with normal cases. Electron Physician. 2017;9(11):5848.

81. Taylor SI, Yazdi ZS, Beitelshees AL. Pharmacological treatment of hyperglycemia in type 2 diabetes. J Clin Invest. 2021;131(2).

82. Seangpraw K, Ong-Artborirak P, Boonyathee S, Bootsikeaw S, Kantow S, Panta P, et al. Effect of health literacy intervention on glycemic control and renal function among Thai older adults at risk of type 2 diabetes mellitus. Clin Interv Aging. 2023;1465–76.

83. Nesti L, Pugliese NR, Sciuto P, Natali A. Type 2 diabetes and reduced exercise tolerance: a review of the literature through an integrated physiology approach. Cardiovasc Diabetol. 2020;19(1):134.

84. Papakonstantinou E, Oikonomou C, Nychas G, Dimitriadis GD. Effects of diet, lifestyle, chrononutrition and alternative dietary interventions on postprandial glycemia and insulin resistance. Nutrients. 2022;14(4):823.

85. Saboo B, Misra A, Kalra S, Mohan V, Aravind SR, Joshi S, et al. Role and importance of high fiber in diabetes management in India. Diabetes & Metabolic Syndrome: Clinical Research & Reviews. 2022;16(5):102480.

86. Krauss RM, Kris-Etherton PM. Public health guidelines should recommend reducing saturated fat consumption as much as possible: NO. Am J Clin Nutr. 2020;112(1):19–24.

87. Chacko E, Signore C. Five evidence-based lifestyle habits people with diabetes can use. Clinical Diabetes. 2020;38(3):273–84.

88. Magkos F, Hjorth MF, Astrup A. Diet and exercise in the prevention and treatment of type 2 diabetes mellitus. Nat Rev Endocrinol. 2020;16(10):545–55.

89. Deng L, Du C, Song P, Chen T, Rui S, Armstrong DG, et al. The role of oxidative stress and antioxidants in diabetic wound healing. Oxid Med Cell Longev. 2021;2021(1):8852759.

90. Gianotti L, Belcastro S, D'Agnano S, Tassone F. The stress axis in obesity and diabetes mellitus: an update. Endocrines. 2021;2(3):334–47.

91. Borse SP, Chhipa AS, Sharma V, Singh DP, Nivsarkar M. Management of type 2 diabetes: current strategies, unfocussed aspects, challenges, and alternatives. Medical Principles and Practice. 2021;30(2):109–21.

92. Chasens ER, Imes CC, Kariuki JK, Luyster FS, Morris JL, DiNardo MM, et al. Sleep and metabolic syndrome. Nurs Clin North Am. 2021;56(2):203.

93. Rajani PS, RANI PS. Influence of Gender on Glycemic Control and Health Related Quality of Life Among Patients with Type 2 Diabetes Mellitus. IJRAR-International Journal of Research and Analytical Reviews (IJRAR). 2024;11(2):730–839.

94. Tandon S, Ayis S, Hopkins D, Harding S, Stadler M. The impact of pharmacological and lifestyle interventions on body weight in people with type 1 diabetes: a systematic review and meta-analysis. Diabetes Obes Metab. 2021;23(2):350–62.

95. Chakraborty S, Verma A, Garg R, Singh J, Verma H. Cardiometabolic risk factors associated with type 2 diabetes mellitus: a mechanistic insight. Clin Med Insights Endocrinol Diabetes. 2023; 16:11795514231220780.

96. Joaquim L, Faria A, Loureiro H, Matafome P. Benefits, mechanisms, and risks of intermittent fasting in metabolic syndrome and type 2 diabetes. J Physiol Biochem. 2022;78(2):295–305.

97. Rahman MS, Hossain KS, Das S, Kundu S, Adegoke EO, Rahman MA, et al. Role of insulin in health and disease: an update. Int J Mol Sci. 2021;22(12):6403.

98. Rachdaoui N. Insulin: the friend and the foe in the development of type 2 diabetes mellitus. Int J Mol Sci. 2020;21(5):1770.

99. Tan Q, Akindehin SE, Orsso CE, Waldner RC, DiMarchi RD, Müller TD, et al. Recent advances in incretin-based pharmacotherapies for the treatment of obesity and diabetes. Front Endocrinol (Lausanne). 2022; 13:838410.

100. Thrasher J. Pharmacologic management of type 2 diabetes mellitus: available therapies. Am J Cardiol. 2017;120(1):S4–16.

101. Kalra S, Das AK, Priya G, Ghosh S, Mehrotra RN, Das S, et al. Fixed-dose combination in management of type 2 diabetes mellitus: expert opinion from an international panel. J Family Med Prim Care. 2020;9(11):5450–7.

102. Dahlén AD, Dashi G, Maslov I, Attwood MM, Jonsson J, Trukhan V, et al. Trends in Antidiabetic Drug Discovery: FDA Approved Drugs, New Drugs in Clinical Trials and Global Sales. Front Pharmacol. 2022;12(January):1–16.

103. Sterrett JJ, Bragg S, Weart CW. Type 2 diabetes medication review. Am J Med Sci. 2016;351(4):342–55.

104. Bramley SE, Dupplin V, Goberdhan DGC, Meakins GD. The Hantzsch thiazole synthesis under acidic conditions: change of regioselectivity. J Chem Soc Perkin 1. 1987;639–43.

105. T. Chhabria M, Patel S, Modi P, S. Brahmkshatriya P. Thiazole: A review on chemistry, synthesis and therapeutic importance of its derivatives. Curr Top Med Chem. 2016;16(26):2841–62.

106. Nyulászi L, Várnai P, Veszprémi T. About the aromaticity of five-membered heterocycles. Journal of Molecular Structure: THEOCHEM. 1995;358(1–3):55–61.

107. Patel M, Bambharoliya T, Shah D, Patel K, Patel M, Shah U, et al. Emerging green synthetic routes for thiazole and its derivatives: Current perspectives. Arch Pharm (Weinheim). 2024;357(2):2300420.

108. Pathan W, Inamdar MN, Asdaq SMB, Asad M, Imran M, Kamal M, et al. The role of thiazole acetate derivatives on isolated heart and blood vessels in experimental rats. Journal of King Saud University-Science. 2022;34(6):102188.

109. Mrowicka M, Mrowicki J, Dragan G, Majsterek I. The importance of thiamine (vitamin B1) in humans. Biosci Rep. 2023;43(10).

110. Mostafa SM, Aly AA, Sayed SM, Raslan MA, Ahmed AE, Nafady A, et al. New quinoline-2-one/thiazolium bromide derivatives; synthesis, characterization and mechanism of formation. J Mol Struct. 2021; 1239:130501.

111. Bert H, Hinde RW. Production of amiphenazole. Google Patents; 1966.

112. Bellani P, Frigerio M, Castoldi P. Process for the synthesis of ritonavir. Google Patents; 2002.

113. Feldman M, Burton ME. Histamine2-receptor antagonists: standard therapy for acid-peptic diseases. New England Journal of Medicine. 1990;323(24):1672–80.

114. Kalashnikov SB, Vinogradov AS. SYNTHESIS OF 4-POLYFLUOROARYLTHIAZOLES. 2021;

115. Kenchappa R, Bodke YD, Telkar S, Aruna Sindhe M. Antifungal and anthelmintic activity of novel benzofuran derivatives containing thiazolo benzimidazole nucleus: an in vitro evaluation. J Chem Biol. 2017; 10:11–23.

116. Moualla H, Mills DA, Hromas R, Verschraegen CF, Castaner R, Bolos J. Voreloxin. Drugs Future. 2009;34(5).

117. Petrou A, Fesatidou M, Geronikaki A. Thiazole ring—A biologically active scaffold. Molecules. 2021;26(11):3166.

118. Fan M, Feng Q, Yang W, Peng Z, Wang G. Thiazole-benzamide derivatives as α-glucosidase inhibitors: Synthesis, kinetics study, molecular docking, and in vivo evaluation. J Mol Struct. 2023; 1291:136011.

119. Hussain R, Rehman W, Khan S, Maalik A, Hefnawy M, Alanazi AS, et al. Imidazopyridine-based thiazole derivatives as potential antidiabetic agents: synthesis, in vitro bioactivity, and in silico molecular modeling approach. Pharmaceuticals. 2023;16(9):1288.

120. Ullah H, Ahmad N, Rahim F, Uddin I, Hayat S, Zada H, et al. Synthesis, molecular docking study of thiazole derivatives and exploring their dual inhibitor potentials against α-amylase and α-glucosidase. Chemical Data Collections. 2022; 41:100932.

121. Yki-Järvinen H. Thiazolidinediones. New England Journal of Medicine. 2004;351(11):1106–18.

122. Zvarec O, Polyak SW, Tieu W, Kuan K, Dai H, Pedersen DS, et al. 5-Benzylidenerhodanine and 5-benzylidene-2-4-thiazolidinedione based antibacterials. Bioorg Med Chem Lett. 2012;22(8):2720–2.

123. Nitsche C, Schreier VN, Behnam MAM, Kumar A, Bartenschlager R, Klein CD. Thiazolidinone–peptide hybrids as dengue virus protease inhibitors with antiviral activity in cell culture. J Med Chem. 2013;56(21):8389–403.

124. Ali AM, Saber GE, Mahfouz NM, El-Gendy MA, Radwan AA, Hamid MAE. Synthesis and three-dimensional qualitative structure selectivity relationship of 3, 5-disubstituted-2, 4-thiazolidinedione derivatives as COX2 inhibitors. Arch Pharm Res. 2007; 30:1186–204.

125. Sethi NS, Prasad DN, Singh RK. Synthesis, anticancer, and antibacterial studies of benzylidene bearing 5-substituted and 3, 5-disubstituted-2, 4-thiazolidinedione derivatives. Med Chem (Los Angeles). 2021;17(4):369–79.

126. Trotsko N, Golus J, Kazimierczak P, Paneth A, Przekora A, Ginalska G, et al. Design, synthesis and antimycobacterial activity of thiazolidine-2, 4-dione-based thiosemicarbazone derivatives. Bioorg Chem. 2020; 97:103676.

127. Mishchenko M, Shtrygol S, Kaminskyy D, Lesyk R. Thiazole-bearing 4-thiazolidinones as new anticonvulsant agents. Sci Pharm. 2020;88(1):16.

128. Ibrahim AM, Shoman ME, Mohamed MFA, Hayallah AM, El-Din A. Abuo-Rahma G. Chemistry and applications of functionalized 2, 4-thiazolidinediones. European J Org Chem. 2023;26(19):e202300184.

129. Dahlén AD, Dashi G, Maslov I, Attwood MM, Jonsson J, Trukhan V, et al. Trends in Antidiabetic Drug Discovery: FDA Approved Drugs, New Drugs in Clinical Trials and Global Sales. Vol. 12, Frontiers in Pharmacology. 2022. p. 1–16.

130. Kallenberg S. Stereochemische Untersuchungen der Diketo-thiazolidine (I.). Berichte der deutschen chemischen Gesellschaft (A and B Series). 1923;56(1):316–31.

131. BOZDAĞ OYA, KILCIGİL GA, Tuncbilek M, Ertan R. Studies on the synthesis of some substituted flavonyl thiazolidinedione derivatives-I. Turk J Chem. 1999;23(2):163–70.

132. Kumar BRP, Nanjan MJ, Suresh B, Karvekar MD, Adhikary L. Microwave induced synthesis of the thiazolidine-2, 4-dione motif and the efficient solvent free-solid phase parallel syntheses of 5-benzylidene-

thiazolidine-2, 4-dione and 5-benzylidene-2-thioxo-thiazolidine-4-one compounds. J Heterocycl Chem. 2006;43(4):897–903.

133. Brown FC. 4-Thiazolidinones. Chem Rev. 1961;61(5):463–521.

134. Heintz W. Beiträge zur Kenntniss der Glycolamidsäuren. Justus Liebigs Ann Chem. 1865;136(2):213–23.

135. Lobo PL, Poojary B, Manjunatha K, Prathibha A, Kumari NS. Novel thiazolidine-2, 4-dione mannich bases: Synthesis, characterization and antimicrobial activity. Der Pharma Chemica. 2012; 4:867–71.

136. Meng G, Gao Y, Zheng ML. Improved preparation of 2, 4-thiazolidinedione. Org Prep Proced Int. 2011;43(3):312–3.

137. Cariou B, Charbonnel B, Staels B. Thiazolidinediones and PPARγ agonists: time for a reassessment. Trends in Endocrinology & Metabolism. 2012;23(5):205–15.

138. Tripathi AC, Gupta SJ, Fatima GN, Sonar PK, Verma A, Saraf SK. 4-Thiazolidinones: the advances continue…. Eur J Med Chem. 2014; 72:52–77.

139. Ahsan W. The journey of thiazolidinediones as modulators of PPARs for the management of diabetes: a current perspective. Curr Pharm Des. 2019;25(23):2540–54.

140. Appaturi JN, Ratti R, Phoon BL, Batagarawa SM, Din IU, Selvaraj M, et al. A review of the recent progress on heterogeneous catalysts for Knoevenagel condensation. Dalton Transactions. 2021;50(13):4445–69.

141. Maccari R, Ottanà R, Curinga C, Vigorita MG, Rakowitz D, Steindl T, et al. Structure–activity relationships and molecular modelling of 5-arylidene-2, 4-thiazolidinediones active as aldose reductase inhibitors. Bioorg Med Chem. 2005;13(8):2809–23.

142. Wang Z, Liu Z, Lee W, Kim SN, Yoon G, Cheon SH. Design, synthesis and docking study of 5-(substituted benzylidene) thiazolidine-2, 4-dione derivatives as inhibitors of protein tyrosine phosphatase 1B. Bioorg Med Chem Lett. 2014;24(15):3337–40.

143. Mahapatra MK, Kumar R, Kumar M. N-alkylated thiazolidine-2, 4-dione analogs as PTP1B inhibitors: synthesis, biological activity, and docking studies. Medicinal Chemistry Research. 2017; 26:1176–83.

144. Li Q, Al-Ayoubi A, Guo T, Zheng H, Sarkar A, Nguyen T, et al. Structure–activity relationship (SAR) studies of 3-(2-amino-ethyl)-5-(4-ethoxy-benzylidene)-thiazolidine-2, 4-dione: Development of potential substrate-

specific ERK1/2 inhibitors. Bioorg Med Chem Lett. 2009;19(21):6042–6.

145. Mohan R, Sharma AK, Gupta S, Ramaa CS. Design, synthesis, and biological evaluation of novel 2, 4-thiazolidinedione derivatives as histone deacetylase inhibitors targeting liver cancer cell line. Medicinal Chemistry Research. 2012; 21:1156–65.

146. Romagnoli R, Baraldi PG, Salvador MK, Camacho ME, Balzarini J, Bermejo J, et al. Anticancer activity of novel hybrid molecules containing 5-benzylidene thiazolidine-2, 4-dione. Eur J Med Chem. 2013; 63:544–57.

147. Tshiluka NR, Bvumbi M V, Ramaite II, Mnyakeni-moleele SS. Synthesis of some new 5-arylidene-2 , 4-thiazolidinedione esters. 2020;1–16.

148. Sergio Alves Palma M. Use of Piperidine and Pyrrolidine in Knoevenagel Condensation. Organic & Medicinal Chemistry International Journal. 2018;5(4).

149. Russell AJ, Westwood IM, Crawford MHJ, Robinson J, Kawamura A, Redfield C, et al. Selective small molecule inhibitors of the potential breast cancer marker, human arylamine N-acetyltransferase 1, and its murine homologue, mouse arylamine N-acetyltransferase 2. Bioorg Med Chem. 2009;17(2):905–18.

150. Thirupathi G, Venkatanarayana M, Dubey PK, Bharathi Kumari Y. Facile and green syntheses of substituted-5-arylidene-2, 4-thiazolidine diones using l-tyrosine as an eco-friendly catalyst in aqueous medium. Der Pharma Chemica. 2012;4(5).

151. Mohamed M, Aziz MA, Abuo-Rahma GEDA. Ultrasound-assisted green synthesis of 2, 4-thiazolidinedione and diaryl substituted pyrazolylthiazolidinediones catalyzed by β-alanine. Int J Phar Sci Drug Anal. 2021;1(1):18–25.

152. Pratap UR, Jawale D V, Waghmare RA, Lingampalle DL, Mane RA. Synthesis of 5-arylidene-2, 4-thiazolidinediones by Knoevenagel condensation catalyzed by baker's yeast. New Journal of Chemistry. 2011;35(1):49–51.

153. Barros FWA, Silva TG, da Rocha Pitta MG, Bezerra DP, Costa-Lotufo L V, de Moraes MO, et al. Synthesis and cytotoxic activity of new acridine-thiazolidine derivatives. Bioorg Med Chem. 2012;20(11):3533–9.

154. Chadha N, Bahia MS, Kaur M, Silakari O. Thiazolidine-2, 4-dione derivatives: programmed chemical weapons for key protein targets of

various pathological conditions. Bioorg Med Chem. 2015;23(13):2953–74.

155. Date K. Regulatory functions of α-amylase in the small intestine other than starch digestion: α-glucosidase activity, glucose absorption, cell proliferation, and differentiation. In: New Insights into Metabolic Syndrome. IntechOpen; 2020.

156. Williams JA. Amylase. Pancreapedia: The Exocrine Pancreas Knowledge Base. 2019;

157. Corrado M. Understanding the intrinsic and extrinsic properties of a starch branching enzyme II wheat mutant and their impact on glucose response. University of East Anglia; 2020.

158. Proença C, Ribeiro D, Freitas M, Fernandes E. Flavonoids as potential agents in the management of type 2 diabetes through the modulation of α-amylase and α-glucosidase activity: A review. Crit Rev Food Sci Nutr. 2022;62(12):3137–207.

159. Dandekar P, Ramkumar S, RaviKumar A. Structure–activity relationships of pancreatic α-amylase and α-glucosidase as antidiabetic targets. Studies in Natural Products Chemistry. 2021; 70:381–410.

160. Lebovitz HE. Alpha-glucosidase inhibitors. Endocrinol Metab Clin North Am. 1997;26(3):539–51.

161. Dandekar P, Ramkumar S, RaviKumar A. Structure–activity relationships of pancreatic α-amylase and α-glucosidase as antidiabetic targets. Studies in Natural Products Chemistry. 2021; 70:381–410.

162. Srinivasa MG, Paithankar JG, Saheb Birangal SR, Pai A, Pai V, Deshpande SN, et al. Novel hybrids of thiazolidinedione-1,3,4-oxadiazole derivatives: synthesis, molecular docking, MD simulations, ADMET study, in vitro, and in vivo anti-diabetic assessment. RSC Adv. 2023;13(3):1567–79.

163. Bosetti C, Rosato V, Buniato D, Zambon A, La Vecchia C, Corrao G. Cancer risk for patients using thiazolidinediones for type 2 diabetes: A meta-analysis. Oncologist. 2013;18(2):148–56.

164. Jain AK, Vaidya A, Ravichandran V, Kashaw SK, Agrawal RK. Recent developments and biological activities of thiazolidinone derivatives: A review. Bioorg Med Chem. 2012;20(11):3378–95.

165. Jain VS, Vora DK, Ramaa CS. Thiazolidine-2, 4-diones: Progress towards multifarious applications. Bioorg Med Chem. 2013;21(7):1599–620.

166. Bérubé G. An overview of molecular hybrids in drug discovery. Expert Opin Drug Discov. 2016;11(3):281–305.

167. Kamerlin N, Delcey MG, Manzetti S, Van der Spoel D. Toward a computational ecotoxicity assay. J Chem Inf Model. 2020;60(8):3792–803.

168. Liu XF, Zheng CJ, Sun LP, Liu XK, Piao HR. Synthesis of new chalcone derivatives bearing 2, 4-thiazolidinedione and benzoic acid moieties as potential anti-bacterial agents. Eur J Med Chem. 2011;46(8):3469–73.

169. Zheng Y, Li M, Wu S, Li L, Xiong Z, Xu X, et al. Synthesis and biological evaluation of chromone-thiazolidine-2, 4-dione derivatives as potential α-glucosidase inhibitors. Arabian Journal of Chemistry. 2023;16(11):105279.

170. Nishida S, Maruoka H, Yoshimura Y, Goto T, Tomita R, Masumoto E, et al. Synthesis and biological activities of some new thiazolidine derivatives containing pyrazole ring system. J Heterocycl Chem. 2012;49(2):303–9.

171. Doddagaddavalli MA, Kalalbandi VKA, Seetharamappa J. Synthesis, characterization, crystallographic, binding, in silico and antidiabetic studies of novel 2, 4-thiazolidinedione-phenothiazine molecular hybrids. J Mol Struct. 2023; 1276:134625.

172. Reddy KA, Lohray BB, Bhushan V, Bajji AC, Reddy KV, Reddy PR, et al. Novel antidiabetic and hypolipidemic agents. 3. Benzofuran-containing thiazolidinediones. J Med Chem. 1999;42(11):1927–40.

173. Daş-Evcimen N, Bozdağ-Dündar O, Sarikaya M, Ertan R. In vitro aldose reductase inhibitory activity of some flavonyl-2, 4-thiazolidinediones. J Enzyme Inhib Med Chem. 2008;23(3):297–301.

174. Garberová M, Kudličková Z, Michalková R, Tvrdoňová M, Sabolová D, Bekešová S, et al. Design, Synthesis, and Characterization of Novel Thiazolidine-2, 4-Dione-Acridine Hybrids as Antitumor Agents. Molecules. 2024;29(14):3387.

175. Mahapatra MK, Saini R, Kumar M. Synthesis, anti-hyperglycaemic activity, and in-silico studies of N-substituted 5-(furan-2-ylmethylene) thiazolidine-2,4-dione derivatives. Research on Chemical Intermediates. 2016;42(12):8239–51.

176. Gowdru Srinivasa M, Revanasiddappa BC, Prabhu A, Rani V, Ghate SD, Kumar B. R P. Development of novel thiazolidine-2,4-dione derivatives as PPAR-γ agonists through design, synthesis, computational docking, MD simulation, and comprehensive in vitro and in vivo evaluation. RSC Med Chem. 2023;14(11):2401–16.

177. Patel S, Sen AK, Dash DK, Sadhu P, Kumari M, Baile SB. Synthesis, Characterization and Biological Evaluation of Thiazolidinedione Derivative as Novel Antidiabetic Agents. J Pharm Res Int. 2021;33(35A):123–33.

178. Kim BY, Ahn JB, Lee HW, Kang SK, Lee JH, Shin JS, et al. Synthesis and biological activity of novel substituted pyridines and purines containing 2, 4-thiazolidinedione. Eur J Med Chem. 2004;39(5):433–47.

179. Bansal G, Singh S, Monga V, Thanikachalam PV, Chawla P. Synthesis and biological evaluation of thiazolidine-2, 4-dione-pyrazole conjugates as antidiabetic, anti-inflammatory and antioxidant agents. Bioorg Chem. 2019;92:103271.

180. Abdellatif KRA, Fadaly WAA, Kamel GM, Elshaier YAMM, El-Magd MA. Design, synthesis, modeling studies and biological evaluation of thiazolidine derivatives containing pyrazole core as potential anti-diabetic PPAR-γ agonists and anti-inflammatory COX-2 selective inhibitors. Bioorg Chem. 2019;82:86–99.

181. Naim MJ, Alam MJ, Nawaz F, Naidu VGM, Aaghaz S, Sahu M, et al. Synthesis, molecular docking and anti-diabetic evaluation of 2,4-thiazolidinedione based amide derivatives. Bioorg Chem. 2017;73:24–36.

182. Shakour N, Sahebkar A, Karimi G, Paseban M, Tasbandi A, Mosaffa F, et al. Design, synthesis and biological evaluation of novel 5-(imidazolyl-methyl) thiazolidinediones as antidiabetic agents. Bioorg Chem. 2021;115:105162.

183. Fettach S, Thari FZ, Hafidi Z, Karrouchi K, Bouathmany K, Cherrah Y, et al. Biological, toxicological and molecular docking evaluations of isoxazoline-thiazolidine-2, 4-dione analogues as new class of anti-hyperglycemic agents. J Biomol Struct Dyn. 2023;41(3):1072–84.

184. Iqbal AKM, Khan AY, Kalashetti MB, Belavagi NS, Gong YD, Khazi IAM. Synthesis, hypoglycemic and hypolipidemic activities of novel thiazolidinedione derivatives containing thiazole/triazole/oxadiazole ring. Eur J Med Chem. 2012;53:308–15.

185. Nazreen et al. Design, synthesis, in silico molecular docking and biological evaluation of novel oxadiazole based thiazolidine-2, 4-diones bis-heterocycles as PPAR-γ agonists. Eur J Med Chem. 2014;87:175–85.

186. Srikanth Kumar K, Lakshmana Rao A, Basaveswara Rao M V. Design, synthesis, biological evaluation and molecular docking studies of novel 3-substituted-5-[(indol-3-yl)methylene]-thiazolidine-2,4-dione derivatives. Heliyon. 2018;4(9):e00807.

187. Verma RK, Mall R, Singh A. Indolyl linked meta-substituted benzylidene-based novel PPAR ligands: synthetic and docking studies. Medicinal Chemistry Research. 2015;24:1396–407.

188. Sameeh MY, Khowdiary MM, Nassar HS, Abdelall MM, Alderhami SA, Elhenawy AA. Discovery potent of thiazolidinedione derivatives as antioxidant, α-amylase inhibitor, and antidiabetic agent. Biomedicines. 2021;10(1):24.

189. Sameeh MY, Khowdiary MM, Nassar HS, Abdelall MM, Amer HH, Hamed A, et al. Thiazolidinedione Derivatives: In Silico, In Vitro, In Vivo, Antioxidant and Anti-Diabetic Evaluation. Molecules. 2022;27(3):1–15.

190. Jeon R, Park S. Synthesis and biological activity of benzoxazole containing thiazolidinedione derivatives. Arch Pharm Res. 2004;27:1099–105.

191. Jeon R, Kim YJ, Cheon Y, Ryu JH. Synthesis and biological activity of [[(heterocycloamino) alkoxy] benzyl]-2, 4-thiazolidinediones as PPARγ agonists. Arch Pharm Res. 2006;29:394–9.

192. Srikanth L, Raghunandan N, Srinivas P, Reddy GA. Synthesis and evaluation of newer quinoline derivatives of thiazolidinedione for their ant diabetic activity. Int J Pharm Bio Sci. 2010;1(4).

193. Gupta D, Ghosh NN, Chandra R. Synthesis and pharmacological evaluation of substituted 5-[4-[2-(6, 7-dimethyl-1, 2, 3, 4-tetrahydro-2-oxo-4-quinoxalinyl) ethoxy] phenyl] methylene] thiazolidine-2, 4-dione derivatives as potent euglycemic and hypolipidemic agents. Bioorg Med Chem Lett. 2005;15(4):1019–22.

194. Mishra G, Sachan N, Chawla P. Synthesis and evaluation of thiazolidinedione-coumarin adducts as antidiabetic, anti-inflammatory and antioxidant agents. Lett Org Chem. 2015;12(6):429–55.

195. Nazreen S, Alam MS, Hamid H, Yar MS, Dhulap A, Alam P, et al. Thiazolidine-2, 4-diones derivatives as PPAR-γ agonists: Synthesis, molecular docking, in vitro and in vivo antidiabetic activity with hepatotoxicity risk evaluation and effect on PPAR-γ gene expression. Bioorg Med Chem Lett. 2014;24(14):3034–42.

196. Madhavan GR, Chakrabarti R, Kumar SKB, Misra P, Mamidi RNVS, Balraju V, et al. Novel phthalazinone and benzoxazinone containing thiazolidinediones as antidiabetic and hypolipidemic agents. Eur J Med Chem. 2001;36(7–8):627–37.

197. Madhavan GR, Chakrabarti R, Vikramadithyan RK, Mamidi RNVS, Balraju V, Rajesh BM, et al. Synthesis and biological activity of novel

pyrimidinone containing thiazolidinedione derivatives. Bioorg Med Chem. 2002;10(8):2671–80.

198. Lee HW, Kim BY, Ahn JB, Kang SK, Lee JH, Shin JS, et al. Molecular design, synthesis, and hypoglycemic and hypolipidemic activities of novel pyrimidine derivatives having thiazolidinedione. Eur J Med Chem. 2005;40(9):862–74.

199. Hulin B, McCarthy PA, Gibbs EM. The glitazone family of antidiabetic agents. Curr Pharm Des. 1996;2(1):85–102.

200. Nazreen S, Alam MS, Hamid H, Yar MS, Dhulap A, Alam P, et al. Design, synthesis, and biological evaluation of thiazolidine-2, 4-dione conjugates as PPAR-γ agonists. Arch Pharm (Weinheim). 2015;348(6):421–32.

201. da Costa Leite LFC, Mourão RHV, de Lima M do CA, Galdino SL, Hernandes MZ, Neves F de AR, et al. Synthesis, biological evaluation and molecular modeling studies of arylidene-thiazolidinediones with potential hypoglycemic and hypolipidemic activities. Eur J Med Chem. 2007;42(10):1263–71.

202. Rathod CH, Nariya PB, Maliwal D, Pissurlenkar RRS, Kapuriya NP, Patel AS. Design, Synthesis and Antidiabetic Activity of Biphenylcarbonitrile-Thiazolidinedione Conjugates as Potential α-Amylase Inhibitors. ChemistrySelect. 2021;6(9):2464–9.

203. Zask A, Jirkovsky I, Nowicki JW, McCaleb ML. Synthesis and antihyperglycemic activity of novel 5-(naphthalenylsulfonyl)-2, 4-thiazolidinediones. J Med Chem. 1990;33(5):1418–23.

204. Kumar A, Salahuddin, Mazumder A, Kumar R, Sahu R, Mishra S, et al. Synthesis, Characterization, and Antidiabetic Evaluation of Substituted 5-(2-Chloro-Quinolin-3-Ylmethylene)-Thiazolidine-2,4-Dione. Indian Journal of Heterocyclic Chemistry. 2021;31(3):357–64.

205. Patnam N, Chevula K, Chennamsetti P, Aleti B, Kotha AK, Manga V. Synthesis, antidiabetic activity and molecular docking studies of novel aryl benzylidenethiazolidine-2,4-dione based 1,2,3-triazoles. Mol Divers. 2024 Jun 1;28(3):1551–63.

206. Yasmin S, Capone F, Laghezza A, Piaz FD, Loiodice F, Vijayan V, et al. Novel Benzylidene Thiazolidinedione Derivatives as Partial PPARγ Agonists and their Antidiabetic Effects on Type 2 Diabetes. Sci Rep. 2017;7(1):1–17.

207. Shukla S, Kumar P, Das N, Hari Narayana Moorthy NS, Kumar Shrivastava S, Trivedi P, et al. Synthesis, characterization, biological evaluation and docking of coumarin coupled thiazolidinedione derivatives

and its bioisosteres as PPARγ agonists. Med Chem (Los Angeles). 2012;8(5):834–45.

208. Mishra LK, Sarkar D, Mentreddy R, Shetty K. Evaluation of phenolic bioactive-linked anti-hyperglycemic and Helicobacter pylori inhibitory activities of Asian Basil (Ocimum spp.) varieties. J Herb Med. 2020;20:100310.

209. Telagari M, Hullatti K. In-vitro α-amylase and α-glucosidase inhibitory activity of Adiantum caudatum Linn. and Celosia argentea Linn. extracts and fractions. Indian J Pharmacol. 2015;47(4):425–9.

210. Bhardwaj N, Puri S, Kumari A, Chauhan A, Kumar A. Investigation on antioxidant, antimicrobial, anti-inflammatory, and neuropsychiatry potential of phyto-mediated ZnONPs using Colebrookea oppositifolia. J Drug Deliv Sci Technol. 2024;97:105748.

211. Haleshappa R, Patil SJ, Siddalinga Murthy KR. Phytochemical analysis, in vitro evaluation of antioxidant and free radical scavenging activity of Simarouba glauca seeds. Advances in Pharmacology and Pharmacy. 2021;9(1):1–8.

212. Staszak M, Staszak K, Wieszczycka K, Bajek A, Roszkowski K, Tylkowski B. Machine learning in drug design: Use of artificial intelligence to explore the chemical structure–biological activity relationship. Wiley Interdiscip Rev Comput Mol Sci. 2022;12(2):e1568.

213. Zhang B, Li H, Yu K, Jin Z. Molecular docking-based computational platform for high-throughput virtual screening. CCF Transactions on High Performance Computing. 2022;1–12.

214. Niazi SK, Mariam Z. Computer-aided drug design and drug discovery: a prospective analysis. Pharmaceuticals. 2023;17(1):22.

215. Bhatia AS, Saggi MK, Kais S. Quantum machine learning predicting ADME-Tox properties in drug discovery. J Chem Inf Model. 2023;63(21):6476–86.

216. Cavasotto CN, Scardino V. Machine learning toxicity prediction: latest advances by toxicity end point. ACS Omega. 2022;7(51):47536–46.

217. Swargiary A, Roy MK, Mahmud S. Phenolic compounds as α-glucosidase inhibitors: A docking and molecular dynamics simulation study. J Biomol Struct Dyn. 2023;41(9):3862–71.

218. Ogunyemi OM, Gyebi AG, Adebayo JO, Oguntola JA, Olaiya CO. Marsectohexol and other pregnane phytochemicals derived from

Gongronema latifolium as α-amylase and α-glucosidase inhibitors: In vitro and molecular docking studies. SN Appl Sci. 2020;2:1–11.

219. Khaldan A, Bouamrane S, El-mernissi R, Ouabane M, Alaqarbeh M, Maghat H, et al. Design of new α-glucosidase inhibitors through a combination of 3D-QSAR, ADMET screening, molecular docking, molecular dynamics simulations and quantum studies. Arabian Journal of Chemistry. 2024;17(3):105656.

220. Shridhar Deshpande N, Shivakumar, Udayakumar D, Prabhu A, Rani V, Dixit SR, et al. Synthesis, Molecular Docking, MD Simulation and Evaluation of Anticancer Activity of Novel 1, 3, 4-Oxadiazole derivatives against Ehrlich Ascites Carcinoma (EAC) Cell lines. Journal of Computational Biophysics and Chemistry. 2024;

221. Maliwal D, Pissurlenkar RRS, Telvekar V. Identification of novel potential anti-diabetic candidates targeting human pancreatic α-amylase and human α-glycosidase: An exhaustive structure-based screening. Can J Chem. 2022;100(5):338–52.

222. Ibeyaima A, Manna P. In Silico Analysis of Anti-Diabetic Compounds: A Reference Study to Determine the Lipinski Rule of 5, Bioavailability, Pharmacokinetics, and Toxicity of Unknown Compound (S) from Bioresources Using Web-Based Tools. Bioavailability, Pharmacokinetics, and Toxicity of Unknown Compound (S) from Bioresources Using Web-Based Tools.

223. Rauf A, Khan H, Khan M, Abusharha A, Serdaroğlu G, Daglia M. In silico, SwissADME, and DFT studies of newly synthesized oxindole derivatives followed by antioxidant studies. J Chem. 2023;2023(1):5553913.

224. Bui TQ, Dat TTH, Quy PT, Hai NTT, Thai NM, Phu NV, et al. Identification of potential anti-hyperglycemic compounds in Cordyceps militaris ethyl acetate extract: in vitro and in silico studies. J Biomol Struct Dyn. 2025;43(2):627–43.

225. Kaur N, Kumar V, Nayak SK, Wadhwa P, Kaur P, Sahu SK. Alpha-amylase as molecular target for treatment of diabetes mellitus: A comprehensive review. Chem Biol Drug Des. 2021;98(4):539–60.

226. Hawash M, Jaradat N, Shekfeh S, Abualhasan M, Eid AM, Issa L. Molecular docking, chemo-informatic properties, alpha-amylase, and lipase inhibition studies of benzodioxol derivatives. BMC Chem. 2021;15(1):40.

227. da Silva SEB, da Silva Moura JA, Branco Júnior JF, de Moraes Gomes PAT, de Paula SKS, Francisco Viana DC, et al. Synthesis and In vitro and in silico Anti-inflammatory Activity of New Thiazolidinedione-quinoline Derivatives. Curr Top Med Chem. 2024;24(14):1264–77.

228. Kumar A, Salahuddin Mazumder A, Kumar R, Sahu R, Mishral S, Singh C, et al. Synthesis, characterization, and antidiabetic evaluation of substituted 5-(2-chloro-quinolin-3-ylmethylene)-thiazolidine-2, 4-dione. Indian Journal of Heterocyclic Chemistry. 2021; 31:357–64.

229. Alminderej F, Bakari S, Almundarij TI, Snoussi M, Aouadi K, Kadri A. Antioxidant activities of a new chemotype of Piper cubeba L. fruit essential oil (Methyleugenol/Eugenol): In Silico molecular docking and ADMET studies. Plants. 2020;9(11):1534.

APPENDICES

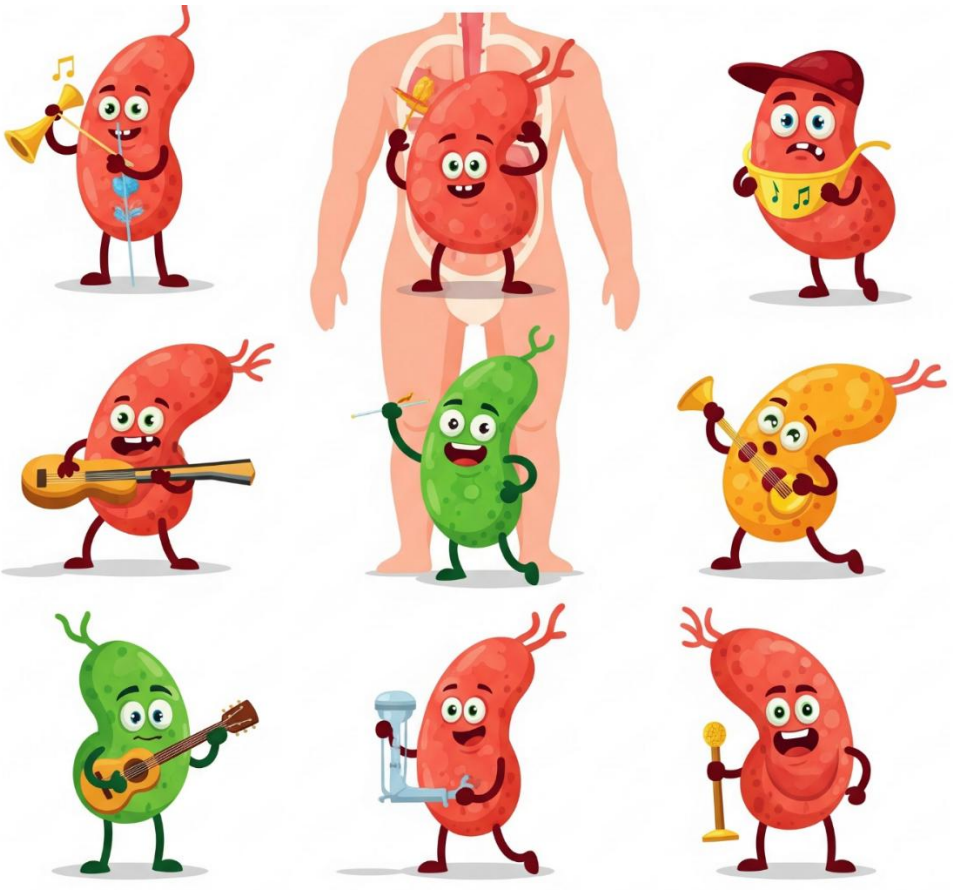

LIST OF APPENDICES

I. Letter of candidacy

LOVELY PROFESSIONAL UNIVERSITY

Centre for
Research Degree Programmes

LPU/CRDP/PHD/EC/20200225/001364

Dated: 12 Oct 2019

Sharfuddin Mohd
VID: 41700271
Programme Name: Doctor of Philosophy (Pharmaceutical Chemistry)

Subject: Letter of Candidacy for Ph.D.

Dear Candidate,

We are very pleased to inform you that the Department Doctoral Board has approved your candidacy for the Ph.D. Programme on 12 Oct 2019 by accepting your research proposal entitled: "Synthesis and Antidiabetic Investigation on Thiazole Derivatives"

As a Ph.D. candidate you are required to abide by the conditions, rules and regulations laid down for Ph.D. Programme of the University, and amendments, if any, made from time to time.

We wish you the very best!!

In case you have any query related to your programme, please contact Centre of Research Degree Programmes.

Head

Centre for Research Degree Programmes

Note:-This is a computer generated certificate and no signature is required. Please use the reference number generated on this certificate for future conversations.

Jalandhar-Delhi G.T.Road, Phagwara, Punjab (India) - 144411
Ph : +91-1824-444594 E-mail : drp@lpu.co.in website : www.lpu.in

II. Spectral data of all synthesized compounds; Series 1 (NT1-NT18)

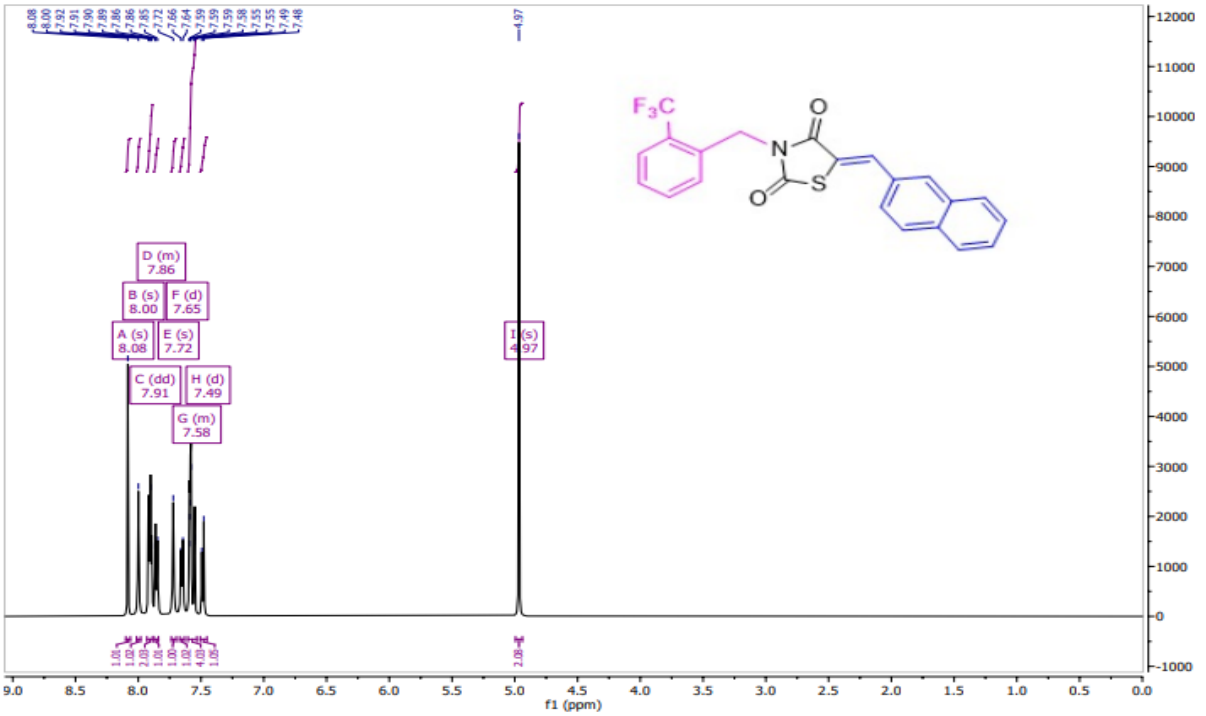

^{1}H-NMR spectrum of compound NT1

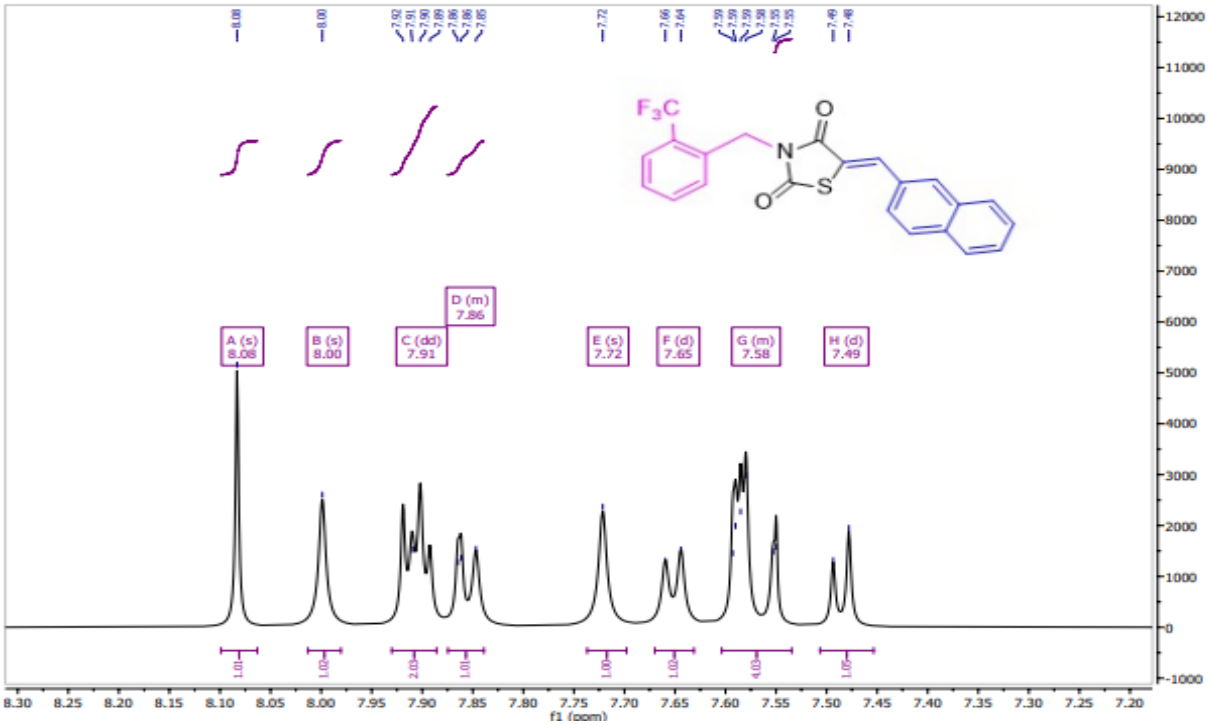

Expanded (aromatic hydrogens) spectrum of compound NT1

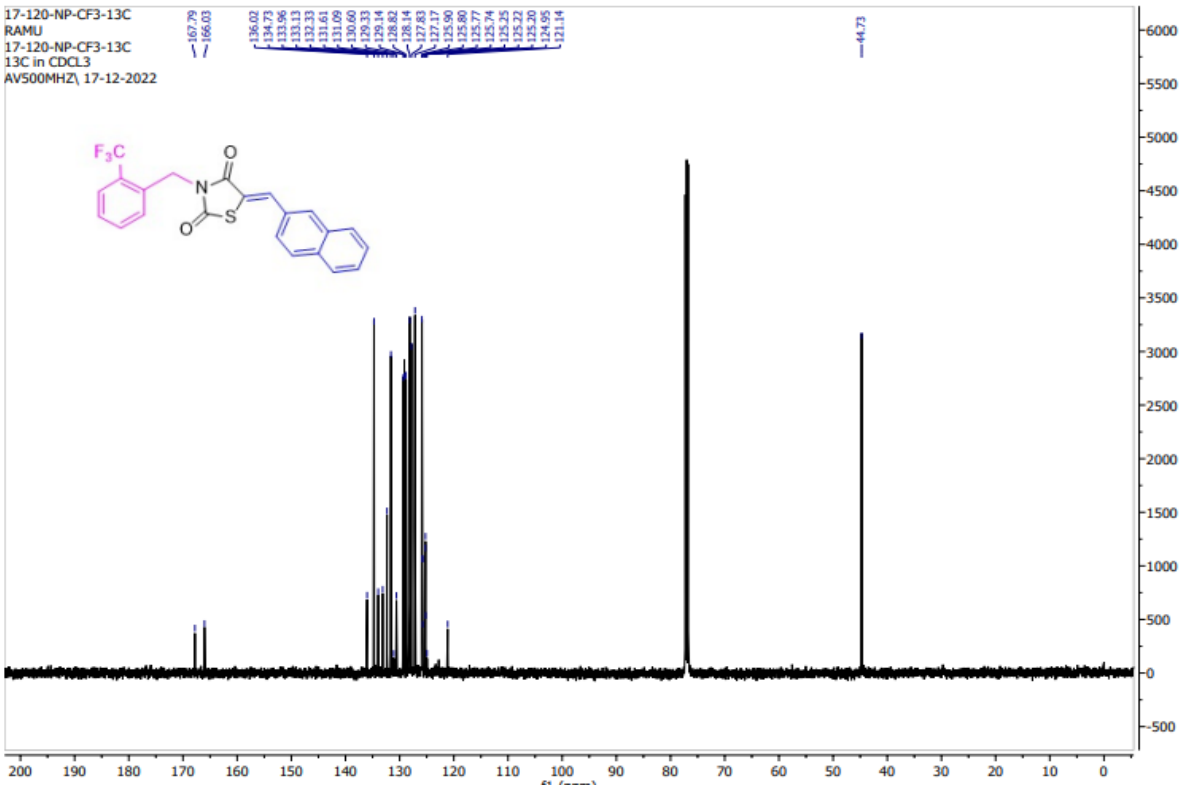

^{13}C-NMR Spectrum of compound NT1

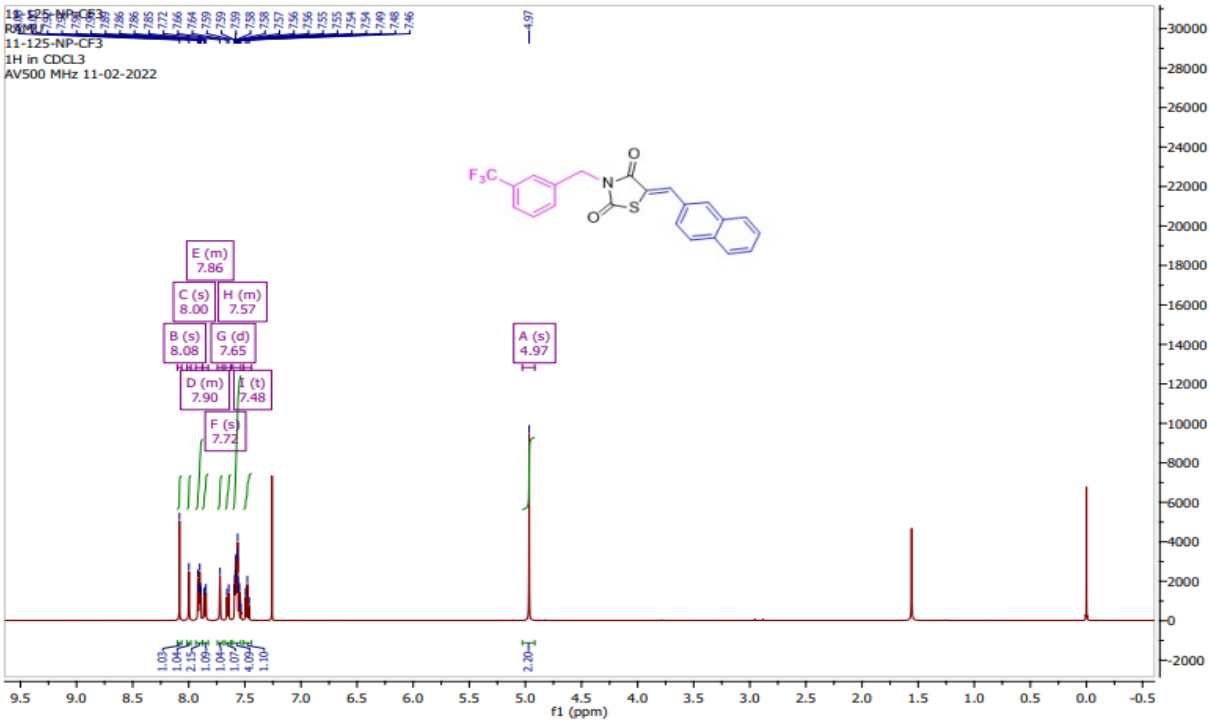

^{1}H-NMR spectrum of compound NT2

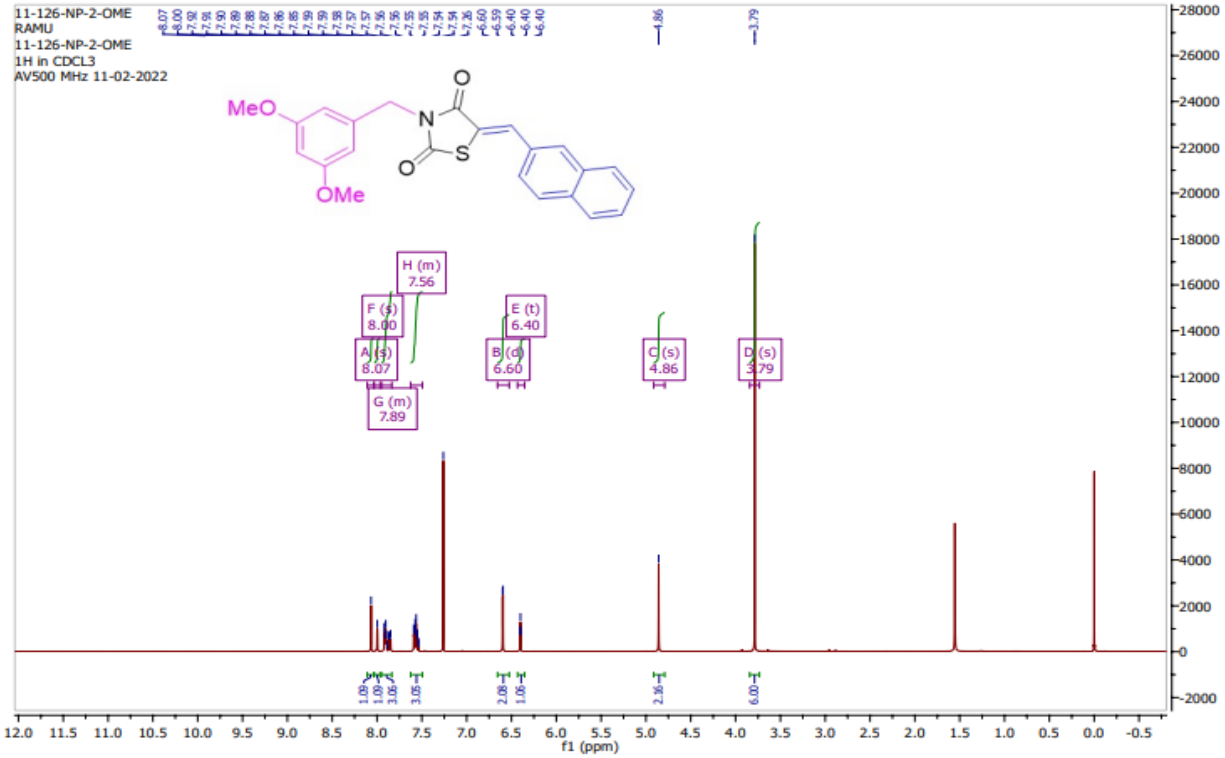

^{1}H-NMR spectrum of compound NT3

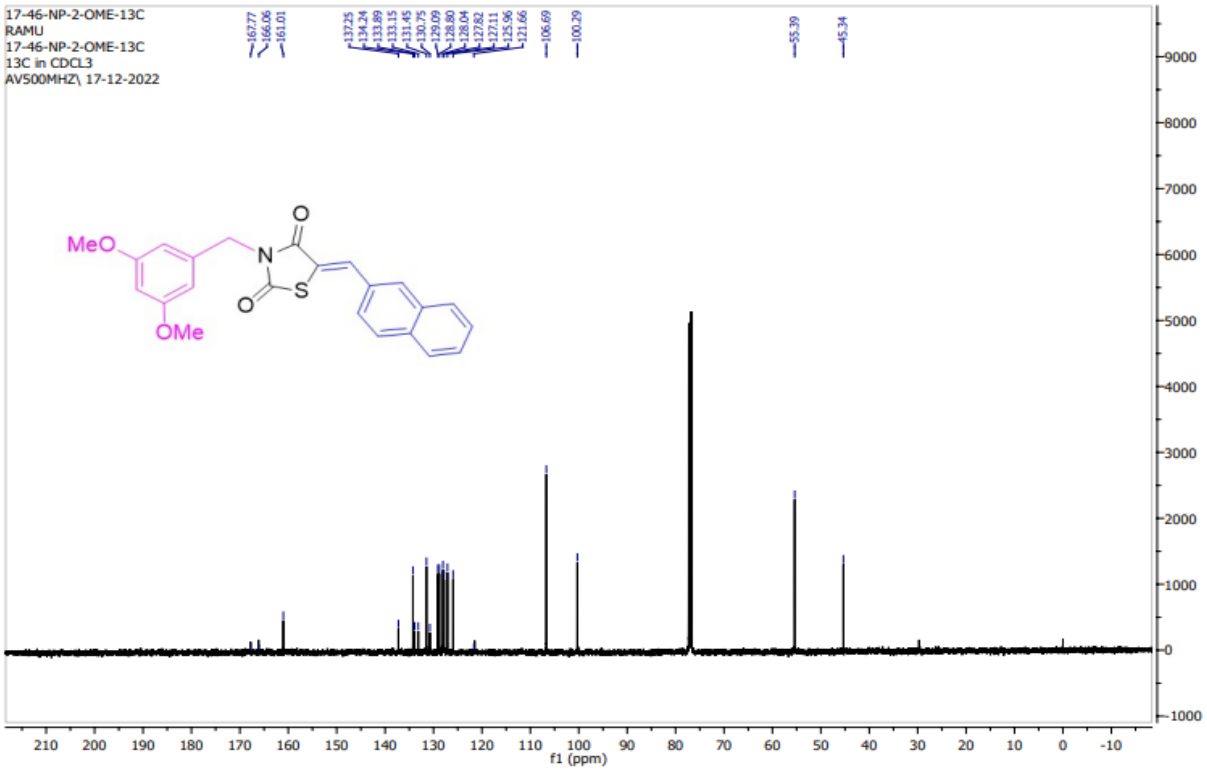

^{13}C-NMR Spectrum of compound NT3

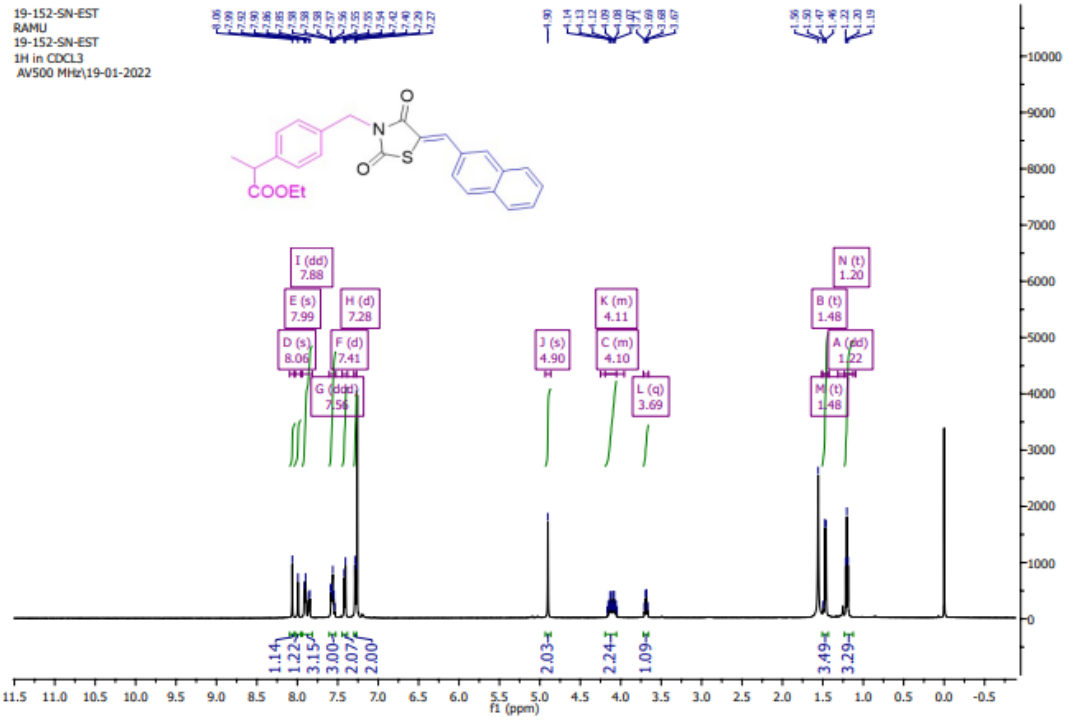

^{1}H-NMR spectrum of compound NT4

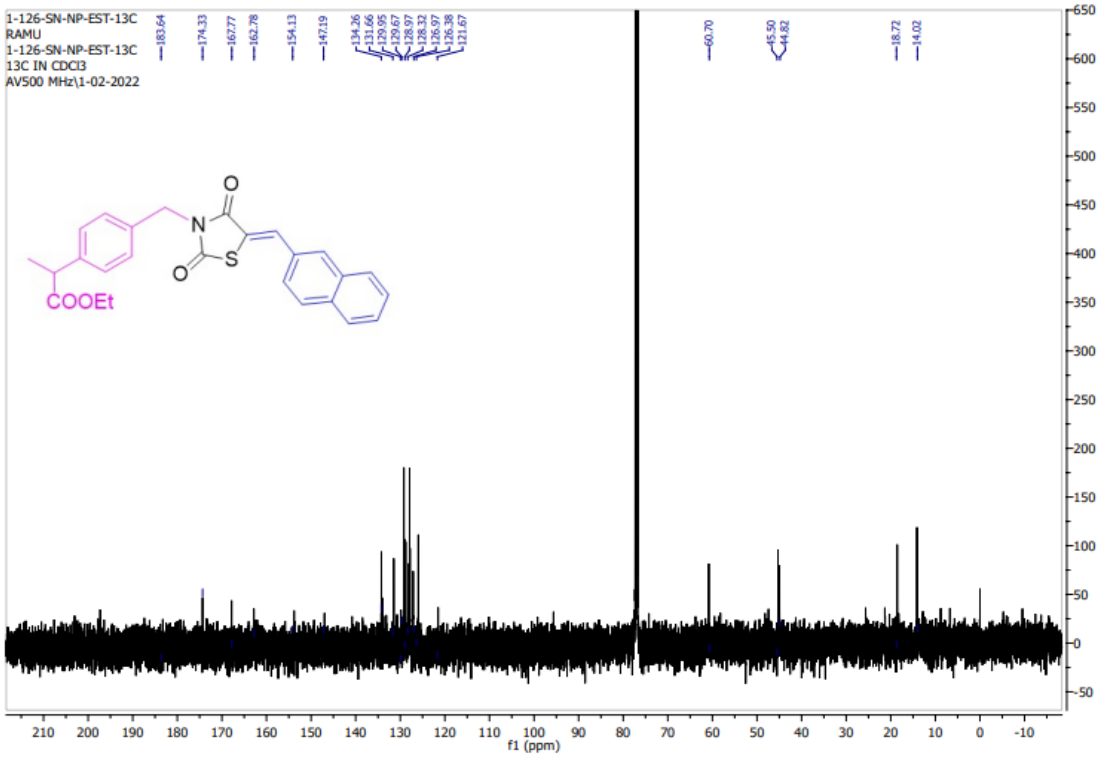

^{13}C-NMR Spectrum of compound NT4

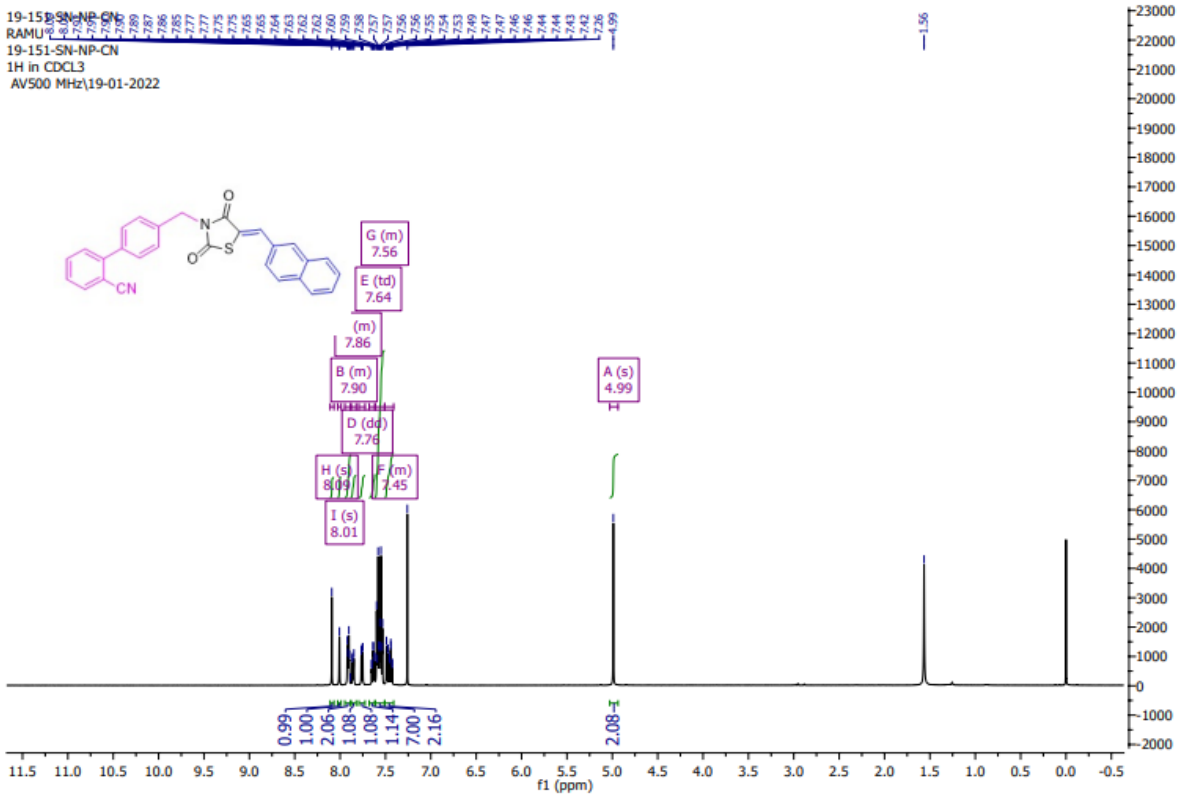

[1]H-NMR spectrum of compound NT5

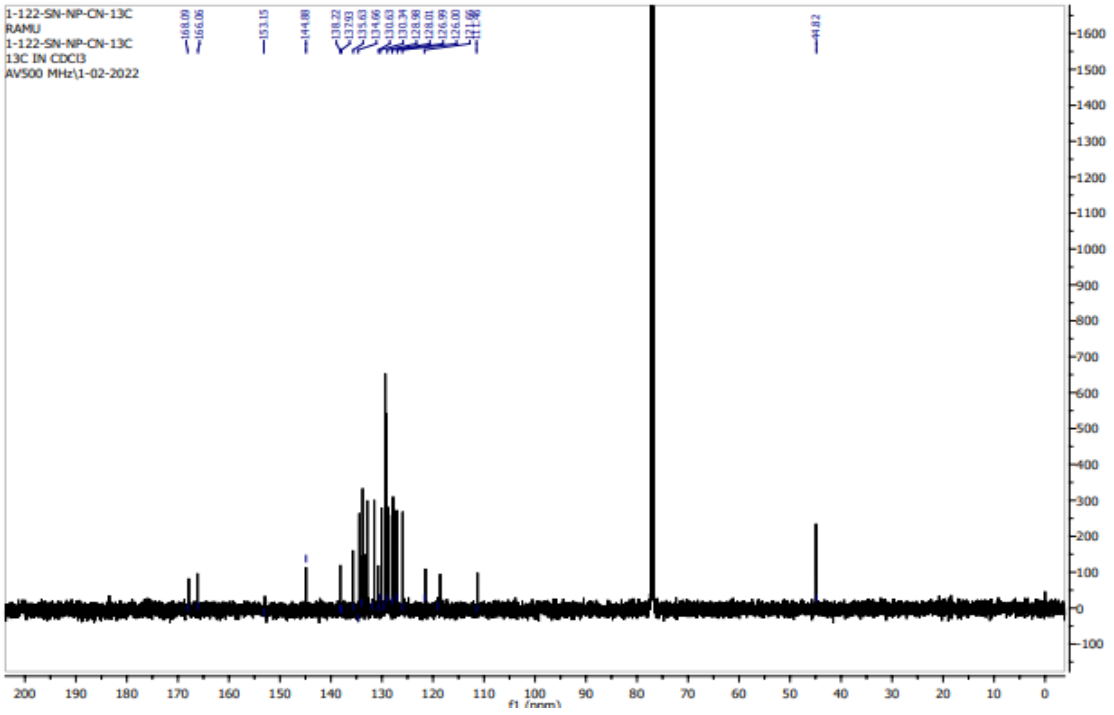

[13]C-NMR Spectrum of compound NT5

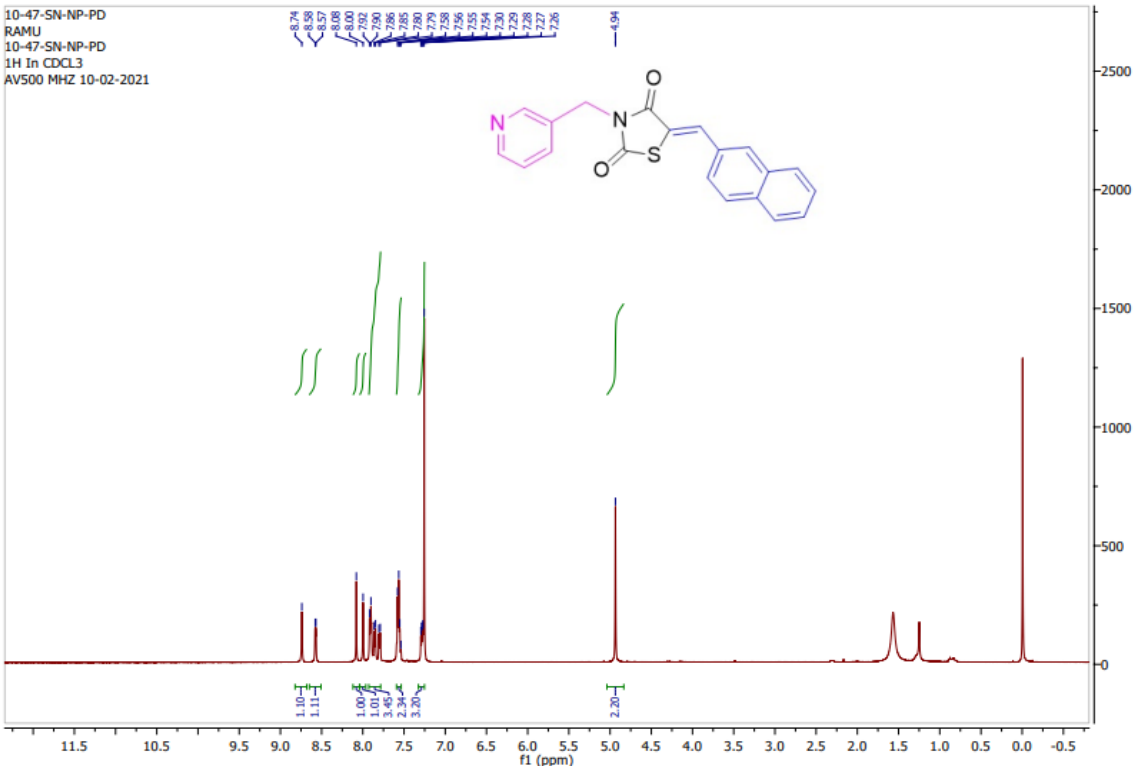

^{1}H-NMR spectrum of compound NT6

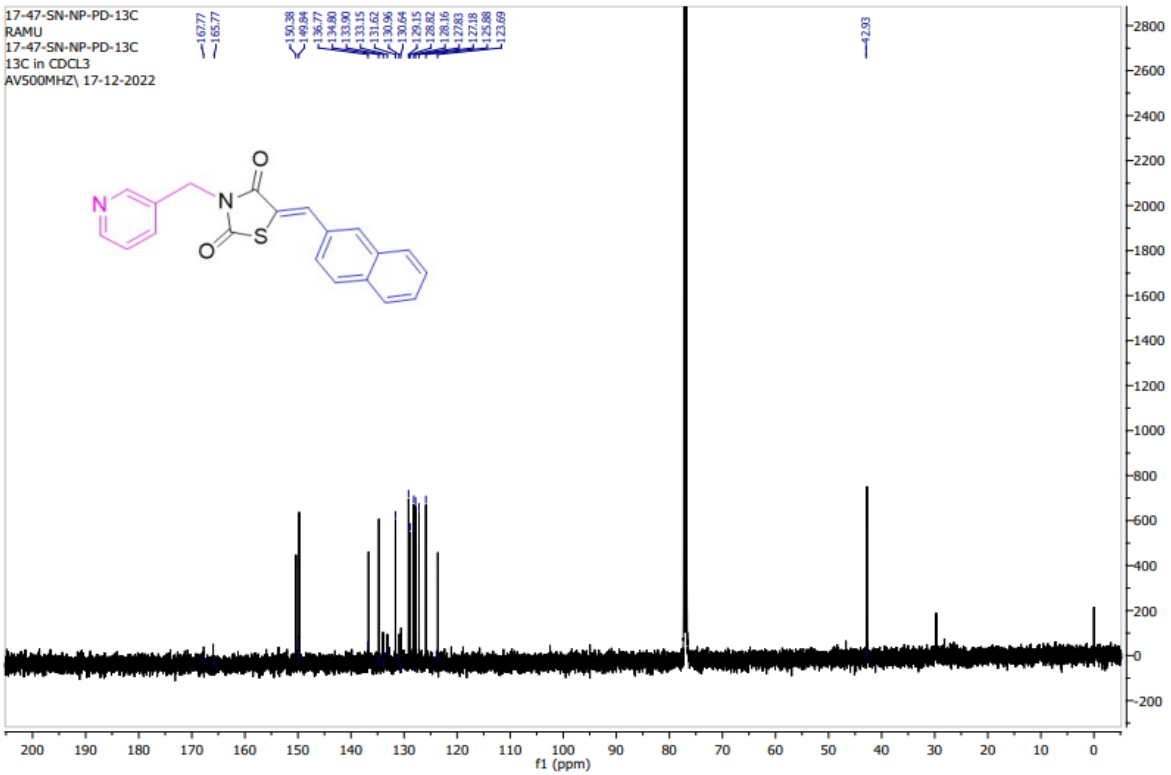

^{13}C-NMR Spectrum of compound NT6

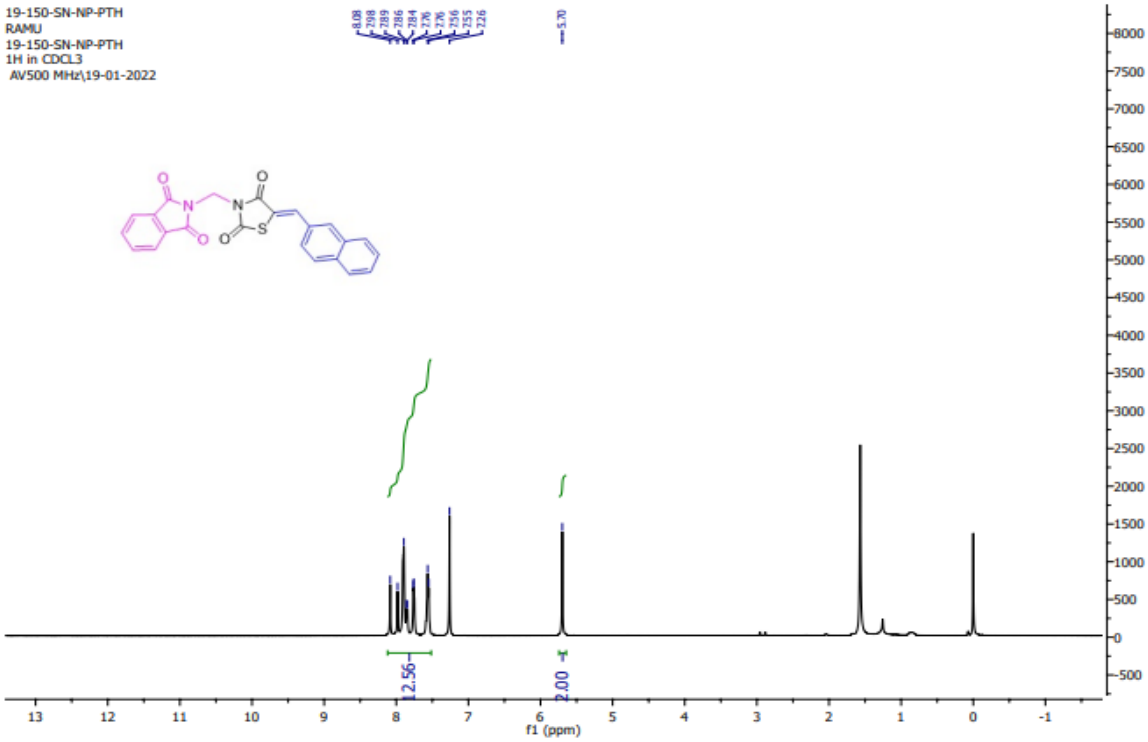

^{1}H-NMR spectrum of compound NT7

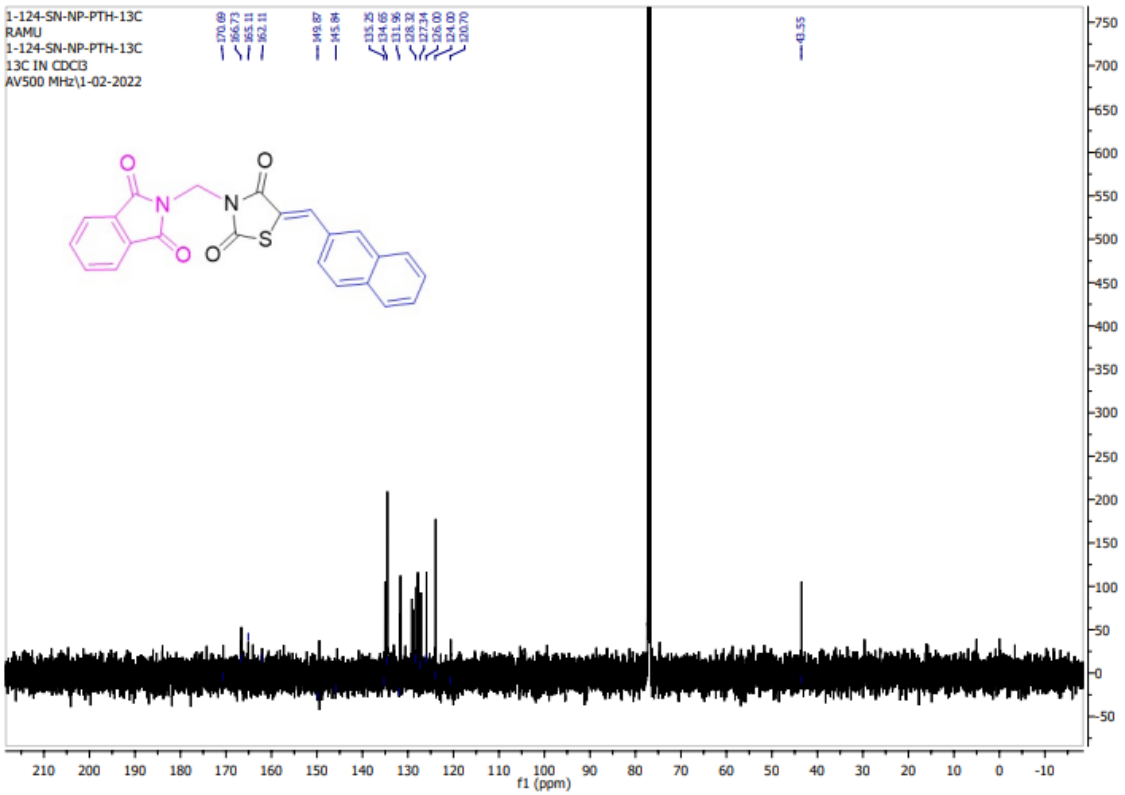

^{13}C-NMR Spectrum of compound NT7

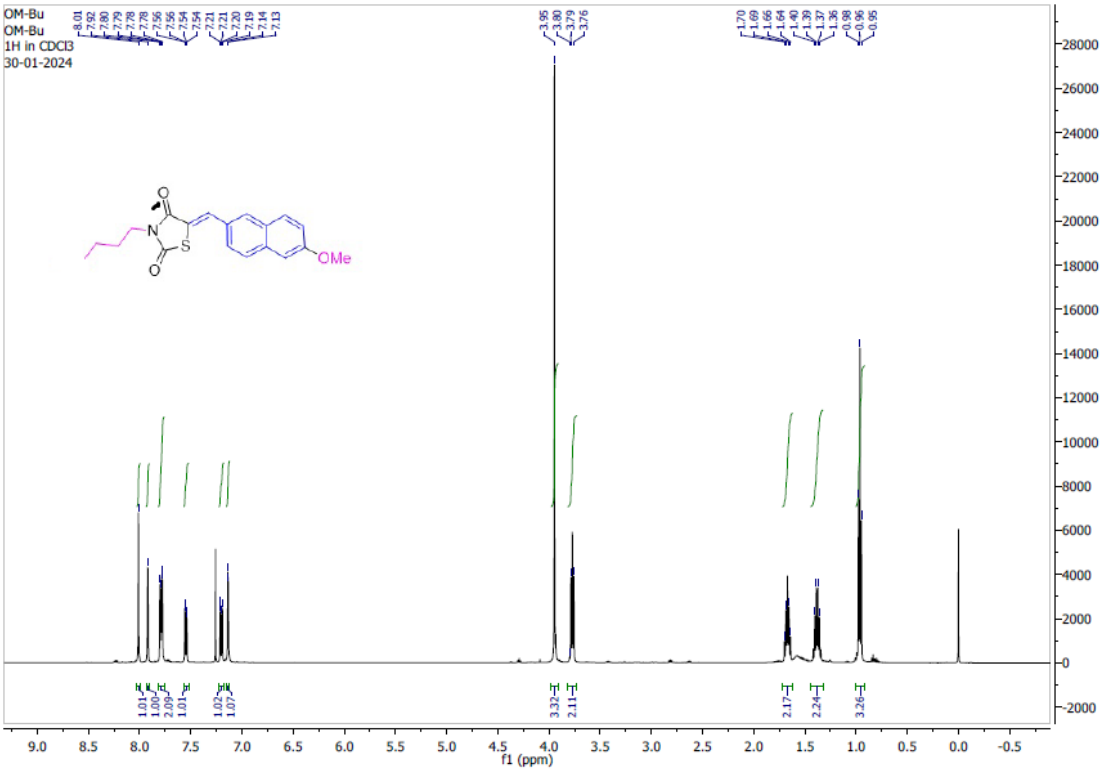

^{1}H-NMR spectrum of compound NT8

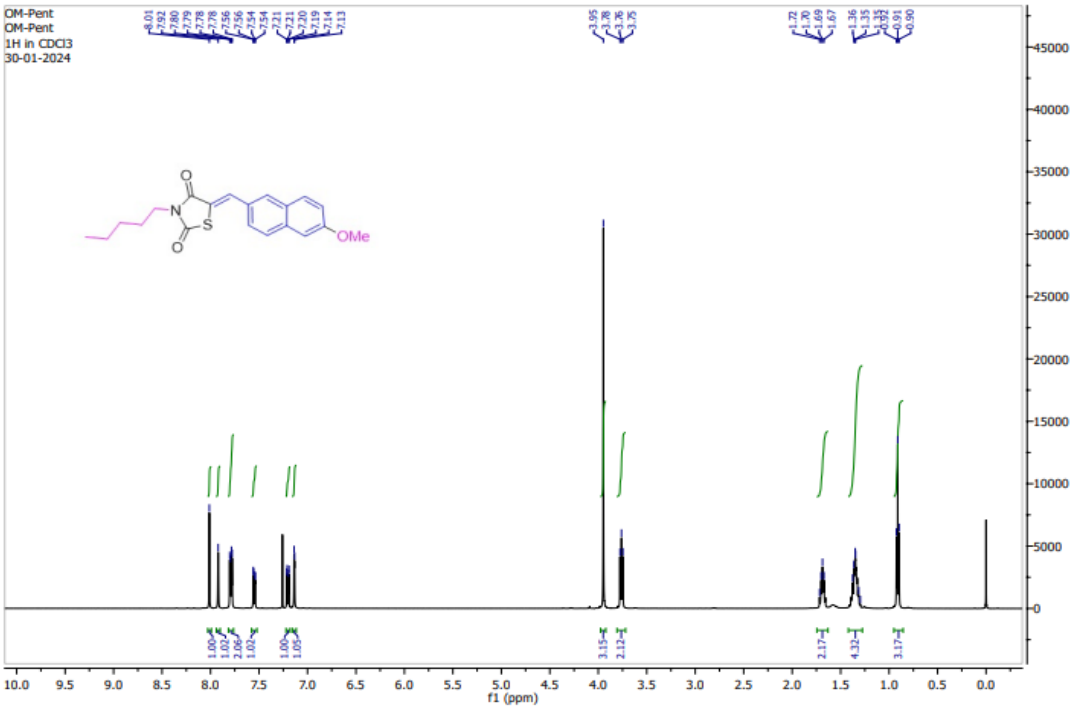

^{1}H-NMR spectrum of compound NT9

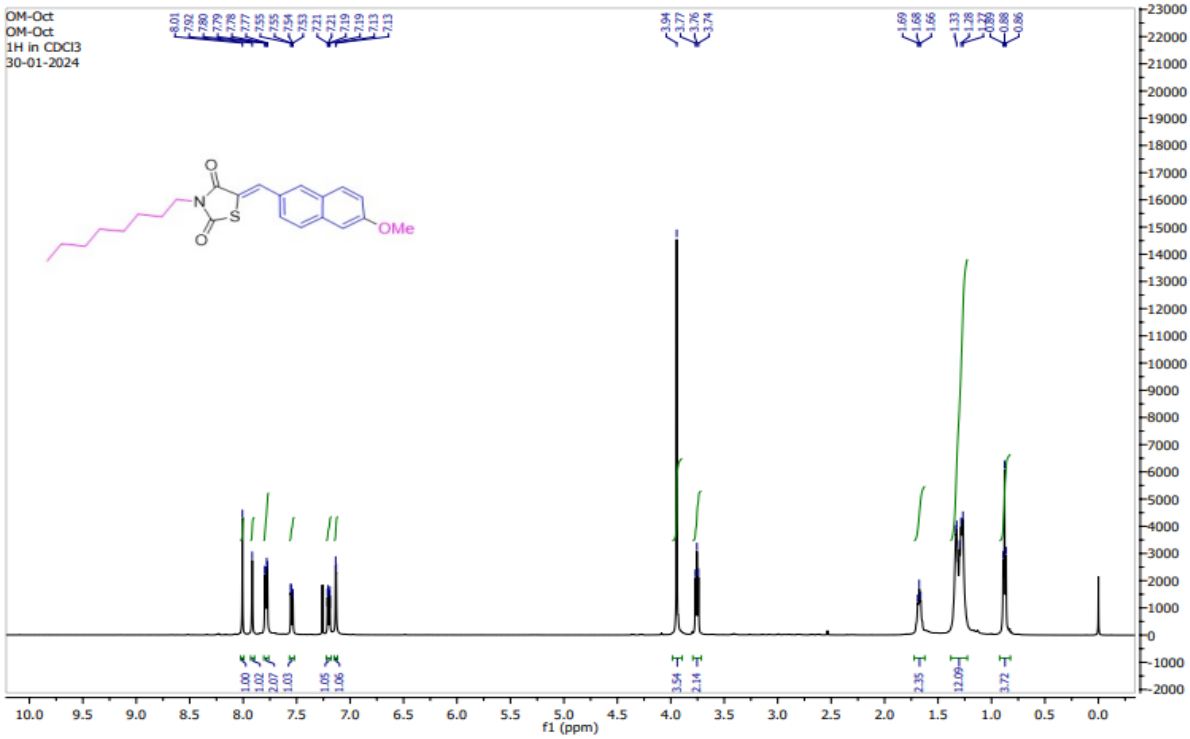

^{1}H-NMR spectrum of compound NT10

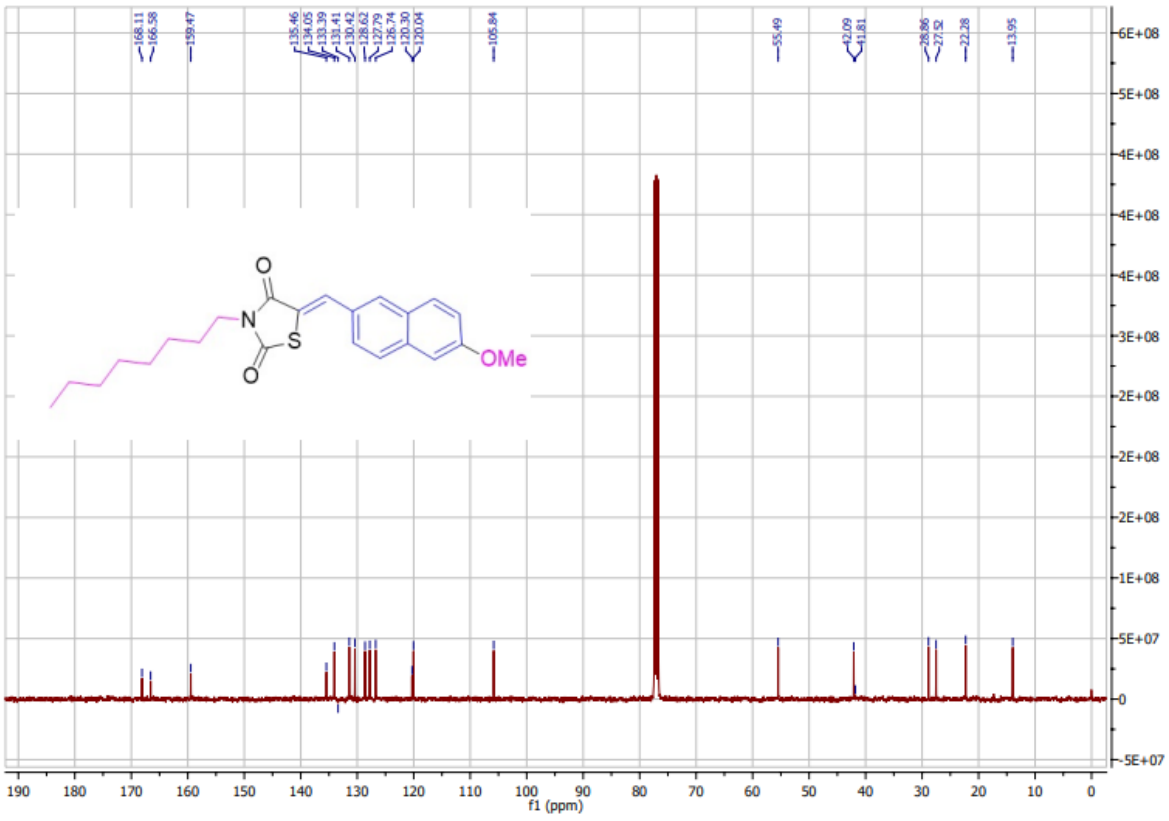

^{13}C-NMR Spectrum of compound NT10

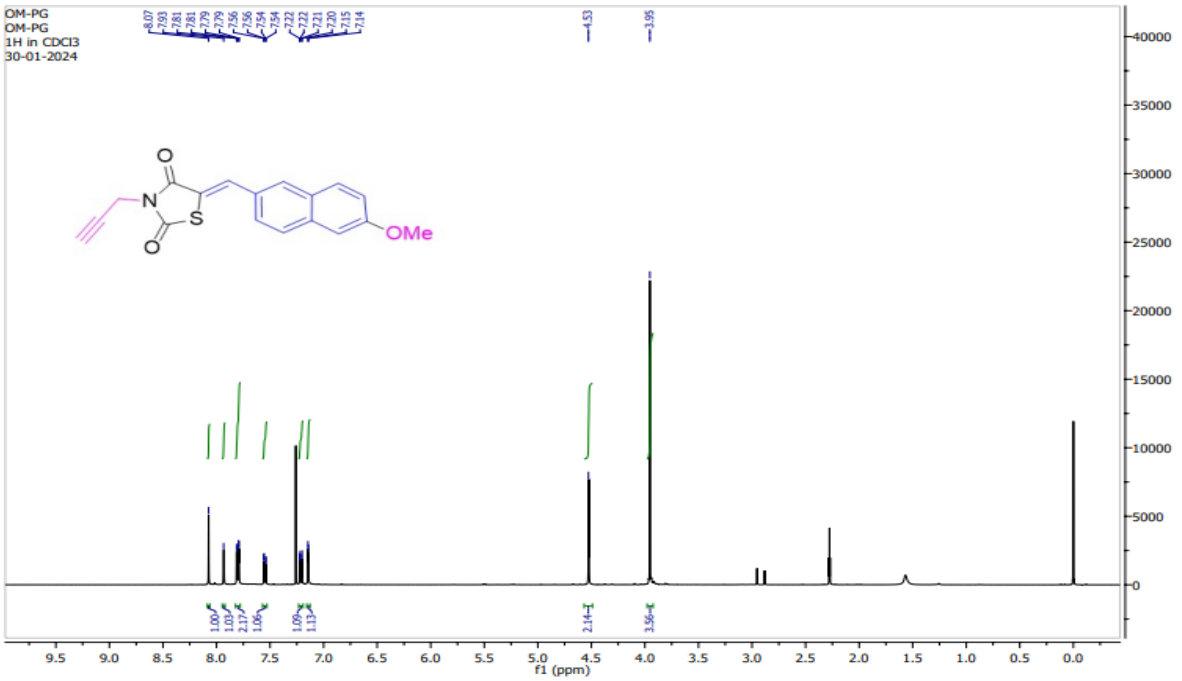

^{1}H-NMR spectrum of compound NT11

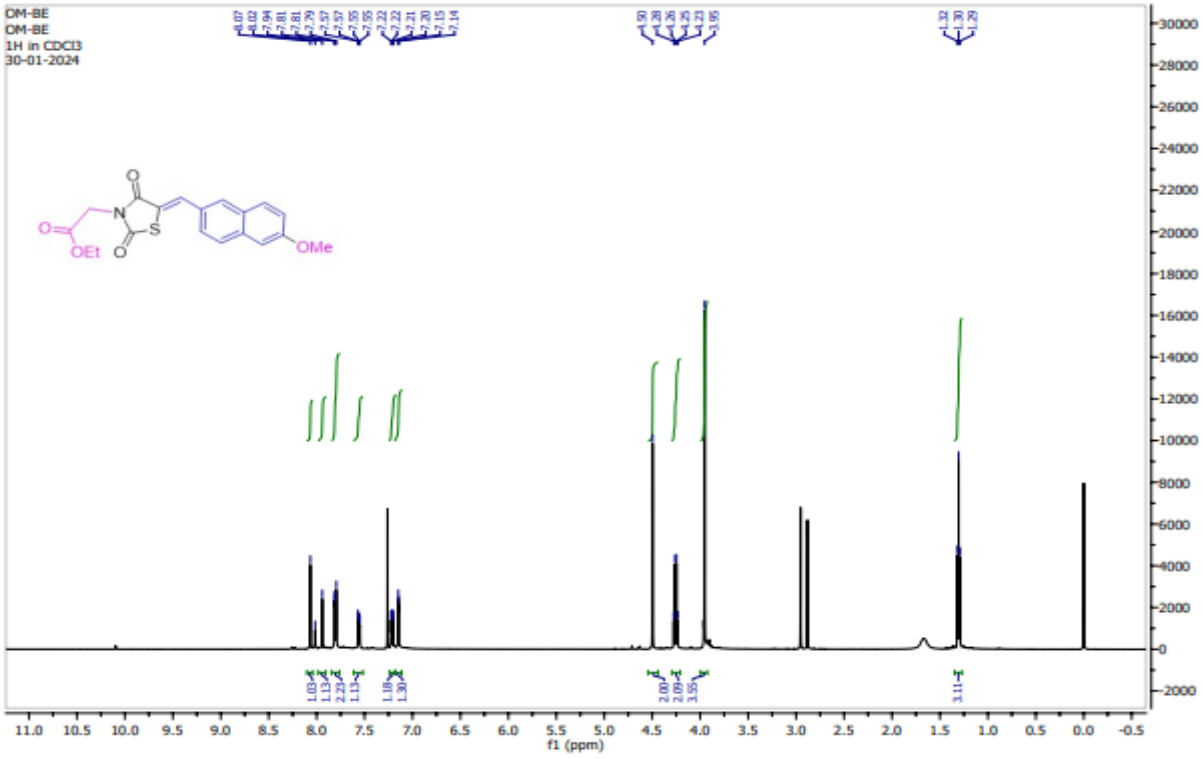

^{1}H-NMR spectrum of compound NT12

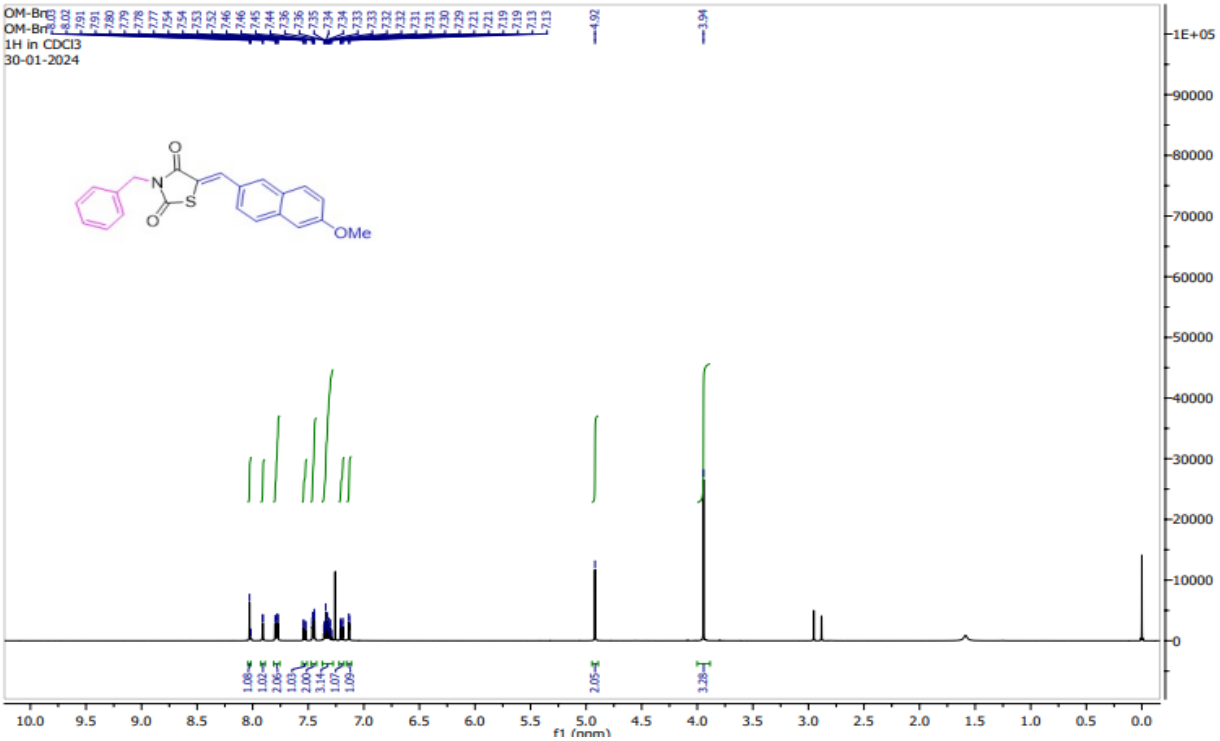

^{1}H-NMR spectrum of compound NT13

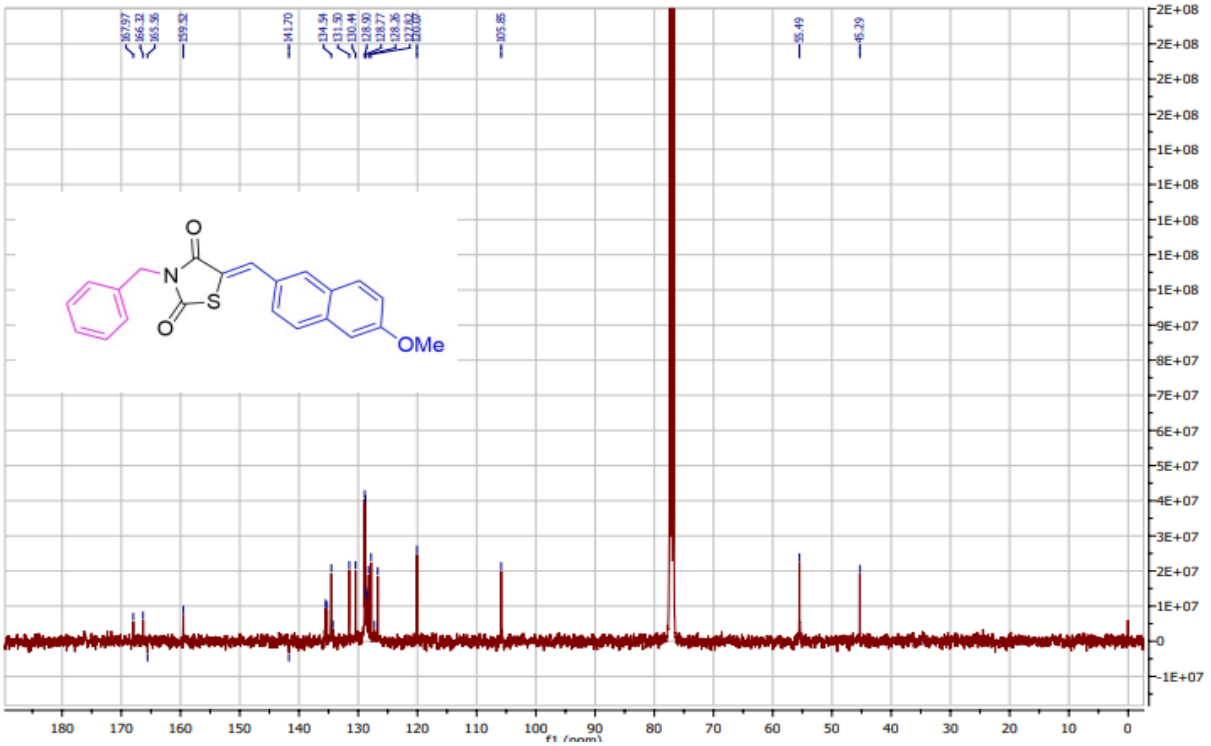

^{13}C-NMR Spectrum of compound NT13

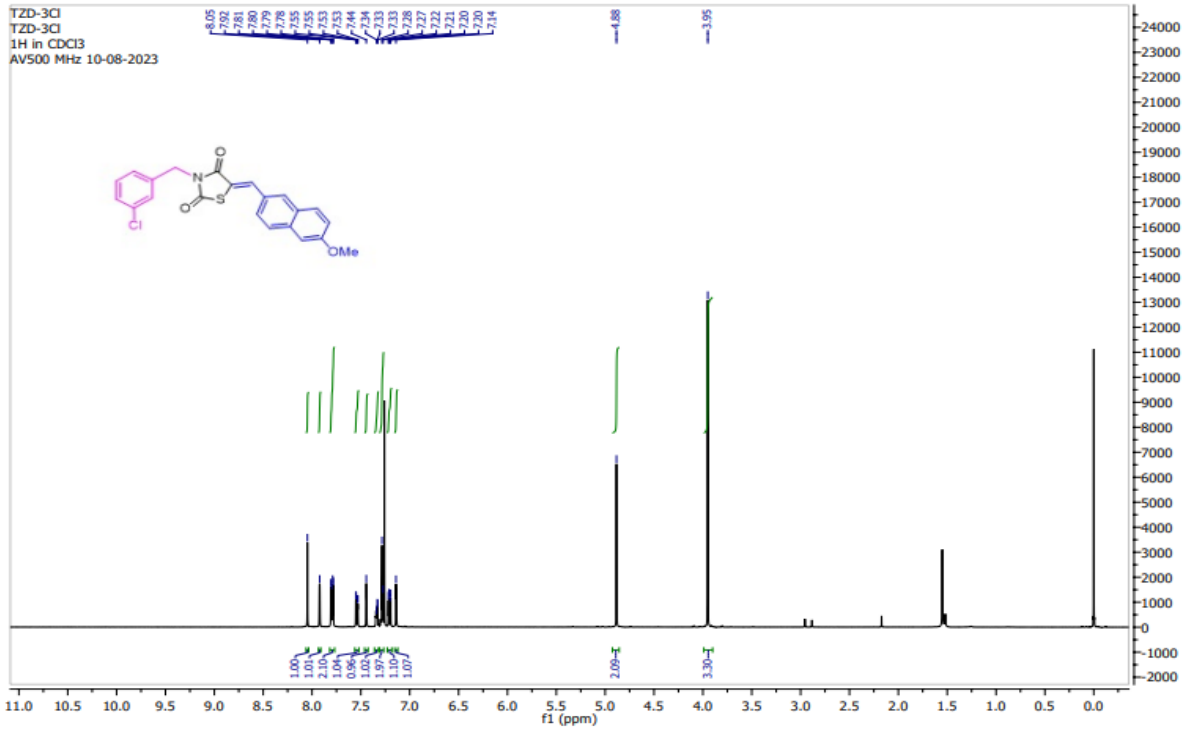

^{1}H-NMR spectrum of compound NT14

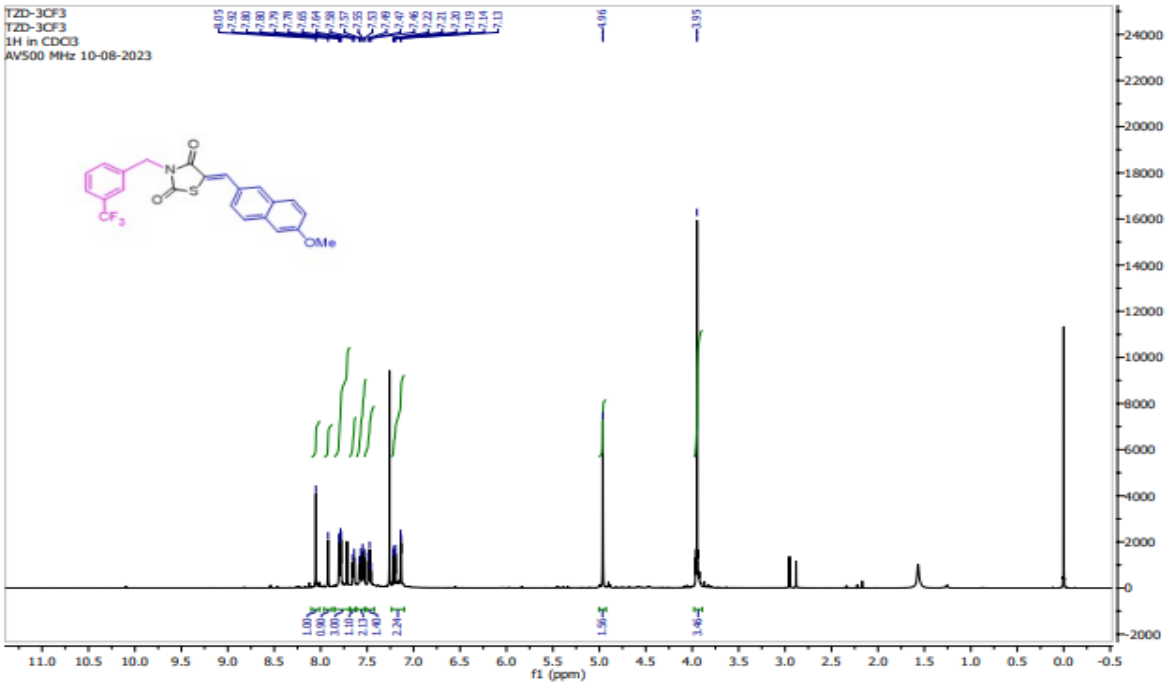

^{1}H-NMR spectrum of compound NT15

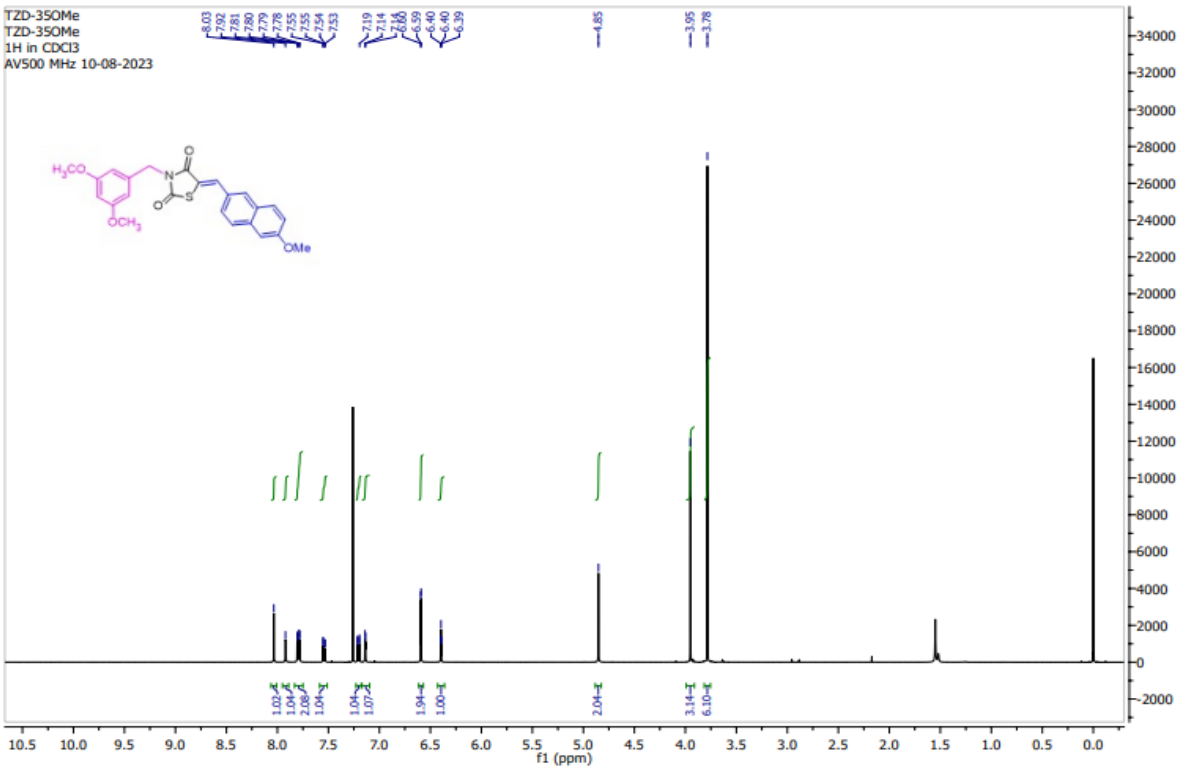

^{1}H-NMR spectrum of compound NT16

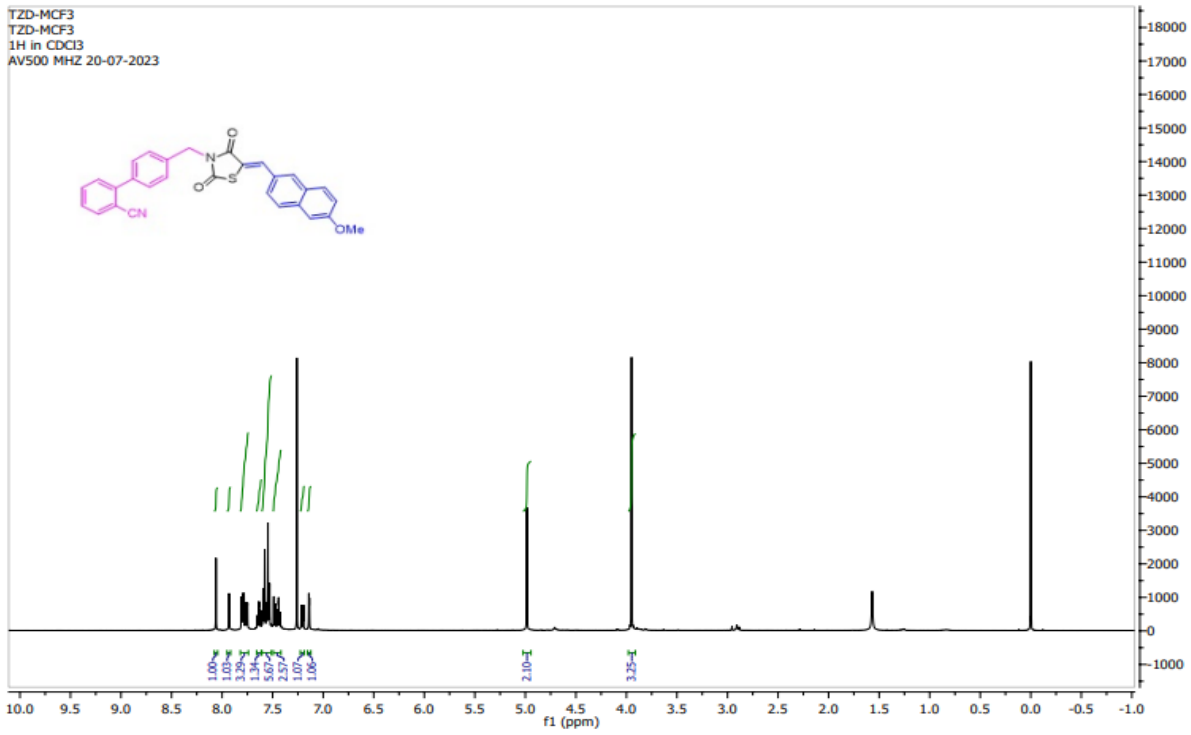

^{1}H-NMR spectrum of compound NT17

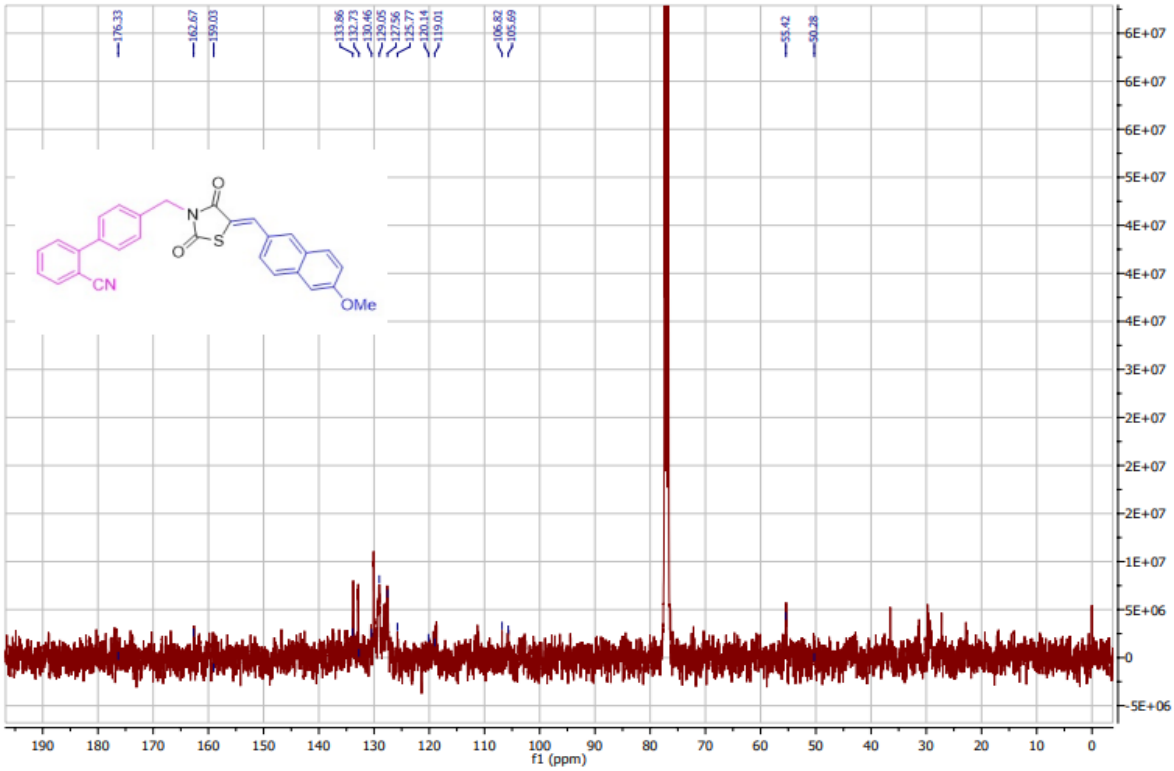

^{13}C-NMR Spectrum of compound NT17

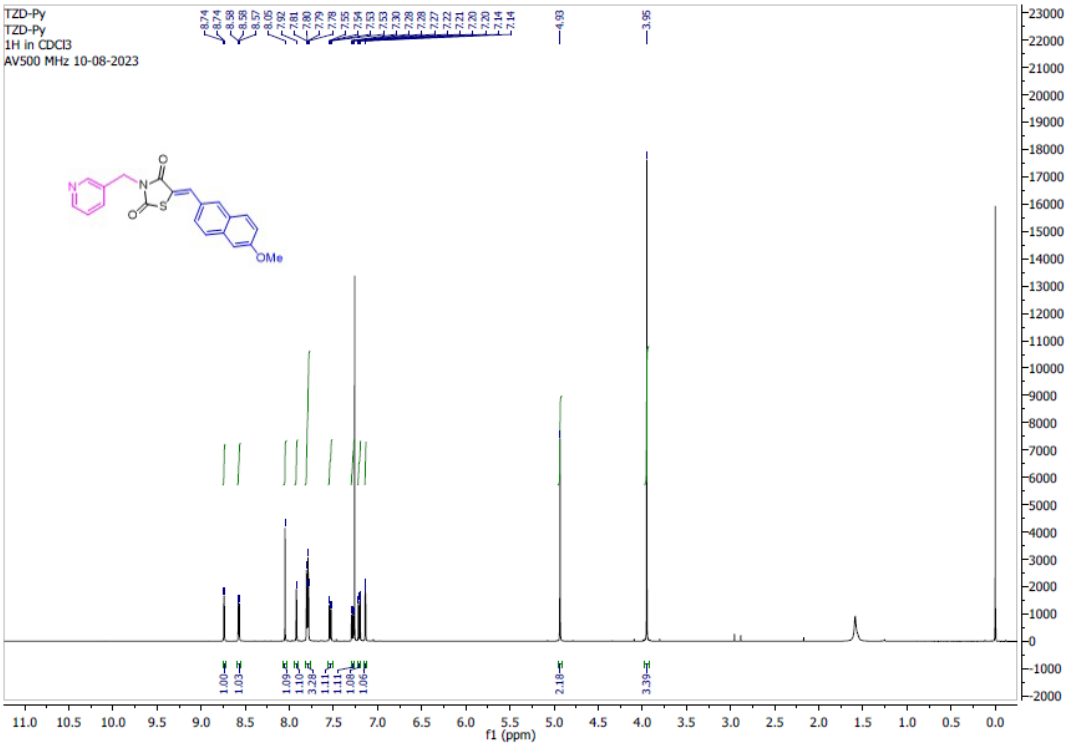

^{1}H-NMR spectrum of compound NT18

Spectral data of all synthesized compounds; Series 2 (QT1-QT8)

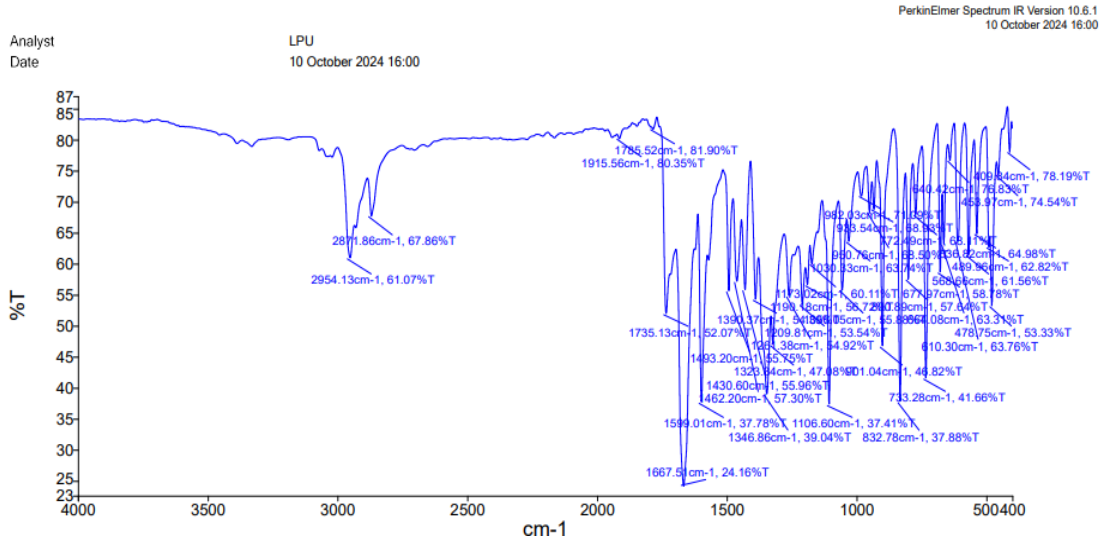

FTIR Spectrum of compound QT1

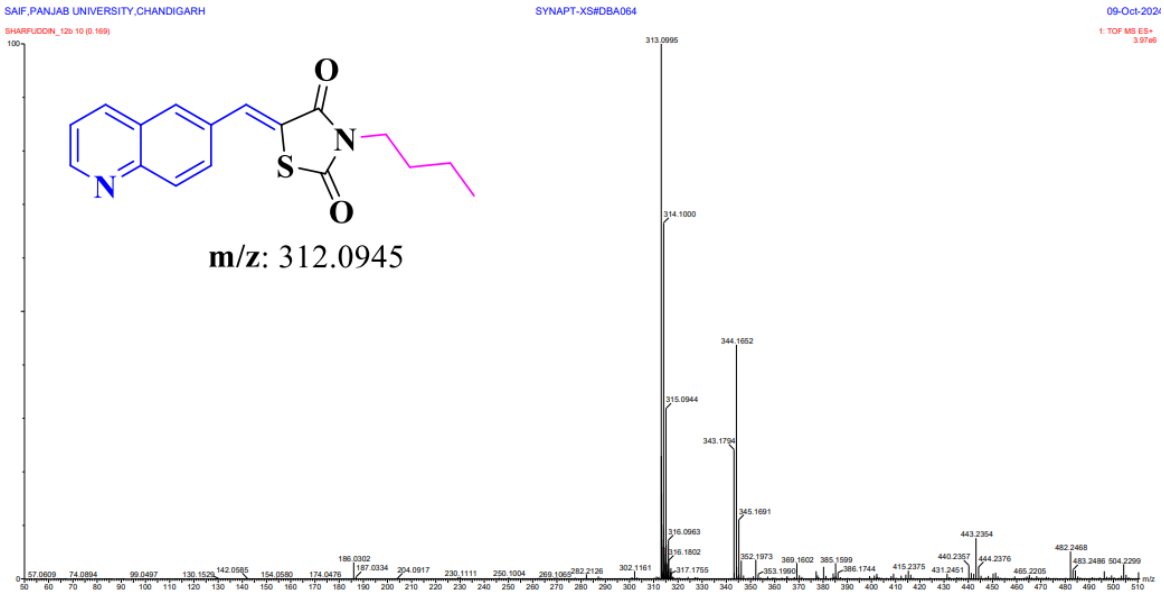

HRMS Spectrum of compound QT1

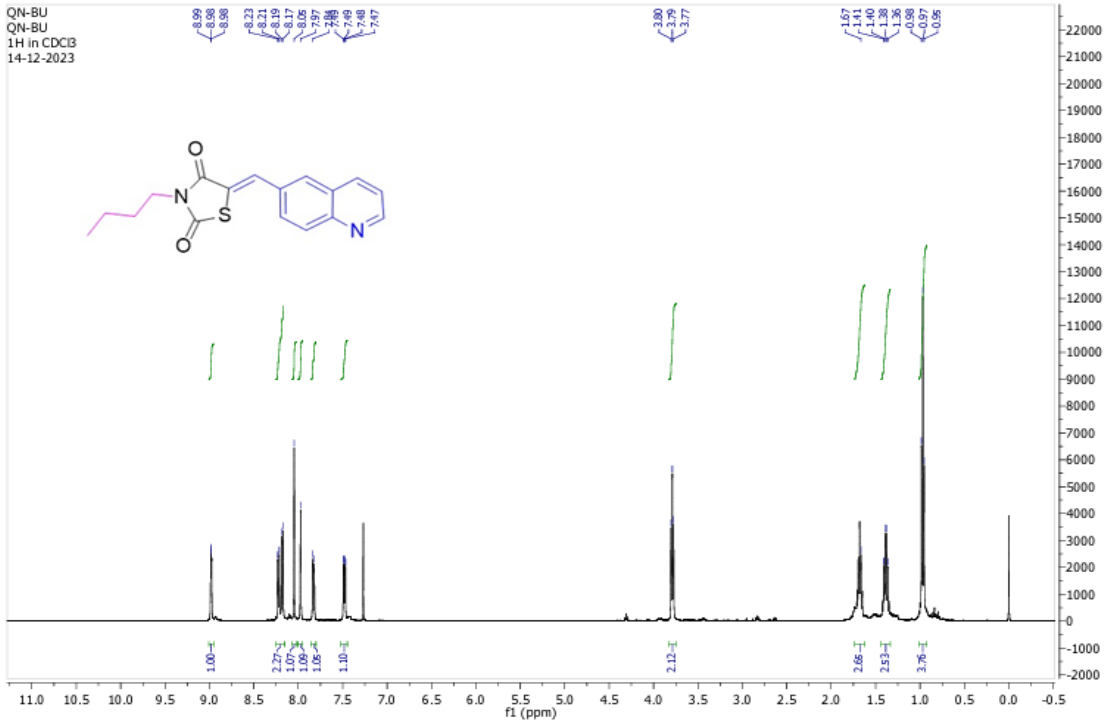

^{1}H-NMR Spectrum of compound QT1

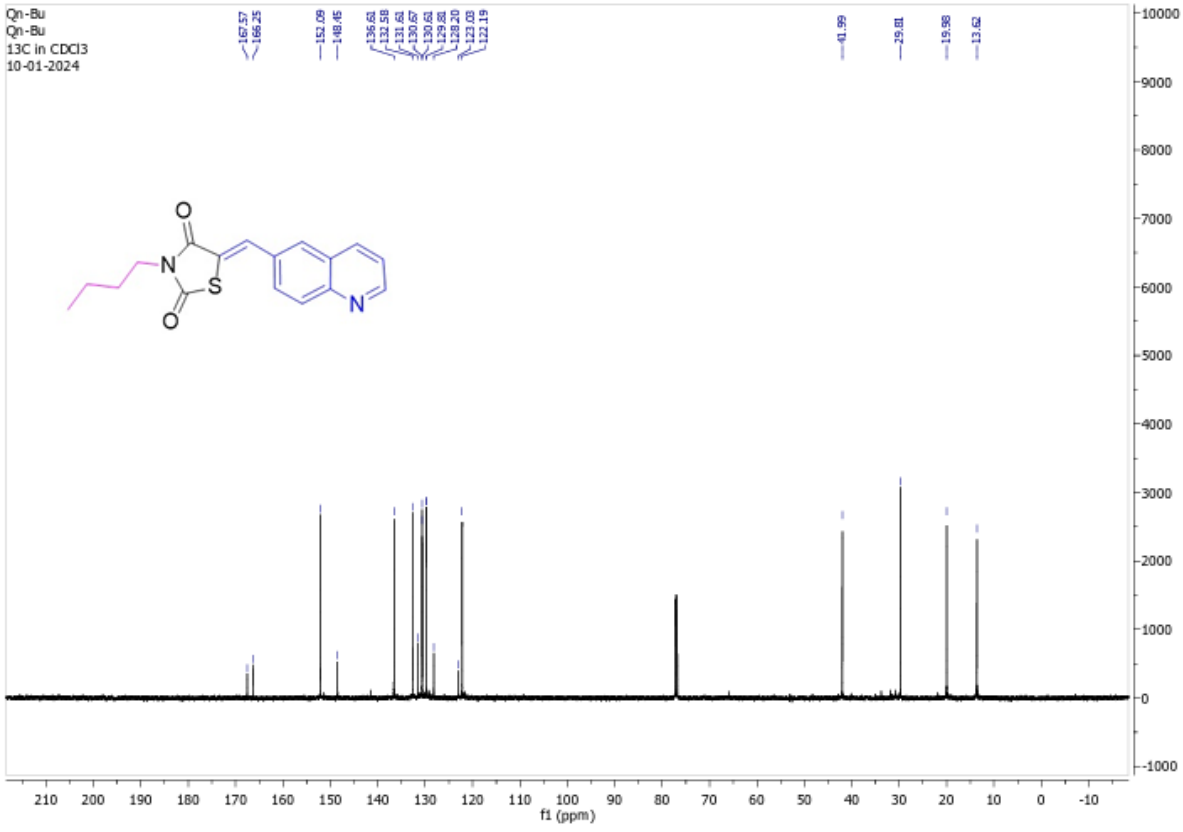

: ^{13}C-NMR Spectrum of compound QT1

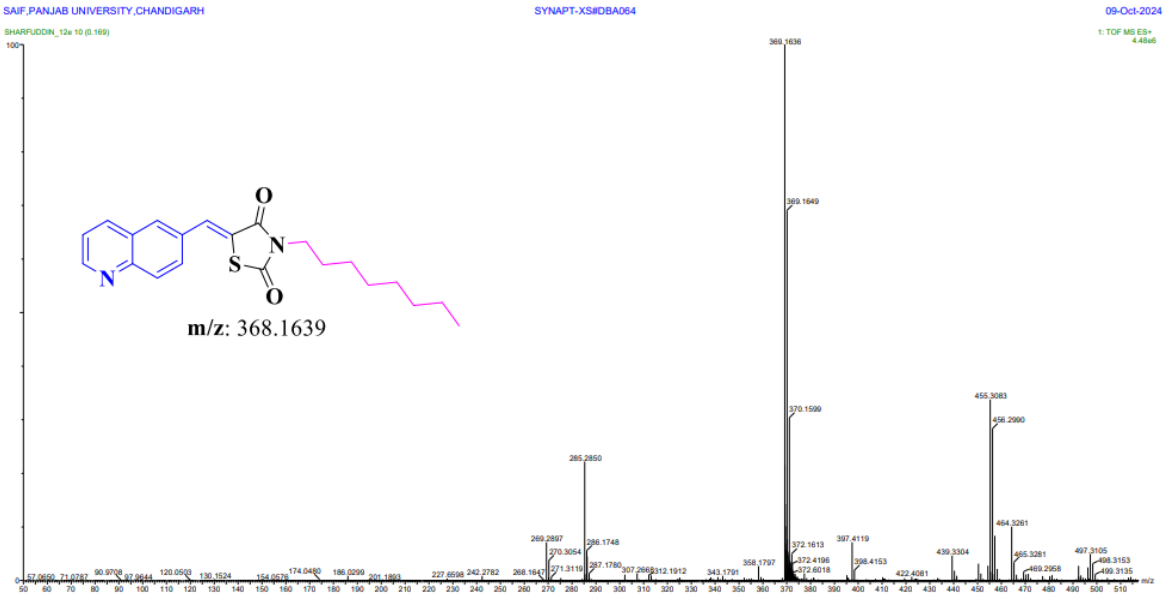

HRMS Spectrum of compound QT2

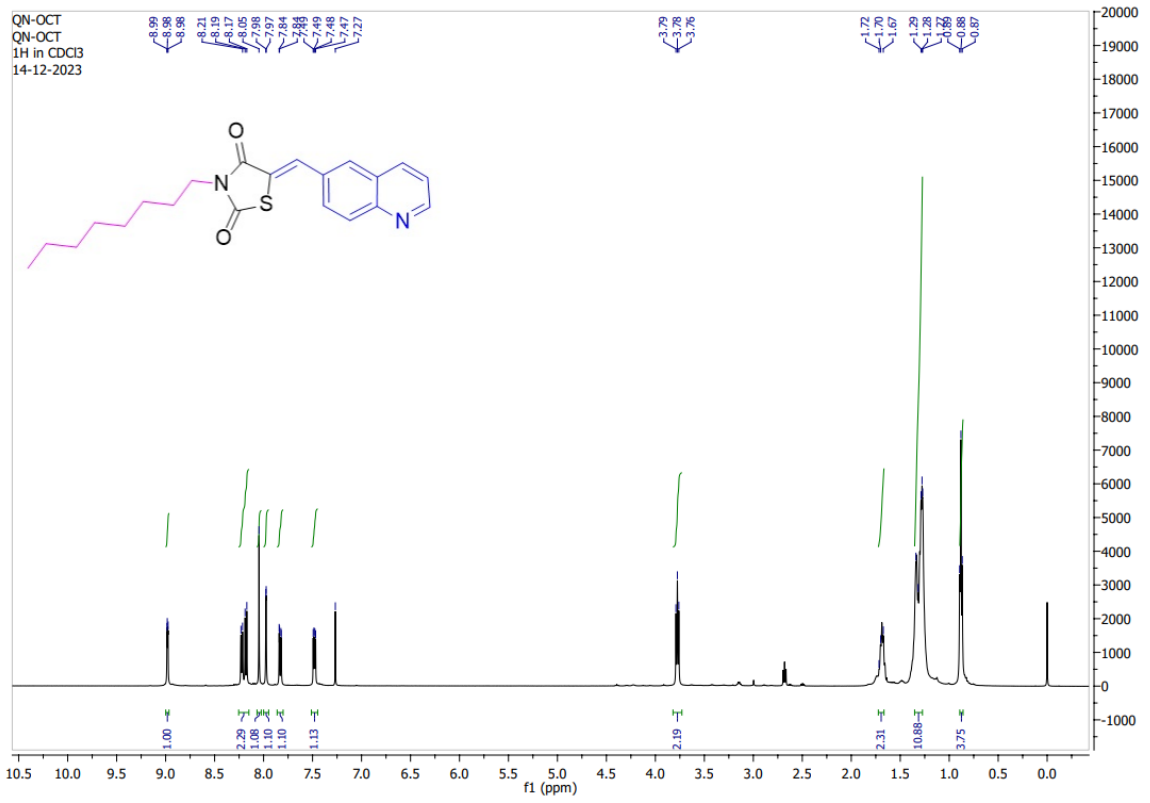

^{1}H-NMR Spectrum of compound QT2

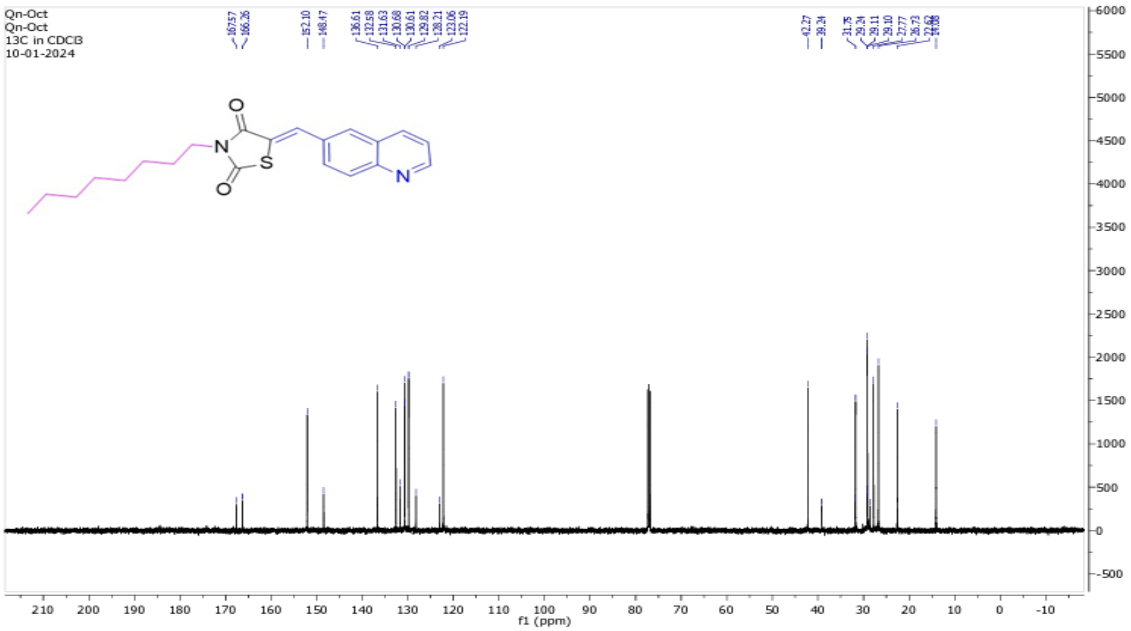

^{13}C-NMR Spectrum of compound QT2

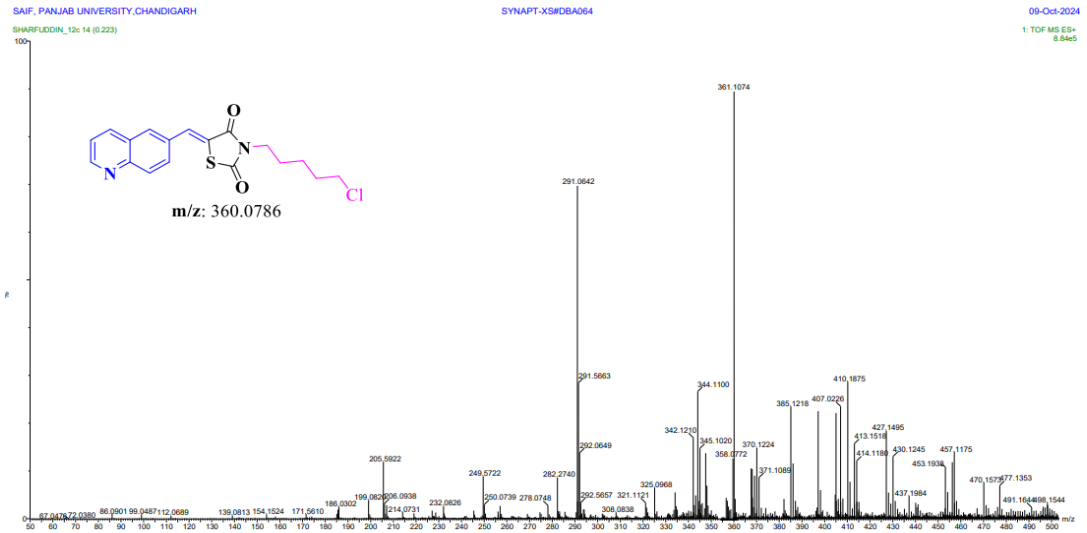

HRMS Spectrum of compound QT3

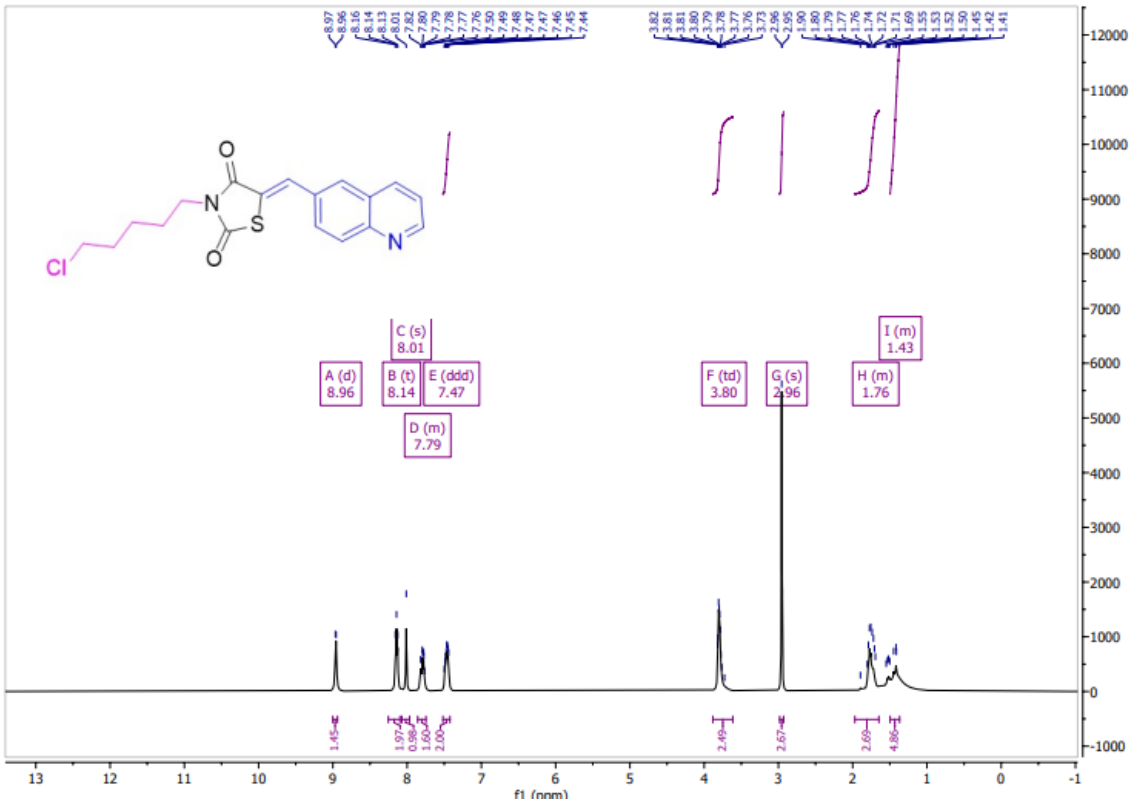

^{1}H-NMR Spectrum of compound QT3

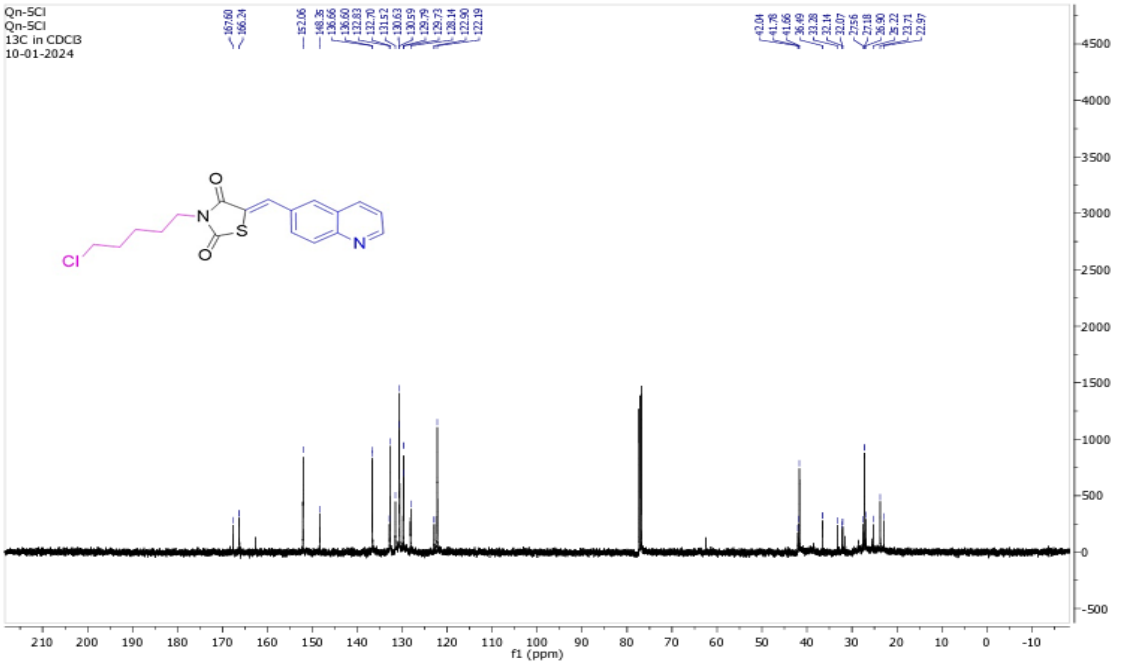

^{13}C-NMR Spectrum of compound QT3

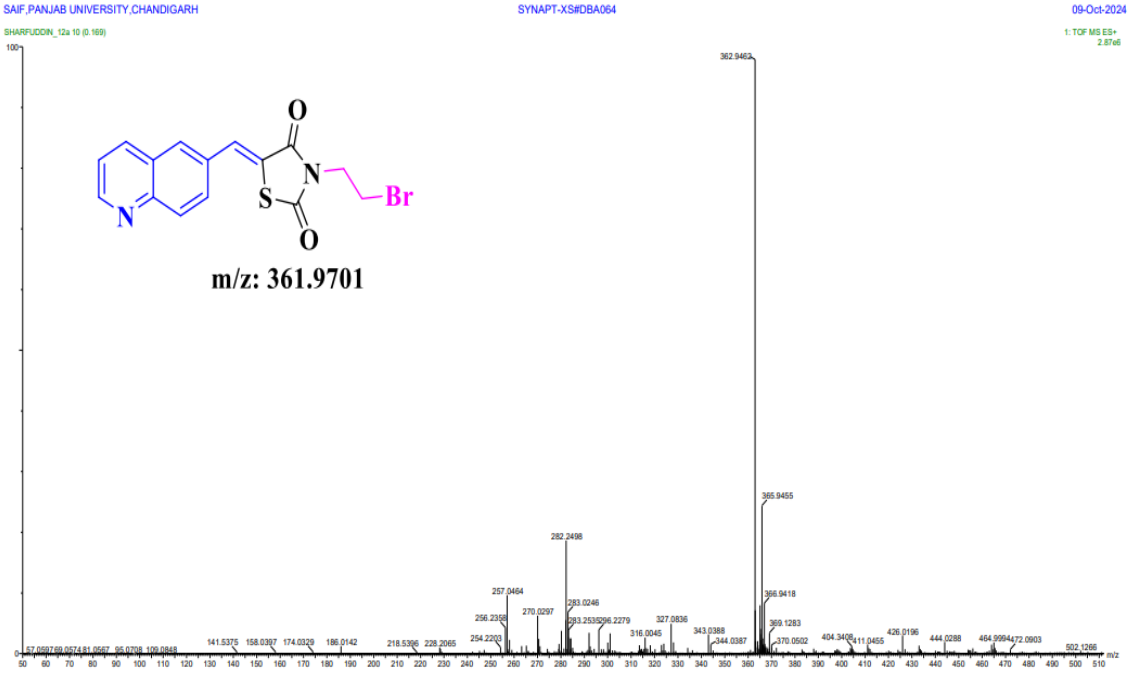

HRMS Spectrum of compound QT4

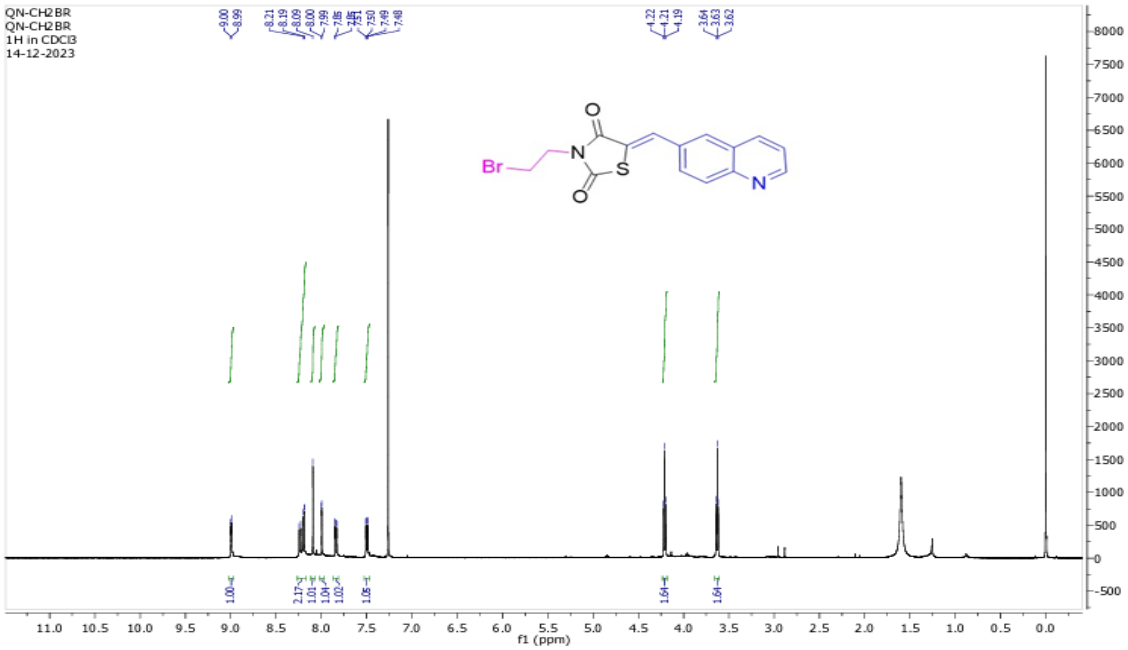

^{1}H-NMR Spectrum of compound QT4

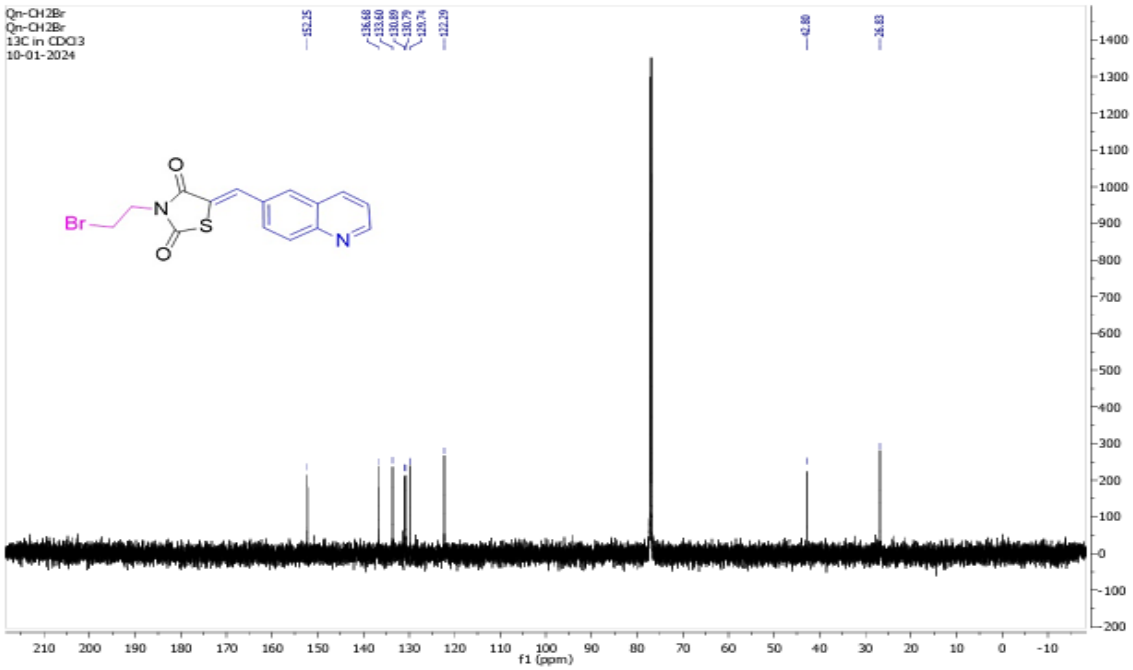

^{13}C-NMR Spectrum of compound QT4

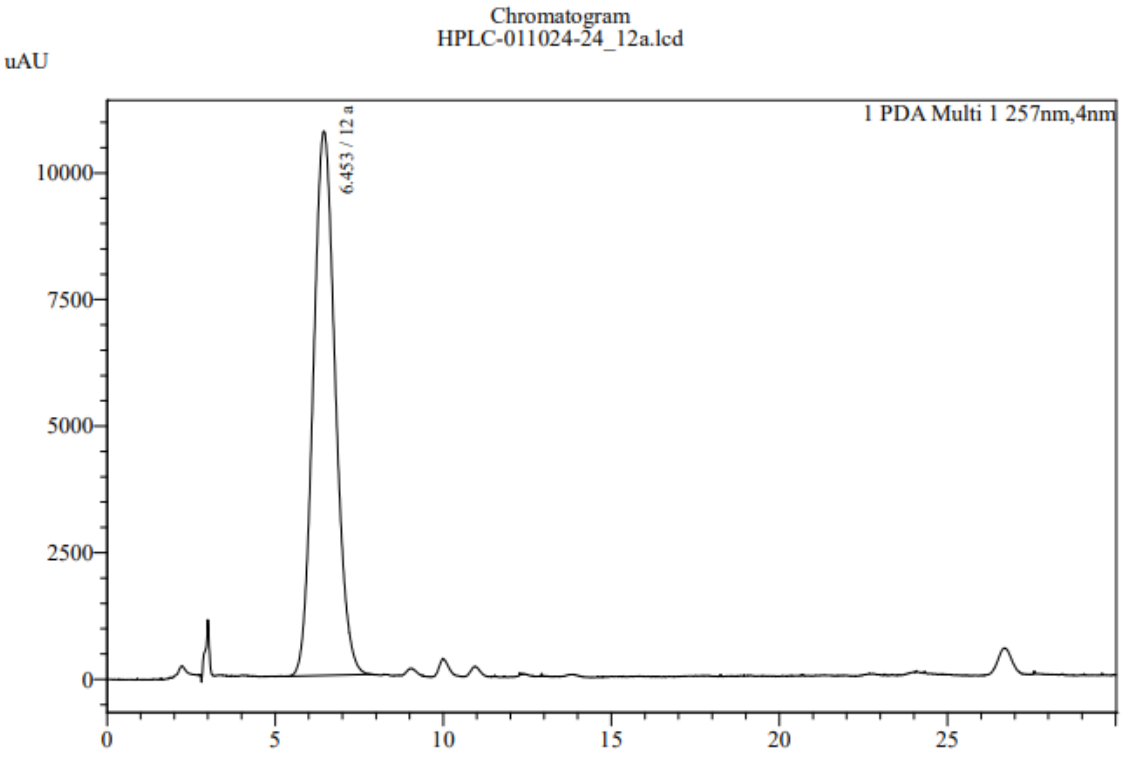

Figure S25: HPLC Chromatogram of compound QT4

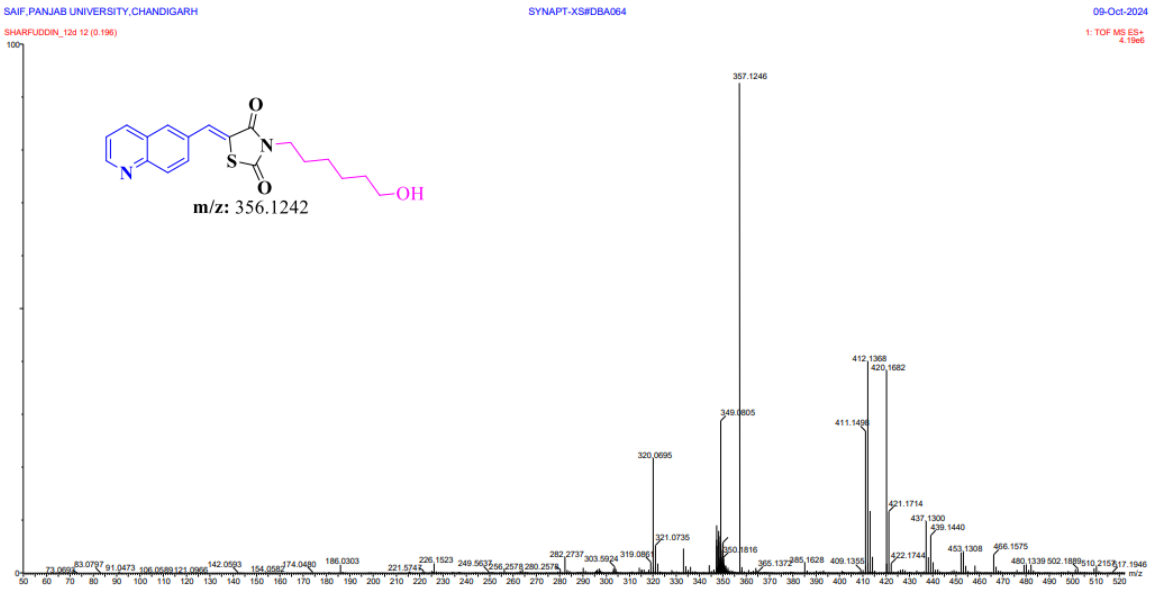

HRMS Spectrum of compound QT5

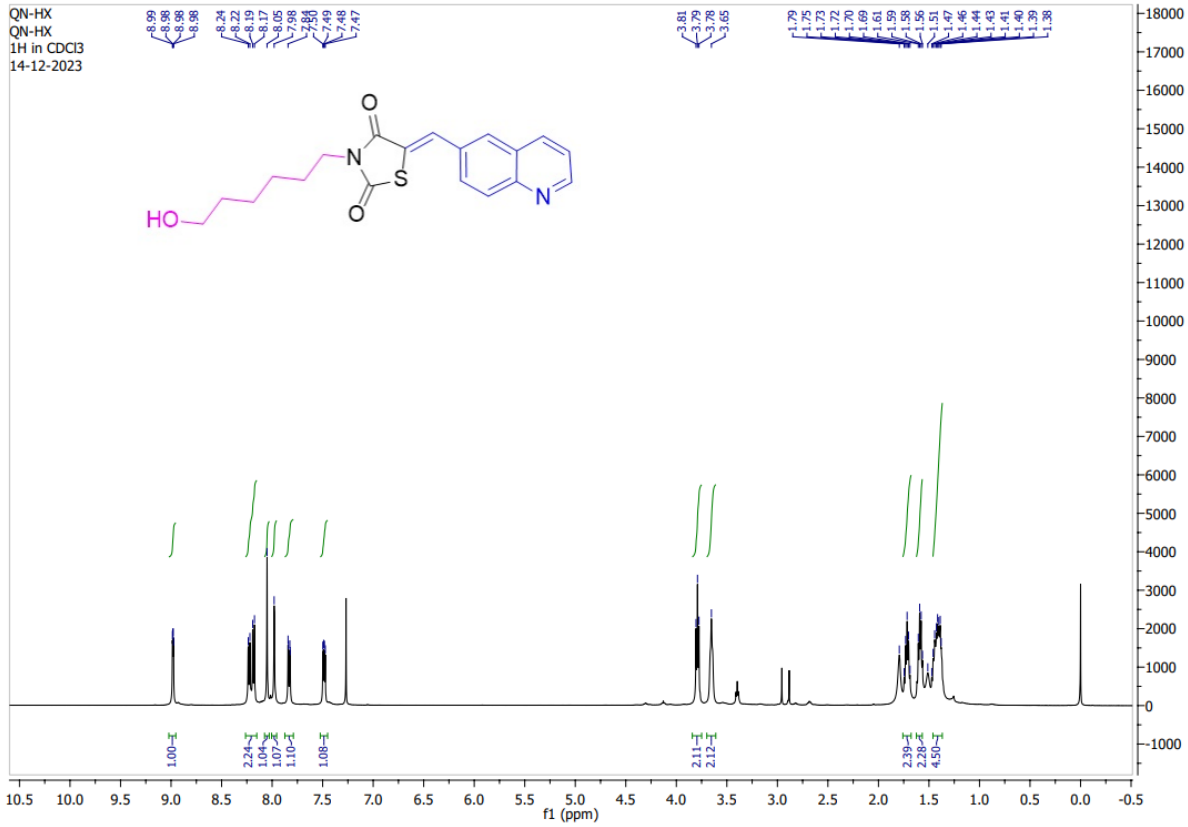

^{1}H-NMR Spectrum of compound QT5

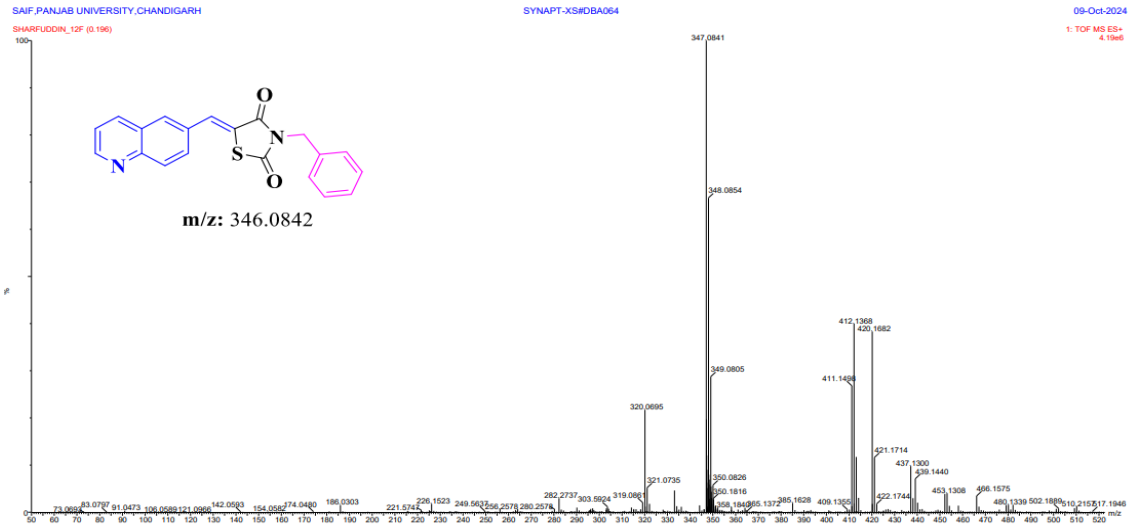

HRMS Spectrum of compound QT6

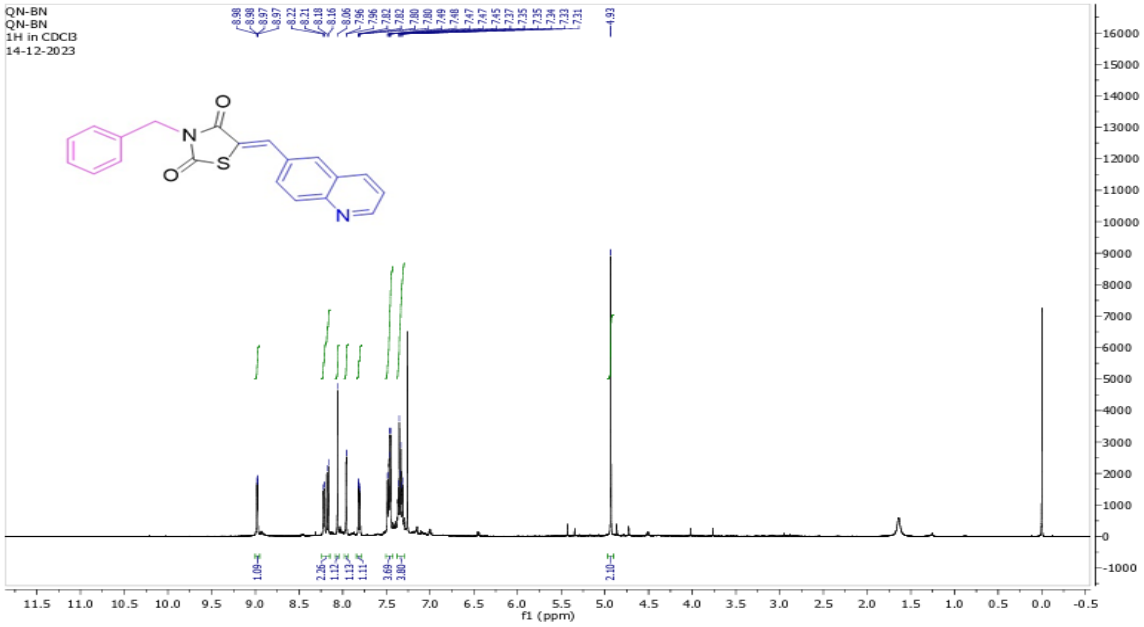

^{1}H-NMR Spectrum of compound QT6

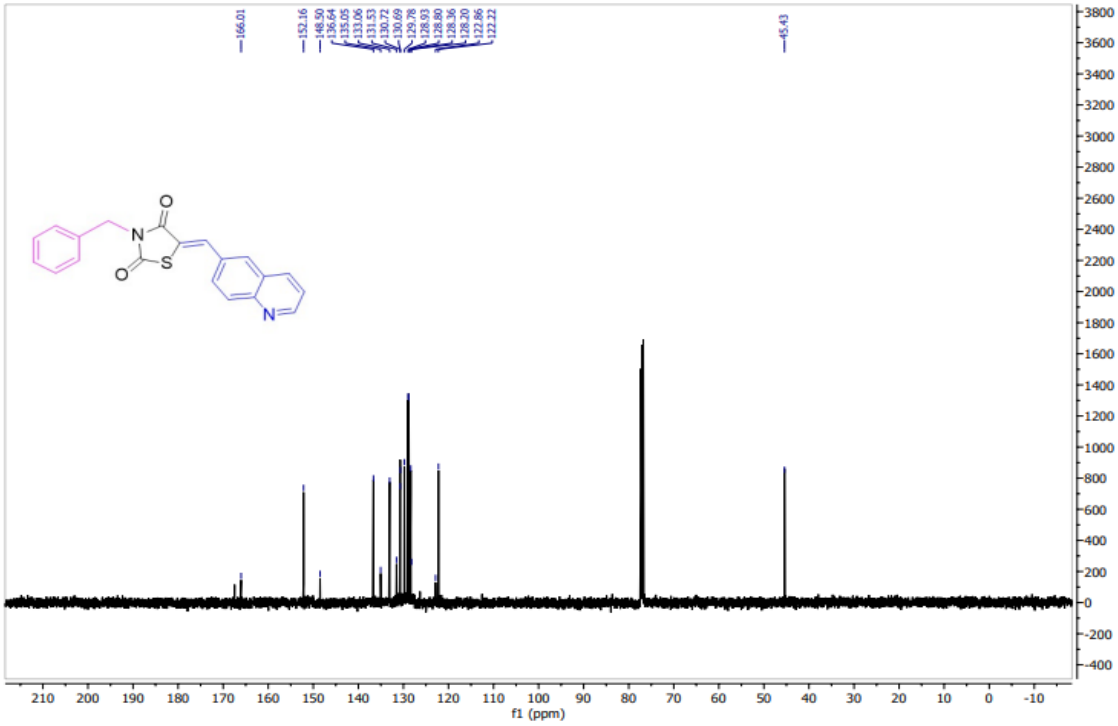

^{13}C-NMR Spectrum of compound QT6

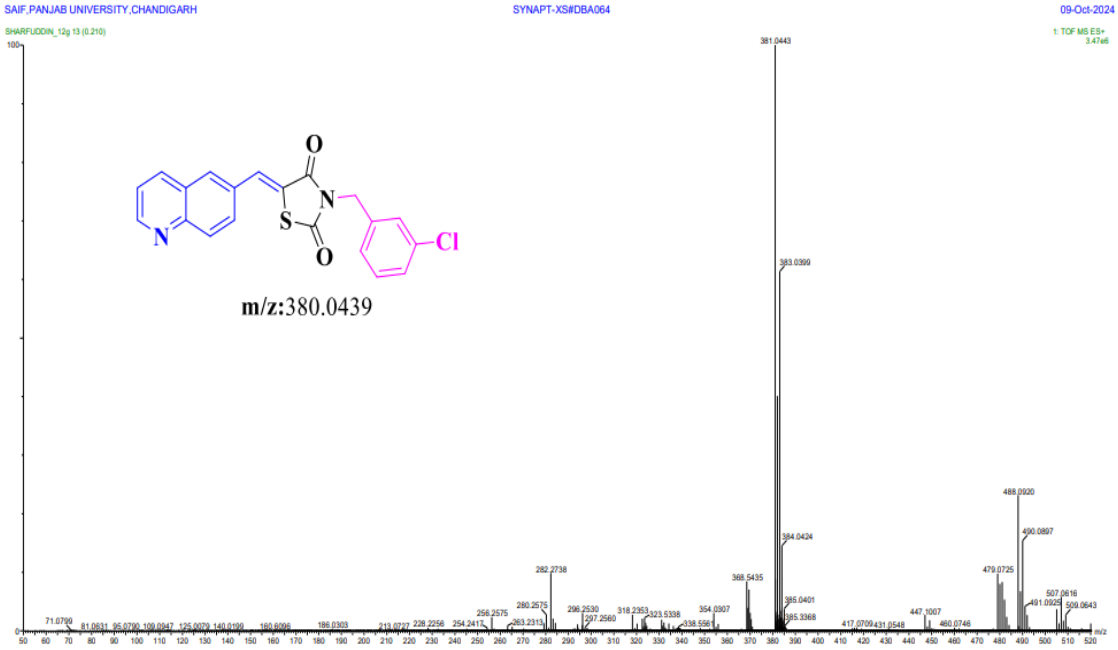

HRMS Spectrum of compound QT7

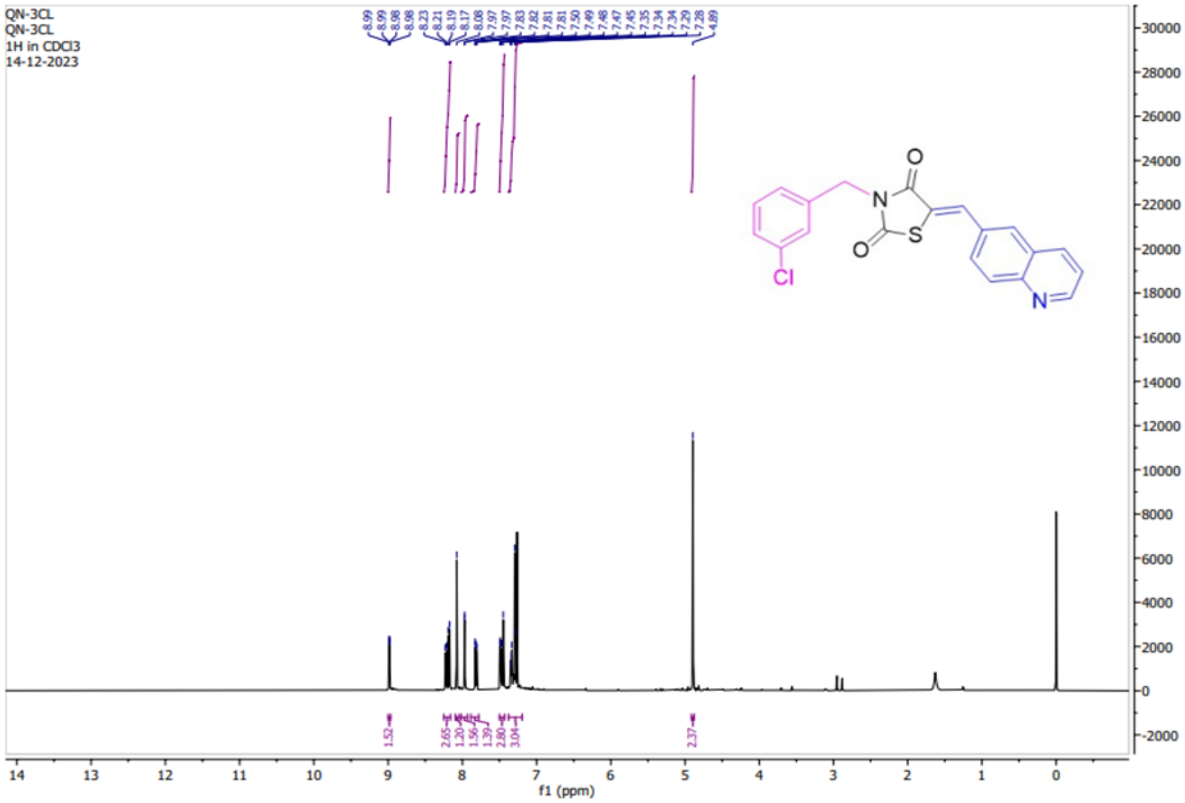

^{1}H-NMR Spectrum of compound QT7

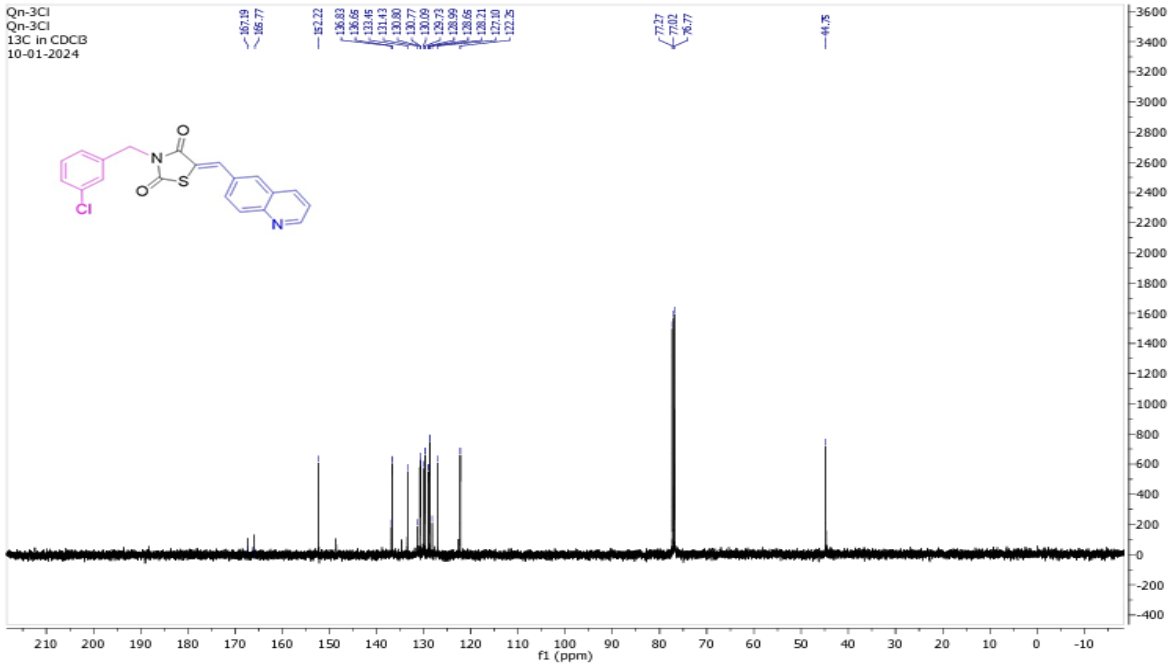

^{13}C-NMR Spectrum of compound QT7

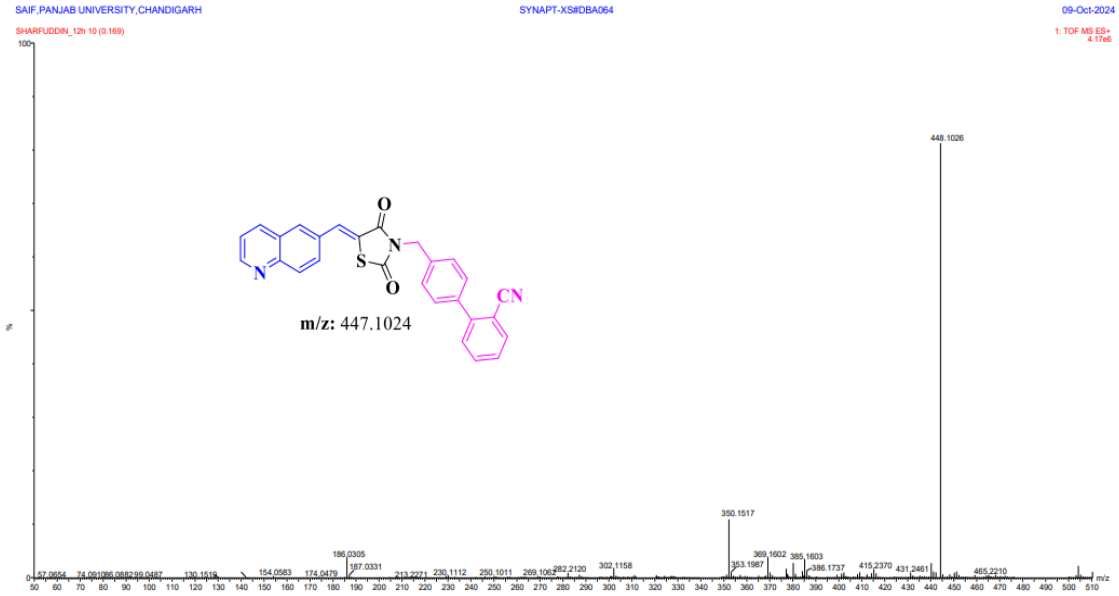

HRMS Spectrum of compound QT8

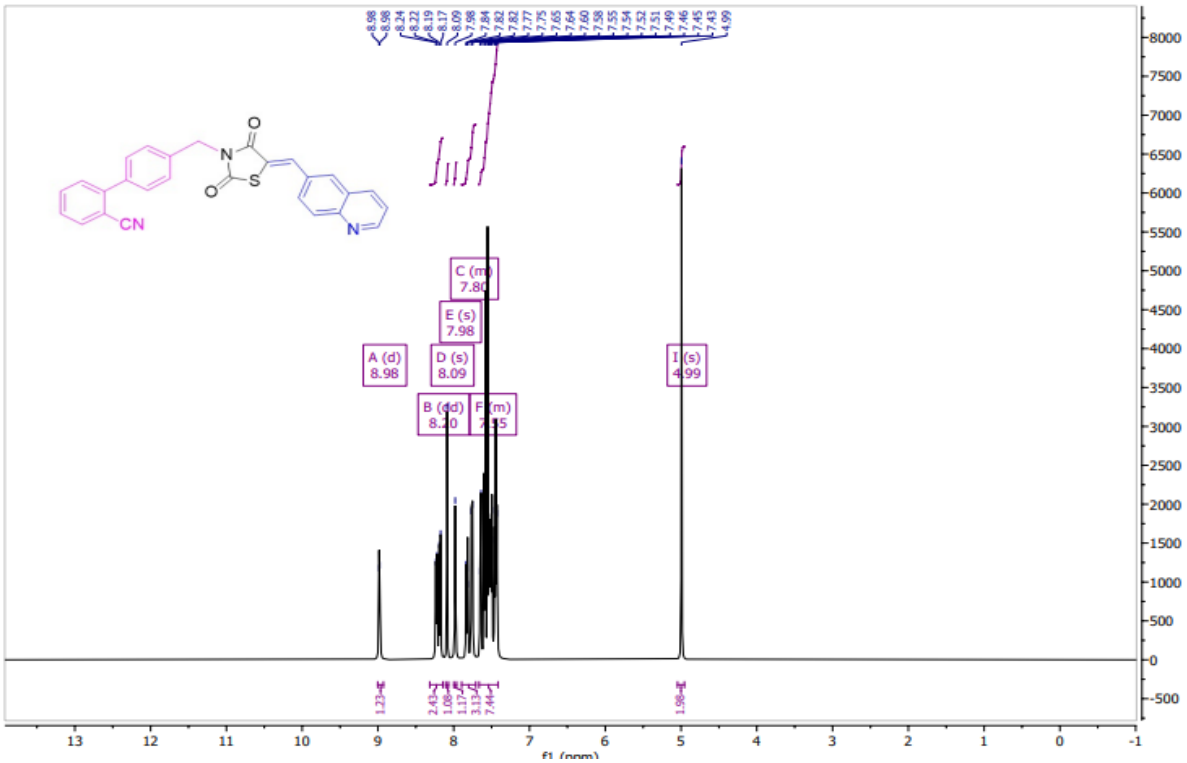

^{1}H-NMR Spectrum of compound QT8

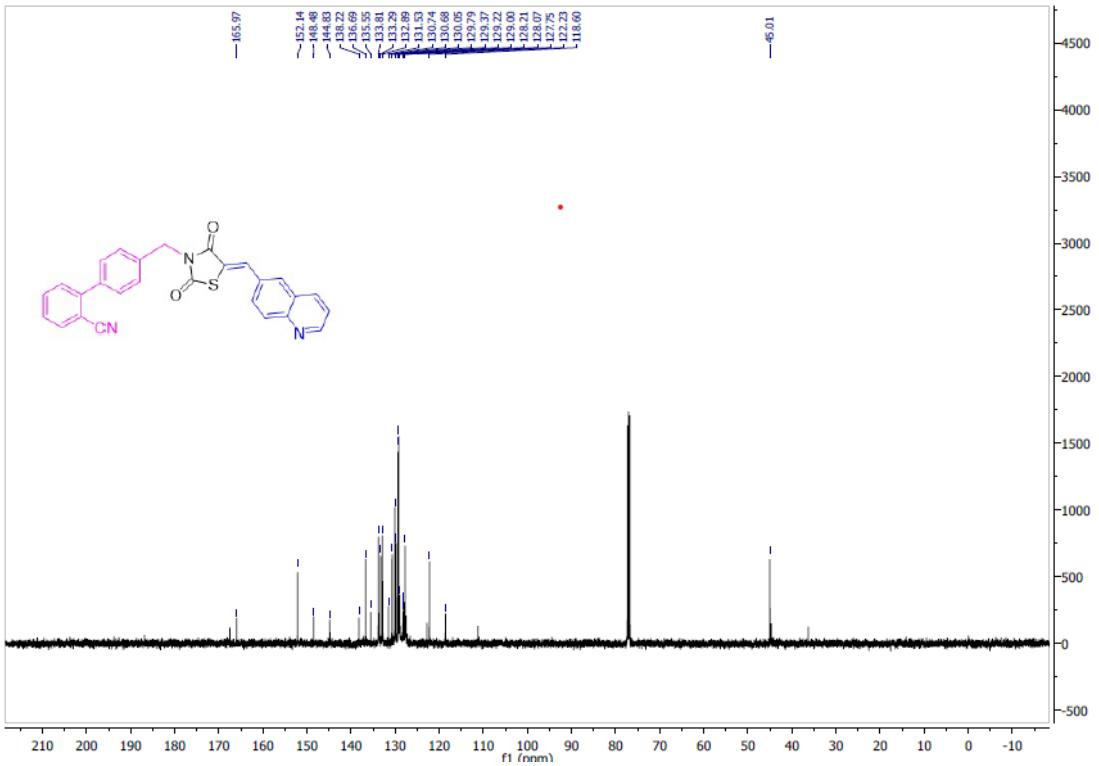

^{13}C-NMR Spectrum of compound QT8

III. List of publications

Research article from current work

1. **Sharfuddin Mohd**, Vikas Sharma, Harish Vancha, Rakesh Kumar, Govindaiah Pilli, Exploring Thiazolidinedione-Naphthalene Analogues as Potential Antidiabetic Agents: Design, Synthesis, Molecular Docking and In-vitro Evaluation. *Cell Biochemistry and Biophysics*. 2024 Dec 13:1-4, https://doi.org/10.1007/s12013-024-01632-y.
2. **Sharfuddin Mohd**, Durhesh Paresh Bidye, sheshagiri R Dixit, B.C. Revanasiddappa, Harish Vancha, Rakesh Kumar, Vikas Sharma, Quinoline Based thiazolidinediones: Design, Synthesis, In Silico, In Vitro, Antioxidant and Antidiabetic Evaluation. *ChemistrySelect*. 2024 Nov;9(41), https://doi.org/10.1002/slct.202402281

Cell Biochemistry and Biophysics
https://doi.org/10.1007/s12013-024-01632-y

ORIGINAL PAPER

Exploring Thiazolidinedione-Naphthalene Analogues as Potential Antidiabetic Agents: Design, Synthesis, Molecular Docking and In-vitro Evaluation

Sharfuddin Mohd[1] · Vikas Sharma[1] · Vancha Harish[1] · Rakesh Kumar[1] · Govindaiah Pilli[2]

Accepted: 21 November 2024

Abstract
Thiazolidinedione-naphthalene analogues were synthesized and evaluated for antidiabetic activity as Pancreatic α-Amylase (PAA) and intestinal α-glucosidase (IAG) inhibitors. The activity of the compounds (**14a–g**,**17a–k**) is compared with acarbose as the standard drug and all the compounds shows good to moderate antidiabetic activity. In-vitro PAA and IAG inhibition assay is performed for the all compounds, the compounds **17e** shows superior PAA and IAG inhibitory activity with respective to standard (IC_{50} = **12.455 ± 0.04** µM and **9.145 ± 0. 01** µM). The molecular interaction with PAA and IAG protein was also studied with the help of molecular docking studies using AutoDock software. while SwissADME and Osiris property explorer tools computed in-silico drug likeliness and toxicity properties. The in-silico results confirmed the **17e** molecule as a superior drug with high binding affinity and good drug likeness against PAA and IAG, confirming in-vitro results. We also studied antioxidant activity (AOA) of all synthesized compounds and results confined that the compound **14g and 17e** has good antioxidant potential IC_{50} = **8.04 ± 0.02** µM **and 6.36 ± 0.03** µM respectively among all compounds. In conclusion, in-vitro, in-silico antidiabetic and antioxidant studies revealed **17e** compound was found to be potential compound.

Keywords Diabetes · Thiazolidinediones · Naphthalene · Pancreatic α-amylase · Intestinal α-glucosidase · Antioxidant

Introduction

Diabetes mellitus (DM) is a chronic, non-communicable metabolic condition characterized by acquired insulin insufficiency and decreased responsiveness of pancreatic beta-cells to generate insulin which leads to hyperglycaemia [1]. The most frequent types are Type 1 (deficiency of insulin secretion) DM and Type 2 (inadequate insulin secretion) DM. Among the different types of diabetes, Type-2 Diabetes mellitus(T2DM) is most common in all most all age groups [2] and its complex and can be accomplished by the conditions like stimulation of pancreatic insulin secretion, increasing β cell sensitivity to secrete insulin and retardation of glucose absorption from kidneys and intestine [3]. These conditions are achieved by identifying the potential targets having capacity to manage the blood glucose levels. The most effective targets include Sodium glucose-cotransporter-2 (SGLT-2) [4], peroxisome proliferator-activated receptor (PPARs) [5], Glucose-dependent insulinotropic polypeptide (GIP) [6], glucagon-like peptide-1 (GLP-1) receptor [7], Dipeptidyl peptidase-4 (DPP-IV) [8], Tyrosine phosphatase 1B [9], Pancreatic α-amylase (PAA) [10] and intestinal α-glucosidase (IAG) [11]. Among all the targets PAA and IAG are the well-known therapeutic targets for the treatment and maintenance of T2DM because they play vital role in the elevation of blood glucose levels. Also, they are the integral enzymes involved in the metabolism of various sources of glucose like carbohydrates, proteins and fats [12]. Inhibiting the activity of these enzymes (PAA and IAG) can lower the risk of developing T2DM.

The U.S. food and drug administration approved PAA and IAG inhibitors like acarbose [13], miglitol [14], Voglibose [15] have encouraged the researchers to design

✉ Govindaiah Pilli
govipharma@gmail.com

[1] School of pharmaceutical sciences, Lovely Professional University, Phagwara, Punjab, India

[2] Faculty of medicine, Department of Pathology, Wayne state University, Detroit, MI, USA

Published online: 13 December 2024

ChemistrySelect | Research Article
doi.org/10.1002/slct.202402281
Chemistry Europe
European Chemical Societies Publishing
www.chemistryselect.org

Quinoline Based thiazolidinediones: Design, Synthesis, In Silico, In Vitro, Antioxidant and Antidiabetic Evaluation

Sharfuddin Mohd,[a] Durgesh Paresh Bidye,[b] Sheshagiri R Dixit,[b] B. C. Revanasiddappa,[c] Vancha Harish,[a] Rakesh Kumar,[a] and Vikas Sharma*[a]

In the present research work a sequence of substituted quinoline based thiazolidinedione moieties (**12a–h**) were designed and synthesized as potential antidiabetic agents. Pancreatic α-amylase (PAA) and intestinal α-glucosidase (IAG) enzymes were considered as potential targets for effective treatment of diabetes. The potential of all compounds **(12a–h)** was assessed in vitro against PAA and IAG using acarbose as standard. The results suggested that compound **12h** has shown superior PAA and IAG inhibitory activity with respective to standard (IC_{50} = **4.683 ± 0.06 µM** and **2.456 ± 0.07 µM**). Furthermore, using computational (in silico) studies like AutoDock and Desmond, predicted the significant binding interactions responsible for the activity of all compounds **(12a–h)** at the active site of enzymes, while SwissADME and Osiris property explorer tools computed in silico drug likeliness and toxicity properties. The RMSD, RMSF, Rg and protein ligand contacts, confirmed the stable binding of compound **12h and 12g** with the both PAA and IAG proteins. The in silico results confirmed the **12h** molecule as a superior drug with high binding affinity and good drug likeness against PAA and IAG, confirming in vitro results. We also studied antioxidant activity (AOA) of all synthesized compounds and results confined that the compound **12h** has good antioxidant potential (IC_{50} **= 5.04 ± 0.054 µM)** among all other compounds. In conclusion, in vitro, in silico and antioxidant studies revealed **12h** compound was found to be potential compound.

1. Introduction

Diabetes mellitus (DM) is a chronic health condition, which is characterized by persistent high blood sugar levels can lead to serious complications affecting various organs and systems in the body. The body's inability to produce enough or effectively use its existing insulin leads to this condition.[1]To avoid the complications of DM, like retinopathy, coronary heart disease, nephropathy, neuropathy and peripheral arteriopathy, postprandial and baseline hyperglycemia should be reduced.[2] Therefore, the therapeutic use of antioxidants has been considered for the treatment and prevention of diabetic complications.[3] Currently, numerous medications for treating Type-2 diabetes mellitus (T2DM) have side effects with less efficacy, often failing to maintain normal glucose levels in the blood.[4] The intestinal α-glucosidase (IAG) and pancreatic α-amylase (PAA) are important targets in the treatment of diabetes due to its involvement in digestion of carbohydrates and its absorption into human body.[5,6] By Restricting the activity of these two enzymes can lower the risk of developing diabetes and postprandial hyperglycemia.[7] Thus, IAG and PAA inhibitors are helpful in the management of hyperglycemia by delaying the digestion of carbohydrates (Figure 1).

In recent years heterocyclic molecules (HCM) grasped the attention of the medicinal chemists because of their unique pharmacological characteristics.[8] Among all HCM, nitrogen(N) containing analogues are most predominant and key structural unit in various bioactive compounds. This flashed the development of new techniques and various synthetic methods.[9] Thiazole core skeleton is composed of around 200 naturally occurring alkaloids found in various plant and animal sources.[10] Thiazolidinedione (TZD), containing thiazole core skeleton, have been found to exhibit significant biological activities including anti-diuretic, anti-Alzheimer, and anti-bacterial properties.[11,12] Due to the wide biological profile of the TZDs ring, it has been shown that the thiazolidine ring is present in several glitazones that are sold commercially, such as pioglitazone, rosiglitazone, troglitazone, lobeglitazone, netoglitazone, and rivoglitazone (Figure 2).[13] The TZD-based hybrid analogs are employed as pharmacologically interesting derivatives and have demonstrated significant biological activities, such as antidiabetic,[14] anti-cancer,[15] antioxidant.[16]

In addition to being a necessary drug discovery approach, nitrogen-containing heterocyclic analogues have gained significant biological and pharmaceutical applications, making them essential for their study. Among all one specific substance is quinoline, with both pyridine and benzene rings, is a widely investigated heterocyclic molecule having significant

[a] S. Mohd, V. Harish, R. Kumar, Dr. V. Sharma
School of Pharmaceutical Sciences, Lovely Professional University, Phagwara, Punjab 144411, India
E-mail: vikas.26231@lpu.co.in
[b] D. P. Bidye, S. R Dixit
Computer Aided Drug Design Laboratory, JSS College of Pharmacy Mysore, JSS Academy of Higher Education and Research, Mysore, Karnataka 570015, India
[c] B. C. Revanasiddappa
NGSM Institute of Pharmaceutical Sciences (A Constituent College of Nitte Deemed to be University), Mangalore, Karnataka 575018, India

Supporting information for this article is available on the WWW under https://doi.org/10.1002/10.1002/slct.202402281

IV. Conference Attended

CHANDIGARH GROUP OF COLLEGES
Building Careers. Transforming Lives.

Sponsored by:
Pharmacy Council of India, New Delhi

CERTIFICATE

This is to certify that Prof./Dr./Mr./Ms. Sharfuddin Mohd has been awarded IInd prize in Poster Presentation on Insilico design of novel Insulysin (IDE) Inhibitors as Antidiabetic agents. in the International Conference on the theme "Emerging Techniques in Drug Discovery and Drug Delivery: Current Challenges and Future Prospects", organized by Chandigarh College of Pharmacy, Landran, Mohali, on 10th-11th February 2020.

Prof. (Dr.) M. Arockia Babu
Organising Secretary
Director-Principal, CCP

Prof. (Dr.) P. N. Hrisheekesha
Patron
Campus Director, CGC

Prof. (Dr.) B. Suresh
President, PCI
New Delhi

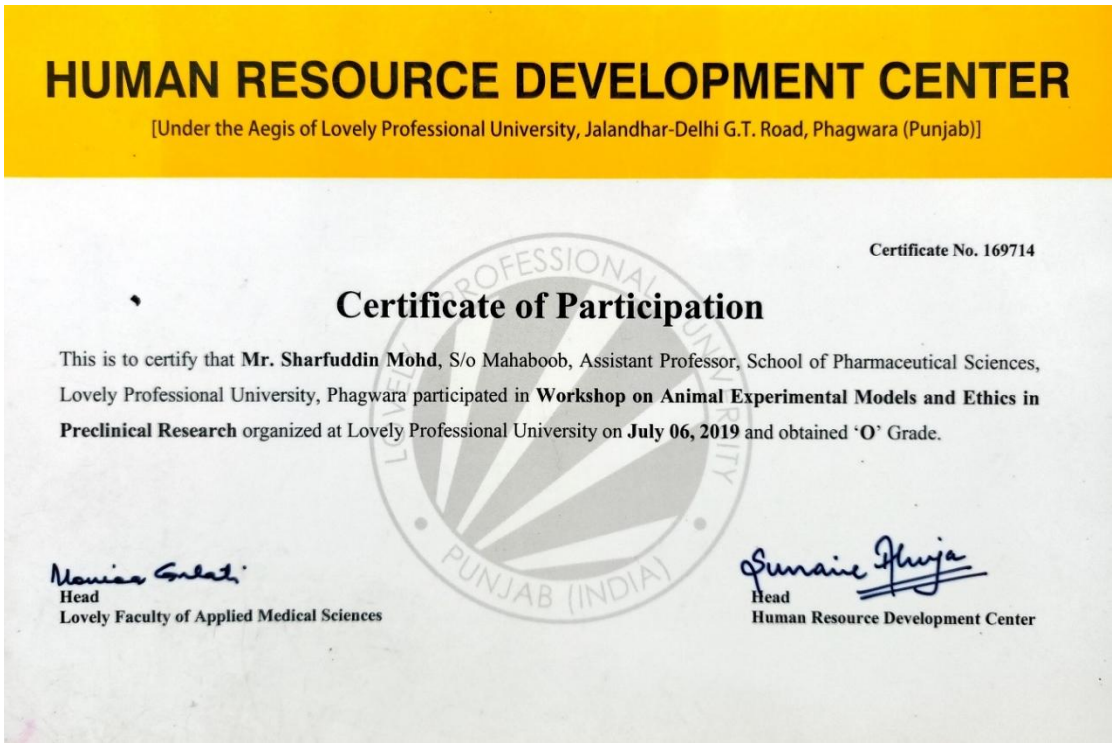

HUMAN RESOURCE DEVELOPMENT CENTER

[Under the Aegis of Lovely Professional University, Jalandhar-Delhi G.T. Road, Phagwara (Punjab)]

Certificate No. 169714

Certificate of Participation

This is to certify that **Mr. Sharfuddin Mohd**, S/o Mahaboob, Assistant Professor, School of Pharmaceutical Sciences, Lovely Professional University, Phagwara participated in **Workshop on Animal Experimental Models and Ethics in Preclinical Research** organized at Lovely Professional University on **July 06, 2019** and obtained '**O**' Grade.

Head
Lovely Faculty of Applied Medical Sciences

Head
Human Resource Development Center

HUMAN RESOURCE DEVELOPMENT CENTER

[Under the Aegis of Lovely Professional University, Jalandhar-Delhi G.T. Road, Phagwara (Punjab)]

Certificate No. 190195

Certificate of Participation

This is to certify that **Mr. Sharfuddin Mohd** S/o Mahaboob participated in **Workshop on Protein Molecular Modeling and Computer Aided Drug Design** organized at Lovely Professional University w.e.f. **November 08, 2019** to **November 09, 2019** and obtained '**A**' Grade.

Head
School of Bio Engineering and Biosciences

Head
Human Resource Development Center

ICRAHS INTERNATIONAL CONFERENCE ON RECENT ADVANCES IN HEALTH SCIENCES

LPU SCHOOL OF PHARMACEUTICAL SCIENCES

Certificate No. 333713

NAAC GRADE A++

Certificate of Participation

This is to certify that **Prof./Dr./Mr./Ms. Sharfuddin Mohd** has successfully participated as Delegate and Oral Presenter on topic **Quinoline based thiazolidinediones: Design, synthesis, In-Silico, In-Vitro, Antioxidant and Anti-Diabetic Evaluation** in offline mode at **"International Conference on Recent Advances in Health Sciences" (ICRAHS-2024)** under the Theme **"Innovations in Sustainable Health Sciences and Research"** held on **27th April 2024**, organized by School of Pharmaceutical Sciences, Lovely Professional University, Punjab.

Date of Issue : 29-05-2024
Place : Phagwara (Punjab), India

Prepared by
(Administrative Officer-Records)

Organizing Secretory
Dr. Vikas Sharma
School of Pharmaceutical Science

Head of School
Dr. Monica Gulati
School of Pharmaceutical Science

SCHOOL OF
PHARMACEUTICAL
SCIENCES

NAAC A++

Certificate No. 354601

Certificate of Presentation

This is to certify that **Dr./Mr./Ms. Sharfuddin Mohd** of **School of Pharmaceutical Sciences, Lovely Professional University, Punjab** has given Oral Presentation on **Quinoline based thiazolidinediones: Design, synthesis, In-Silico, In-Vitro, Antioxidant and Anti-Diabetic Evaluation** in the **4th International Conference of Pharmacy (ICP-2024)** held from 18th to 19th October 2024, organized by **School of Pharmaceutical Sciences** at Lovely Professional University, Punjab in association with **Indian Pharmacy Graduates Association.**

Date of Issue : 05-11-2024
Place : Phagwara (Punjab), India

Prepared by
(Administrative Officer-Records)

Organizing Secretary & Convenor
ICP-2024 (School of Pharmaceutical Sciences)

Executive Dean
Lovely Professional University

ICRAHS
INTERNATIONAL CONFERENCE ON RECENT ADVANCES IN HEALTH SCIENCES

LOVELY PROFESSIONAL UNIVERSITY
Transforming Education Transforming India

Certificate No. 269921

Certificate of Participation

This is to certify that **Prof./Dr./Mr./Ms. Sharfuddin Mohd** has successfully participated as **"Delegate and Oral Presenter"** in the International Conference on **"Recent Advances in Health Sciences" (ICRAHS-2023)** on the Theme of "Interdisciplinary Research: A key to transform Health care." from 14th April, 2023 to 15th April, 2023 organized by School of Pharmaceutical Sciences in association with Komar University of Sciences and Technology at Lovely Professional University, Punjab.

Date of Issue : 24-05-2023
Place : Phagwara (Punjab), India

Prepared by
(Administrative Officer-Records)

Dr. Navneet Khurana
Program Chair

Prof. Dr. Kawis Aziz Faraj
Conference Co-Chair

Dr. Monica Gulati
Conference Chair

Serial No. 31CP2022151S

LOVELY PROFESSIONAL UNIVERSITY
Transforming Education Transforming India

सत्यमेव जयते
IPC

Certificate of Participation

This is to certify that Prof./Dr./Mr./Ms. SHARFUDDIN. MOHD has successfully participated as Delegate & Presented Poster/ Oral Presentation on Therapeutic importance of Heterocyclic compounds. in the 3rd International Conference of Pharmacy (ICP-2022) on the Theme of "Practice, Promotion & Publication of Innovation : A Way of Transforming Health" held on 09th & 10th November 2022 organized by School of Pharmaceutical Sciences in a collaboration with Indian Pharmaceutical Association (IPA) at Lovely Professional University, Punjab.

Mr. Suresh Khanna	Dr. Bimlesh Kumar	Dr. T.V. Naryana	Dr. Monica Gulati
National Hon. Gen. Secretary, IPA	Organizing Secretary	National President IPA	LOC Chairperson

Sri Herbasia Biotech | Tishk International University, Iraq